Bioremediation of chromate in alkaline sediment-water systems

Robert Andrew Whittleston

Submitted in accordance with the requirements for the degree of Doctor of Philosophy

The University of Leeds

School of Earth and Environment

September 2011

The candidate confirms that the work submitted is his own, except where work which has formed part of jointly-authored publications has been included. The contribution of the candidate and the other authors to this work has been explicitly indicated below. The candidate confirms that appropriate credit has been given within the thesis where reference has been made to the work of others.

Paper status and collaborator contributions

Due to the breadth of knowledge required to produce high quality academic research, three of the results chapters within this thesis form all or part of jointly-authored work prepared for publication. Therefore, collaborator contributions and submission status of each article are clarified below.

Chapter 4 "Chromate reduction in Fe(II)-containing soil affected by hyperalkaline leachate from chromite ore processing residue" (Submitted to Journal of Hazardous Materials in June 2011, in press August 2011).

> R. A. Whittleston – principal author, site sampling, geochemical analyses, microcosm experiments, reoxidation experiments, XAS data collection and analyses, culturing of iron reducers, DNA extraction, 16S rRNA gene analysis, clone libraries and phylogenetic tree construction; D. I. Stewart – site sampling, extensive manuscript review; R. J. G Mortimer – manuscript review; Z. C. Tilt – site sampling, XRD, XRF and TOC analyses; A. P. Brown – TEM analysis; K. Geraki – XAS data collection guidance; I. T. Burke – site sampling, SEM preparation, guidance on XAS data collection and analysis, extensive manuscript review.

Chapter 5 "Effect of microbially induced anoxia on Cr(VI) mobility at a site contaminated with hyperalkaline residue from chromite ore processing" (Submitted to Geomicrobiology Journal April 2010, published January 2011 28, 68-82).

> R. A. Whittleston – principal author, geochemical analyses, DNA extraction, 16S rRNA gene analyses, clone libraries and phylogenetic tree construction; D. I. Stewart – site sampling, provided guidance for DNA extraction and 16S rRNA gene analysis, extensive manuscript review; R. J. G Mortimer –

manuscript review; D. J. Ashley – IC technical guidance; I. T. Burke – site sampling, microcosm experiments, extensive manuscript review.

Chapter 6 “Enhancing microbial reduction in hyperalkaline, chromium contaminated sediments by pH amendment” (Submitted to Journal of Hazardous Materials September 2011).

R. A. Whittleston – principal author, site sampling, microcosm experiments, geochemical analyses, DNA extraction, 16S rRNA gene analysis, clone libraries, MOTHUR, rarefaction and MDS analyses, phylogenetic tree construction; R. J. G Mortimer – manuscript review; I. T. Burke – site sampling, extensive manuscript review; D. I. Stewart – site sampling, guidance on MOTHUR, rarefaction and MDS analyses, extensive manuscript review.

ACKNOWLEDGEMENTS

I would like to express my deepest gratitude to Ian Burke, Doug Stewart, and Rob Mortimer for their unwavering support in my academic development. They have provided me with priceless guidance from their vast range of expertise, without which this project would not have been possible. I am also incredibly grateful to them for the personal help and advice they have given me over the last three or more years. Your ability to remain good humoured in the most frustrating situations was invaluable! I would also like to thank the many others who have had input in one form or another, including but not limited to; David Ashley, Andy Brown, Louise Fletcher, Lesley Neve and Eric Condliffe for technical guidance and data collection, Michael Marsden, Zana Tilt and James Atkins for help with sample collection and interpretation. Thanks also to Kalotina Geraki and Fred Mosselmans for their help with XAS data collection and interpretation, and to Dr Phil Studds and Mark Bell from Ramboll UK for enabling site access and sample collection. Beyond these, I am grateful to everyone that made my time at the university memorable. Ian Burke, for teaching me to remain calm in stressful situations through his unique mini bus driving style and endless supply of British Isles coffee (two not explicitly linked). Mat Evans for repeatedly allowing me to outperform him in the gym, not pressing charges in Arran, and for listening to my endless rants. Sam Allshorn, for patience and understanding despite his militaristic running of the Cohen Labs, and to Damian Howells, for always being up for a pint. I also owe huge thanks to my office mates and fellow postgraduate students for their tolerance of me over the last three years, including; Chris Hubbard, Jenn Brooke, Ross Herbert, Mike Hollaway, Cat Scott, Amber Leeson, David Tupman, Ryan Hossaini, Eimear Dunne, James Pope for not being quite as good at sport as I am, Ben Parkes for his t-shirts bringing colour into an otherwise bland office, and Bradley Jemmett-Smith and Rachael Berman for their continued friendship over the last 6 years. For having the dubious honour of sitting next to me for the last two years special thanks must go to Sarah Wallace, who willingly provided me with all office supplies, a chronological banana skin decompositional time piece, cakes, mugs, plates, cutlery and rescued me from a dire Czech situation. Thanks are also due to all those who have helped me keep in touch with some form of reality over the years; Dave McClane, Rebecca “Pearbear” Perry, Andrew “Mexican” Mason and his beautiful geometric features, Phil Rooney, Oliver

Wade, Jack “Jack-bot” Ellery, Felicity Ford, Jo Minnitt, Joseph Weiler for that ticket we were just talking about, Nishal Palawan and his gatecrasher hoodie, Nick Bell 10L and his love of small animals, Simon Burton, Tom Dawson and his paddle, Matt Charles and his pear juice, Dan Faben for always wanting to get married, everyone at Bradford Bulldogs IHC, and even Eli Rosenblatt. A huge thank you to my parents for always supporting me with whatever I decided to do and for funding my various exploits over the years, and to both my brothers. Special thanks are also owed to Mr Hamshaw for spending his free time all those years ago to teach me AS-level physical geography, without which I probably would never have started university. Finally, I would also like to thank “my muse, my flame” Ashlea “gets there in the end” Henshaw for helping me get there in the end, and in the words of Jimmy MacElroy: “if you can dream it, you can do it!”

This project has been jointly funded by the University of Leeds School of Earth and Environment and the John Henry Garner Endowed Scholarship. Funding for XAS analysis at the Diamond Lightsource was awarded through Burke I. T., Stewart D. I., Mortimer R. J. G. and Whittleston R. A. (2009) Micro-focus XAS study of chromium behaviour in alkaline soil-water systems. STFC Diamond Light Source AP6-1493 (4 days).

ABSTRACT

The poorly controlled disposal of chromium ore processing residue (COPR) is a globally widespread problem due to its potential to form chromium contaminated hyperalkaline (pH > 12) leachates. These highly oxidising leachates typically contain chromium in the Cr(VI) oxidation state as its chromate anion (CrO_4^{2-}). This anion is highly mobile, toxic, carcinogenic, and exhibits a high degree of bioavailability. Under reducing conditions chromium exists in the non-toxic and poorly soluble Cr(III) oxidation state. Thus, the reduction of Cr(VI) to Cr(III) is often the goal of remediative strategies. In anaerobic subsurface environments where reducing conditions are established by the indigenous microbial population, chromium reduction can occur naturally. The microbial transformation of Cr(VI) to Cr(III) can be both a result of its direct use in microbial metabolism, or through its indirect reaction with microbially produced reduced species, e.g. Fe(II). This study has used a multidisciplinary approach to investigate the biogeochemical influences on the fate and stability of Cr(VI) leaching from a site of COPR in the north of England. Reducing sediments encountered directly beneath the COPR waste were found contain elevated concentrations of chromium. These sediments were shown to be able to remove aqueous Cr(VI) from solution when incubated with contaminated site groundwater in microcosm incubation experiments. This removal is likely a result of the abiotic reduction by soil associated microbially produced Fe(II), followed by precipitation as insoluble Cr(III) hydroxides. X-ray absorption spectroscopy (XAS) and electron microscopy confirms the association of chromium as Cr(III) with iron in these soils, hosted as a mixed Cr(III)-Fe(III) oxyhydroxide phase. Upon air oxidation, only minor amounts of chromium was remobilised from these sediments as Cr(VI). A diverse population of alkaliphilic microorganisms are indigenous to this horizon, capable of successful metabolism despite elevated pH values. This population was found to contain a consortium of microorganisms capable of iron reduction when incubated at pH 9 to 9.5. Microbial community analysis found taxonomic similarity to several known metal reducing alkaliphiles from the phylum *Firmicutes.* These results suggest that the novel action of iron reducing alkaliphiles indigenous to reducing sediments beneath COPR sites may provide zones of natural chromium attenuation via microbially mediated mechanisms of Cr(VI) transformation.

TABLE OF CONTENTS

LIST OF FIGURES

LIST OF TABLES

ABBREVIATIONS

ACGIH	American Conference of Industrial Hygienists
ADP	Adenosine diphosphate
ANC	Acid Neutralisation Capacity
ATP	Adenosine triphosphate
ATSDR	Agency for Toxic Substances and Disease Registry
BSE	Backscatter Electrons
COPR	Chromate Ore Processing Residue
EDX	Energy-dispersive X-ray spectroscopy
EMBL	European Molecular Biology Laboratory
EPMA	Electron Probe Micro-analyser
EXAFS	Extended X-Ray Absorption Fine Structure
FT	Fourier Transform
IC	Ion Chromatography
LOI	Loss on Ignition
MPN	Most Probable Number
OSHA	Occupational Safety and Health Administration
OTU	Operational Taxonomic Unit
PCR	Polymerase Chain Reaction
PEL	Permissible Exposure Limit
RDP	Ribosomal Database Project
SEM	Scanning Electron Microscopy
SR	Synchrotron Radiation
STEM	Scanning Transmission Electron Microscopy
TEAP	Terminal Electron Accepting Process
TEM	Transmission Electron Microscopy
TOC	Total Organic Carbon
USEPA	United States Environmental Protection Agency
WHO	World Health Organisation
XANES	X-ray Absorption Near Edge Structure
XAS	X-ray Absorption Spectroscopy

Chapter 1 Project context, significance and structure

1.1 Project context and significance

Chromium is among the most extensively used heavy metals in both the chemical and alloy industries (Wang, 2000). Its use is included in leather tanning, wood preservation, chrome metal finishing, and the manufacturing of dyes, paints, pigments, and stainless steel (Morales-Barrera and Cristiani-Urbina, 2008; Rehman and Shakoori, 2001; Thacker et al., 2007; Yewalkar et al., 2007). The high demand for chromium means that world production from its ore, chromite ($FeCr_2O_4$), is of the order of 10^7 tons per year (Cervantes et al., 2001). Chromite typically exhibits a spinel structure (Cr, Fe, Al)$_2O_3$(Fe, Mg)O, and has a chromium oxide content of between 15 and 65% (Darrie, 2001; Farmer et al., 1999). In order to obtain chromium from this ore, it is first oxidised to facilitate extraction with water due to the greater solubility of its oxidised hexavalent form. Traditionally this was achieved using the "high lime" method of chromium ore processing. During this process, chromite ore is first roasted at 1150ºC in the presence of lime (CaO) and alkali carbonate for several hours to oxidise Cr(III) to Cr(VI) (Farmer et al., 1999). The Cr(VI) compounds produced (either potassium or sodium chromate), are then extracted with water and further reacted with sulphuric acid to yield dichromate *(Eqn. 1 - 2).*

$$4FeCr_2O_4 + 8Na_2CO_3 + 7O_2 \rightarrow 8Na_2CrO_4 + 2Fe_2O_3 + 8CO_2 \quad (1)$$

$$2Na_2CrO_4 + H_2SO_4 \rightarrow Na_2Cr_2O_7 + Na_2SO_4 + H_2O \quad (2)$$

As its name suggests, lime was added to the smelting process to act a catalyst for chromium oxidation through improved O_2 penetration and by helping to prevent the reactants from fusing (Darrie, 2001; Farmer et al., 1999). It was eventually replaced by dolomite or limestone fillers which, although cheaper, produced huge volumes of waste material (Darrie, 2001; Hillier et al., 2003; Wang et al., 2007). Despite being no longer used in Europe or the USA, this high lime method is still responsible for up to 40% of world chromium production today, producing approximately 600,000 tonnes of waste in 2001 (Darrie, 2001; Walawska and Kowalski, 2000). The inefficiencies of the process mean that this waste, termed chromite ore processing residue (COPR), contains substantial amounts of residual chromium. While this is predominantly present in the relatively benign and immobile Cr(III) form, significant concentrations are also found in the toxic, carcinogenic and highly mobile Cr(VI) form.

The disposal of COPR material has traditionally been achieved by landfill, commonly in or around urban areas (Wang et al., 2007). Historically these sites have been poorly managed, and as a result contamination from the formation of hazardous Cr(VI) bearing hyperalkaline plumes is considered a globally widespread problem (Geelhoed et al., 2002; Higgins et al., 1998; Stewart et al., 2007). The high mobility of Cr(VI) allows it to migrate substantial distances from the source of contamination within these leachates, posing a significant danger to surrounding ecosystems and water sources. Indeed, cases of aquifer contamination by hexavalent chromium as a result of its use in industry can become nationally significant, and cost companies millions in compensation payments. One such example that highlights the need to understand the behaviour of Cr(VI) within the subsurface was the poisoning of the

entire water supply for the town of Hinkley, California. Here, Cr(VI) was used by a gas and electric firm between 1952 and 1966 to fight corrosion of cooling towers, before being discharged directly into unlined ponds. The high mobility of Cr(VI) subsequently enabled it to percolate into the surrounding groundwater, contaminating a wide area. This case was eventually settled in 1996 for $333 million, and was such high profile that it has subsequently formed the basis of the Hollywood film "Erin Brockovich", released in the year 2000.

In addition to the hazards associated with contaminated aqueous systems, Cr(VI) bearing dusts have also been identified as a human carcinogen through inhalation (Nurminen, 2006). This complicates remediation efforts as dig and dump strategies at sites of Cr(VI) contamination are inadvisable due to the risk of forming these carcinogenic dusts. As environmental awareness continues to grow, pressure is mounting on companies responsible for contaminated environments to not only produce successful remediation strategies, but also to perform them in an environmentally conscious manner. Traditional remediation of COPR sites has focused on the hazardous relocation of the waste, and/or the implementation of a variety of costly chemical treatments (Bewley, 2007; Geelhoed et al., 2003; Su and Ludwig, 2005; Wazne et al., 2007). There is therefore a clear need to develop *in-situ* remediation technologies for COPR contaminated environments that do not require large volumes of chemical treatments or the disturbance of the waste itself. Such remediation strategies need to be successful at a relatively low cost to both the investing company, and the environment.

Bioremediation is a technique that can be applied *in-situ* which is increasingly being employed as a sustainable remediation solution to a variety of contaminated environments. It is defined by Andrews et al. (2004) as "*The elimination, attenuation or transformation of polluting or contaminating substances by the use of biological processes, to minimize the risk to human health and the environment"*. The successful implementation of bioremediation therefore relies on the exploitation of natural biological processes, to either directly or indirectly transform or immobilise a contaminant (Hazen and Tabak, 2005; Krishna and Philip, 2005; NABIR, 2003). The ability of soil microorganisms to couple the oxidation of soil organic matter to the reduction of transition metals in a process known as dissimilatory metabolism is widely known in a variety of subsurface environments (Lovley, 1993). Soil microorganisms can therefore influence the fate of metal contaminants within the subsurface because oxidation state often plays a significant role in metal mobility. The reduced Cr(III) form of chromium is considered substantially less toxic and environmentally mobile compared to Cr(VI), due to its decreased solubility and increased retention within the solid phase (Lin, 2002). Its reduction is therefore desirable. Microbial reducing environments occur naturally within the subsurface, and provide potential reactive zones for the natural transformation of redox active contaminants. Such microbially active zones have previously been encountered under COPR contaminated sites in New Jersey, and were appearing to facilitate the accumulation of chromium (Higgins et al., 1998; Martello et al., 2007).

Harnessing the ability of soil microorganisms to directly or indirectly bio-reduce Cr(VI) therefore provides a potential mechanism of remediation that could be enhanced through the stimulation of the influential microbial population. The

stimulation of bio-reduction is usually achieved through the addition of nutrients to nutrient starved systems, or the altering of subsurface conditions to favour the development of reducing conditions. However, the toxicity of Cr(VI) and high pH characteristic of COPR contaminated environments puts significant stress on microbial metabolism, making these challenging environments for successful bioremediation. Detailed multidisciplinary investigations are therefore crucial at COPR sites in order develop an understanding of the fate of Cr(VI) in the environment, and determine the extent of chromium contamination. This subsequently allows for the feasibility of *in-situ* ecologically favourable remediation strategies, such as bioremediation, to be assessed.

1.2 Thesis structure

This thesis begins with an overview of chromium chemistry and the processes that govern its fate in the environment. This is followed by an introduction to the COPR landfill site that is the focus of this research, detailed project aims and objectives, and the approaches adopted to achieve them. Results in the form of four working chapters, three of which have been prepared for publication, are then presented. The thesis is concluded with a summary chapter, detailing the project findings. This summary chapter concludes with suggestions for additional work and considerations for future remediation strategies. In addition, comprehensive appendices are included, providing detailed descriptions of the methods employed throughout, additional results, and associated publications.

1.3 References

Andrews, J.E., Brimblecombe, P., Jickells, T.D., Liss, P.S., Reid, B.J., 2004. Chapter 4 - The Chemistry of Continental Solids. An Introduction to Environmental Chemistry 2nd ed, 121.

Bewley, R.J.F., 2007. Treatment of Chromium Contamination and Chromium Ore Processing Residue. URS Corpotation Ltd., Technical paper.

Cervantes, C., Campos-Garcia, J., Devars, S., Gutierrez-Corona, F., Loza-Tavera, H., Torres-Guzman, J.C., Moreno-Sanchez, R., 2001. Interactions of chromium with microorganisms and plants. FEMS. Microbiol. Rev. 25, 335-347.

Darrie, G., 2001. Commercial extraction technology and process waste disposal in the manufacture of chromium chemicals from ore. Environ. Geochem. Health 23, 187-193.

Farmer, J.G., Graham, M.C., Thomas, R.P., Licona-Manzur, C., Licona-Manzur, C., Paterson, E., Campbell, C.D., Geelhoed, J.S., Lumsdon, D.G., Meeussen, J.C.L., Roe, M.J., Conner, A., Fallick, A.E., Bewley, R.J.F., 1999. Assessment and modelling of the environmental chemistry and potential for remediative treatment of chromium-contaminated land. Environ. Geochem. Health 21, 331-337.

Geelhoed, J.S., Meeussen, J.C.L., Hillier, S., Lumsdon, D.G., Thomas, R.P., Farmer, J.G., Paterson, E., 2002. Identification and geochemical modeling of processes controlling leaching of Cr(VI) and other major elements from chromite ore processing residue. Geochim. Cosmochim. Acta 66, 3927-3942.

Geelhoed, J.S., Meeussen, J.C.L., Roe, M.J., Hillier, S., Thomas, R.P., Farmer, J.G., Paterson, E., 2003. Chromium remediation or release? Effect of iron(II) sulfate addition on chromium(VI) leaching from columns of chromite ore processing residue. Environ. Sci. Technol. 37, 3206-3213.

Hazen, T.C., Tabak, H.H., 2005. Developments in bioremediation of soils and sediments polluted with metals and radionuclides: 2. Field research on bioremediation of metals and radionuclides. Rev. Env. Sci. Biot. 4, 157-183.

Higgins, T.E., Halloran, A.R., Dobbins, M.E., Pittignano, A.J., 1998. In situ reduction of hexavalent chromium in alkaline soils enriched with chromite ore processing residue. Japca J. Air. Waste Ma. 48, 1100-1106.

Hillier, S., Roe, M.J., Geelhoed, J.S., Fraser, A.R., Farmer, J.G., Paterson, E., 2003. Role of quantitative mineralogical analysis in the investigation of sites contaminated by chromite ore processing residue. Sci. Total Environ. 308, 195-210.

Krishna, K.R., Philip, L., 2005. Bioremediation of Cr(VI) in contaminated soils. J. Hazard. Mater. 121, 109-117.

Lin, C.J., 2002. The chemical transformations of chromium in natural waters - A model study. Water Air Soil Poll. 139, 137-158.

Lovley, D.R., 1993. Dissimilatory Metal Reduction. Annu. Rev. Microbol 47, 263-290.

Martello, L., Fuchsman, P., Sorensen, M., Magar, V., Wenning, R.J., 2007. Chromium geochemistry and bioaccumulation in sediments from the lower Hackensack River, New Jersey. Arch. Environ. Con. Tox. 53, 337-350.

Morales-Barrera, L., Cristiani-Urbina, E., 2008. Hexavalent chromium removal by a Trichoderma inhamatum fungal strain isolated from tannery effluent. Water Air Soil Poll. 187, 327-336.

NABIR, 2003. Bioremediation of metals and radionuclides: what it is and how it works, A NABIR primer, 2nd ed. NABIR primer prepared for US Department of Energy, p. p.78.

Nurminen, M., 2006. Human Carcinogenicity Risk Assessment of Metallic Chromium and Trivalent Chromium. International Chromium Development Association, [Accessed 21/10/2008] Available at: http://www.icdachromium.com/pdf/publications/8909_CHROMIUM_ICDA_N_2014.pdf.

Rehman, A., Shakoori, A.R., 2001. Heavy metal resistance Chlorella spp., isolated from tannery effluents, and their role in remediation of hexavalent chromium in industrial waste water. B. Environ. Contam. Tox. 66, 542-547.

Stewart, D.I., Burke, I.T., Mortimer, R.J.G., 2007. Stimulation of microbially mediated chromate reduction in alkaline soil-water systems. Geomicrobiol. J. 24, 655-669.

Su, C.M., Ludwig, R.D., 2005. Treatment of hexavalent chromium in chromite ore processing solid waste using a mixed reductant solution of ferrous sulfate and sodium dithionite. Environ. Sci. Technol. 39, 6208-6216.

Thacker, U., Parikh, R., Shouche, Y., Madamwar, D., 2007. Reduction of chromate by cell-free extract of Brucella sp isolated from Cr(VI) contaminated sites. Bioresource Technol 98, 1541-1547.

Walawska, B., Kowalski, Z., 2000. Model of technological alternatives of production of sodium chromate (VI) with the use of chromic wastes. Waste Manage. 20, 711-723.

Wang, T.G., He, M.L., Pan, Q., 2007. A new method for the treatment of chromite ore processing residues. J. Hazard. Mater. 149, 440-444.

Wang, Y.T., 2000. In Lovley D.R. "Environmental Microbe-Metal Interactions" ASM Press. Chapter 10: Microbial Reduction of Chromate, 225-235.

Wazne, M., Jappilla, A.C., Moon, D.H., Jagupilla, S.C., Christodoulatos, C., Kim, M.G., 2007. Assessment of calcium polysulfide for the remediation of hexavalent chromium in chromite ore processing residue (COPR). J. Hazard. Mater. 143, 620-628.

Yewalkar, S.N., Dhumal, K.N., Sainis, J.K., 2007. Chromium(VI)-reducing Chlorella spp. isolated from disposal sites of paper-pulp and electroplating industry. J. Appl. Phycol. 19, 459-465.

Chapter 2 Background information and site processes

This chapter provides an overview of chromium chemistry and toxicity, sources of environmental pollution, and fate in the environment. The potential of soil microorganisms to influence trace metal behaviour within the subsurface is discussed, and a detailed introduction to the study site also provided.

2.1 Overview

Chromium is the 7th most abundant element on earth, and the 21st in crustal rocks which contain concentrations ranging from 100 to 300 $\mu g.g^{-1}$ (Cervantes et al., 2001). Chromium concentrations within soils are more variable, and typically range between 1 and 2000 $mg.kg^{-1}$ dependent on the composition and source of the parent material (Shewry and Peterson, 1976; USGS, 1984). Background concentrations in the air can range from <10 $ng.m^3$ in rural environments to between 0 and 30 $ng.m^3$ in urban areas (ATSDR, 2008). It can exist in nine valence states ranging from +6 to -2, but under natural environmental conditions it is the tri (Cr(III)) and hexavalent (Cr(VI)) forms which dominate due to their superior thermodynamic stability (Krishna and Philip, 2005; Nurminen, 2006; Richard and Bourg, 1991). While Cr(III) occurs naturally in the environment, Cr(VI) is primarily sourced anthropogenically (Stewart et al., 2003). These two forms exhibit significantly differing geochemical and ecotoxicological characteristics, with Cr(III) widely regarded as non-toxic and poorly mobile (James, 2001, 2002; Martello et al., 2007). In contrast Cr(VI) is considered a priority pollutant by the US Environmental Protection Agency due to its toxic, carcinogenic, and mutagenic properties (Nurminen, 2006; Rowbotham et al., 2000; USEPA, 2005b; Wielinga et al., 2001). In addition, Cr(VI) is also considered

much more soluble than Cr(III) under normal environmental conditions. It is these characteristics that result in Cr(VI) posing a significant hazard within the environment, complicated by its ability to migrate away from sources of contamination (Lin, 2002; Richard and Bourg, 1991). Cr(VI) species are also considered to have a high bioavailability due to the ease at which it is absorbed into cells. This occurs via the sulphate transport system as its dominant anion, chromate (CrO_4^{2-}), exhibits similar structural characteristics to the sulphate anion (SO_4^{2-}) (Cervantes et al., 2001; Daulton et al., 2007). As a result, the accumulation of chromium in crops due to uptake in the rhizosphere has led to food being a major concern as a source of exposure (Hullebusch et al., 2005). The estimated oral intake for children and adults ranges from 123-171 and 246-343 µg per day respectively (Rowbotham et al., 2000). However, James (2002) explains that Cr(VI) uptake by roots is normally limited due to the coupled process of reduction to Cr(III) as a detoxification mechanism followed by its organic complexation onto the root surface. Early studies by Breeze (1973) identified high alkalinity and Cr(VI) concentrations associated with chromate manufacture as directly responsible for reduced vegetation diversity, as a consequence of this high bioavailability.

2.2 Exposure and health effects

The widespread use of chromium in industry has meant that areas with the highest levels of contamination primarily result from anthropogenic sources (Breeze, 1973; Levy et al., 2001). Cr(VI) is classified by the American Conference of Industrial Hygienists (ACGIH) as a confirmed human carcinogen in both water soluble and insoluble forms (Nurminen, 2006). Elevated Cr(VI) concentrations in air and water systems can be the result of close proximity to industries that use or manufacture chromium, hazardous waste facilities, and cigarette smoke. Those deemed most at

risk of exposure to airborne Cr(VI) are workers in the metallurgy or tanning industries (ATSDR, 2008). Recent mortality estimates among workers at several industrial sites are reported at 6 deaths per 1000 persons at 1 $\mu g.m^3$ Cr(VI) and ~1 per 1000 persons at 0.2 $\mu g.m^3$ Cr(VI) (NIOSH, 2008). The toxicity of Cr(VI) is mainly due to its ability to act as an oxidising agent in living cells (James, 2002). Independent experiments exposing human bronchial (BEAS-2B) and skin cells to Cr(VI) have demonstrated its genotoxic nature through direct oxidative DNA damage, and supported its link with lung cancer and skin irritation (Bagchi et al., 1997; Cavallo et al., 2008; Rudolf et al., 2008). The dangers associated with airborne Cr(VI) have led the Occupational Safety and Health Administration (OSHA) to set a Permissible Exposure Limit (PEL) of 5 $\mu g.m^3$ in air averaged over an 8-hour working day (OSHA, 2006). The risk associated with Cr(VI) ingestion is considered much less than that of inhalation, in part due to the reduction of Cr(VI) to the less toxic Cr(III) within the digestive system. However, excessive ingestion of Cr(VI) has been found to result in irritation or ulcer formation in the stomach and small intestine, as well as causing blood anaemia (ATSDR, 2008). Although these risks posed by ingestion are considered small, a significantly elevated mortality rate due to stomach cancer has been observed in areas exposed to Cr(VI) contaminated drinking water (Beaumont et al., 2008). The World Health Organisation has therefore established 0.05 $mg.l^{-1}$ total Cr guideline for drinking water (WHO, 2008).

In contrast to the dangers associated with its hexavalent form, trivalent chromium, Cr(III), is regarded as an essential plant and animal nutrient in trace amounts. It is required for successful amino and nucleic acid synthesis, correct insulin function and fat and glucose metabolism creating improved lean body mass (Jain et al., 2007;

Krishna and Philip, 2005; Pechova and Pavlata, 2007; Richard and Bourg, 1991). Cr(III) has also been shown to reduce blood cholesterol levels, and is suggested to help decrease the risk of cardio-vascular disease (Jain et al., 2007). An early study investigating the different mutagenic properties of Cr(III) and Cr(VI) on *salmonella typhimurium* found a Cr(III) concentration 1000 times greater than that of Cr(VI) was required to produce the same levels of mutation (Lofroth and Ames, 1978). As Cr(III) toxicity is considered much lower than that of Cr(VI), intake via ingestion has a large safety range with no detrimental effects observed up to 1 mg per day. Cr(III) therefore has a suggested adequate minimum daily intake of 50 µg (Anderson, 1996). Despite this, most diets have been found to contain less than 60% of the recommended minimum intake of Cr(III), therefore increasing the risk of developing symptoms similar to diabetes or cardiovascular disease (Anderson, 1996).

2.3 Chromite ore processing residue (COPR)

The poor management of COPR legacy disposal sites has led to contamination derived from these wastes becoming a globally widespread problem. The impurities within chromite ore (e.g. Mg, Fe, Al), and the inefficiency of the high lime process leaves up to 70% (w/w) chromite ore discarded, with ~30% by weight converted to chromate (Deakin et al., 2001). The use of alkali carbonates (K_2CO_3 until c.1880, Na_2CO_3 thereafter) and lime (eventually replaced by cheaper dolomite or limestone) in the smelting process create highly alkaline wastes, dominated by alkaline and alkali earth oxides (Farmer et al., 1999; Geelhoed et al., 2003; Stewart et al., 2007). During the process, the reaction of lime with water forms calcium hydroxides, and as a result COPR and surrounding porewaters have characteristically high pH values of between 9 and 12 (Geelhoed et al., 2003; Stewart et al., 2007). Stoichiometric dissolution studies on common COPR mineral phases have found that hydroxide and

carbonate phases cannot solely be responsible for maintaining such high pH values as their equilibrium pH values are too low (Geelhoed et al., 2002). Instead, the dissolution of other COPR minerals such as hydrogarnet and hydrocalumite, is considered an important factor as they are shown to produce equilibrium pH's between 11 and 12 (Farmer et al., 2006; Geelhoed et al., 2002; Hillier et al., 2003; Tinjum et al., 2008). The diverse mineralogical makeup of COPR creates a huge buffering capacity. A study into the acid neutralising capacity (ANC) of COPR by Tinjum et al. (2008) found nearly 8 moles of HNO_3 per kg of waste was required to reduce its pH from 11.3 to 7.5. This has important implications on the feasibility of Cr(VI) remediation strategies through further *in-situ* acid extraction due to the large volumes of chemicals that would be required.

Quantative information on the solid mineral phases present within COPR has been acquired using a variety of analytical techniques, including X-ray Powder Diffraction (XRD), Scanning Electron Microscopy (SEM), and Energy Dispersive X-ray detection (EDX). These phases can be subdivided into four categories: unreacted chromite ore; high temperature phases formed during the extraction process (brownmillerite, periclase and portlandite); minerals produced by *in-situ* weathering (brucite, hydrocalumite, hydrogarnet, ettringite and calcite derived from the addition of lime and dolomite); and cementing agents e.g. tricalcium aluminate (Geelhoed et al., 2002; Geelhoed et al., 2003; Sreeram and Ramasami, 2001; Tinjum et al., 2008; Walawska and Kowalski, 2000). Reports of total residual chromium within COPR by oxide weight vary considerably between landfill sites but typically fall between 2-8% Cr (w/w), although it has been reported to be as high as 15% (Deakin et al., 2001; Tinjum et al., 2008). This is probably in part due to its heterogeneous makeup, and

commonly relates to residual concentrations ranging from 2000-40,000 $mg.kg^{-1}$ (Tinjum et al., 2008), although it can reach as much as 70,000 $mg.kg^{-1}$ (Higgins et al., 1998). Most of this residual chromium is present in the relatively insoluble Cr(III) form. For example, a COPR site in south-east Glasgow was reported to contain up to 80% of the total chromium present in the reduced Cr(III) form, as unreacted chromite ore and Cr(III) containing brownmillerite (Farmer et al., 2006; Hillier et al., 2003; James, 1994; Tinjum et al., 2008). However, the inefficiency of the extraction process has also led to COPR containing significant amounts of highly mobile Cr(VI). The amount again varies dependant on site, with concentrations measured from XANES analysis of bulk material ranging from 1-35% of total chromium (Geelhoed et al., 2002; Tinjum et al., 2008). At the COPR site in south-eastern Glasgow, Cr(VI) accounted for the remaining 20% of residual chromium (Hillier et al., 2003). Cr(VI) is primarily hosted within COPR minerals such as Cr(VI)-hydrocalumite ($Ca_4Al_2(OH)_{12}CrO_4 \cdot 6H_2O$), Cr(VI)-substituted hydrogarnet ($Ca_3Al_2((Cr/Si/H4)O4)_3$) and Cr(VI)-ettringite ($Ca_6Al_2(OH)_{12}(CrO_4)_3 \cdot 26H_2O$) (Geelhoed et al., 2002; Hillier et al., 2003). Of these minerals, hydrogarnet is considered to be the most significant hosting phase and is a primary constituent of COPR, existing at up to 25% (w/w) (Hillier et al., 2007). It is calculated that this phase is responsible for hosting up to 50% of the total residual Cr(VI) present in some COPR samples (Hillier et al., 2003). Ettringite is a secondary precipitate phase formed when hydrocalumite dissolves. It is considered to only be a minor Cr(VI) host phase, accounting for as little as 1-3% of total residual Cr(VI) within COPR (Farmer et al., 2006). The high stability of these hosting minerals at high pH is responsible for the residual Cr(VI) concentrations within COPR following the extraction process.

Batch studies by Geelhoed, Meeussen et al. (2002) have indicated that the subsequent dissolution of these minerals is likely to be the key process responsible for Cr(VI) leaching to groundwaters. Their models were able to accurately predict Cr(VI) concentrations in solution between pH 10-12. Hydrocalumite and hydrogarnet were again identified as the most important solid phases existing in COPR that control Cr(VI) solubility above pH 11, with Cr(VI)-ettringite reported to become increasingly influential at pH values between 9.5 and 11. Cr(VI) hosted within hydrogarnet and hydrocalumite exists in its anionic CrO_4^{2-} form, substituted within the mineral structure (Geelhoed et al., 2002; Geelhoed et al., 2003). As this anion is readily exchangeable with other anions such as SO_4^{2-} in hydrocalumite, and SiO_4^{-} in hydrogarnet, it is readily leached into surrounding porewaters (Farmer et al., 2002). Despite the stability of these phases at high pH leaching studies have shown that only a slight lowering of the pH is required to promote their partial dissolution, and result in a significant release of Cr(VI) to solution (Hillier et al., 2003). As a result of this and the buffering effect of the dissolution of calcite minerals, COPR affected aqueous systems at sites of landfill are often hyperalkaline and contaminated with high concentrations of Cr(VI). These concentrations have been reported as up to 1.6 $mmol.l^{-1}$ Cr(VI), nearly 1000 times greater than environmental health standards (Geelhoed et al., 2002; Whittleston et al., 2011).

Concern has grown in recent years over the treatment of Cr(VI) contaminated residues as understanding of the leaching behaviour and detrimental health effects improves (Wang et al., 2007). Once Cr(VI) is leached from COPR, understanding the

geochemical controls on its mobility is considered paramount in order to mitigate resulting environmental hazards.

2.4 Chromium fate in the environment

2.4.1 Geochemical behaviour

The aqueous chemistry of chromium is complex as its mobility is highly variable depending on its existence in the cationic Cr(III), or anionic Cr(VI) state (Chen and Hao, 1998; Richard and Bourg, 1991). The principle dissolved species of Cr(III) are $Cr(OH)^{2+}$ and $Cr(OH)_3^0$, with $HCrO_4^-$ and CrO_4^{2-} the most common Cr(VI) species found in natural waters (Mohan and Pittman, 2006). The prevailing phase existing in aqueous systems is initially governed by the Eh and pH of the environment (Mohan and Pittman, 2006). Figure 2.1 gives the stability fields for common aqueous chromium species, with the red and blue boarders indicating +6 and +3 valence states respectively.

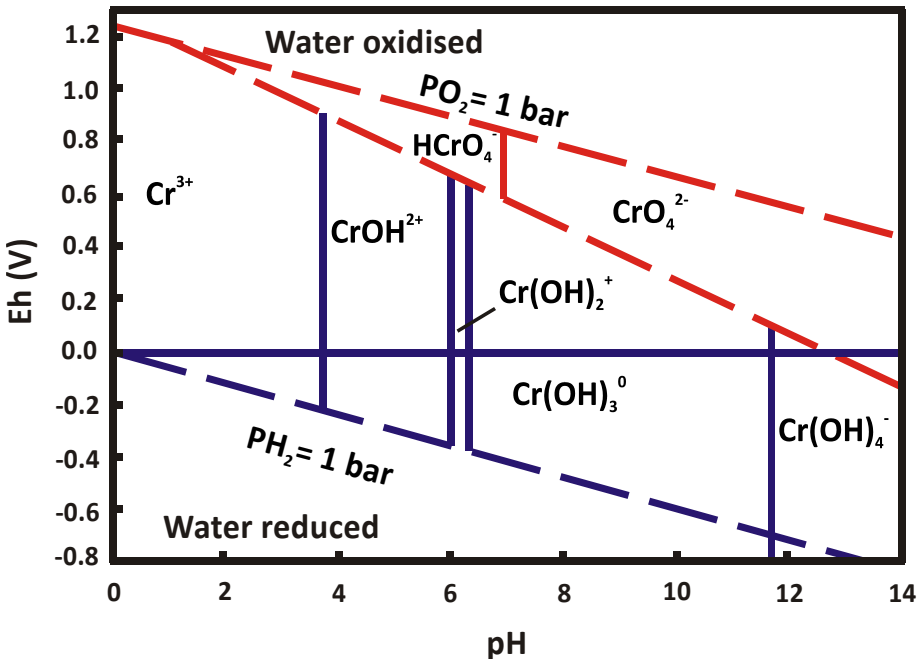

Figure 2.1 Eh-pH diagram for aqueous chromium species, red boarder = Cr(VI) species, blue boarder = Cr(III) species. Redrawn from Mohan and Pittman (2006)

Cr(III) species are found to be most stable at low pH values, or under reducing conditions. At pH values >3.5 the progressive hydrolysis of Cr(III) produces Cr(III)-hydroxyl species $CrOH^{2+}$, $Cr(OH)_2^{+}$, $Cr(OH)_3^{0}$ and $Cr(OH)_4^{-}$ (Mohan and Pittman, 2006; Rai et al., 1987). Although the hydrolysis of Cr(III) is very complex, under aqueous conditions with environmentally relevant pH's of between 6 and 12 it is considered highly insoluble and will readily precipitate as the amorphous Cr(III) hydroxide, $Cr(OH)_3^{0}$ (Spiccia, 1988). Despite this, the solubility of Cr(III) increases slightly at pH values greater than 8 (as $Cr(OH)_3$), and significantly below pH 5.5 (Lide, 1995). Chromium in aqueous systems is therefore predominantly present as Cr(VI), and exists as either bichromate ($HCrO_4^{-}$) or chromate (CrO_4^{2-}), formed from the acid dissociation of chromic acid ($H_2CrO_4^{0}$) *(Eqn. 3 - 4)* (Palmer and Wittbrodt, 1991). At chromium concentrations above 1 $g.l^{-1}$, this may further become polymerised to form dichromate *(Eqn. 5)* ($Cr_2O_7^{2-}$) (Mohan and Pittman, 2006).

$$H_2CrO_4^{0} \leftrightarrow H^{+} + HCrO_4^{-} \qquad (3)$$

$$HCrO_4^{-} \leftrightarrow H^{+} + CrO_4^{2-} \qquad (4)$$

$$HCrO_4^{-} + HCrO_4^{-} \leftrightarrow Cr_2O_7^{2-} \qquad (5)$$

The prevailing form of Cr(VI) within solutions is therefore further governed by its concentration (Figure 2.2). Bichromate is considered to be the stable Cr(VI) species at pH values 1-6 and at concentrations less that 1 $g.l^{-1}$, with dichromate formation beginning at concentrations above 1 $g.l^{-1}$. Solutions with pH values >6.5 are shown to have an affinity to Cr(VI) in the chromate form. (Richard and Bourg, 1991; Tokala et al., 2008).

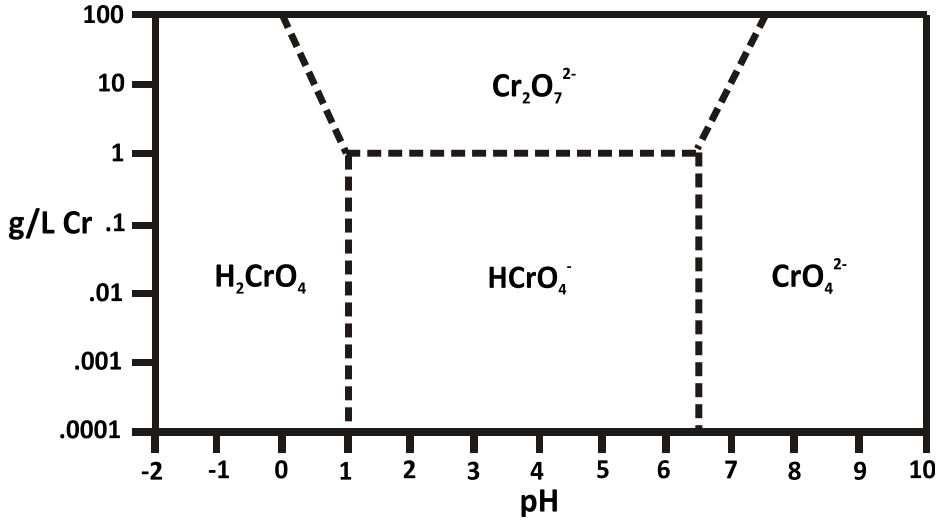

Figure 2.2 Effect of concentration and pH on Cr(VI) speciation, redrawn from Mohan and Pittman (2006)

In practice, chromium speciation and subsequent mobility, bioavailability and toxicity in sub-surface aqueous-sediment systems does not behave ideally, and is influenced by a number of environmental factors (Table 2.1). For example, although Cr(III) is considered immobile in the pH range 6-12, primarily existing as insoluble $Cr(OH)_3$, the formation of several organic and inorganic complexes has been shown to increase its solubility (Geelhoed et al., 2002). It is therefore important to consider these influences when investigating the potentially hazardous migration of Cr(VI), sourced from desorption of sorbed Cr(VI), oxidation of Cr(III), and dissolution of Cr(VI)-containing solid phases (Martello et al., 2007).

Table 2.1 Factors affecting chromium speciation and subsequent mobility in sediment-water systems (taken from Andrews et al., (2004) and Krauskopf and Bird (1995))

Factor	Influence
AVS (acid volatile sulphide)	Cr(VI) is rapidly reduced to Cr(III) in the presence of AVS.
Fe(II)	Similar to AVS, Fe(II) is an important reducing agent mediating the transformation of Cr(VI) to Cr(III).
Mn(III,IV) (hydr)oxides	Mn-oxides are widely known as strong metal sorbents, scavengers, and oxidizers. Mn-oxides have been shown to oxidize Cr(III) to Cr(VI) under laboratory conditions.
Dissolved Oxygen (DO)	Reducing agents for chromium (AVS and Fe(II)) are typically abundant in anaerobic sediments (i.e., in the absence of DO). DO can vary with temperature and season.
Eh	Eh affects the dissolution or precipitation of various metals. Cr(III) is stable, even under oxidizing conditions, whereas Cr(VI) is unstable under reducing or even mildly oxidizing conditions.
Total Organic Carbon (TOC)	Metals can form complexes with organic material; therefore, metals will be less bioavailable at higher concentrations of TOC. Organic ligands also can serve as reducing agents for chromium transformation, although the reduction kinetics are slower than for AVS or Fe(II).
Dissolved organic carbon (DOC)	Chromium has been shown to form complexes with dissolved organic carbon, which may increase the apparent solubility of Cr(III) but likewise decreases its bioavailability and oxidation potential.
pH	Cr(III) solubility increases at low pH; such low pH levels occur in acidic soils but are rarely encountered in sediments. Chromium speciation is affected by both Eh and pH, such that Cr(VI) is stable under moderately oxidizing conditions at high pH.
Grain size	Grain size can affect metal bioavailability both directly and as it is correlated with TOC. Generally, increased fines content is associated with decreased bioavailability.

2.4.2 Sorption

Sorption is defined as the accumulation of ions, complexes or molecules to a mineral surface or structure. This occurs as two main phenomena; adsorption (sorption of aqueous species to a surface, without the formation of three-dimensional molecular arrangement), and absorption (incorporation into a mineral structure, e.g. ion exchange mediated Cr(VI) hosting in COPR) (Appelo and Postma, 2005). Surface precipitation is another form of sorption, where insoluble precipitates form on the surface of solid phases, often as a result of chemical transformations. The adsorption of trace metals in solution occurs on the charge surfaces of solid oxides and organic matter, and varies dependent on the pH of a system (Richard and Bourg, 1991). Cr(III) sorption is typical of cationic species with adsorption increasing with pH, but decreasing with competing cations. In contrast, Cr(VI) exhibits typical anionic sorption behaviour with adsorption decreasing with increasing pH and in the presence of competing anions (Wielinga et al., 2001). As a result Cr(VI) is weakly retained by solids in soils at circumneutral to alkaline pH values, largely accounting for the high mobility of Cr(VI) within sediment-water systems (Schmieman et al., 1998). Cr(III) however exhibits strong affinity to negatively charged surfaces such as hydroxyl and carboxyl groups on sediment minerals and solid phase organic ligands and is strongly retained in the solid phase**.** The extent of chromium adsorption is therefore controlled by the concentration of clay minerals and inorganic carbon, as well as the pH value and cation exchange capacity of a system (Loyaux-Lawniczak et al., 2001; Pagilla and Canter, 1999; Raghu and Hsieh, 1989). Studies have demonstrated the preferential precipitation of Cr(III) hydroxides on clay grains (<2μm), highlighting its importance as a contributor to the immobilisation of Cr(III) within sediments (Loyaux-Lawniczak et al., 2001; Stewart et al., 2003). It is also

suggested that this retention could be a result of Cr(III) binding to iron oxides, found in naturally high concentrations within the fine sediment fraction (Onyancha et al., 2008).

Biosorption is another important sorption process in subsurface environments where metal cations are sequested by natural organic compounds, both living and dead, on the functional groups of the biopolymers (Han et al., 2007; Onyancha et al., 2008). For Cr(III), this adsorption primarily occurs on the carboxylate ($-COO^-$) and hydroxide ($-OH^-$) groups, with amino groups (NH_2) believed to be important sites of Cr(VI) affinity (Han et al., 2006; Han et al., 2007, 2008; Onyancha et al., 2008). The capacity of microalgal isolates such as *Spirogyra condensate*, *Rhizoclonium hieroglyphicum* and *Chlorella miniata* to immobilise Cr(III) through complexation with cell carboxyl groups has been reported (Han et al., 2007, 2008). Notably in the case of *Chlorella miniata* Cr(III) in its hydroxide form appears to more readily complex directly to the cell surface. Biosorption onto algal biomass also has the ability to indirectly sequest Cr(VI). This occurs through the initial biosorption (onto amino groups), followed by bioreduction to Cr(III) and subsequent biosorption onto oxidised biomass *(Eqn. 6)* (Han et al., 2008).

$$HCrO_4^- + H^+ + biomass \leftrightarrow HCrO_4^- - H^+ - biomass \rightarrow Cr^{3+} + H_2O + biomass\ (oxidised) \quad (6)$$

Cr(III) is also able to adsorb directly to the surface of humic acids through ion exchange, binding with electronegative carboxyl groups formed during their dissociation *(Eqn. 7)* (Li et al., 2008). The dissociation of humic acid also releases

electrons that can facilitate the bioreduction of Cr(VI) to Cr(III) *(Eqn. 8)* (Han et al., 2007; Onyancha et al., 2008)

$$3R\text{–}COOH + Cr^{3+} \rightarrow (R\text{–}COO)3Cr + 3H^{+} \quad (7)$$

$$2H^{+} + R\text{–}OH + CrO_4^{2-} \rightarrow ROCrO_3H + H_2O \quad (8)$$

Aqueous Cr(III) and Cr(VI) biosorption by both microalgal isolates and humic acids has been shown to be most efficient at low pH values, and at low concentrations of competing metal ions (Erdem et al., 2004; Farmer et al., 1999). As discussed, Cr(III) is less soluble, more easily retained through sorption mechanisms, and has a lower affinity to remobilisation through ion exchange than Cr(VI). This, along with the much lower health risks associated with Cr(III) means that the reduction of Cr(VI) to Cr(III) is often the aim of remediation strategies (Pagilla and Canter, 1999; Schroeder and Lee, 1975). The reduction of Cr(VI) within sediment-water systems is predominantly governed by redox pathways with both organic and inorganic species (Housecroft and Sharpe, 2005).

2.4.3 Redox interactions

Redox reactions in metals release energy as electrons flow from one substance to another in an effort to reach chemical equilibrium (USEPA, 2005b). In doing so one species will be reduced, gaining electrons, and the other oxidised, losing electrons (Hazen and Tabak, 2005). Thus, the valence state of a metal species is dependent on its ability to lose or gain electrons within the environment, termed its “redox potential”.

Cr(VI) is thermodynamically unstable in anoxic sediment-water systems (Katz and Salem, 1994; Palmer and Wittbrodt, 1991). This instability is a result of its strongly oxidising nature allowing it to be readily reduced in the presence of naturally occurring reductants (Lin, 2002). In contrast, Cr(III) is considered much more thermodynamically stable due to its resistance to oxidation by to O_2. Under anoxic conditions, the presence of high concentrations of manganese oxides can catalyse the oxidation of Cr(III) to Cr(VI) through direct sorption onto the active sites of the oxide (Schroeder and Lee, 1975). However, in natural environments competition from other metal cations was found to significantly inhibit this reaction. Natural aqueous systems are therefore predominantly reductive environments for Cr(VI) under normal conditions, due to the presence of natural reductants and the slow oxidation kinetics of Cr(III) (Deakin et al., 2001; Lin, 2002). Although there are a number of potential chemical reductants of Cr(VI), rate expressions indicate that ferrous iron (Fe(II)) and reduced sulphur species will be the dominant reducers in natural subsurface aqueous environments (Palmer and Wittbrodt, 1991). This reduction can be expressed by the reactions below *(Eqn. 9 - 10)* (Buerge and Hug, 1997).

$$3Fe(OH)_2 + Cr(VI) \rightarrow 3Fe(OH)^{2+} + Cr(III) \quad (9)$$

$$4HSO_3^- + 2Cr(VI) + 6H^+ \rightarrow 2Cr(III) + 2SO_4^{2-} + S_2O_6^{2-} + 6H_2O \quad (10)$$

Model studies of natural waters by Lin (2002) found that the primary reductant of Cr(VI) is dependent on pH, with low values (<5) favouring sulphite (S(IV)), and high values (>6) favouring ferrous iron (Fe(II)). It has also been found that reduction

becomes increasingly more difficult as the pH of a system increases (Wielinga et al., 2001). The rate of Cr(VI) reduction by Fe(II) is shown by Erdem and Tumen (2004b) to follow first-order reaction kinetics, with faster removal observed with lower initial Cr(VI) concentration. The practical application of these redox pathways has been used to produce Cr(III) bearing species with ferrous sulphate and sodium sulphite as reductants *(Eqn. 11 - 12)*. The pH was also lowered during these reactions using sulphuric acid to increase the solubility of the reagents (Erdem and Tumen, 2004a).

$$K_2Cr(VI)_2O_7 + 6Fe(II)SO_4 + 7H_2SO_4 \rightarrow Cr(III)_2(SO_4)_3 + 3Fe(III)_2(SO_4)_3 + 7H_2O + K_2SO_4 \quad (11)$$

$$K_2Cr(VI)_2O_7 + 3Na_2S(IV)O_3 + 4H_2SO_4 \rightarrow Cr(III)_2(SO_4)_3 + 3Na_2S(VI)O_4 + K_2SO_4 + 4H_2O \quad (12)$$

Where aqueous Cr(VI) is reduced by Fe(II), the resulting Cr(III) species can become both incorporated into the Fe(III) crystal structure as Cr(III)-substituted iron oxides, and precipitated on the surface as Cr(III)-hydroxide due to its lower solubility. Using Fe(II) as a reductant has been applied successfully in the remediation of a variety of Cr(VI) contaminated environments, including municipal landfill leachate. Here the ability of microorganisms to re-reduce Fe(III) produced during its abiotic reaction with Cr(VI) was also observed (Li et al., 2009). This highlights the importance of biogeochemical processes occurring within the subsurface, as the indigenous microbial population may directly or indirectly influence the transformation of contaminants.

2.5 Soil microorganisms

Prokaryote microorganisms have evolved over 3.8 billion years to survive in every ecological niche on the planet. In soils the diversity of indigenous microorganisms is

huge, and is estimated to exceed that of vegetation by several orders of magnitude (Torsvik et al., 2002). The existence of these vast populations is crucial to maintaining all life as they are the primary driving force behind every biogeochemical cycle on earth. As a result of such a long period of evolution, many microorganisms display adaptations that allow them to thrive in extreme environments where no other forms of life could survive. Such microorganisms are broadly termed *extremophiles.* These include environments with natural extremes of temperature (e.g. hydrothermal vents), pH (e.g. soda lakes), and pressure (e.g. deep sea sediments). Microorganisms adapted to survive such conditions are deemed *thermophiles*, *alkaliphiles*, and *piezophiles* respectively. In more recent times, these natural adaptations have also allowed microorganisms to populate areas of anthropogenic pollution where extremes of pH, heavy metal contamination, radiation, and temperature exist. Indeed, some of these adaptations may prove useful in developing methods to remediate polluted environments, due to the ability of many microorganisms to influence their surrounding as a mechanism of survival. Sites of COPR characteristically portray both high pH and Cr(VI) metal toxicity, and therefore provide significantly challenging environments to microbial metabolism.

2.6 Alkaliphiles

A broad range of microbial taxa can grow optimally and robustly in high pH environments like those found at COPR disposal sites, or natural soda lakes (Pollock et al., 2007; Roadcap et al., 2006; Stewart et al., 2007; Wani et al., 2006). These microbes have evolved adaptations to this challenging environment and consist of two main groups, alkaliphiles and haloalkaliphiles. True alkaliphiles are reported to require a pH $\geq$ 9 to grow with an optimal growth pH of between 9 and 10. Haloalkaliphiles require similar pH conditions but also high salt concentrations of up

to 33% NaCl (w/v) (Horikoshi, 2004). Alkaliphiles are found in both aerobic and anaerobic environments, and display a variety of physiological features that set them apart from microorganisms adapted to live in circumneutral pH environments. Although alkaliphiles commonly have optimal growth pH values of between 9 and 10, the optimal pH of intracellular enzymes critical for microbial metabolism is often lower. As a result, many alkaliphiles have adapted mechanisms to regulate cytoplasmic pH in order to keep them as close as possible to the optimal functional values of internal enzymes. This can produce a difference of several pH units between the cytoplasmic and external pH values. These pH gradients have been observed in numerous alkaliphiles and haloalkaliphies including *Bacillus halodurans* where intracellular values were measured at up to 2 pH units lower than the surrounding medium (Horikoshi, 1999; Muntyan et al., 2005)

In order to maintain this pH homeostasis, it has been suggested that many alkaliphiles utilise the Na^+/H^+ and K^+/H^+ antiporter systems across plasma membranes. These are traditionally are used to establish an electrochemical gradient during respiration. Cells utilising the Na^+ antiporter can respond to chances in external pH by exchanging Na^+ ions from within the cell with external H^+ ions across its plasma membranes, effectively increasing acidity within the cell (Horikoshi, 1999; Krulwich et al., 1997). This is also thought to result in an increase in solute uptake and motility (Detkova and Pusheva, 2006; Horikoshi, 1999; Krulwich et al., 2001). In effect this ability increases the cytoplasmic buffering capacity within the cells, and explains why the majority of alkaliphiles require environments containing NaCl for growth. Adaptations to cell external walls also have been found to provide additional passive protection to microorganisms in high pH environments. Acidic

cell wall macro molecules produced via fermentation are believed to create a partial barrier to certain ion flux (Krulwich and Guffanti, 1989; Krulwich et al., 1997). In the case of the alkaliphile *Bacillus* sp. these acidic polymers, phosphoric, galacturonic, glutamic and aspartic acid, are believed help make the surface of the cell negatively charged (Aono et al., 1997). This in turn helps repel negatively charged hydroxide ions, as well as aiding in the uptake of Na^+ ions essential for the maintenance of internal pH homeostasis (Horikoshi, 1999). Alkaliphiles are also able to influence the pH of their surroundings through the production of organic acids such as acetic acids, as observed in various alkaliphilic *Bacillus* species when grown on carbohydrates (Paavilainen et al., 1994). This reduces the pH of the environment immediately adjacent to the microorganism and will aid in solute uptake and motility.

In addition to these pH regulatory mechanisms, a wide range of enzymes within alkaliphiles have been found to be specifically adapted to function optimally at a higher pH. The first alkaliphilic enzyme was reported to be an alkali protease recovered from *Bacillus* bacterium in 1971 (Horikosh.K, 1971a). This was found to have an optimum operational pH of 11.5, and was able to function at 75% efficiency even at pH 13. Since then, many others have been isolated from alkaliphiles including further proteases, cellulases, lipases, pectinases, xylanases, catalase and starch degrading enzymes including amylases (Horikosh.K, 1971a, b, 1972; Kurono and Horikosh.K, 1973). These enzymes are of particular commercial interest due to their potential applications within biotechnology (Horikoshi, 1999).

2.7 Microbial metal reduction

Soil microorganisms obtain energy for growth through the respiration of organic molecules present in the soil. This energy is released when organic matter is oxidised and coupled to the reduction of a terminal electron accepting species. Oxygen is the primary terminal electron accepting species as its reduction coupled to the oxidation of an organic compound releases the most amount of energy during metabolism. In subsurface environments where sufficient organic matter is available for oxidation, progressively more anoxic conditions develop as oxygen is consumed. This produces a cascade of terminal-electron-accepting processes (TEAPs) occurring in sequence as microorganisms utilise other oxidised species present (Froelich et al., 1979). Reactions releasing most energy are favoured, so the sequence in which electron acceptors are used typically follows the decreasing order of redox potentials shown in Table 2.2.

The ability of indigenous soil microorganisms to couple simple organic matter oxidation to the reduction of heavy metals such as iron, manganese, selenium, chromium, and the radionuclide uranium, during metabolism, is no longer a new concept (Burke et al., 2005). Numerous bacteria have now been identified which are able to gain energy from the transfer of electrons from an organic compound to metal species where the ultimate electron acceptor, oxygen, is absent. In anaerobic environments the reduced metal formed during this process often displays more favourable properties compared to that of its oxidised form, for example Cr(III) compared with Cr(VI). Reduced species are formed as electrons are “dumped” to it following use in the respiratory electron transport train. Thus, the utilisation of this process can be advantageous at sites of heavy metal and radionuclide contamination.

Table 2.2 Microbially significant half-reaction reduction potentials: Standard Reduction Potential, E^0, and redox potential, Eh, at pH 7 and 10.5 (at 25°C and atmospheric pressure)

Transformation	Reaction	E_0 (V)	Eh @ pH 7 (V)	Eh @ pH 10.5 (V)	Assumptions
O_2 Depletion[+]	$O_2 + 4H^+ + 4e^- = 2H_20$	1.23	0.805	0.598	P_{O2} = 0.2 bar
Denitrification[+]	$NO_3^- + 6H^+ + 5e^- = 1/2N_2 + 3H_2O$	1.24	0.713	0.464	$[NO_3^-]$ = 1 mmol L^{-1} P_{N2} = 0.8 bar
Cr reduction[*] Cr(VI) to Cr(III)	$CrO_4^{2-} + 5H^+ + 3e^- = Cr(OH)_3 + H_2O$	1.198	0.508	0.163	$[CrO_4^{2-}]$=250 μM
Mn reduction [+] Mn(III) to Mn(II)	$Mn_3O_4 + 2H^+ + 2H_2O + 2e^- = 3Mn(OH)_2$	0.480	0.066	-0.140	-
Fe reduction[*] Fe(III) to Fe(II)	$Fe(OH)_3 + H^+ + e^- = Fe(OH)_2 + H_2O$	0.257	-0.157	-0.364	-
Fe reduction[+] Fe(III) to Fe(II)	$Fe(OH)_3 + HCO_3^- + 2H^+ + e^- = FeCO_3 + 3H_2O$	1.078	-	-0.266 -0.321	$[HCO_3^-]$ = 20 mmol L^{-1} $[HCO_3^-]$ = 1 mmol L^{-1}
Sulfate reduction[+] S(VI) to S(-II)	$SO_4^{2-} + 10H^+ + 8e^- = H_2S + 4H_2O$	0.301	-0.217	-0.476	$[SO_4^{2-}] = [H_2S]$
Bicarbonate reduction to acetate[×] C(VI) to C(0)	$2HCO_3^- + 9H^+ + 8e^- = CH_3COO^- + 4H_2O$	0.187	-0.292	-0.525	$[HCO_3^-] = [CH_3COO^-]$ = 20 mmol L^{-1}

[+] after Langmuir (1997)
[*] calculated using thermodynamic data from Stumm and Morgan (1996)
[×] calculated using thermodynamic data from Thauer (1977)

Numerous studies have demonstrated the potential for the biostimulation of microbial metal reducing populations within contaminated systems, through the addition of different electron donors including acetate, glucose, yeast extract, lactate, and H_2 (Higgins et al., 1998; Lovley, 1993b; McLean et al., 2006; NABIR, 2003; Stucki et al., 2007; Vrionis et al., 2005). The practical *in-situ* application of such a process for site remediation is known as bioremediation, and is increasingly being favoured over traditional, more environmentally and financially costly remediation strategies (NABIR, 2003). According to Torsvik et al. (2002) only a fraction of the total diversity of soil bacteria has so far been characterised (about 4500 species). As a result, the potential for utilising microbial processes in remediation strategies in the future is likely to continue to grow.

2.8 Microbial iron reduction

The ability of soil microorganisms to reduce metals, specifically iron, has been known since the 19th century. However, it wasn't until 1987 that this ability was first attributed to the action of a specific microorganism, *Geobacter metallireducens* (Lovley et al., 1987). Since then the ability to reduce iron has been described in numerous microbial taxa from a broad range of environments including some iron reducing alkaliphiles isolated from natural high pH environments, such as *Bacillus sp*. *Alkaliphilius peptidofermentans* and *Geoalkalibacter ferrihydriticus* (Pollock et al., 2007; Zavarzina et al., 2006; Zhilina et al., 2009). As iron is the most abundant redox-active metal in soils, the establishment of microbial Fe(III) reducing conditions has been described as the most important to develop during the development of anaerobic soils due to its influence on trace metal behaviour (Lovley, 1991, 1997; Pollock et al., 2007; Zavarzina et al., 2006).

Alkaliphilius peptidofermentans and *geoalkalibacter ferrihydriticus* are two high pH iron reduces, isolated from an alkaline soda lake environment, capable of using amorphous Fe(III) hydroxides as electron acceptors during growth (Zavarzina et al., 2006; Zhilina et al., 2009). The biomineral formed as a result of microbial iron reduction is dependent on the metabolic pathway utilised and growth conditions. The obligate anaerobic alkaliphile *geoalkalibacter ferrihydriticus* has been reported to produce siderite (ferrous carbonate) or magnetite dependent on concentration of amorphous Fe(III) hydroxide available (Fredrickson et al., 1998). Other biominerisation products of amorphous Fe(III) hydroxide reduction include vivianite and green rust type compounds. These were found to be produced along with magnetite and siderite when *schewanella putrefaciens* was incubated under a variety of conditions (Ona-Nguema et al., 2000). The stability of the iron phase existing in soil systems have been reported to be governed by pH, rate, and type of microbial Fe(II)/Fe(III) cycling occurring *in-situ.* Metastable iron oxyhydroxides such as ferrihydrite ($Fe_5HO_8 \cdot 4H_2O$) (Hansel et al., 2005) are considered important sinks for metals due to their reactive nature, high surface area, and high bioavailability (Cudennec and Lecerf, 2006; Schwertmann et al., 1999). This amorphous, poorly crystalline phase is often the first product of Fe(III) precipitation and over time has been reported to transform into more thermodynamically stable phases such as hematite at circumneutral pH, and goethite at low and high (10-14) pH (Liu et al., 2007). Fe(II) adsorbed to ferrihydrite was also found to increase the rate of its transformation, as well as to lead to the production of lepidocrocite (γ-FeOOH) at low pH values (Chistyakova et al., 2007; Zhilina et al., 2009).

Iron phase formation and stability is further complicated where intermediate iron phases such as lepidocrocite are subsequently involved in bioreduction. This produces different products dependent on reduction rate. For *schewanella putrefaciens* a high rate of lepidocrocite reduction results in the formation of magnetite, whereas slower rates yield hydroxycarbonate green rusts ($[Fe_2^{II}Fe_2^{III}(OH)_8]^{2+}\cdot[CO_3^{2-}]^{2-}$) (Ona-Nguema et al., 2002). Green rust compounds are metastable in environmental mixtures that contain lepidocrocite and magnetite as they exist in equilibrium with Fe^{2+} ions. Thus, the adsorption of Fe(II) onto lepidocrocite during its bioreduction induces dissolution of green rust to magnetite (Chistyakova et al., 2007). Iron biominerals are also altered in the presence of metal ions able to fill vacancies on the mineral structure, such as Magnesoferrite ($MgFe_2O_4$) formed from Mg addition into magnetite during the stationary phase of microbial incubation (Stucki et al., 2007). An increase in the Fe(II):Fe(III) ratio of aluminosilicate clay minerals has been reported as a result of Fe(III) bioreduction. This suggests the Fe(III) content of such minerals can also be utilised as an electron sink during microbial metabolism (Lovley, 1993b, 1997; Lovley et al., 2004; Tebo and Obraztsova, 1998)

2.9 Microbial chromium reduction

Microbial reduction of Cr(VI) was first observed with *Pseudomonas dechromaticans* in 1977 by Romanenko and Koren’kov. Since then, Cr(VI) reduction has been reported for a number of other gram negative genera including *Desulfovibro* and *Shewanella,* and members of the gram positive *Bacillus* and *Cellulomonas* genera (Table 2.3) (Francis et al., 2000; Lovley, 1993a; Romanenko and Koren'kov, 1977; Sani et al., 2002; Sau et al., 2008). Microbial reduction of Cr(VI) results in the

subsequent precipitation of insoluble Cr(III) hydroxides at neutral pH, and can generally be described by the reaction below *(Eqn. 13)*, and (Chen and Hao, 1998).

$$CrO_4^{2-} + H^+ + 3^{e-} \rightarrow Cr^{3+} + 4H_2O \rightarrow Cr(OH)_{3(s)} + 3H^+ + H_2O \quad (13)$$

Microbial Cr(VI) reduction has been attributed to both the reaction of Cr(VI) with chromium reductase enzymes, and through its use as the sole electron acceptor during microbial respiration within mitochondrial membranes (Chen and Hao, 1998). Enzymatic reduction of Cr(VI) is a complex process and occurs both in cell cytoplasmic membranes and the soluble fraction depending on mechanism and species present (Chen and Hao, 1998; Laxman and More, 2002). Intracellular Cr(VI) reduction in the soluble fraction of the cell is attributed to enzymatic reaction with soluble proteins, and has been observed in many Cr(VI) reducing microorganisms e.g. *Desulfovibrio vulgaris* and *Pseudomonas putida* (Daulton et al., 2007; Ishibashi et al., 1990; Lovley et al., 1993). Other cases of enzymatic Cr(VI) reduction have been found to be associated with membrane bound Cr(VI) reductases e.g. *Pseudomonas fluorescens* and *Enterobacter cloacae* (Bopp and Ehrlich, 1988; Wang et al., 1989).

Table 2.3 Summary of Cr(VI) reducing microorganisms (developed from Chen and Hao (1998))

Organism	Confirmed carbon source	Reduction conditions	Reference
Shewanella putrefaciens	Lactate	Anaerobic	(Liu et al., 2002)
Halomonas sp.	Acetate	Anaerobic	(VanEngelen et al., 2008)
Microbacterium sp. MP30	Acetate	Anaerobic	(Pattanapipitpaisal et al., 2001)
Leucobacter sp. CRB1	Yeast extract, glucose or lactate	Aerobic	(Zhu et al., 2008)
Pseudomonas stutzeri CMG462	Acetate	Anaerobic	(Badar et al., 2000)
Pseudomonas stutzeri CMG463	Acetate	Anaerobic	(Badar et al., 2000)
Pseudomonas synxantha K2	Acetate	Anaerobic	(Badar et al., 2000)
Pseudomonas aeruginosa	Acetate or glucose	Anaerobic	(Cervantes and Ohtake, 1988)
Pseudomonas dechromaticans	Peptone or glucose	Anaerobic	(Romanenko and Koren'kov, 1977)
Pseudomonas chromatophila	Ribose, fructose, fumarate, lactate, acetate, succinate, butyrate, glycerol, or ethylene glycol.	Anaerobic	(Lebedeva and Lyalikova, 1979)
Pseudomonas ambigua G-1	Nutrient broth	Aerobic	(Suzuki et al., 1992)
Pseudomonas fluorescens LB 300	Glucose, NAD(P)H or citrate	Aerobic	(Bopp and Ehrlich, 1988; Deleo and Ehrlich, 1994)
Pseudomonas putida PRS 2000	NAD(P)H	Aerobic	(Ishibashi et al., 1990)
Achromobacter eurydice	Acetate or glucose	Aerobic	(Lovley, 1995)
Aeromonas dechromatica	Galactose, mannose, melibiose, sucrose, fructose, lactose, cellobiose, arabinose, mannitol dulcitol, sorbitol, or glycerol	Anaerobic	(Kvasnikov et al., 1985)
Agrobacterium radiobacter	Glucose, fructose, maltose, lactose, mannitol or glycerol	Aerobic and Anaerobic	(Llovera et al., 1993)
Bacillus sp.	NAD(P)H, citrate, acetate	Aerobic	(Desai et al., 2008; Rehman et al., 2008)
Bacillus subtilis	Glucose or acetate	Anaerobic	(Mangaiyarkarasi et al., 2011)
Desulfovibrio vulgaris	Hydrogen, citrate	Anaerobic	(Mabbett et al., 2002)
Enterobacter cloacae	Acetate, glycerol or glucose	Anaerobic	(Wang et al., 1989)
Escherichia coli	Acetate	Anaerobic	(Wang, 2000)
Escherichia coli ATCC 33456	Glucose, acetate or propionate	Aerobic and anaerobic	(Shen and Wang, 1993)
Micrococcus roseus	Acetate or glucose	Anaerobic	(Gvozdyak et al., 1986)
Pantoea agglomerans	Acetate, hydrogen or lactate	Anaerobic	(Francis et al., 2000)
Desulfotomaculum reducens	Lactate	Anaerobic	(Tebo and Obraztsova, 1998)
Pannonibacter phragmitetus	Yeast extract and acetate	Aerobic	(Chai et al., 2009)
Streptomyces griseus	Glucose and yeast extract	Anaerobic	(Laxman and More, 2002)
Cellulomonas flavigena	Lactate	Anaerobic. Nongrowth.	(Sani et al., 2002)

Direct microbial reduction of Cr(VI) has been observed during aerobic (Ishibashi et al., 1990) and anaerobic respiration (Daulton et al., 2007; Suzuki et al., 1992). Only a few studies have clearly demonstrated anaerobic growth dependent on the use of Cr(VI) as the sole electron acceptor, although it is suggested for a number of organisms including *Desulfotomaculum reducens* and *Pantoea agglomerans* (Francis et al., 2000; Tebo and Obraztsova, 1998). Anaerobic enzymatic Cr(VI) reduction has been found associated with both membrane bound or soluble internal Cr(VI) reductases (Cervantes et al., 2001) as Cr(VI) is readily able to cross cell membranes by utilising the sulphate transport system (Daulton et al., 2007). Cr(VI) reduction has also been observed in the growth phase by fermentation in *Cellulomonas sp,* where it is hypothesised that Cr(VI) acts as an external electron dump, receiving electrons outside of the cell via metabolite shuttles (such as cytochromes, and glucose) (Chai et al., 2009; VanEngelen et al., 2008; Zhu et al., 2008). Even fewer studies have demonstrated direct microbial Cr(VI) reduction at high pH although this ability has been reported for *Pannonibacter phragmitetus, leucobacter sp* (aerobic), and *halomonas maura* (anaerobic) at pH 9.8, 11.0 and 9.0 respectively (Chai et al., 2009; VanEngelen et al., 2008; Zhu et al., 2008). It is therefore suggested that microbially mediated Cr(VI) reduction in alkaline, chromium contaminated environments will usually occur by an indirect pathway involving extracellular reaction with reduced species, e.g. Fe(II) produced by microbial respiration (Lloyd et al., 1998). This iron promoted reduction of Cr(VI) via a coupled biotic-abiotic mechanism has been demonstrated in laboratory experiments for the dissimilatory iron reducer *Shewenella* sp under anaerobic conditions (Wielinga et al., 2001).

2.9.1 Cr(VI) resistance mechanisms

The toxicity of heavy metals provides further challenges for microbial taxa. Cr(VI) is particularly hazardous to microorganisms as it is readily able to cross cell membranes by utilising the sulphate transport system. Environments with an influx of Cr(VI), such as those surrounding sites of COPR, therefore put significant stress on microbial metabolism as a build-up of Cr(VI) would ultimately destroy the cell (Cervantes et al., 2001; Daulton et al., 2007). Cr(VI) is also known to cause direct oxidative DNA degradation via the production of hydroxyl free radicals (Bagchi et al., 1997; Cavallo et al., 2008). As a result, bacterial tolerance to Cr(VI) may indicate an evolutionary response to Cr(VI) toxicity. Indeed many microorganisms have demonstrated tolerance to Cr(VI) including *Pannonibacter phragmitetus*, which showed no evidence of cell degradation at 500 $mg.l^{-1}$ Cr(VI), and *Leucobacter* sp which could tolerate up to 4,000 $mg.l^{-1}$ Cr(VI) (Chai et al., 2009; Chen and Hao, 1998; Rehman et al., 2008; Zhu et al., 2008).

One possible resistance mechanism to Cr(VI) toxicity expressed by several bacteria is their ability to either internally or externally reduce Cr(VI) to Cr(III). It has been suggested that the terminal microbial reduction step in internal Cr(VI) reduction is Cr(II), which is subsequently expelled from the cell and oxidises to Cr(III) on the cell surface (Chai et al., 2009; Chen and Hao, 1998; Rehman et al., 2008; Zhu et al., 2008). It is hypothesised that this, along with extracellular Cr(VI) reduction, may therefore provide physical barrier to further Cr(VI) toxicity by forming a protective layer of insoluble Cr(III) hydroxides.

The combination of high Cr(VI) concentration and high pH commonly found at sites of COPR disposal therefore provide a testing environment for microbial metabolism. As a result, it is likely that adaptations to these extreme conditions exist within the indigenous microbial populations at COPR affected sites to enable successful metabolism.

2.10 Study site

Contamination at sites of COPR disposal provide a challenging environment for successful remediation due to the environmental mobility of Cr(VI) contained in high pH leachates, and the dangers associated with the disturbance of the waste itself. The focus of this research project was the impact that one such COPR disposal site, located in the north of England, is having on the adjacent environment. The total area of the site, known locally as "old tip" is approximately 2.2 hectares in size, and is made up of two landforms situated within a glacial valley between a canal to its northern boundary and river to its south-western edge (Figure 2.3). The canal itself is approximately 7 metres above the level of the river, with landform 1 approximately 1.5 meters above the level of the canal towpath at its highest point. A drainage ditch runs along the southern edge of the site, flowing east to west parallel to the railway viaduct, and feeds directly into the river (Stewart et al., 2010; Whittleston et al., 2007). Vegetation on site is dominated by grasses and sparse small trees, with erosion as a result of recreational activity leaving several steeper areas of the waste bare and exposed. Some of these areas have subsequently been fenced off.

As the site is located in an urban area publicity of its existence could have harmful socioeconomic impacts. As a result, it was requested by those now responsible for site maintenance that its precise location remains confidential.

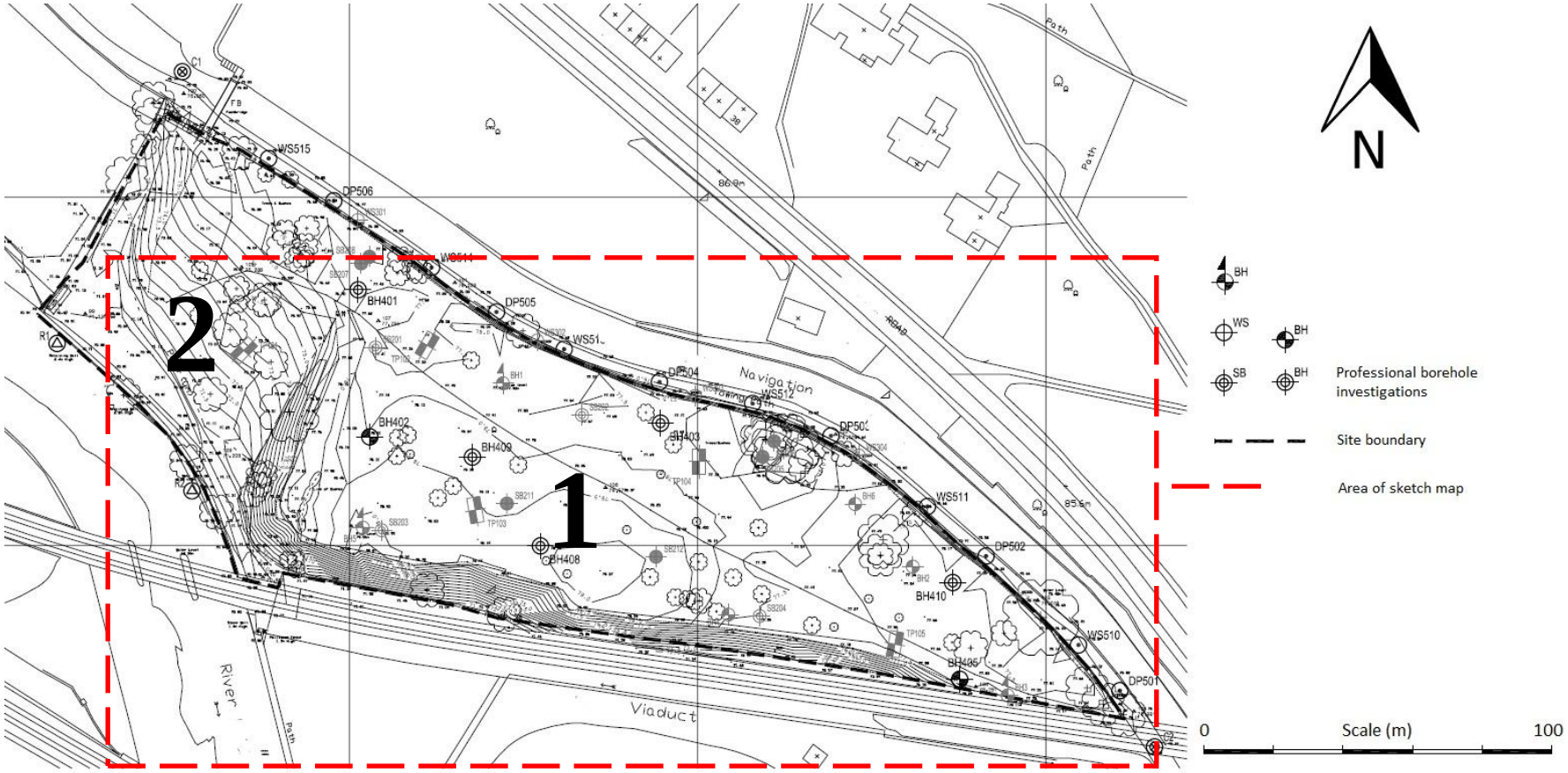

Figure 2.3 Professional plan of the "old tip" showing the location of two distinct landforms, and boreholes produced during professional site investigations (From WYG report 2005, edited to remove proprietary information)

2.10.1 Site history

Landform 1 (Figure 2.3) first appeared on historical OS maps in the late 19th century (see Appendix B.1). It is plausible that the waste may have been tipped here as a way of supporting the canal bank, and/or transported by barge to this location from nearby industrial works. Indeed, the appearance of a dye works roughly half a kilometre to the south east during the same period is interesting as chromium was widely used in the dying and leather tanning industries. Although it cannot be said with any confidence that this dye-works is responsible for the source of the COPR, it is a good indication that industries existed within the area that would have required chromium. Therefore it would be reasonable to assume that chromium ore processing plants are likely to be located nearby. A second landform (Landform 2, Figure 2.3) approximately 0.3 hectares in size appears to the west of the COPR tip on historical OS maps by 1922 (see Figure B.2). Landform 1 has subsequently been identified during professional site investigations as made ground consisting of chromite ore processing residue, the extent of which is highlighted in yellow in Figure 2.4. In contrast, landform 2 is recorded in a professional report compiled in 2005 to consist of canal dredging's, and is not COPR material.

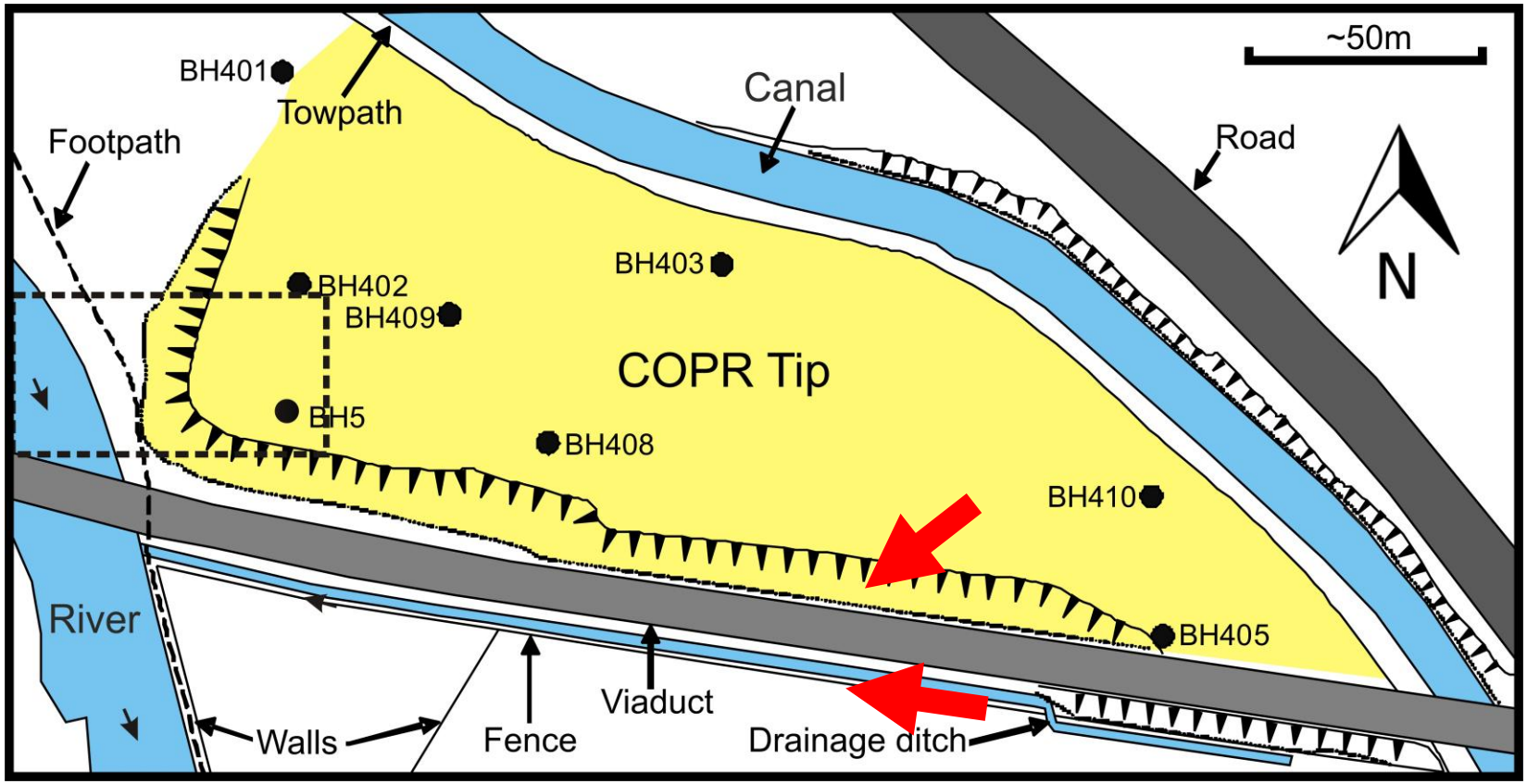

Figure 2.4 Sketch map showing the extent of the COPR material. Red arrows indicate the location and orientation of the photographs taken presented below. Dotted section highlights the area of recent geotechnical investigations in March 2009.

2.10.2 Site investigations

Since 1993 the site has been subject to a series of professional investigations including the production of numerous boreholes (see Figure 2.3). As well as these, ground investigations were conducted for the sole purpose of gathering material for this research project in March 2009, and focused on the south western edge of the COPR material (see Figure 2.4, dotted selection).

1. *Surface investigations*

A preliminary report at the site by the Environment Agency into the state of the drainage ditch in March 2000 found chromium concentrations of 24 $mg.l^{-1}$ and a pH value of 11.7. It concluded that the presence of this contaminated surface leachate meant the area could be determined a Special Site under Part IIA of the Environmental Protection Act 1990. To date no such official designation has been made, despite surface chromium contamination continuing to be clearly evident on site. The drainage ditch is visibly yellow in colour (Figure 2.5), with Cr(VI) concentrations measured over the course of this investigation to vary seasonally between 5 and 16 $mg.l^{-1}$ (100-300 µM), well above the 0.05 $mg.l^{-1}$ WHO guideline. Zana Tilt an MSc student from The University of Leeds demonstrated that the greatest source of Cr(VI) flux into this drainage ditch are adjacent surface seeps located at the base of the waste between the viaduct arches to the south of the site (Tilt, 2009). These surface seeps are also visibly contaminated with Cr(VI) (Figure 2.6). The pH value of the drainage ditch remains elevated, most notably downstream of the contaminated seeps, and ranges from pH 10.50 – 12.55.

This drainage ditch discharges directly into the river to the west of the site and could therefore potentially become a source of wider pollution. However, the rate of discharge from the drainage ditch is very small, and therefore once dispersed it is unlikely that Cr(VI) concentration and hyperalkalinity will pose significant danger to the aquatic ecosystem. In addition, the drainage ditch can easily be monitored, and has already been isolated from the public having recently been fenced off. In contrast, behaviour of Cr(VI) contaminated leachates that may be migrating away from the COPR within the subsurface is more difficult to assess.

2. Professional geotechnical investigations

Initial borehole logs from professional investigations describe much of the site to be covered in a layer of topsoil that varies in thickness between 0.5 and 2.1 meters. The COPR material itself is described as made ground, comprising of grey, bright green, yellow sandy silts, and was present beneath the thin topsoil layer to a maximum depth of approximately 10 meters below ground level. This in turn overlies a dark grey and brown silty clay layer that varies in thickness and composition. Professional reports postulate that these grey and brown clay layers encountered directly beneath the COPR represents the original topsoil layer that existed prior to the placement of the waste. Geological maps and borehole logs further indicate the entire site is underlain by alluvial material including gravels. Taken together, this information was used to construct a simplified geological cross section providing a preliminary assessment of the waste position, shown in Figure 2.7

Figure 2.5 Chromium contaminated site drainage ditch.

Figure 2.6 Chromium contaminated surface seeps.

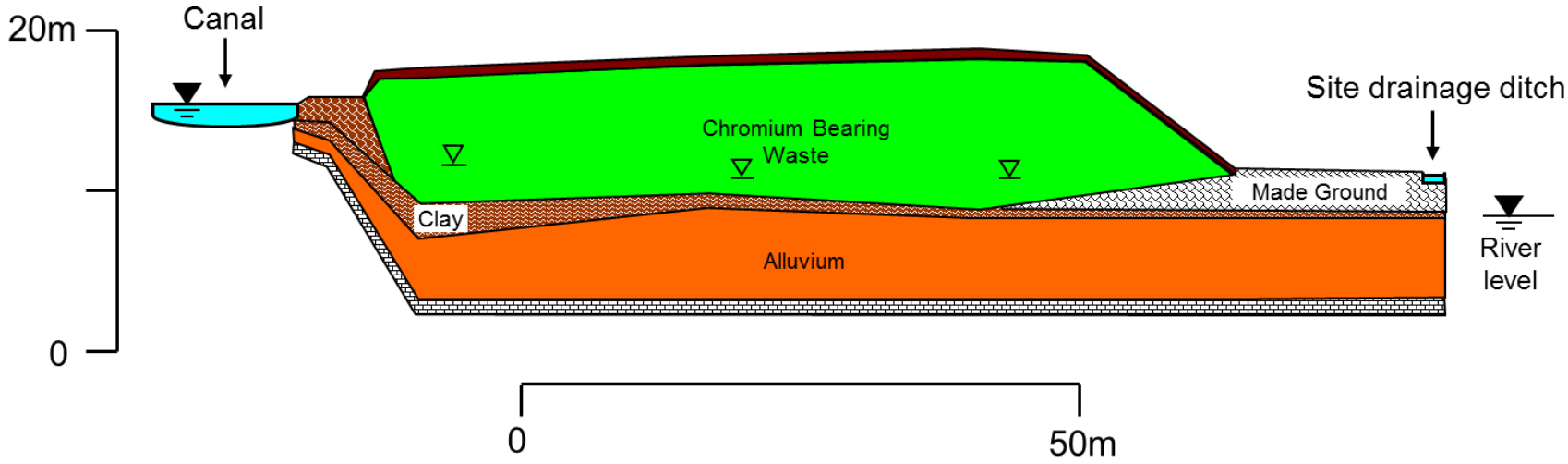

Figure 2.7 Simplified geological cross section showing waste position, constructed from borehole logs produced during professional site investigations (Whittleston et al., 2007)

2.10.3 Geochemical characterisation

Geochemical analysis of COPR material recovered during a professional site investigation in November 2003 found a maximum total chromium concentration of 19,000 $mg.kg^{-1}$. 380 $mg.kg^{-1}$ (2%) of this chromium was reported to be present in the hexavalent form. As a result, soil leach tests of this material were able to remobilise up to 33 $mg.l^{-1}$ of soluble Cr(VI). A hydrogeology study in April 2009 conducted by James Atkins, an MSc student at the University of Leeds, revealed the presence of a perched water table within the waste. This was located roughly 2 meters above the underlying groundwater, which is inferred to be flowing in an approximately south westerly direction within the alluvial gravels underlying the site (Figure B.3) (Atkins, 2009). This perched water table is highly contaminated with Cr(VI) as a result of being in direct contact with the COPR waste. Water from this perched water table was retrieved for this project in March 2009 from BH5 (Figure 2.4), and was found to contain 51 $mg.l^{-1}$ Cr(VI) and have a pH value of 12.2. These concentrations are up to ten times that of the contaminated surface waters, demonstrating a clear hazard to of potential subsurface migration. Geochemical analysis of groundwater within the underlying alluvial gravels undertaken by previous professional site investigations reported Cr(VI) concentrations of up to 42 $mg.l^{-1}$ and pH values in excess of 12. Cr(VI) is therefore clearly mobile within subsurface waters at this site, and poses a significant hazard to the adjacent environment.

2.11 References

Anderson, R.A., 1996. Chromium as an essential nutrient for humans, Chromium Symposium - 1996. Academic Press Inc Jnl-Comp Subscriptions, Arlington, Va, pp. S35-S41.

Andrews, J.E., Brimblecombe, P., Jickells, T.D., Liss, P.S., Reid, B.J., 2004. Chapter 4 - The Chemistry of Continental Solids. An Introduction to Environmental Chemistry 2nd ed, 121.

Aono, R., Ito, M., Horikoshi, K., 1997. Measurement of cytoplasmic pH of the alkaliphile Bacillus lentus C-125 with a fluorescent pH probe. Microbiology-Uk 143, 2531-2536.

Appelo, C.A.J., Postma, D., 2005. Chapter 7 - Sorption of Trace Metals. Geochemistry, groundwater and pollution 2nd ed, 311.

Atkins, J., 2009. Modelling groundwater and chromite migration through an old spoil tip in Copley., MSc Dissertation School of Earth and Environment. University of Leeds, Leeds, UK.

ATSDR, 2008. Toxicological Profile for Chromium, in: Services, U.S.D.o.H.a.H. (Ed.). Agency for Toxic Substances and Disease Registry, Atlanta.

Badar, U., Ahmed, N., Beswick, A.J., Pattanapipitpaisal, P., Macaskie, L.E., 2000. Reduction of chromate by microorganisms isolated from metal contaminated sites of Karachi, Pakistan. Biotechnol. Lett. 22, 829-836.

Bagchi, D., Vuchetich, P.J., Bagchi, M., Hassoun, E.A., Tran, M.X., Tang, L., Stohs, S.J., 1997. Induction of oxidative stress by chronic administration of sodium dichromate chromium VI and cadmium chloride cadmium II to rats. Free Radical Bio. Med. 22, 471-478.

Beaumont, J.J., Sedman, R.M., Reynolds, S.D., Sherman, C.D., Li, L.H., Howd, R.A., Sandy, M.S., Zeise, L., Alexeeff, G.V., 2008. Cancer mortality in a Chinese population exposed to hexavalent chromium in drinking water. Epidemiology 19, 12-23.

Bopp, L.H., Ehrlich, H.L., 1988. Chromate resistance and reduction in *pseudomonas-fluorescens* strain LB300. Arch. Microbiol. 150, 426-431.

Breeze, V.G., 1973. Land Reclamation and River Pollution Problems in Croal Valley Caused by Waste from Chromate Manufacture. J. Appl. Ecol. 10, 513-525.

Buerge, I.J., Hug, S.J., 1997. Kinetics and pH dependence of chromium(VI) reduction by iron(II). Environ. Sci. Technol. 31, 1426-1432.

Burke, I.T., Boothman, C., Lloyd, J.R., Mortimer, R.J.G., Livens, F.R., Morris, K., 2005. Effects of progressive anoxia on the solubility of technetium in sediments. Environ. Sci. Technol. 39, 4109-4116.

Cavallo, D., Maiello, R., Ursini, C.L., Fresegna, A.M., Ciervo, A., Iavicoli, S., 2008. Evaluation of genotoxic and oxidative effects on human bronchial cells exposed to low doses of hexavalent chromium. Toxicol. Lett. 180, S97-S98.

Cervantes, C., Campos-Garcia, J., Devars, S., Gutierrez-Corona, F., Loza-Tavera, H., Torres-Guzman, J.C., Moreno-Sanchez, R., 2001. Interactions of chromium with microorganisms and plants. FEMS. Microbiol. Rev. 25, 335-347.

Cervantes, C., Ohtake, H., 1988. Plasmid-determined resistance to chromate in pseudomonas-aeruginosa. FEMS Microbiol. Lett. 56, 173-176.

Chai, L.Y., Huang, S.H., Yang, Z.H., Peng, B., Huang, Y., Chen, Y.H., 2009. Hexavalent chromium reduction by Pannonibacter phragmitetus BB isolated from soil under chromium-containing slag heap. J. Environ. Sci. Heal. A 44, 615-622.

Chen, J.M., Hao, O.J., 1998. Microbial chromium (VI) reduction. Crit. Rev. Env. Sci. Tec. 28, 219-251.

Chistyakova, N.I., Rusakov, V.S., Nazarova, K.A., Koksharov, Y.A., Zavarzina, D.G., Greneche, J.M., 2007. Iron minerals formed by dissimilatory iron-and sulfur reducing bacteria studied by Mossbauer spectrometry, 29th Interenational Conference on Applications of the Mossbauer Effect, Kanpur, INDIA, pp. 55-63.

Cudennec, Y., Lecerf, A., 2006. The transformation of ferrihydrite into goethite or hematite, revisited. J. Solid State Chem. 179, 716-722.

Daulton, T.L., Little, B.J., Jones-Meehan, J., Blom, D.A., Allard, L.F., 2007. Microbial reduction of chromium from the hexavalent to divalent state. Geochim. Cosmochim. Acta 71, 556-565.

Deakin, D., West, L.J., Stewart, D.I., Yardley, B.W.D., 2001. Leaching behaviour of a chromium smelter waste heap. Waste Manage. 21, 265-270.

Deleo, P.C., Ehrlich, H.L., 1994. Reduction of hexavalent chromium by Pseudomonas fluorescens LB300 in batch and continuous cultures. Appl. Microbol. Biot. 40, 756-759.

Desai, C., Jain, K., Madamwar, D., 2008. Evaluation of In vitro Cr(VI) reduction potential in cytosolic extracts of three indigenous Bacillus sp isolated from Cr(VI) polluted industrial landfill. Bioresource Technol 99, 6059-6069.

Detkova, E., Pusheva, M., 2006. Energy metabolism in halophilic and alkaliphilic acetogenic bacteria. Microbiol. 75, 1.

Erdem, M., Gur, F., Tumen, F., 2004. Cr(VI) reduction in aqueous solutions by siderite. J. Hazard. Mater. 113, 219-224.

Erdem, M., Tumen, F., 2004a. Chromium removal from aqueous solution by ferrite process. J. Hazard. Mater. 109, 71-77.

Erdem, M., Tumen, F., 2004b. A study on dissolution properties of the sludges from Cr(VI) reduction-precipitation processes. J. Environ. Sci. Heal. A 39, 253-267.

Farmer, J.G., Graham, M.C., Thomas, R.P., Licona-Manzur, C., Licona-Manzur, C., Paterson, E., Campbell, C.D., Geelhoed, J.S., Lumsdon, D.G., Meeussen, J.C.L., Roe, M.J., Conner, A., Fallick, A.E., Bewley, R.J.F., 1999. Assessment and modelling of the environmental chemistry and potential for remediative treatment of chromium-contaminated land. Environ. Geochem. Health 21, 331-337.

Farmer, J.G., Paterson, E., Bewley, R.J.F., Geelhoed, J.S., Hillier, S., Meeussen, J.C.L., Lumsdon, D.G., Thomas, R.P., Graham, M.C., 2006. The implications of integrated assessment and modelling studies for the future remediation of chromite ore processing residue disposal sites. Sci. Total Environ. 360, 90-97.

Farmer, J.G., Thomas, R.P., Graham, M.C., Geelhoed, J.S., Lumsdon, D.G., Paterson, E., 2002. Chromium speciation and fractionation in ground and surface waters in the vicinity of chromite ore processing residue disposal sites. J. Environ. Monitor. 4, 235-243.

Francis, C.A., Obraztsova, A.Y., Tebo, B.M., 2000. Dissimilatory metal reduction by the facultative anaerobe Pantoea agglomerans SP1. Appl. Environ. Microbiol. 66, 543-548.

Fredrickson, J.K., Zachara, J.M., Kennedy, D.W., Dong, H.L., Onstott, T.C., Hinman, N.W., Li, S.M., 1998. Biogenic iron mineralization accompanying the dissimilatory reduction of hydrous ferric oxide by a groundwater bacterium. Geochim. Cosmochim. Acta 62, 3239-3257.

Froelich, P.N., Klinkhammer, G.P., Bender, M.L., Luedtke, N.A., Heath, G.R., Cullen, D., Dauphin, P., Hammond, D., Hartman, B., Maynard, V., 1979. Early Oxidation Of Organic-Matter In Pelagic Sediments Of The Eastern Equatorial Atlantic - Suboxic Diagenesis. Geochim. Cosmochim. Acta 43, 1075-1090.

Geelhoed, J.S., Meeussen, J.C.L., Hillier, S., Lumsdon, D.G., Thomas, R.P., Farmer, J.G., Paterson, E., 2002. Identification and geochemical modeling of processes controlling leaching of Cr(VI) and other major elements from chromite ore processing residue. Geochim. Cosmochim. Acta 66, 3927-3942.

Geelhoed, J.S., Meeussen, J.C.L., Roe, M.J., Hillier, S., Thomas, R.P., Farmer, J.G., Paterson, E., 2003. Chromium remediation or release? Effect of iron(II) sulfate addition on chromium(VI) leaching from columns of chromite ore processing residue. Environ. Sci. Technol. 37, 3206-3213.

Gvozdyak, P.I., Mogilevich, N.F., Rylskii, A.F., Grishchenko, N.I., 1986. Reduction of hexavalent chromium by collection strains of bacteria. Microbiol. 55, 770-773.

Han, X., Wong, Y.S., Tam, N.F.Y., 2006. Surface complexation mechanism and modeling in Cr(III) biosorption by a microalgal isolate, Chlorella miniata. J. Colloid Interface Sci. 303, 365-371.

Han, X., Wong, Y.S., Wong, M.H., Tam, N.F.Y., 2007. Biosorption and bioreduction of Cr(VI) by a microalgal isolate, Chlorella miniata. J. Hazard. Mater. 146, 65-72.

Han, X., Wong, Y.S., Wong, M.H., Tam, N.F.Y., 2008. Effects of anion species and concentration on the removal of Cr(VI) by a microalgal isolate, Chlorella miniata. J. Hazard. Mater. 158, 615-620.

Hansel, C.M., Benner, S.G., Fendorf, S., 2005. Competing Fe(II)-induced mineralization pathways of ferrihydrite. Environ. Sci. Technol. 39, 7147-7153.

Hazen, T.C., Tabak, H.H., 2005. Developments in bioremediation of soils and sediments polluted with metals and radionuclides: 2. Field research on bioremediation of metals and radionuclides. Rev. Env. Sci. Biot. 4, 157-183.

Higgins, T.E., Halloran, A.R., Dobbins, M.E., Pittignano, A.J., 1998. In situ reduction of hexavalent chromium in alkaline soils enriched with chromite ore processing residue. Japca J. Air. Waste Ma. 48, 1100-1106.

Hillier, S., Lumsdon, D.G., Brydson, R., Paterson, E., 2007. Hydrogarnet: A host phase for Cr(VI) in chromite ore processing residue (COPR) and other high pH wastes. Environ. Sci. Technol. 41, 1921-1927.

Hillier, S., Roe, M.J., Geelhoed, J.S., Fraser, A.R., Farmer, J.G., Paterson, E., 2003. Role of quantitative mineralogical analysis in the investigation of sites contaminated by chromite ore processing residue. Sci. Total Environ. 308, 195-210.

Horikosh.K, 1971a. Production of alkaline enzymes by alkalophilic microorganisms .1. Alkaline protease produced by bacillus N-2210. Agricultural and Biological Chemistry 35, 1407-&.

Horikosh.K, 1971b. Production of alkaline enzymes by alkalophilic microorganisms .2. Alkaline amylase produced by bacillus no A-40-2. Agricultural and Biological Chemistry 35, 1783-&.

Horikosh.K, 1972. Production of alkaline enzymes by alkalophilic microorganisms .3. Alkaline pectinase of bacillus no P-4-N. Agricultural and Biological Chemistry 36, 285-&.

Horikoshi, K., 1999. Alkaliphiles: Some applications of their products for biotechnology. Microbiol. Mol. Biol. R. 63, 735-+.

Horikoshi, K., 2004. Alkaliphiles. P. Jpn. Acad. A-Phys. 80, 166-178.

Housecroft, C.E., Sharpe, A.G., 2005. Inorg. Chem. 2nd ed.

Hullebusch, E.D., Lens, P.N.L., Tabak, H.H., 2005. Developments in bioremedtiaon of soils and sediments polluted with metals and radionuclides: 3. Influence of chemical speciation and bioavailability on contaminants immobilization/mobilization bio-process. Rev. Env. Sci. Biot. 4, 185-212.

Ishibashi, Y., Cervantes, C., Silver, S., 1990. Chromium reduction in *pseudomonas-putida*. Appl. Environ. Microbiol. 56, 2268-2270.

Jain, S.K., Rains, J.L., Croad, J.L., 2007. Effect of chromium niacinate and chromium picolinate supplementation on lipid peroxidation, TNF-alpha, IL-6, CRP, glycated hemoglobin, triglycerides, and cholesterol levels in blood of streptozotocin-treated diabetic rats. Free Radical Bio. Med. 43, 1124-1131.

James, B.R., 1994. Hexavalent Chromium Solubility and Reduction in Alkaline Soils Enriched with Chromite Ore Processing Residue. J. Environ. Qual. 23, 227-233.

James, B.R., 2001. Remediation-by-reduction strategies for chromate-contaminated soils. Environ. Geochem. Health 23, 175-179.

James, B.R., 2002. Chemical Transformations of Chromium in Soils: Relevance to Mobility, Bio-availability and Remediation. International Chromium Development Association, [Accessed 21/10/2008] Available at: http://www.icdachromium.com/pdf/publications/crfile2008feb2002.htm.

Katz, S.A., Salem, H., 1994. The Biological and Environmental Chemistry of Chromium.

Krauskopf, K.B., Bird, D.K., 1995. Chapter 6 - Surface Chemistry: The solution-mineral interface. Introduction to Geochemistry 3rd ed, 142.

Krishna, K.R., Philip, L., 2005. Bioremediation of Cr(VI) in contaminated soils. J. Hazard. Mater. 121, 109-117.

Krulwich, T.A., Guffanti, A.A., 1989. Alkalophilic Bacteria. Annu. Rev. Microbol 43, 435-463.

Krulwich, T.A., Ito, M., Gilmour, R., Guffanti, A.A., 1997. Mechanisms of cytoplasmic pH regulation in alkaliphilic strains of Bacillus. Extremophiles 1, 163-169.

Krulwich, T.A., Ito, M., Guffanti, A.A., 2001. The Na+-dependence of alkaliphily in Bacillus. BBA-Bioenergetics 1505, 158-168.

Kurono, Y., Horikosh.K, 1973. Production of alkaline enzymes by alkalophilic microorganisms .6. Alkaline catalase produced by bacillus no KU-1. Agricultural and Biological Chemistry 37, 2565-2570.

Kvasnikov, E.I., Stepanyuk, V.V., Klyushnikova, T.M., Serpokrylov, N.S., Simonova, G.A., Kasatkina, T.P., Panchenko, L.P., 1985. A new chromium reducing, gram variable bacterium with mixed type of flagellation. Microbiol. 54, 69-75.

Langmuir, D., 1997. Aqueous Environmental Geochemistry. Englewood Cliffs, NJ: Prentice Hall.

Laxman, R.S., More, S., 2002. Reduction of hexavalent chromium by Streptomyces griseus. Miner. Eng. 15, 831-837.

Lebedeva, E.V., Lyalikova, N.N., 1979. Reduction of crocoite by pseudomonas-chromatophila sp-nov. Microbiol. 48, 405-410.

Levy, L.S., Shuker, L.K., Rowbotham, A.L., 2001. An evaluation of total personal exposure to chromium in the UK environment and associated possible adverse health effects. Environ. Geochem. Health 23, 181-186.

Li, Y., Yue, Q.Y., Gao, B.Y., Li, Q., Li, C.L., 2008. Adsorption thermodynamic and kinetic studies of dissolved chromium onto humic acids. Colloid Surface. B. 65, 25-29.

Li, Y.R., Low, G.K.C., Scott, J.A., Amal, R., 2009. The role of iron in hexavalent chromium reduction by municipal landfill leachate. J. Hazard. Mater. 161, 657-662.

Lide, D.R., 1995. Handbook of chemistry and physics. CRC Press 76th Ed.

Lin, C.J., 2002. The chemical transformations of chromium in natural waters - A model study. Water Air Soil Poll. 139, 137-158.

Liu, C.X., Gorby, Y.A., Zachara, J.M., Fredrickson, J.K., Brown, C.F., 2002. Reduction kinetics of Fe(III), Co(III), U(VI) Cr(VI) and Tc(VII) in cultures of dissimilatory metal-reducing bacteria. Biotechnol. Bioeng. 80, 637-649.

Liu, H., Li, P., Zhu, M.Y., Wei, Y., Sun, Y.H., 2007. Fe(II)-induced transformation from ferrihydrite to lepidocrocite and goethite. J. Solid State Chem. 180, 2121-2128.

Llovera, S., Bonet, R., Simonpujol, M.D., Congregado, F., 1993. Chromate Reduction by Resting Cells of Agrobacterium radiobacter EPS-916. Appl. Environ. Microbiol. 59, 3516-3518.

Lloyd, J.R., Nolting, H.F., Sole, V.A., Bosecker, K., 1998. Technetium reduction and precipitation by sulfate-reducing bacteria. Geomicrobiol. J. 15, 45-58.

Lofroth, G., Ames, B.N., 1978. Mutagenicity of Inorganic-Compounds in Salmonella-Typhimurium - Arsenic, Chromium and Selenium. Mutat. Res. 53, 65-66.

Lovley, D.R., 1991. Dissimilatory Fe(III) and Mn(IV) Reduction. Microbiol. Rev. 55, 259-287.

Lovley, D.R., 1993a. Anaerobes into Heavy-Metal - Dissimilatory Metal Reduction in Anoxic Environments. Trends Ecol. Evol. 8, 213-217.

Lovley, D.R., 1993b. Dissimilatory Metal Reduction. Annu. Rev. Microbol 47, 263-290.

Lovley, D.R., 1995. Microbial reduction of iron, manganese, and other metals, Advances in Agronomy, Vol 54, pp. 175-231.

Lovley, D.R., 1997. Microbial Fe(III) reduction in subsurface environments. FEMS. Microbiol. Rev. 20, 305-313.

Lovley, D.R., Holmes, D.E., Nevin, K.P., 2004. Dissimilatory Fe(III) and Mn(IV) reduction, Advances in Microbial Physiology, Vol. 49. Academic Press Ltd, London, pp. 219-286.

Lovley, D.R., Stolz, J.F., Nord, G.L., Phillips, E.J.P., 1987. Anaerobic Production of Magnetite by a Dissimilatory Iron-Reducing Microorganism. Nature 330, 252-254.

Lovley, D.R., Widman, P.K., Woodward, J.C., Phillips, E.J.P., 1993. Reduction of Uranium by Cytochrome-C(3) of Desulfovibrio-Vulgaris. Appl. Environ. Microbiol. 59, 3572-3576.

Loyaux-Lawniczak, S., Lecomte, P., Ehrhardt, J.J., 2001. Behavior of hexavalent chromium in a polluted groundwater: Redox processes and immobilization in soils. Environ. Sci. Technol. 35, 1350-1357.

Mabbett, A.N., Lloyd, J.R., Macaskie, L.E., 2002. Effect of complexing agents on reduction of Cr(VI) by Desulfovibrio vulgaris ATCC 29579. Biotechnol. Bioeng. 79, 389-397.

Mangaiyarkarasi, M.S.M., Vincent, S., Janarthanan, S., Rao, T.S., Tata, B.V.R., 2011. Bioreduction of Cr(VI) by alkaliphilic Bacillus subtilis and interaction of the membrane groups. Saudi J. Biol. Sci. 18, 157-167.

Martello, L., Fuchsman, P., Sorensen, M., Magar, V., Wenning, R.J., 2007. Chromium geochemistry and bioaccumulation in sediments from the lower Hackensack River, New Jersey. Arch. Environ. Con. Tox. 53, 337-350.

McLean, J.E., Dupont, R.R., Sorensen, D.L., 2006. Iron and arsenic release from aquifer solids in response to biostimulation. J. Environ. Qual. 35, 1193-1203.

Mohan, D., Pittman, C.U., 2006. Activated carbons and low cost adsorbents for remediation of tri- and hexavalent chromium from water. J. Hazard. Mater. 137, 762-811.

Muntyan, M.S., Popova, I.V., Bloch, D.A., Skripnikova, E.V., Ustiyan, V.S., 2005. Energetics of alkalophilic representatives of the genus Bacillus. Biochemistry-Moscow+ 70, 137-142.

NABIR, 2003. Bioremediation of metals and radionuclides: what it is and how it works, A NABIR primer, 2nd ed. NABIR primer prepared for US Department of Energy, p. p.78.

NIOSH, 2008. Occupational Exposure to Hexavalent Chromium. National Institute for Occupational Safety and Health: Hexavalent Chromium Criteria Document Update.

Nurminen, M., 2006. Human Carcinogenicity Risk Assessment of Metallic Chromium and Trivalent Chromium. International Chromium Development Association, [Accessed 21/10/2008] Available at: http://www.icdachromium.com/pdf/publications/8909_CHROMIUM_ICDA_N_2014.pdf.

Ona-Nguema, G., Abdelmoula, M., Jorand, F., Benali, O., Gehin, A., Block, J.C., Genin, J.M.R., 2000. Microbial reduction of lepidocrocite gamma-FeOOH by Shewanella putrefaciens; The formation of green rust, 5th International Symposium on the Industrial Applications of the Mossbauer Effect, Virginia Beach, Virginia, pp. 231-237.

Ona-Nguema, G., Abdelmoula, M., Jorand, F., Benali, O., Gehin, A., Block, J.C., Genin, J.M.R., 2002. Iron(II,III) hydroxycarbonate green rust formation and stabilization from lepidocrocite bioreduction. Environ. Sci. Technol. 36, 16-20.

Onyancha, D., Mavura, W., Ngila, C., Ongoma, P., Chacha, J., 2008. Studies of chromium removal from tannery wastewaters by algae biosorbents, Spirogyra condensata and Rhizoclonium hieroglyphicum J. Hazard. Mater. 158, 605-614.

OSHA, 2006. Small Entity Compliance Guide for the Hexavalent Chromium Standards, in: Labor, U.S.D.o. (Ed.). Occupational Safety and Health Administration.

Paavilainen, S., Helisto, P., Korpela, T., 1994. Conversion of carbohydrates to organic-acids by alkaliphilic bacilli. J. Ferment. Bioeng. 78, 217-222.

Pagilla, K.R., Canter, L.W., 1999. Laboratory studies on remediation of chromium-contaminated soils. J. Environ. Eng-ASCE 125, 243-248.

Palmer, C.D., Wittbrodt, P.R., 1991. Processes Affecting the Remediation of Chromium-Contaminated Sites. Environ. Health Persp. 92, 25-40.

Pattanapipitpaisal, P., Brown, N.L., Macaskie, L.E., 2001. Chromate reduction and 16S rRNA identification of bacteria isolated from a Cr(VI)-contaminated site. Appl. Microbol. Biot. 57, 257-261.

Pechova, A., Pavlata, L., 2007. Chromium as an essential nutrient: a review. Vet. Med-Czech 52, 1-18.

Pollock, J., Weber, K.A., Lack, J., Achenbach, L.A., Mormile, M.R., Coates, J.D., 2007. Alkaline iron(III) reduction by a novel alkaliphilic, halotolerant, Bacillus sp isolated from salt flat sediments of Soap Lake. Appl. Microbol. Biot. 77, 927-934.

Raghu, D., Hsieh, H.-N., 1989. Origin, properties and disposal problems of chromium ore residue. Int. J. Environ. Stud. 34, 227-235.

Rai, D., Sass, B.M., Moore, D.A., 1987. Chromium(Iii) Hydrolysis Constants and Solubility of Chromium(Iii) Hydroxide. Inorg. Chem. 26, 345-349.

Rehman, A., Zahoor, A., Muneer, B., Hasnain, S., 2008. Chromium tolerance and reduction potential of a Bacillus sp.ev3 isolated from metal contaminated wastewater. B. Environ. Contam. Tox. 81, 25-29.

Richard, F.C., Bourg, A.C., 1991. Aqueous geochemistry of Cr: A review. Water Res. 25, 807-816.

Roadcap, G.S., Sanford, R.A., Jin, Q.S., Pardinas, J.R., Bethke, C.M., 2006. Extremely alkaline (pH > 12) ground water hosts diverse microbial community. Ground Water 44, 511-517.

Romanenko, V.I., Koren'kov, V.N., 1977. Pure culture of bacteria using chromates and bichromates as hydrogen acceptors during development under anaerobic conditions. Mikrobiologiia 46, 414-417.

Rowbotham, A.L., Levy, L.S., Shuker, L.K., 2000. Chromium in the environment: an evaluation of exposure of the UK general population and possible adverse health effects. J. Toxicol. Env. Heal. B 3, 145-178.

Rudolf, E., Schroterova, L., Kralova, V., Cervinka, M., 2008. Hexavalent chromium induces DNA damage and activates DNA-damage-response pathway in human skin cells. Toxicol. Lett. 180, S114.

Sani, R.K., Peyton, B.M., Smith, W.A., Apel, W.A., Petersen, J.N., 2002. Dissimilatory reduction of Cr(VI), Fe(III), and U(VI) by Cellulomonas isolates. Appl. Microbol. Biot. 60, 192-199.

Sau, G.B., Chatterjee, S., Sinha, S., Mukherjee, S.K., 2008. Isolation and Characterization of a Cr(VI) Reducing Bacillus firmus Strain from Industrial Effluents. Polish Journal of Microbiology 57, 327-332.

Schmieman, E.A., Yonge, D.R., Rege, M.A., Petersen, J.N., Turick, C.E., Johnstone, D.L., Apel, W.A., 1998. Comparative kinetics of bacterial reduction of chromium. J. Environ. Eng-ASCE 124, 449-455.

Schroeder, D.C., Lee, G.F., 1975. Potential Transformations of Chromium in Natural-Waters. Water Air Soil Poll. 4, 355-365.

Schwertmann, U., Friedl, J., Stanjek, H., 1999. From Fe(III) ions to ferrihydrite and then to hematite. J. Colloid Interface Sci. 209, 215-223.

Shen, H., Wang, Y.T., 1993. Characterization of enzymatic reduction of hexavalent chromium by Escherichia coli ATCC 33456. Appl. Environ. Microbiol. 59, 3771-3777.

Shewry, P.R., Peterson, P.J., 1976. Distribution of Chromium and Nickel in Plants and Soil from Serpentine and Other Sites. J. Ecol. 64, 195-212.

Spiccia, L., 1988. Solubility of Chromium(Iii) Hydroxides. Inorg. Chem. 27, 432-434.

Sreeram, K.J., Ramasami, T., 2001. Speciation and recovery of chromium from chromite ore processing residues. J. Environ. Monitor. 3, 526-530.

Stewart, D.I., Burke, I.T., Hughes-Berry, D.V., Whittleston, R.A., 2010. Microbially mediated chromate reduction in soil contaminated by highly alkaline leachate from chromium containing waste. Ecol. Eng. 36, 211-221.

Stewart, D.I., Burke, I.T., Mortimer, R.J.G., 2007. Stimulation of microbially mediated chromate reduction in alkaline soil-water systems. Geomicrobiol. J. 24, 655-669.

Stewart, M.A., Jardine, P.M., Barnett, M.O., Mehlhorn, T.L., Hyder, L.K., McKay, L.D., 2003. Influence of soil geochemical and physical properties on the sorption and bioaccessibility of chromium(III). J. Environ. Qual. 32, 129-137.

Stucki, J.W., Lee, K., Goodman, B.A., Kostka, J.E., 2007. Effects of in situ biostimulation on iron mineral speciation in a sub-surface soil. Geochim. Cosmochim. Acta 71, 835-843.

Stumm, W., Morgan, J.J., 1996. Aquatic Geochemistry 3rd ed. John Wiley and Sons, New York.

Suzuki, T., Miyata, N., Horitsu, H., Kawai, K., Takamizawa, K., Tai, Y., Okazaki, M., 1992. NAD(P)H-dependent chromium (VI) reductase of Pseudomonas ambigua G-1: a Cr(V) intermediate is formed during the reduction of Cr(VI) to Cr(III). J. Bacteriol. 174, 5340-5345.

Tebo, B.M., Obraztsova, A.Y., 1998. Sulfate-reducing bacterium grows with Cr(VI), U(VI), Mn(IV), and Fe(III) as electron acceptors. FEMS Microbiol. Lett. 162, 193-198.

Thauer, R.K., Jungermann, K., Decker, K., 1977. Energy conservation in chemotrophic anaerobic bacteria. Bacteriol. Rev. 41, 100-180.

Tilt, Z., 2009. The subsurface migration of Cr(VI) at a chromium waste tip in the North of England., School of Earth and Environment. University of Leeds.

Tinjum, J.M., Benson, C.H., Edil, T.B., 2008. Mobilization of Cr(VI) from chromite ore processing residue through acid treatment. Sci. Total Environ. 391, 13-25.

Tokala, R.K., Yonge, D., Puzon, G.J., Sivaswarny, V., Xun, L., Peyton, B.M., 2008. Subsurface mobility of organo-Cr(III) complexes formed during biological reduction of Cr(VI). J. Environ. Eng-ASCE 134, 87-92.

Torsvik, V., Ovreas, L., Thingstad, T.F., 2002. Prokaryotic diversity - Magnitude, dynamics, and controlling factors. Science 296, 1064-1066.

USEPA, 2005b. Procedures for the Derivation of Equilibrium Partitioning Sediment Benchmarks (ESBs) for the Protection of Benthic Organisms: Metal Mixtures (Cadmium, Copper, Lead, Nickel, Silver, and Zinc). United States Environmental Protection Agency. Online., [Accessed 17/10/2008] Available at: http://www.epa.gov/nheerl/publications/.

USGS, 1984. Element concentrations in soils and other surficial materials of the conterminous United States. United States Geological Survey. USGS Professional Paper 1270. Goverment Printing Office, Washington, DC: U.S.

VanEngelen, M.R., Peyton, B.M., Mormile, M.R., Pinkart, H.C., 2008. Fe(III), Cr(VI), and Fe(III) mediated Cr(VI) reduction in alkaline media using a Halomonas isolate from Soap Lake, Washington. Biodegradation 19, 841-850.

Vrionis, H.A., Anderson, R.T., Ortiz-Bernad, I., O'Neill, K.R., Resch, C.T., Peacock, A.D., Dayvault, R., White, D.C., Long, P.E., Lovley, D.R., 2005. Microbiological and geochemical heterogeneity in an in situ uranium bioremediation field site. Appl. Environ. Microbiol. 71, 6308-6318.

Walawska, B., Kowalski, Z., 2000. Model of technological alternatives of production of sodium chromate (VI) with the use of chromic wastes. Waste Manage. 20, 711-723.

Wang, P.C., Mori, T., Komori, K., Sasatsu, M., Toda, K., Ohtake, H., 1989. Isolation and Characterization of an Enterobacter cloacae Strain That Reduces Hexavalent Chromium under Anaerobic Conditions. Appl. Environ. Microbiol. 55, 1665-1669.

Wang, T.G., He, M.L., Pan, Q., 2007. A new method for the treatment of chromite ore processing residues. J. Hazard. Mater. 149, 440-444.

Wang, Y.T., 2000. In Lovley D.R. "Environmental Microbe-Metal Interactions" ASM Press. Chapter 10: Microbial Reduction of Chromate, 225-235.

Wani, A.A., Surakasi, V.P., Siddharth, J., Raghavan, R.G., Patole, M.S., Ranade, D., Shouche, Y.S., 2006. Molecular analyses of microbial diversity associated with the Lonar soda lake in India: An impact crater in a basalt area. Res. Microbiol. 157, 928-937.

Whittleston, R.A., Hughes-Berry, D.V., Stewart, D.I., Burke, I.T., 2007. A Natural In-situ Reactive Zone beneath a COPR Tip, 3rd International Symposium on Permeable Reactive Barriers and Reactive Zones, Rimini, Italy.

Whittleston, R.A., Stewart, D.I., Mortimer, R.J.G., Ashley, D.J., Burke, I.T., 2011. Effect of Microbially Induced Anoxia on Cr(VI) Mobility at a Site Contaminated with Hyperalkaline Residue from Chromite Ore Processing. Geomicrobiol. J. 28, 68-82.

WHO, 2008. Guidlines for drinking-water quality, 3 ed. World Health Organization, Geneva.

Wielinga, B., Mizuba, M.M., Hansel, C.M., Fendorf, S., 2001. Iron promoted reduction of chromate by dissimilatory iron-deducing bacteria. Environ. Sci. Technol. 35, 522-527.

Zavarzina, D.G., Kolganova, T.V., Boulygina, E.S., Kostrikina, N.A., Tourova, T.P., Zavarzin, G.A., 2006. Geoalkalibacter ferrihydriticus gen. nov sp nov., the first alkaliphilic representative of the family Geobacteraceae, isolated from a soda lake. Microbiol. 75, 673-682.

Zhilina, T.N., Zavarzina, D.G., Kolganova, T.V., Lysenko, A.M., Tourova, T.P., 2009. Alkaliphilus peptidofermentans sp nov., a new alkaliphilic bacterial soda lake isolate capable of peptide fermentation and Fe(III) reduction. Microbiol. 78, 445-454.

Zhu, W.J., Yang, Z.H., Ma, Z.M., Chai, L.Y., 2008. Reduction of high concentrations of chromate by Leucobacter sp CRB1 isolated from Changsha, China. World J. Microb. Biot. 24, 991-996.

Chapter 3 Project aims, objectives and approach

3.1 Objectives and research hypotheses

This thesis reports the findings of a detailed investigation into the fate and stability of Cr(VI) within COPR derived hyperalkaline leachates, as it percolates into the underlying soil horizon. Its primary objective was to develop a thorough understanding of the extent of chromium contamination within the subsurface, and the implications this could have on the design of future remediation strategies. The biogeochemical processes influencing Cr(VI) mobility within the subsurface were investigated, and the stability of the resulting host phase assessed. Emphasis was placed on characterising the diversity of the indigenous microbial population, and their influence on the biogeochemical processes occurring *in-situ.*

The following research hypotheses were used as a guide to this investigation:

- COPR waste will be a source for the spread of toxic, carcinogenic Cr(VI) into adjacent environments.
- The main mode of Cr(VI) migration will be via leaching within hyperalkaline, Cr(VI) contaminated liquors into soils below the waste.
- It is possible to intervene beneath the waste to attenuate this soluble transport mechanism through implementing *in-situ* remediation strategies.
- Soil microorganisms indigenous to the soils beneath the waste will have adapted to survive in a COPR contaminated environment.
- Indigenous soil microorganisms may be able to respire anaerobically using organic matter coupled to the reduction of Fe(III), to produce Fe(II) *in-situ,*

therefore providing a natural reactive zone for redox active metals such as Cr(VI).

- Reducing soil pH to approximately 9 to 9.5 may enhance Fe(III) reduction by reducing the metabolic stresses associated with hyperalkalinity, and aid the activity of indigenous alkaliphilic microorganisms.
- The addition of exogenic electron donors, such as acetate, can further induce bioreduction, despite the elevated pH.
- The reduction of Cr(VI) within the high pH soil systems will result in the precipitation of insoluble Cr(III) hydroxide phases, resistant to reoxidation to Cr(VI), thus providing a method of natural attenuation.
- The stability of chromium hosted within the sediments beneath the waste will be largely determined by the speciation in which it is found.
- That understanding the influence of novel indigenous alkaliphilic microbial populations on contaminant fate will be important in predicting the limiting factors for bioreduction at hyperalkaline, metal containing waste sites.

3.2 Approach

To test these hypotheses, a multidisciplinary approach was taken. This was essential in order to produce a coherent and comprehensive understanding of the processes occurring on site. To this end, research methods and analytical techniques from a variety of scientific disciplines including geochemistry, molecular biology, biogeochemistry, and geotechnical engineering were employed.

Although numerous site investigations have occurred in the past, little spatial analysis existed between the samples recovered. For the purpose of this investigation a series of boreholes were produced in March 2009 leading away from the COPR in

the direction of inferred groundwater flow. These boreholes encountered a variety of topsoil, waste and clay horizons depending on location, and were periodically sampled as both disturbed and undisturbed samples for analysis. Additional soil samples were recovered from previous professional investigations. Samples were stored carefully before being characterised using a variety of geochemical and analytical techniques including XRD and XRF. The resulting vertical geochemical profiles (see Appendix B.3) were compared and provided an indication of the extent of vertical and horizontal influence of a hyperalkaline, Cr(VI) contaminated plume. Material from the clay horizon immediately beneath the waste assumed to be the original top soil layer was collected for the detailed investigation into *in-situ* biogeochemical processes controlling the fate and stability of Cr(VI) entering this horizon leached from the COPR immediately above.

The influence of microorganisms indigenous to this former topsoil layer on biogeochemical processes controlling Cr(VI) solubility was investigated using microcosm incubation experiments. COPR contaminated leachates and underlying soils were mixed and sampled periodically for a range of redox indicators including nitrate, nitrite, Fe(II) Cr(VI), Eh and pH. This enabled the production of a time series of geochemical response during the development of microbial anoxia. These experiments were also conducted under pH amendment and with the addition of an exogenic carbon source, acetate, to investigate their effect on community development. At points of key interest, 16s rRNA gene fragments were recovered in order to determine the microbial community present. The quality of each sequence was assessed and non-chimeric sequences uploaded to the EMBL GenBank database. A combination of the Ribosomal Database Project (RDP) Naïve Bayesian classifier

(Wang et al., 2007), construction of phylogenetic trees, MOTHUR analysis, and Multidimensional Scaling analysis (MDS) was then used to assign these sequences to taxonomy and investigate community structure. This enabled comparisons to be made to the original soil population as well as to known microbial type species.

The solid phase speciation and association of chromium contained within borehole and experimental samples was determined using a combination of Cr-XAS, TEM and SEM techniques. As the two prevailing oxidation states of chromium within the environment (+3 and +6) exhibit significantly different geochemical behaviour, determination of its speciation is crucial to understanding its fate in the environment. Chromium K-edge XANES spectra were therefore collected as the existence of a characteristic pre-edge feature at 5994 eV is indicative of Cr(VI) compounds (Parsons et al., 2007). Information on the hosting environment for chromium within these samples was obtained from chromium K-edge EXAFS modelling of the backscatter bond distances from nearest neighbour atoms, and TEM analysis including STEM elemental mapping.

As Cr(VI) is much more mobile in the environment, oxidation of any Cr(III) phases is a potential source of secondary leaching. Therefore, to investigate the stability of chromium phases accumulating within soils beneath the COPR waste against remobilisation via this method, air reoxidation experiments were established. These experiments used air oxygenated deionised H_2O as a proxy for rainwater to represent the possible impact of relocation on the waste and subsequent exposure of the underlying soils to the atmosphere. The percentage of total chromium remobilised was measured over time.

In an attempt to produce viable cultures and isolates of iron reducing microorganisms that are indigenous to the former topsoil horizon beneath the COPR, a variety of culturing techniques were employed. These included the development of an iron reducing alkaline growth media (pH 9.2), serial dilution and plate incubation techniques. Successful cultures were subsequently profiled using 16s rRNA gene sequence analysis and the phylogenetic assignment techniques listed above.

3.3 References

Parsons, J.G., Dokken, K., Peralta-Videa, I.R., Romero-Gonzalez, J., Gardea-Torresdey, J.L., 2007. X-ray absorption near edge structure and extended X-ray absorption fine structure analysis of standards and biological samples containing mixed oxidation states, of chromium(III) and Chromium(VI). Appl. Spectrosc. 61, 338-345.

Wang, Q., Garrity, G.M., Tiedje, J.M., Cole, J.R., 2007. Naive Bayesian classifier for rapid assignment of rRNA sequences into the new bacterial taxonomy. Appl. Environ. Microbiol. 73, 5261-5267.

Chapter 4 Chromate reduction in Fe(II)-containing soil affected by hyperalkaline leachate from chromite ore processing residue

Abstract

Highly alkaline (pH 12.2) chromate contaminated leachate (990 μmol L^{-1}) has been entering soils below a chromite ore processing residue disposal (COPR) site for over 100 years. The soil immediately beneath the waste has a pH of 11→12.5, contains 0.3→0.5% (w/w) chromium, and 45→75% of the microbially available iron is Fe(II). Despite elevated pH, a viable microbial consortium of *Firmicutes* dominated iron reducers was isolated from this COPR affected soil. Soil pH and Cr concentration decrease with distance from the waste. XAS analysis of soil samples indicated that Cr is present as a mixed Cr(III)-Fe(III) oxy-hydroxide phase, suggesting that the elevated soil Cr content is due to reductive precipitation of Cr(VI) by Fe(II). Microcosm results demonstrate the capacity of COPR affected soil to abiotically remove all Cr(VI) from the leachate within 40 days. In air oxidation experiments less than 2% of the total Cr in the soil was remobilised despite significant Fe(II) oxidation. XAS analysis after air oxidation showed no change in Cr-speciation, indicating the Cr(III)-containing phase is a stable long term host for Cr. This work suggests that reductive precipitation of Cr(VI) is an effective method of contaminant immobilisation in soils where microbially produced Fe(II) is present.

4.1 Introduction

Chromium is a widely used industrial metal extracted commercially from the mineral chromite. Chromite ore is processed by roasting with an alkali-carbonate at 1150 °C to oxidise insoluble Cr(III) to soluble Cr(VI) which is extracted with water upon cooling. Traditionally, limestone was added to the reaction to improve air penetration, and this "high-lime" process was the primary commercial method of chromium production up to the 1960s (Darrie, 2001). Although now superseded by lime-free processes, high-lime Cr extraction recently accounted for 40% of Cr production worldwide (Darrie, 2001). The process is inefficient, and is responsible for producing large quantities of waste (600,000 $t.yr^{-1}$ in 2001 (Darrie, 2001)) known as chromite ore processing residue (COPR). COPR from the high-lime process is highly alkaline and typically contains 2–7% total chromium by weight (Deakin et al., 2001; Geelhoed et al., 2002; Geelhoed et al., 2003), and although much is unreacted insoluble chromite ore (i.e. Cr(III)), up to 30% can be in the oxidised Cr(VI) form (Geelhoed et al., 2003). Water in contact with COPR has a pH of 11→12, and can contain up to 1.6 mmol L^{-1} Cr(VI) as the highly mobile and toxic anion chromate (Geelhoed et al., 2003).

Poorly controlled landfilling of COPR is a global problem (Darrie, 2001; Geelhoed et al., 2002), and locally such sites can be major sources of pollution. Remediation of COPR legacy sites is challenging because they are often in urban areas and date from times when COPR disposal was poorly managed (Stewart et al., 2007). Traditional "dig and dump" remediation strategies are costly due to the large volumes involved, and inadvisable due to the risk of forming carcinogenic Cr(VI) bearing dusts (Broadway et al., 2010; USEPA, 1998). In contrast to the harmful properties of

Cr(VI), the reduced Cr(III) form is an essential trace nutrient in plants and animals (Pechova and Pavlata, 2007; Richard and Bourg, 1991), readily sorbs to soil minerals, and (co)-precipitates as insoluble Cr(III) hydroxides in neutral and alkaline environments (Rai et al., 1987; Richard and Bourg, 1991).

In natural environments a number of chemical species are known to reduce Cr(VI), including Fe(II), organic matter and sulphide (Lin, 2002). In anaerobic soils Fe(II) is probably the most important, as iron is abundant and microbial reduction of Fe(III) occurs as anoxia develops (Lovley, 1991, 1997; Pollock et al., 2007; Zavarzina et al., 2006). Cr(VI) is readily reduced by oxidation of Fe(II) (Richard and Bourg, 1991), and as Cr(III) can substitute for Fe(III), the resulting Cr(III) is likely to be incorporated into iron(III) oxyhydroxides (Fendorf, 1995). However, such metastable iron oxyhydroxides can exhibit high bioavailability (Hansel et al., 2005) and thus Fe(II)/Fe(III) cycling may continue in environments where microbial iron reduction can occur. Iron cycling is likely to be important at COPR sites as a broad range of microbes have adapted to allow them to respire and grow in high pH and metal contaminated environments (Horikoshi, 2004; Rehman and Shakoori, 2001; Rehman et al., 2008; Zavarzina et al., 2006).

This chapter describes a site in the North of England where COPR has been deposited next to a canal on the side of a valley and close to a river in the bottom (Stewart et al., 2010). It is of environmental concern because water emerging from the waste pile, which enters both the groundwater and the surface water systems, has an elevated Cr(VI) concentration (Stewart et al., 2010). Previous investigations have found that the anoxic soils beneath the waste have accumulated Cr (Stewart et al.,

2010; Whittleston et al., 2011). These studies suggest that microbially mediated reduction of COPR derived chromate is naturally attenuating contaminant transport. Here a combination of field investigation, microcosm experiments, microbial community analysis and X-ray absorption spectroscopy are used to investigate the controls on geochemical transformation of Cr(VI) in COPR contaminated water as it enters underlying anoxic soil horizons.

4.2 Materials and methods

4.2.1 Field sampling and sample handling

A 19th century COPR tip is located in the North of England. It is in a glacial valley, through undifferentiated siltstone and mudstone, in-filled with alluvial deposits (Figure 4.1a; see also (Stewart et al., 2010; Whittleston et al., 2011)). A thin layer of topsoil covers much of the tip, however to date no chemical remediation strategy has been employed at the site. Soil samples were collected in March 2009 from six boreholes in a line away from the tip using a hand auger and 1m core sampler (Figure 4.1b and c). Water was taken from a standpipe in BH5 screened into the COPR using a PVC bailer (BH5 dates from a 2002 commercial site investigation, Figure 4.1b). Samples were stored at 4°C in the dark in sealed polythene containers (XAS samples were stored at −80°C in glass vials). Sealed containers with samples for microbial community analysis were stored anaerobically using Anaerogen^{tm} sachets.

4.2.2 Sample characterisation

Soil samples were characterised using X-ray powder diffraction (XRD), X-ray fluorescence (XRF), total organic carbon analysis, pH analysis, deionised water (DIW) soluble Cr(VI) content, scanning electron microscopy (SEM) and scanning

transmission electron microscopy (STEM) using standard protocols (ASTM, 2006; Schumacher, 2002; Vitale et al., 1997) (see Appendix A.2). Water chemistry was determined using the standard methods below.

4.2.3 Reduction microcosm experiments

Triplicate microcosms were prepared using 10g of homogenised soil from sample B2-310 and 100ml of COPR leachate in 120ml glass serum bottles (Whittleston et al., 2011). After sealing, the headspace was purged with nitrogen. A sterilised control was prepared by autoclaving soil with a nitrogen purged headspace (120°C, 20min) and filter sterilised COPR leachate added upon cooling. Bottles (incubated in the dark at 21°C) were periodically sampled aseptically for geochemical analysis. During sampling microcosms were shaken and 3ml soil slurry extracted. Samples were centrifuged (3min, 16,000 x g) and the water analysed for, pH, Eh and Cr(VI), and soil for acid extractable Fe(II).

4.2.4 Geochemical methods

Eh and pH were measured using an Orion meter (pH calibrated at 7 and 10). UV/VIS spectroscopy methods based on reactions with diphenycarbazide and ferrozine were used to determine aqueous Cr(VI) and Fe concentrations using a Cecil CE3021 UV/VIS Spectrophotometer (USEPA, 1992; Viollier et al., 2000), with standard calibrations performed regularly. As a proxy for microbial available Fe (Burke et al., 2006; Weber et al., 2001), the percentage Fe(II) in the soil was determined after extraction by 0.5N HCl and reaction with ferrozine (Lovley and Phillips, 1986). See Appendix A.3 for detail descriptions of methods.

4.2.5 Oxidation experiments

DIW equilibrated with atmospheric O_2 and CO_2 was used as a proxy for rain water in leaching tests that evaluated the potential for Cr remobilisation. 500ml conical flasks containing 10g B2-310 soil and 100ml DIW were left open to the atmosphere using a foam bung, placed on an orbital shaker (150rpm), and incubated in the dark at 21°C. Duplicate experiments were sampled periodically over 60 days. At each sample point, 1.5ml soil slurry was extracted using a sterile syringe, and centrifuged (3min 16,000 x g). The supernatant was then analysed for pH, Eh aqueous Cr(VI) concentration, and the soil pellet analysed for Fe(II) in solids, as described above.

4.2.6 X-ray absorption spectroscopy (XAS)

XANES and EXAFS spectra were collected on station I18 at Diamond Light Source, UK, from seven soil samples from below the local water table and the B2-310 oxidation sample. Spectra were compared to standard laboratory chemicals, natural chromite ore, and amorphous Cr-hydroxide (precipitated by dropwise neutralisation of $CrCl_3$ solution using NaOH (Saraswat and Vajpei, 1984)). XANES and EXAFS spectra were summed and normalised using Athena v0.8.056. Background subtracted EXAFS spectra were prepared for selected B2 and B3 samples using PySpline v1.1, and were modelled using DLexcurv v1.0 with improvement in *R* value used to measure fit (see Appendix A.2.7).

4.2.7 Culturing of iron reducers

An alkaline (pH 9.2) growth media was used to culture a consortium of Fe(II)-reducing anaerobes. Fe(III) citrate and yeast extract were used as sole electron acceptors and donors (See Appendix A.4.1). 5mL of B2-310 soil in sterile growth media (20g L^{-1}) was sealed into 10mL glass serum bottles with nitrogen headspace.

The resulting culture was progressed repeatedly to obtain a viable consortium. Precipitate colour change from orange to black indicating Fe(II) production was confirmed using the method described above.

4.2.8 Microbial community analysis

Microbial DNA was extracted from B2-310 and the Fe(III)-reducing culture. A 16S rRNA gene fragment (~500bp) was amplified from each sample by polymerase chain reaction (PCR) using broad specificity primers. The PCR product was ligated into a standard cloning vector, and transformed into E. coli competent cells to isolate plasmids containing the insert, which were sent for sequencing (see Appendix A.5.2). The quality of each gene sequence was evaluated, and non-chimeric sequences were classified using the Ribosomal Database Project (RDP) naïve Bayesian Classifier (Wang et al., 2007) in August 2010 (GenBank accession numbers FR695903-FR695964, and FR820910-FR820956).

4.3 Results

4.3.1 Ground investigation

Borehole B1 (Figure 4.1c) penetrated a topsoil layer and encountered COPR waste at 55cm but did not enter the underlying soil. B2 penetrated a thicker topsoil layer before entering COPR waste at 190cm, grey sandy clay at 310cm, and terminated in a gravel layer at 365cm. Subsequent boreholes B3→B6 (in order of distance from the waste edge), did not go through the COPR waste, but revealed a sequence of topsoil over brown sandy clay, then grey sandy clay, and terminated in the gravel layer. The pH of water in the COPR (BH5) was 12.2 and the Cr(VI) concentration was 990 µmol L^{-1} (51.5 mg l^{-1} as CrO_4^{2-}).

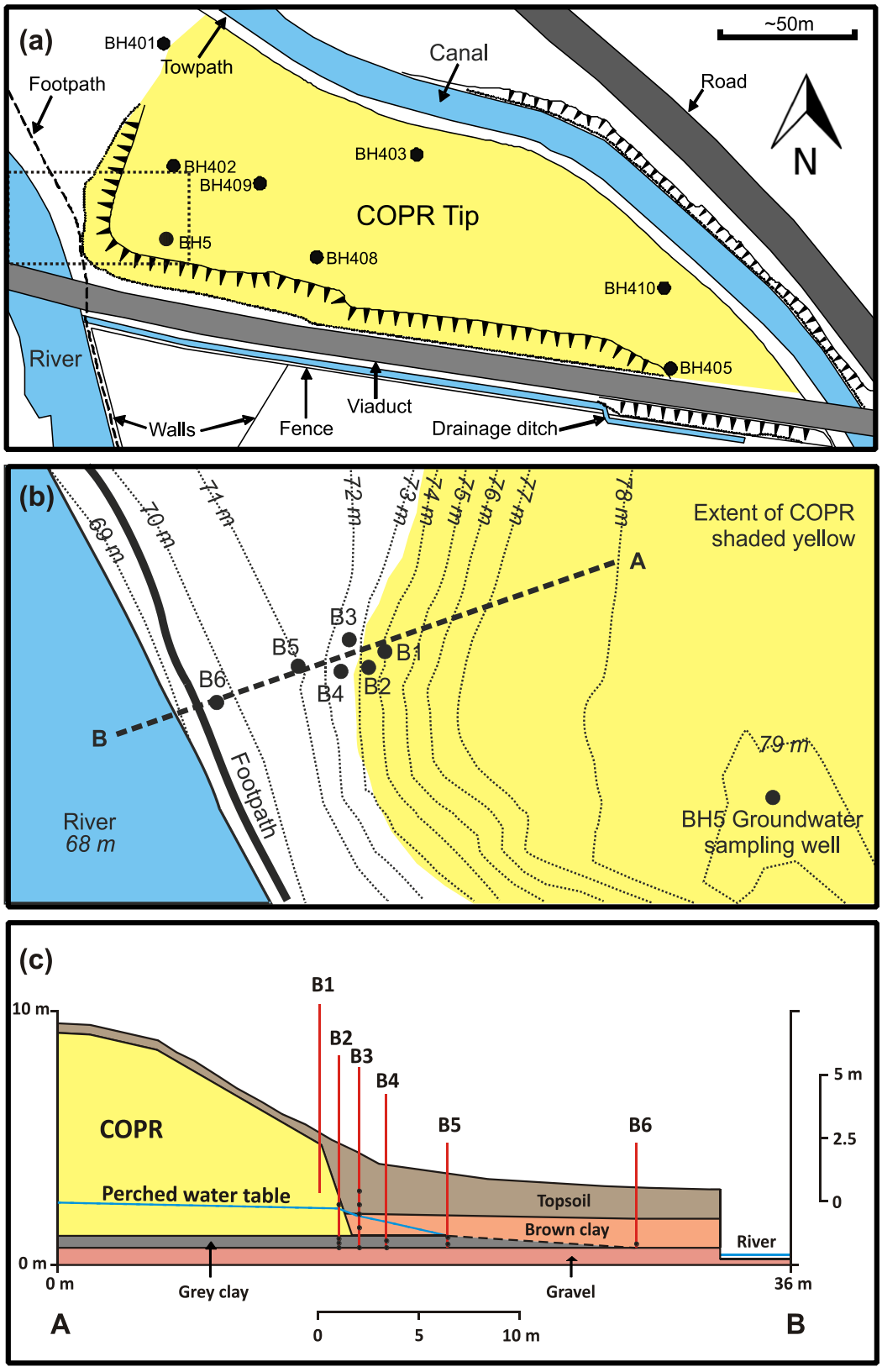

Figure 4.1 COPR site ground investigation; (a) Sketch map of the site indicating the study area and the borehole locations from commercial site investigations undertaken in 2002 and 2007, (b) the study area on the south western edge of the waste showing new borehole locations, and (c) conceptual ground model along line of pseudo-section

4.3.2 Sample characterisation

The properties of COPR and soil samples are shown in Table 4.1, and full XRF analysis is presented in Table 4.2. The COPR sample (B2 190-210) contained 1.27% (w/w) chromium, and 119.1 $mg.kg^{-1}$ of Cr(VI) was leachable with DIW (see Stewart et al. (2010) for full characterisation COPR leachate). The soil samples from closest to the COPR contained between 0.3 and 0.5% (w/w) chromium (samples B2-310 and B2 320-340 from the grey clay immediately beneath the COPR, and B3 150-200 and B3 200-240 from the topsoil immediately next to the COPR). Backscatter SEM images of grey clay sample (B2-310) show it to consist of a largely fine grained matrix, interspaced with angular quartz grains (Figure 4.2). The mean Cr-concentration within fine matrix determined by SEM microprobe was 0.46% ± 0.29% (w/w), consistent with the bulk XRF analysis (0.34% w/w) for this sample. The amount of chromium in the soil samples shows a rough trend of decreasing with depth in B2 and B3, and of decreasing with horizontal distance from the waste pile (B3>B4>B6). These trends are reflected in pH, with the samples closest to the COPR having the highest values, which were above pH 12 immediately below the waste in B2. The percentages of iron extracted by 0.5 N HCl present as Fe(II) in B2 soils from immediately below the waste were 45→75%, and values were similar throughout the grey clay layer. In the overlying brown clay and topsoil layers percentages of iron extracted by 0.5N HCl present as Fe(II) were more variable but generally increased with depth. This suggests that Fe(III) reducing conditions develop rapidly under saturated conditions.

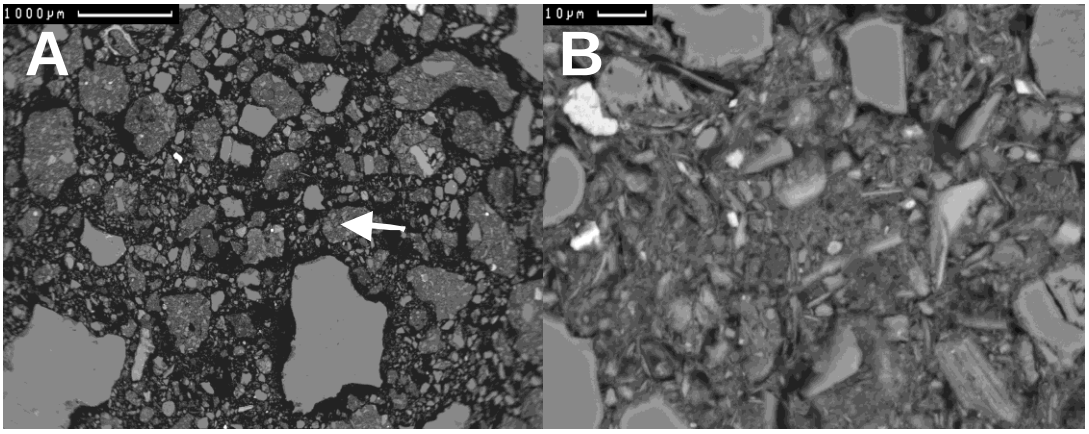

Figure 4.2 Backscatter SEM images from B2-310 soil sample, resin embedded thin section, showing (A) low magnification view of angular quartz grains in a fine grained matrix (scale bar 1000 µM); (B) higher magnification view (from white arrow, frame A) of fine grained clay-like matrix material (scale bar 10 µM)

Table 4.1 Soil composition.

Borehole	Depth (cm)	Soil type	Total Cr ($mgkg^{-1}$)	Leachable Cr(VI) ($mgkg^{-1}$)	pH	% Acid extractable iron as Fe(II)	Major Minerals Present	Water Strike	TOC (%)
B2	190-210	COPR Waste	12716	119.10	12.51	-	Portlandite	No	0.26
	310	Grey clay	3436	6.65	12.16	53	Quartz, Kaolinite, Albite	Yes	0.96
	320-340	Grey grey	3946	4.54	12.51	45	Quartz, Kaolinite	Yes	0.96
	365	Grey clay	846	5.80	11.2	75	Quartz, Kaolinite, Illite	Yes	0.50
B3	150-200	Topsoil	4890	8.76	4.31	4	-	No	13.38
	200-240	Topsoil	4321	1.45	7.03	5	-	No	14.47
	240-250	Brown clay	1431	0.89	7.96	5	Quartz, Kaolinite, Illite	Yes	1.86
	280-335	Brown clay	1511	0.46	7.76	37	Quartz, Kaolinite	Yes	0.54
	360-365	Grey clay	1379	0.46	7.83	31	-	Yes	0.23
B4	240-270	Grey clay	336	0.60	6.58	68	Quartz, Kaolinite	Yes	1.16
	270-280	Grey clay	847	0.60	6.59	92	-	Yes	0.25
B5	190-200	Brown clay	1599	0.74	7.2	60	-	No	0.23
	220-230	Grey clay	1278	0.89	6.62	89	-	No	0.36
B6	220	Brown clay	162	1.59	5.64	N.d	Quartz, Kaolinite	No	0.14

- Not determined

N.d. Not detected

Table 4.2 Selected XRF major and trace elemental composition of soil samples reported as component oxide weight percent and parts per million (ppm) respectively. Major element data corrected for loss on ignition.

Borehole	Depth (cm)	Soil type	SiO_2	MgO	CaO	Fe_2O_3	Cr	As	Ba	Cu	Ni	Pb	Sn	Zn	Zr
B2	190-210	COPR Waste	2.25	6.31	46.63	5.54	12716	331.5	481	17.6	512.1	21.9	2.9	100.8	5.8
B2	310	Grey clay	58.79	1.21	6.12	5.70	3436	86.3	501.3	67.3	78.1	56	43.2	167.7	323.9
B2	320-340	Grey grey	56.81	1.39	4.23	6.13	3946	41.5	552.2	26.7	67.1	44.5	15.8	123.3	278.6
B2	365	Grey clay	78.61	0.36	0.69	4.39	846	17.1	348.9	23.5	28.8	21.2	9.9	76.6	393.2
B3	150-200	Topsoil	53.37	0.7	0.47	5.71	4890	432.6	631.5	655.1	35	596.9	1242.6	152.1	200.2
B3	200-240	Topsoil	54.92	0.73	0.96	6.08	4321	374.7	511.2	537.4	70.2	529	1412.4	710.5	201.9
B3	240-250	Brown clay	63.95	0.82	1.41	5.30	1431	109.5	528.3	38.7	44.9	69	68.6	155.4	322.7
B3	280-333	Brown clay	59.54	0.98	1.65	7.48	1511	28.9	448.5	31.7	46.8	28.3	2.1	140.2	290.9
B3	360-365	Grey clay	76.64	0.65	0.88	3.66	1379	26.2	371.7	22.4	25.2	25.2	12.8	64.5	401.7
B4	240-270	Grey clay	57.29	0.89	0.73	8.88	336	16.8	447.8	65.2	49.3	56.7	48.2	252.7	279.2
B4	270-280	Grey clay	81.57	0.39	0.19	3.61	847	6	361.6	176	40.6	27.2	10	652.6	308.9
B5	190-200	Brown clay	61.75	0.84	0.23	5.82	1599	6.7	467.6	138.5	103.6	42.2	1.3	984.2	298
B5	220-230	Grey clay	60.52	0.81	0.44	7.58	1278	6.6	491.6	226.6	128.3	47.4	1.5	2215	287.3
B6	220	Brown clay	81.1	0.4	0.16	3.97	162	6.2	341.2	36	38.7	21	4.5	491.6	339.4
BH402	8.8-9.0 m	Brown clay	53.43	0.98	3.02	8.71	8846	15.9	499.2	40.5	60	81	4.6	186.1	227.4
BH402	9.5-10.8 m	Grey clay	58.35	0.89	1.4	7.94	868	29.9	420	39.1	37.3	62.5	24	118.5	270.5

XANES spectra from a selection of grey and brown clay samples taken from boreholes with increasing distance from the COPR all lacked the characteristic pre-edge feature associated with Cr(VI) at 5994 eV (Parsons et al., 2007) (Figure 4.3). All XANES spectra indicate that Cr is present predominately in the reduced Cr(III) form although minor amounts of Cr(VI) (up to 3-5% of the total Cr depending on sample concentration) may not be detected in XANES spectra (Peterson et al., 1996). The amount of DIW leachable Cr(VI) in the soil samples (Table 4.1) falls below this detection limit, thus XANES and DIW leaching tests bracket the amount of Cr(VI) within these soils at approximately 0.5–3% of the total Cr. Due to the suspected presence of freshly precipitated Cr(III) hydroxides in these soils, estimates of Cr(VI) content from alkaline extractions were excluded as significant method induced oxidation of Cr(III) was observed in these samples (Vitale et al., 1997). Although XANES spectra from many Cr(III) compounds are superficially similar, the chromite ore spectrum has a distinct shoulder at approximately 6003 eV which is absent in the less crystalline Cr(III) hydroxide spectrum. The spectra from the soil samples do not have this shoulder.

EXAFS spectra from selected samples were fitted with a shell of 6 oxygen atoms at 1.97→1.99 Å and refined to minimise *R*. The spectral features beyond 2Å were fitted with a further 3 shells of Fe(Cr) backscatters at 3.06→3.07Å, 3.30→3.34Å and 3.93→4.02Å, and further refined (Table 4.3), n.b. Fe and Cr backscatters are indistinguishable in EXAFS modelling (He et al., 2004)). EXAFS and Fourier transformed EXAFS spectra are shown on Figure 4.4.

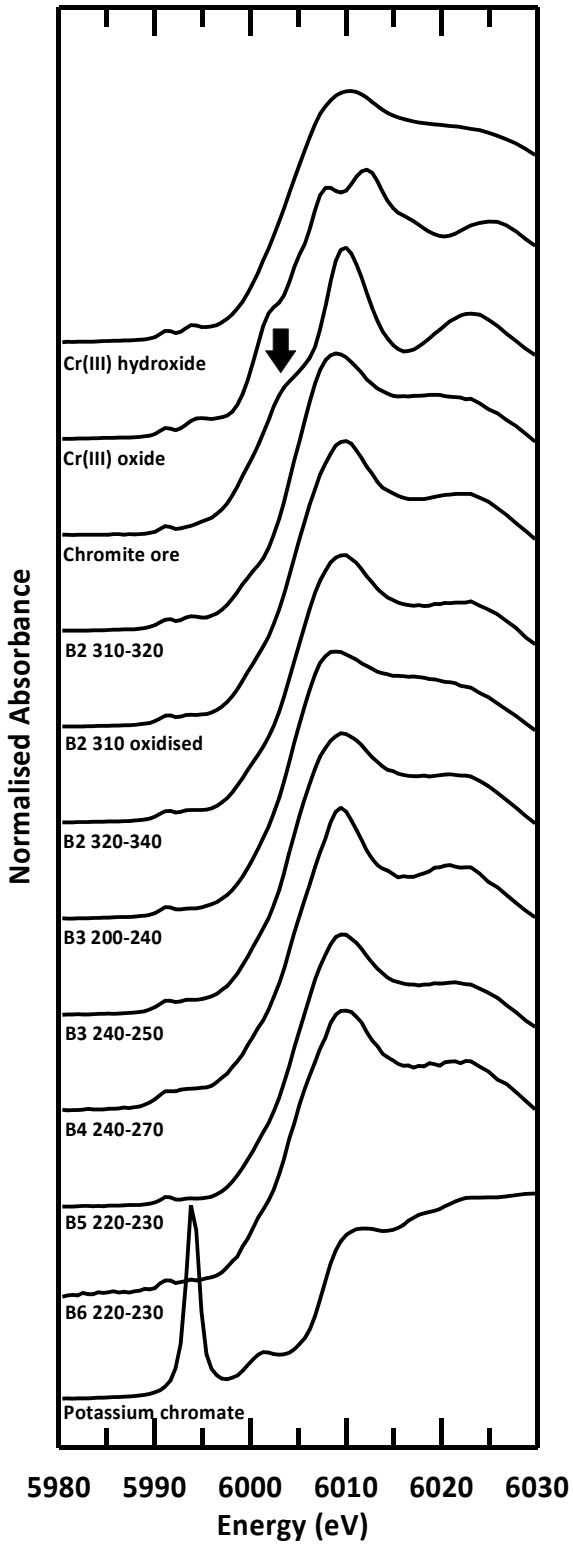

Figure 4.3 Normalised chromium K-edge XANES of soil samples and synthetic standards. Arrow indicates a distinctive curve inflection present at 6003 eV in the chromite ore spectra.

Table 4.3 EXAFS model fitting parameters where n is the occupancy (±25%), r is the interatomic distance (±0.02Å for the first shell, ± 0.05Å for outer shells),$2\sigma^2$ is the Debye-Waller factor (±25%), and *R* is the least squares residual.

Sample	Shell	n	R (Å)	$2\sigma^2$ (Å^2)	*R*	% gain
B2 310-320	O	6	1.99	0.011	49.2	
	Fe(Cr)	2.9	3.06	0.013		
	Fe(Cr)	3.3	3.34	0.010		
	Fe(Cr)	3.3	3.99	0.014	30.1	38.7
B2 320-340	O	6	1.98	0.011	42.9	
	Fe(Cr)	3.1	3.07	0.017		
	Fe(Cr)	3.1	3.33	0.020		
	Fe(Cr)	3.1	3.97	0.022	28.1	34.5
B2 310 oxidised	O	6	1.98	0.010	42.9	
	Fe(Cr)	3.1	3.06	0.014		
	Fe(Cr)	3	3.33	0.020		
	Fe(Cr)	3.4	3.99	0.022	28.2	34.2
B3 200-240	O	6	1.97	0.010	43.3	
	Fe(Cr)	3	3.07	0.018		
	Fe(Cr)	2.9	3.32	0.012		
	Fe(Cr)	3.1	3.93	0.016	30.4	29.9
B3 240-250	O	6	1.99	0.010	40.9	
	Fe(Cr)	3	3.07	0.011		
	Fe(Cr)	3	3.30	0.011		
	Fe(Cr)	3	4.02	0.026	30.6	25.1

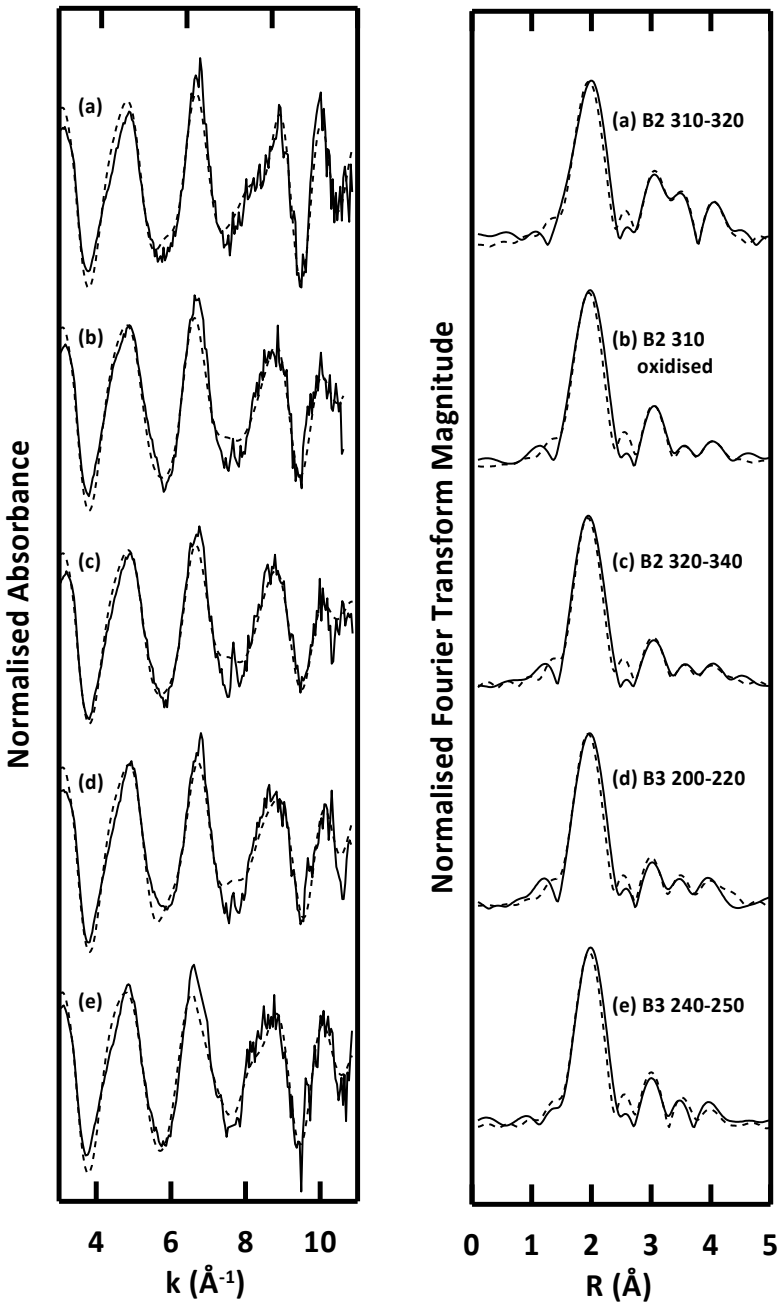

Figure 4.4 Chromium K-edge EXAFS spectra collected from selected soil samples (left) and corresponding Fourier transformations (right). Dashed lines represent model fits produced in DLexcurv v1.0 using the parameters listed in

To further investigate the co-localisation of Cr at the nano-scale, STEM analysis was carried out on sample B2-310. Dark field STEM imaging identified fine-grained aggregates amongst coarser grained material (Figure 4.5). EDX point analysis shows Cr and Fe co-localization in the fine-grained region (Figure 4.5A, point 1; EDX spectrum 1 in Figure 4.6). Bright field TEM imaging (Figure 4.5B) confirms that the Fe and Cr containing material consists of 5-10nm sized particles. STEM-EDX elemental mapping of this area (Figure 4.5) shows Cr (Kα X-rays) localised with Fe in the fine grained region, Al and Si are localised in the surrounding larger particles. EDX point analysis of a crystalline Fe-rich particle (Figure 4.5A, point 2; EDX spectrum 2 Figure 4.6) and a Si and Al rich particle (Figure 4.5A, point 3; EDX spectrum 3 Figure 4.6) confirmed the lack of Cr in these regions.

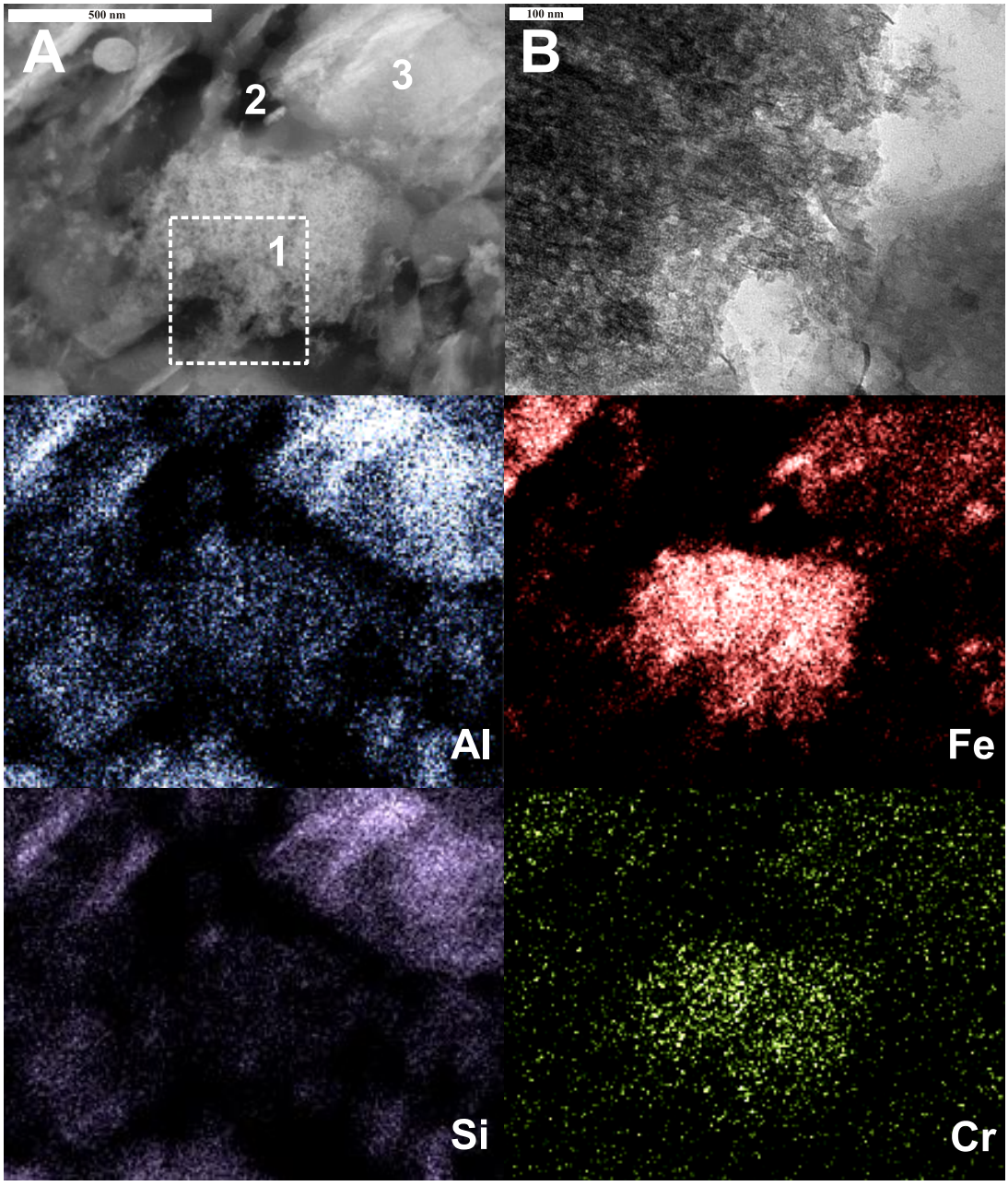

Figure 4.5 TEM images and corresponding STEM-EDX elemental maps of B2-310 soil. (A) Darkfield TEM image with locations of point EDX measurements, marked 1-3 (scale bar 500nm); (B) Higher magnification bright field TEM image of fine-grained area highlighted in (A), rotated 90° (scale bar 100nm). STEM-EDX maps of elemental distribution of aluminium ($K\alpha$ X-ray energy), iron ($K\alpha$), silicon ($K\alpha$) and chromium ($K\alpha$).

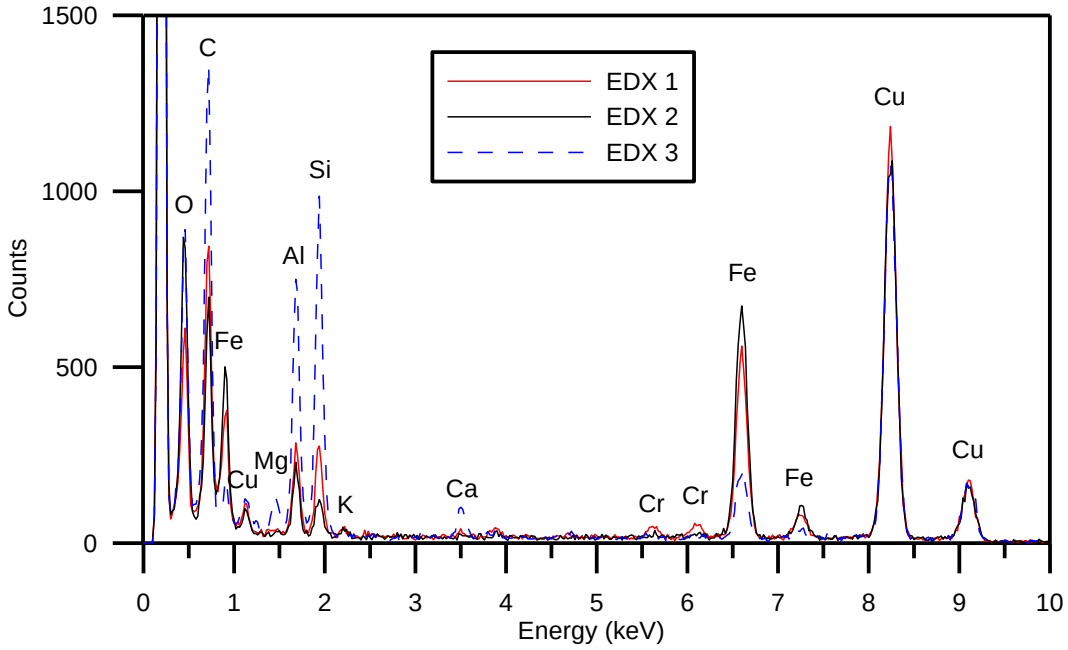

Figure 4.6 Point EDX spectra (10-20 nm probe diameter) from the 3 localities identified by STEM imaging (see Figure 4.5): Point 1, Fe-rich, Cr containing oxide hotspot (red); Point 2 Fe-rich oxide particle (black); Particle 3 Si and Al rich oxide particle.

4.3.3 Reduction microcosm experiments

The microcosm experiments investigated the interaction of COPR leachate with Fe(II)-containing grey clay from below the waste pile (sample B2-310). The initial pH value of microcosms was 12.2, while the corresponding sterile control had an initial pH value of 12. The pH in all microcosms decreased over about 20 days before levelling off at 11.7 (Figure 4.7). At the first sample point (~1hr) the aqueous Cr(VI) concentration had dropped from the leachate value of 990 to 788 ±14 μmol L^{-1}, and Cr(VI) was subsequently removed from solution over the first 30 days in all microcosm bottles. The concentration of Cr(VI) in the corresponding sterile control was 822 μmol L^{-1} at 1 hour and Cr(VI) was also completely removed from solution by 14 days. At the first sample point 36% of the 0.5N HCl extractable iron in the microcosms was present as Fe(II), and by day 4 this had dropped to 30% at the same time as most of the Cr(VI) was removed (788→257 μmol L^{-1}). Percentage 0.5N HCl

extractable Fe as Fe(II) then remains within error of the 4 day value. The percentage of the 0.5N HCl extractable iron in the sterile control as Fe(II) was 45% with no significant change during the experiments. Eh values at the first sampling point were -77 ± 10 and -65 mV for the active microcosms and sterile control, respectively and decreased very slowly to -135 ± 40 and -185mV at 83 days. Aqueous Fe remained at between 2 and 10 μmol L^{-1} in all microcosms throughout the duration of the incubations.

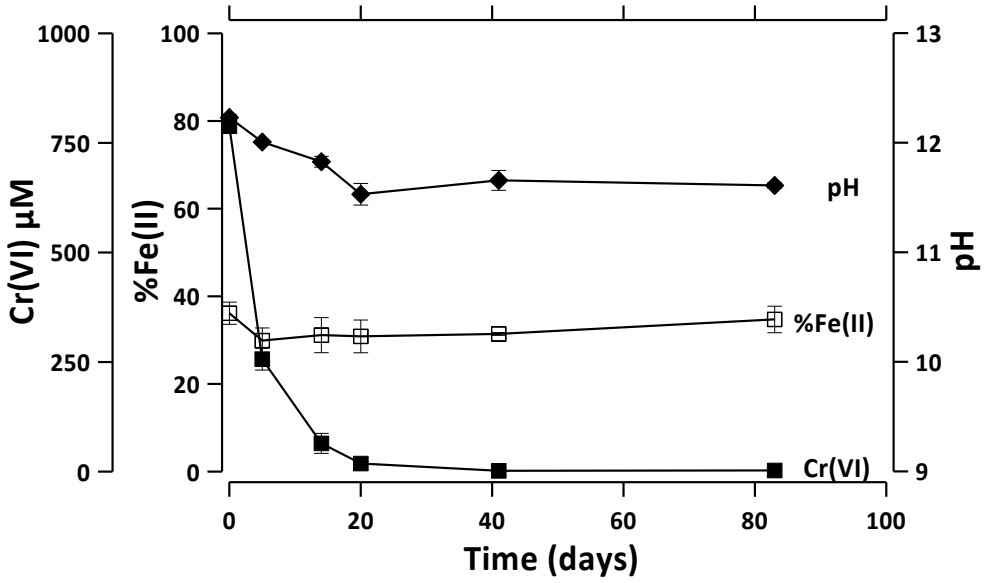

Figure 4.7 Microcosm experiment geochemical profiles; (■) aqueous Cr(VI); (◆) pH; (□) % of 0.5N HCl extractable Fe as Fe(II) in soils. Error bars are one standard deviation from the mean of triplicate experiments.

4.3.4 Microbial community analysis

The 62 16s rRNA gene sequences obtained from B2-310 soil were assigned to 9 different bacterial phyla (confidence threshold >98%) with approximately left 10% unassigned. Three phyla were dominant, with 52%, 19%, and 16% of sequences assigned to *Proteobacteria*, *Firmicutes* and *Bacteriodetes*, respectively (Table B.1). When this soil was incubated in an alkaline Fe-reducing media a microbial consortium was cultured that survived repeated progressions. The 16s rRNA gene

sequences recovered from this consortium were dominated by the phylum *Firmicutes* (91% of the 47 sequences), with just 2% assigned to *Proteobacteria* and 7% left unassigned (Table B.4). Of the *Firmicutes* sequences in this consortium, all were found to be members of the *Clostridiales* order with representatives identified to genus level that were also found in the original soil sample, such as *Anaerobranca* and *Tissierella.*

4.3.5 Oxidation experiments

An aqueous suspension of soil sample B2-310 was oxidised for 60 days with deionised water in equilibrium with atmospheric O_2. After 14 days of oxidation 1.5% of the total Cr within the soil was remobilised as Cr(VI) and no further remobilisation occurred for the remainder of the 60 days experiment (Figure 4.8). The % of 0.5N HCl extractable iron that was Fe(II) decreased, the Eh increased from -37 ± 15 mV to +202 ± 33 mV, and aqueous Fe decreased from 31 ± 23 μmol L^{-1} to 11 ± 2 μmol L^{-1} over the course of the experiment. The pH dropped rapidly from an initial value of 11 to just above 8 after 4 days, and then remained steady about this value.

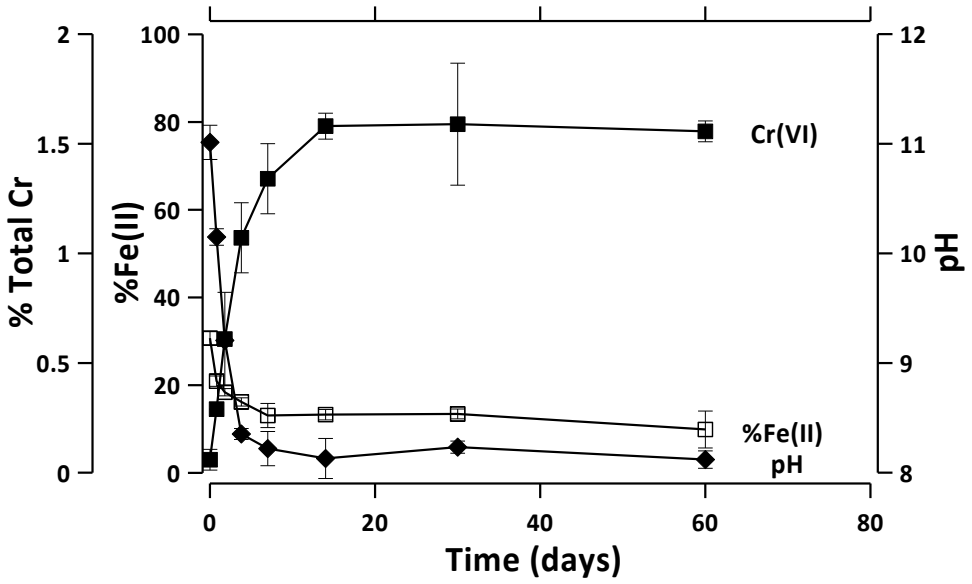

Figure 4.8 Air oxidation experiments; remobilisation of Cr to solution as a percentage of total Cr (■); pH (◆); % of 0.5N HCl extractable iron as Fe(II) (□). Error bars are the range of the duplicate experiments.

4.4 Discussion

4.4.1 Ground model

Data from the six boreholes advanced during this project were used to further develop the existing ground model for the site (Figure 4.1c). They confirm COPR waste has been placed directly over the alluvial soils and then covered with topsoil. The relationship between the brown clay and the COPR indicates that it is made ground that was placed after COPR tipping. The grey clay, which was absent in B6 closest to the river, is thought to have been the surface layer prior to COPR tipping. The gravel layer is part of the alluvial deposits that underlie the entire site. Data from a confidential commercial site investigation conducted in 2007 (locations shown in Figure 4.1a) support the proposed ground model, and reveal that the alluvial deposits are ~8m thick. A hydrogeology study in April 2009 (Atkins, 2009) revealed that there is a perched water table in the waste just over 2 m above the underlying water table in the alluvial deposits, and that the underlying flow in the alluvial deposits is

roughly south-westerly from the valley side towards the river. Together, the local lithology, the perched water table and the direction of underlying flow indicated that water flow from the COPR tip is initially downward and then towards the river roughly along the pseudo-section in Figure 4.1b.

4.4.2 Distribution and speciation of Cr in soils

The general trend in the borehole data (Table 4.1) is that the Cr concentration in the soil decreases with distance from the waste. The variation in the Cr content of samples from B4 and B5 is counter to the general trend, but this may be attributed to non-uniform flow of contaminated water as it migrates away from the tip. Furthermore, B4 and B5 are slightly offset laterally in opposite directions from the line of the pseudo section (Figure 4.1b), and thus may have received slightly different influent water. The trend can be explained either by transport of waste particles into the soil or by interaction with a plume of Cr(VI) containing leachate. Cr(III) in COPR is found predominately in unreacted chromite ore particles (Geelhoed et al., 2003; Stewart et al., 2010; Tinjum et al., 2008). However, XANES analysis suggest that Cr is present in the soil predominately as a poorly crystalline Cr(III) phase (Figure 4.3). EXAFS spectra from samples close to the waste also lack the spectral features characteristic of chromite samples (there are no sub peaks at K=5.1 and 8$Å^{-1}$, Figure 4.9) and the coordination environment is inconsistent with chromite Cr-Fe bond distances (Derbyshire and Yearian, 1958; Doelsch et al., 2006; Peterson et al., 1997) (Table 4.4).

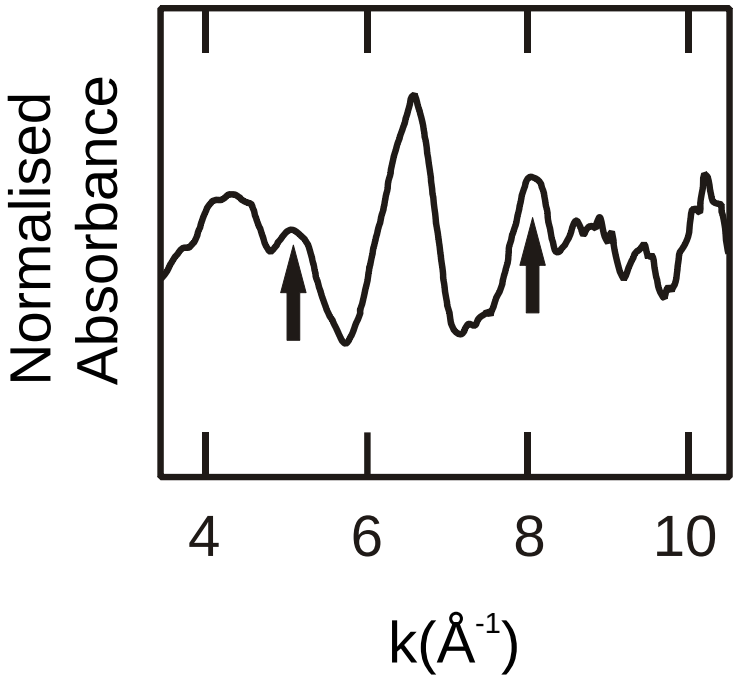

Figure 4.9 Chromite ore Cr K-edge EXAFS spectra. Arrows highlight the characteristic sub peak features at k=5.1 and 8 $Å^{-1}$, redrawn from Doelsch et al. (2006).

Table 4.4 Idealised Cr molecular co-ordination environment in the chromite structure where n is the number of atoms in each shell and R is the bond distance. Calculated from structural information presented in Derbyshire et al. (1958).

Structure	Shell	n	R (Å)
Chromite	O	6	1.99
	Cr-Cr	6	2.97
	Cr-Fe	6	3.47

The Cr(III) coordination environment in all samples with EXAFS analysis was fitted with 6 oxygen atoms at 1.97→1.99Å, indicating octahedral Cr-O coordination. Further shells of Fe(Cr) atoms at distances of 3.06→3.07 and 3.30→3.34Å from the central Cr atom are characteristic of the edge and double corner octahedral sharing geometries present in Cr(III) substituted iron oxy-hydroxides (Charlet and Manceau, 1992; Frommer et al., 2010; Hansel et al., 2005; He et al., 2004). The presence of an additional shell of backscatters at 3.93→4.02Å could indicate that single corner

sharing geometries are present in surface precipitation of γ-CrOOH on hydrous ferric oxides (Charlet and Manceau, 1992). γ-CrOOH also has a Cr-Cr edge sharing bond distance of 3.06Å (Charlet and Manceau, 1992). Therefore the Cr(III) coordination resolved by EXAFS analysis of soil samples can be best described as that of a poorly ordered Cr-Fe-OOH precipitate containing both incorporated and surface precipitated Cr(III). This interpretation is supported by the STEM analysis of B2-310 soil (Figure 4.5), which found that Cr was associated with 5-10nm sized Fe-rich particles. Identification of this mixed Cr(III)-Fe(III) oxy-hydroxide phase indicates that chromium in soils receiving water from the COPR waste is not the result of transport of chromite particles from the waste, and therefore, is most likely the result of *in situ* reduction of Cr(VI) from the contaminated groundwater by reaction with Fe(II).

4.4.3 Reduction of Cr(VI) in microcosms

The microcosm experiments show that soil from B2-310 is capable of removing Cr(VI) from the COPR leachate. Cr(VI) reduction was observed in both sterile and non-sterile microcosms indicating that the reaction was abiotic (Figure 4.7). At pH values greater than 6 the most likely abiotic removal mechanism is reduction to Cr(III) by soil associated Fe(II) followed by precipitation (Lin, 2002). The percentage of Fe(II) in the 0.5N HCl extractions reduced slightly during the incubation which is compatible with Fe(II) being consumed by reaction with the Cr(VI), although the overall change is within the measurement error. This minor reduction in Fe(II) during Cr(VI) removal is consistent with the calculated Fe(II) : Cr(VI) ratio of 20-30:1 present in these experiments.

4.4.4 Capacity for Fe(III)-reduction in alkaline soils

Bioreduction of Fe(III) oxides is commonplace in water saturated soils containing organic matter. The elevated pH and Cr(VI) conditions existing at this site provide additional challenges to microbial respiration. Despite this, a relatively diverse microbial community was characterised from soil B2 310. Many of the sequences in this community are best database matches to bacteria isolated from studies of high pH tufa and soda lake environments (Stougaard et al., 2002; Tiago et al., 2004), as well as unidentified sequences from other COPR affected environments (Stewart et al., 2010; Stewart et al., 2007).

The isolation of a community of microorganisms capable of Fe(III) reduction from B2-310 soil clearly shows that this soil contains indigenous microorganisms capable of iron reduction. Around 40% of the 0.5N HCl extractable Fe present in B2-310 soil is Fe(II), despite the constant exposure to a Cr(VI) flux for over 100 years, which indicates that there must be a mechanism for replenishing Fe(II) within this soil. Taken together, these facts strongly suggest microbial iron reduction is responsible for the Fe(II) present in the soil and, by implication, is indirectly responsible for the reductive precipitation of Cr(VI). The relative dominance of the *Firmicutes* sequences in the consortium extracted by growth in alkaline Fe(III)-citrate media (Table B.4), when compared to the population from the original soil, suggests that members of this phylum are responsible for the Fe(III) reducing capacity. The indigenous population of B2-310 soil did not induce Fe(II) accumulation in soil microcosms at pH 12 where soil organic matter was available as an electron donor (~1% TOC, Table 4.1), indicating that the microbial mechanism for producing the

Fe(II) at high pH is either slow or was not reproduced successfully in these homogenised systems.

4.4.5 Soil oxidation experiments

During oxidation of B2-310 soil only a small amount of Cr(VI) was remobilised (Figure 4.8) despite the increase in Eh and decrease in the percentage of 0.5N HCl extractable iron as Fe(II) indicating that soil oxidation occurred. This minor remobilisation may be attributable to either desorption of Cr(VI) or oxidation of Cr(III). The pH drop observed during soil oxidation can be attributed to both the oxidation and the hydrolysis of Fe minerals, which consume OH^- (Cornell and Schwertmann, 2003), and the development of a carbonate buffered system due to dissolution of atmospheric CO_2. As CrO_4^{2-} adsorbs strongly to surfaces at pH values below 8 (Langmuir, 1997), measurement of the concentration in the aqueous phase will have slightly underestimated the amount of Cr(VI) in the system. However the amount of Cr(VI) present in the soil after oxidation for 60 days is too low to be detected by XAS (Figure 4.3). Also the EXAFS spectra from the oxidised experimental sample is fitted best by the same 3 shell Fe(Cr) model as the other soil samples. This indicates that the majority of the Cr remains in the same coordination environment in the solid phase. This is consistent with the work of others who have shown that Cr(III) is not readily reoxidised in air alone (Schroeder and Lee, 1975). Mn oxides are known to be more effective oxidising agents for Cr(III) (Kim et al., 2002), but this is not an immediate concern at the study site as any Mn-oxides present would probably have been reduced during the development of microbial anoxia that resulted in Fe(II) accumulation in soils (Lovley, 1991). The lack of reactivity suggests that once Cr has accumulated in the soils beneath the waste, it is in a form that is resistant to remobilisation via air oxidation.

4.4.6 Implications for managing legacy COPR waste sites

For the site reported here, the presence of a layer of Fe(II)-containing sandy clay beneath the waste seems to have two beneficial outcomes. Firstly, it acts as an aquitard reducing the water flux from the waste into the aquifer below. Instead, contaminated water at this site is directed to surface discharge, where there is at least an opportunity to intercept and treat it (currently much of the water from the COPR drains into a ditch along the southern boundary; Figure 4.1a). Secondly, reaction of Cr(VI) with soil associated Fe(II) within the clay layer produces a Cr(III)-Fe(III) oxy-hydroxide precipitate that is resistant to oxic remobilisation, significantly reducing the downward migration of Cr(VI).

The presence of a Fe(II)-containing soil beneath the waste may seem fortuitous and site specific in nature, but it appears to be the result of a common metabolic process in soil microorganisms and is driven by natural soil organic matter. At a COPR site in New Jersey (Higgins et al., 1998) it was observed that a anoxic, organic-rich soil horizon directly beneath the waste also prevented Cr(VI) migration from the COPR into underlying aquifers. It therefore seems likely that reductive precipitation of Cr(VI) by soil associated Fe(II) also occurred at that site. Site investigations of COPR contaminated land should therefore determine the redox state of the subsurface below the waste and assess if Fe(II)-containing soils are present and can act as natural "reactive barriers" for Cr(VI) contaminated water. In addition, even where unfavourable oxidising conditions exist, populations of alkali and Cr(VI) tolerant Fe(III)-reducing bacteria are often present (Whittleston et al., 2011) and it may be possible to induce *in situ* microbial Fe(III)-reduction (e.g. by addition of electron donors) to produce Fe(II) in the soil, and thus attenuate Cr(VI) migration.

4.5 Conclusions

Cr(VI) is migrating with water from the legacy COPR tip into the underlying soil layers. Chromium is accumulating in these soils predominately in its reduced Cr(III) form within a mixed Cr(III)-Fe(III) oxy-hydroxide phase which is resistant to air oxidation. The soil directly beneath the waste is sub-oxic, with a substantial proportion of the microbial available iron as Fe(II), and it contains an indigenous microbial population capable of reducing iron from Fe(III) to Fe(II). Thus these results suggest that Cr(VI) derived from the highly alkaline COPR can be effectively sequestered in the soil beneath the waste through reduction by microbially produced soil associated Fe(II), and this results in co-precipitation as Cr(III) within a stable Fe(III) oxide host phase.

4.6 Acknowledgments

RAW is funded by a University of Leeds, John Henry Garner Scholarship. Thanks to: Dr Phil Studds and Mark Bell, Ramboll UK, for enabling field work; Eric Condliffe, University of Leeds, for support during SEM analysis; and Fred Mosselmans for advice during STFC funded EXAFS experiments at the Diamond Light Source.

4.7 References

ASTM, 2006. D4972-01: standard test method for pH of soils. Annual book of ASTM standards. American Society for Testing and Materials 4, 963-965.

Atkins, J., 2009. Modelling groundwater and chromite migration through an old spoil tip in Copley., MSc Dissertation School of Earth and Environment. University of Leeds, Leeds, UK.

Broadway, A., Cave, M.R., Wragg, J., Fordyce, F.M., Bewley, R.J.F., Graham, M.C., Ngwenya, B.T., Farmer, J.G., 2010. Determination of the bioaccessibility of chromium in Glasgow soil and the implications for human health risk assessment. Sci Total Environ 409, 267-277.

Burke, I.T., Boothman, C., Lloyd, J.R., Livens, F.R., Charnock, J.M., McBeth, J.M., Mortimer, R.J.G., Morris, K., 2006. Reoxidation behavior of technetium, iron, and sulfur in estuarine sediments. Environ. Sci. Technol. 40, 3529-3535.

Charlet, L., Manceau, A., 1992. X-Ray Absorption Spectroscopic Study of the Sorption of Cr(Iii) at the Oxide Water Interface .2. Adsorption, Coprecipitation, and Surface Precipitation on Hydrous Ferric-Oxide. J. Colloid Interface Sci. 148, 443-458.

Cornell, R.M., Schwertmann, U., 2003. The Iron Oxides: Structure, Properties, Reactions, Occurances and Uses, 2nd ed. WILEY-VCH, Weinheim.

Darrie, G., 2001. Commercial extraction technology and process waste disposal in the manufacture of chromium chemicals from ore. Environ. Geochem. Health 23, 187-193.

Deakin, D., West, L.J., Stewart, D.I., Yardley, B.W.D., 2001. Leaching behaviour of a chromium smelter waste heap. Waste Manage. 21, 265-270.

Derbyshire, W.D., Yearian, H.J., 1958. X-Ray Diffraction and Magnetic Measurements of the Fe-Cr Spinels. Phys. Rev. 112, 1603-1607.

Doelsch, E., Basile-Doelsch, I., Rose, J., Masion, A., Borschneck, D., Hazemann, J.L., Saint Macary, H., Borrero, J.Y., 2006. New combination of EXAFS spectroscopy and density fractionation for the speciation of chromium within an andosol. Environ. Sci. Technol. 40, 7602-7608.

Fendorf, S.E., 1995. Surface-Reactions of Chromium in Soils and Waters. Geoderma 67, 55-71.

Frommer, J., Nachtegaal, M., Czekaj, I., Kretzschmar, R., 2010. The Cr X-ray absorption K-edge structure of poorly crystalline Fe(III)-Cr(III)-oxyhydroxides. Am. Miner. 95, 1202-1213.

Geelhoed, J.S., Meeussen, J.C.L., Hillier, S., Lumsdon, D.G., Thomas, R.P., Farmer, J.G., Paterson, E., 2002. Identification and geochemical modeling of processes controlling leaching of Cr(VI) and other major elements from chromite ore processing residue. Geochim. Cosmochim. Acta 66, 3927-3942.

Geelhoed, J.S., Meeussen, J.C.L., Roe, M.J., Hillier, S., Thomas, R.P., Farmer, J.G., Paterson, E., 2003. Chromium remediation or release? Effect of iron(II) sulfate addition on chromium(VI) leaching from columns of chromite ore processing residue. Environ. Sci. Technol. 37, 3206-3213.

Hansel, C.M., Benner, S.G., Fendorf, S., 2005. Competing Fe(II)-induced mineralization pathways of ferrihydrite. Environ. Sci. Technol. 39, 7147-7153.

He, Y.T., Chen, C.C., Traina, S.J., 2004. Inhibited Cr(VI) reduction by aqueous Fe(II) under hyperalkaline conditions. Environ. Sci. Technol. 38, 5535-5539.

Higgins, T.E., Halloran, A.R., Dobbins, M.E., Pittignano, A.J., 1998. In situ reduction of hexavalent chromium in alkaline soils enriched with chromite ore processing residue. Japca J. Air. Waste Ma. 48, 1100-1106.

Horikoshi, K., 2004. Alkaliphiles. P. Jpn. Acad. A-Phys. 80, 166-178.

Kim, J.G., Dixon, J.B., Chusuei, C.C., Deng, Y.J., 2002. Oxidation of chromium(III) to (VI) by manganese oxides. Soil Sci. Soc. Am. J. 66, 306-315.

Langmuir, D., 1997. Adsorption-Desorption Reactions, Aqueous Environmental Geochemistry. Prentice-Hall, Inc., Upper Saddle River, NJ, p. 371.

Lin, C.J., 2002. The chemical transformations of chromium in natural waters - A model study. Water Air Soil Poll. 139, 137-158.

Lovley, D.R., 1991. Dissimilatory Fe(III) and Mn(IV) Reduction. Microbiol. Rev. 55, 259-287.

Lovley, D.R., 1997. Microbial Fe(III) reduction in subsurface environments. FEMS. Microbiol. Rev. 20, 305-313.

Lovley, D.R., Phillips, E.J.P., 1986. Availability of Ferric Iron for Microbial Reduction in Bottom Sediments of the Fresh-Water Tidal Potomac River. Appl. Environ. Microbiol. 52, 751-757.

Parsons, J.G., Dokken, K., Peralta-Videa, I.R., Romero-Gonzalez, J., Gardea-Torresdey, J.L., 2007. X-ray absorption near edge structure and extended X-ray absorption fine structure analysis of standards and biological samples containing mixed oxidation states, of chromium(III) and Chromium(VI). Appl. Spectrosc. 61, 338-345.

Pechova, A., Pavlata, L., 2007. Chromium as an essential nutrient: a review. Vet. Med-Czech 52, 1-18.

Peterson, M.L., Brown, G.E., Parks, G.A., 1996. Direct XAFS evidence for heterogeneous redox reaction at the aqueous chromium/magnetite interface. Colloid Surf. A-Physicochem. Eng. Asp. 107, 77-88.

Peterson, M.L., White, A.F., Brown, G.E., Parks, G.A., 1997. Surface passivation of magnetite by reaction with aqueous Cr(VI): XAFS and TEM results. Environ. Sci. Technol. 31, 1573-1576.

Pollock, J., Weber, K.A., Lack, J., Achenbach, L.A., Mormile, M.R., Coates, J.D., 2007. Alkaline iron(III) reduction by a novel alkaliphilic, halotolerant, Bacillus sp isolated from salt flat sediments of Soap Lake. Appl. Microbol. Biot. 77, 927-934.

Rai, D., Sass, B.M., Moore, D.A., 1987. Chromium(Iii) Hydrolysis Constants and Solubility of Chromium(Iii) Hydroxide. Inorg. Chem. 26, 345-349.

Rehman, A., Shakoori, A.R., 2001. Heavy metal resistance Chlorella spp., isolated from tannery effluents, and their role in remediation of hexavalent chromium in industrial waste water. B. Environ. Contam. Tox. 66, 542-547.

Rehman, A., Zahoor, A., Muneer, B., Hasnain, S., 2008. Chromium tolerance and reduction potential of a Bacillus sp.ev3 isolated from metal contaminated wastewater. B. Environ. Contam. Tox. 81, 25-29.

Richard, F.C., Bourg, A.C., 1991. Aqueous geochemistry of Cr: A review. Water Res. 25, 807-816.

Saraswat, I.P., Vajpei, A.C., 1984. Characterization of Chromium-Oxide Hydrate Gel. J. Mater. Sci. Lett. 3, 515-517.

Schroeder, D.C., Lee, G.F., 1975. Potential Transformations of Chromium in Natural-Waters. Water Air Soil Poll. 4, 355-365.

Schumacher, B.A., 2002. Methods for the Determination of Total Organic Carbon (TOC) in Soils and Sediments. United States Environmental Protection Agency, Las Vegas.

Stewart, D.I., Burke, I.T., Hughes-Berry, D.V., Whittleston, R.A., 2010. Microbially mediated chromate reduction in soil contaminated by highly alkaline leachate from chromium containing waste. Ecol. Eng. 36, 211-221.

Stewart, D.I., Burke, I.T., Mortimer, R.J.G., 2007. Stimulation of microbially mediated chromate reduction in alkaline soil-water systems. Geomicrobiol. J. 24, 655-669.

Stougaard, P., Jorgensen, F., Johnsen, M.G., Hansen, O.C., 2002. Microbial diversity in ikaite tufa columns: an alkaline, cold ecological niche in Greenland. Environ. Microbiol. 4, 487-493.

Tiago, I., Chung, A.P., Verissimo, A., 2004. Bacterial diversity in a nonsaline alkaline environment: Heterotrophic aerobic Populations. Appl. Environ. Microbiol. 70, 7378-7387.

Tinjum, J.M., Benson, C.H., Edil, T.B., 2008. Mobilization of Cr(VI) from chromite ore processing residue through acid treatment. Sci. Total Environ. 391, 13-25.

USEPA, 1992. SW-846 Manual: Method 7196a. Chromium hexavalent (colorimetric). Retrieved 6th Jan 2006.

USEPA, 1998. Toxicological review of hexavalent chromium. Available online at http://www.epa.gov/ncea/iris.

Viollier, E., Inglett, P.W., Hunter, K., Roychoudhury, A.N., Van Cappellen, P., 2000. The ferrozine method revisited: Fe(II)/Fe(III) determination in natural waters. Appl. Geochem. 15, 785-790.

Vitale, R.J., Mussoline, G.R., Petura, J.C., James, B.R., 1997. Cr(VI) soil analytical method: A reliable analytical method for extracting and quantifying Cr(VI) in soils. J. Soil Contam. 6, 581-593.

Wang, Q., Garrity, G.M., Tiedje, J.M., Cole, J.R., 2007. Naive Bayesian classifier for rapid assignment of rRNA sequences into the new bacterial taxonomy. Appl. Environ. Microbiol. 73, 5261-5267.

Weber, K.A., Picardal, F.W., Roden, E.E., 2001. Microbially catalyzed nitrate-dependent oxidation of biogenic solid-phase Fe(II) compounds. Environ. Sci. Technol. 35, 1644-1650.

Whittleston, R.A., Stewart, D.I., Mortimer, R.J.G., Ashley, D.J., Burke, I.T., 2011. Effect of Microbially Induced Anoxia on Cr(VI) Mobility at a Site Contaminated with Hyperalkaline Residue from Chromite Ore Processing. Geomicrobiol. J. 28, 68-82.

Zavarzina, D.G., Kolganova, T.V., Boulygina, E.S., Kostrikina, N.A., Tourova, T.P., Zavarzin, G.A., 2006. Geoalkalibacter ferrihydriticus gen. nov sp nov., the first alkaliphilic representative of the family Geobacteraceae, isolated from a soda lake. Microbiol. 75, 673-682.

Chapter 5 Effect of microbially induced anoxia on Cr(VI) mobility at a site contaminated with hyperalkaline residue from chromite ore processing

Abstract

This paper reports an investigation of microbially mediated Cr(VI) reduction in a hyper alkaline, chromium contaminated soil-water system representative of the conditions at a chromite ore processing residue (COPR) site. Soil from the former surface layer that has been buried beneath a COPR tip for over 100 years was shown to have an active microbial population despite a pH value of 10.5. This microbial population was able to reduce nitrate using an electron donor(s) that was probably derived from the soil organic matter. With the addition of acetate, nitrate reduction was followed in turn by removal of aqueous Cr(VI) from solution, and then iron reduction. Removal of ~300μM aqueous Cr(VI) from solution was microbially mediated, probably by reductive precipitation, and occurred over a few months. Thus, in soil that has had time to acclimatize to the prevailing pH value and Cr(VI) concentration, microbially mediated Cr(VI) reduction can be stimulated at a pH of 10.5 on a time scale compatible with engineering intervention at COPR contaminated sites.

5.1 Introduction

Chromium is among the most extensively used transition metals in the chemical and metal alloy industries, including leather tanning, wood preservation, chrome metal finishing, and manufacture of dyes, paints, pigments, and stainless steel (Morales-Barrera and Cristiani-Urbina, 2008; Wang, 2000). In order to obtain chromium from chromite ($FeCr_2O_4$), the ore is roasted with an alkali-carbonate at 1150ºC, to oxidise the relatively insoluble Cr(III) to soluble chromate (Cr(VI)), which is then extracted with water as sodium chromate upon cooling. Lime (CaO) was traditionally added as a diluent to increase air penetration and provide sufficient O_2 for chromite oxidation in a practice known as the "high-lime" process (Farmer et al., 1999). Lime was replaced by cheaper alternatives of limestone ($CaCO_3$) and dolomite ($CaMg(CO_3)_2$) around the turn of the 20th century, and this variant of the high-lime process remained the dominant method of chromium extraction until the early 1960's when it was superseded by lime free processes (Darrie, 2001).

Economically developed nations no longer use the high-lime process to extract chromium, but until recently it still accounted for 40% of chromium production worldwide (Darrie, 2001). Due to its inefficient use of raw materials the high-lime process produces up to 4 tonnes of waste per ton of product (Walawska and Kowalski, 2000). Thus it is still responsible for producing large quantities of chromium containing waste (600,000 t.yr-1 in 2001; Darrie, (2001)). This waste, known as chromite ore processing residue (COPR), is highly alkaline due to the calcium hydroxide (CaOH) produced from the limestone, and typically contains between 2-8% chromium (w/w) (Geelhoed et al., 2003; Sreeram and Ramasami, 2001; Tinjum et al., 2008; Walawska and Kowalski, 2000). Of this, up to 35% can be

in the form of the toxic, carcinogenic and environmentally mobile chromate anion (CrO_4^{2-}) (Farmer et al., 2006; James, 1994; Tinjum et al., 2008). As a result, water in contact with COPR has a characteristically high pH of 9-12 (Geelhoed et al., 2003; Stewart et al., 2007), and can contain up to 1.6 mM Cr(VI) as chromate (Farmer et al., 2002).

Remediation of legacy sites contaminated with COPR is challenging, particularly because these sites are often in urban areas and date from times when COPR disposal was quite poorly managed (Stewart et al., 2007). Traditional "dig and dump" remediation strategies are not only financially costly due to the large volumes of waste involved, but also inadvisable due to the risk of forming Cr(VI) bearing dusts during large scale manipulation. Such an approach would create a pathway to human exposure, as Cr(VI) bearing dust is a confirmed human carcinogen through inhalation (USEPA, 1998).

In contrast to the harmful properties of Cr(VI), the reduced form Cr(III) is an essential trace nutrient in plants and animals, required for fat and glucose metabolism, amino and nucleic acid synthesis, and correct insulin function (Pechova and Pavlata, 2007; Richard and Bourg, 1991). Also the Cr(III) cation is much less mobile in the subsurface environment than the CrO_4^{2-} anion as it readily sorbs to soil minerals, and (co)-precipitates as insoluble Cr(III) hydroxides in neutral and alkaline environments (Fonseca, 2009; Han et al., 2006; Lee et al., 2003; Rai et al., 1987; Richard and Bourg, 1991). Thus the reduction of Cr(VI) to Cr(III) in-situ would significantly reduce the hazard posed by chromium contaminated groundwater.

The ability of indigenous soil microorganisms to couple organic matter oxidation to the reduction of transition metals, such as iron and manganese, during dissimilatory metabolism is well documented (Lovley, 1993b). Where sufficient organic matter is available for oxidation, progressively more anoxic conditions develop and a cascade of terminal-electron-accepting processes (TEAPs) occur in sequence (Froelich et al., 1979). Microbial processes releasing most energy are favoured, so the sequence in which electron acceptors are used typically follows the decreasing order of redox potentials shown in Table 2.2.

Iron is by far the most abundant redox-active metal in soils, and cycling between Fe(II) and Fe(III) is a prominent factor affecting other chemical processes (Stucki et al., 2007). Fe(III) is relatively insoluble except in acidic solutions and precipitation usually proceeds via intermediates, $Fe_2(OH)_2^{4+}$ and ferrihydrite, which are metastable with regard to goethite (α-FeO(OH) and hematite (α-Fe_2O_3); goethite being favoured in alkaline conditions (Cudennec and Lecerf, 2006; Schwertmann et al., 1999). Aqueous Fe(II) is stable in acidic and neutral conditions, but can precipitate as siderite ($FeCO_3$) if carbonate is present and will precipitate as $Fe(OH)_2$ at high pH values (Langmuir, 1997). Fe(II)/Fe(III) cycling occurs naturally in soils particularly where there are periodic changes in water content (Stucki et al., 2007), and iron cycling can be important where there is a redox active contaminant flux (Lovley, 1993b). For example Cr(VI) is readily reduced to Cr(III) by Fe(II) oxidation to Fe(III) (Richard and Bourg, 1991). As Cr(III) can substitute for Fe(III) in many iron minerals, any Cr(VI) that is reduced by Fe(II) is likely to be incorporated into iron(III) oxyhydroxides (Fendorf, 1995). Such metastable iron oxyhydroxides exhibit high bioavailability (Hansel et al., 2005) and thus Fe(II)/Fe(III) cycling continues.

A broad range of microbial taxa can grow optimally and robustly in high pH environments like those found at COPR disposal sites (Roadcap et al., 2006). These microbes, called alkaliphiles, have adapted to this challenging environment with mechanisms for regulating cytoplasmic pH and by producing surface layer enzymes that function at high pH. For example many alkaliphiles use a Na^+ electrochemical gradient to maintain pH homeostasis and to energize solute uptake and motility (Detkova and Pusheva, 2006; Krulwich et al., 2001). Similarly many microorganisms have demonstrated tolerance to Cr(VI) including *Pannonibacter phragmitetus*, which showed no evidence of cell degradation at 500 mg l^{-1} Cr(VI) (Chai et al., 2009; Chen and Hao, 1998; Rehman et al., 2008; Zhu et al., 2008). As Cr(VI) is readily able to cross cell membranes by utilising the sulphate transport system (Cervantes et al., 2001), tolerance to Cr(VI) may indicate an evolutionary response to Cr(VI) toxicity.

Microbial reduction of Cr(VI) was first observed with *Pseudomonas dechromaticans* (Romanenko and Koren'kov, 1977), and has since been reported in a number of Gram negative genera including *Pseudomonas*, *Desulfovibro* and *Shewanella*, and members of the Gram positive *Bacillus* and *Cellulomonas* (Francis et al., 2000; Lovley, 1993a; Sani et al., 2002; Sau et al., 2008). Direct microbial Cr(VI) reduction has been observed during aerobic (Bopp and Ehrlich, 1988; Ishibashi et al., 1990) and anaerobic respiration (Daulton et al., 2007; Neal et al., 2002; Suzuki et al., 1992), but only a few studies have clearly demonstrated anaerobic growth dependent solely on the use of Cr(VI) as an electron acceptor (e.g. Pantoea agglomerans, Francis et al., 2000). Even fewer studies have demonstrated direct microbial Cr(VI) reduction at high pH (although notable examples are reported by Chai et al., 2009;

VanEngelen et al., 2008; Zhu et al., 2008). Thus it has been suggested that microbially mediated Cr(VI) reduction in alkaline, chromium contaminated environments usually occurs by an indirect pathway involving extracellular reaction with reduced species, e.g. Fe(II) produced by respiration (Lloyd et al., 1998).

This chapter reports an investigation of microbially mediated Cr(VI) reduction in hyper alkaline soils (pH >10) from a COPR contaminated site in the north of England. It uses a multidisciplinary approach to gain an understanding into microbially induced anoxia at high pH, the microbial communities that develop, and their influence on Cr(VI) geochemistry in closed systems.

5.2 Materials and methods

5.2.1 Site description

The study site is in a glacial valley in-filled with alluvial deposits, which is located in the north of England (Figure 5.1). COPR waste has been tipped against the valley side between a canal and a river (the canal follows the valley side and locally is ~7 metres above the level of the river). The waste tip is approximately 2.2 hectares in area with a relatively flat top surface ~1.5m above the canal bank and steep side-slopes down to the valley floor (Stewart et al., 2010; Whittleston et al., 2007). This landform first appeared on historical maps in the late 19th century. Currently there is a thin soil cover on the waste with vegetation dominated by grasses and occasional small trees; however erosion has left the waste exposed on steeper slopes. A drainage ditch along the southern waste boundary frequently contains water that is alkaline, visibly yellow in colour, and has elevated Cr(VI) concentrations.

5.2.2 Site sampling

Several exploratory boreholes were advanced in March 2007 using cable percussion drilling. The soil sample used in this study was taken from ~1m below the waste, at a depth 7 metres below ground level (the soil sampling location is shown in Figure 5.1). It consisted of grey silty clay that is representative of the alluvial soils that would have been the surface layer prior to waste tipping. A water sample was collected from the leachate drainage ditch in February 2008 from a location close to where it enters the river. Samples were placed in sealed polythene containers at time of sampling and were stored at 4ºC in the dark within 4 hours of collection. Sample manipulations were kept to a minimum until they were required for experiments in March 2008. The soil sample was homogenised prior to use.

5.2.3 Sample characterisation

X-ray powder diffraction (XRD) analysis of the alluvial soil (ground to < 75 μm) was performed on a Philips PW1050 Goniometer, and X-ray fluorescence (XRF) analysis was undertaken using a fused sample on a Philips PW2404 wavelength dispersive sequential X-ray spectrometer (data were corrected for loss on ignition). Approximately 25g of homogenised soil was oven dried at 105°C and disaggregated with a mortar and pestle for carbon content determination. A portion of each sample was pre-treated with 10% HCl to remove any carbonates present (Schumacher, 2002). The total organic and inorganic carbon content of oven dried and HCl treated subsamples was measured using Carlo-Erba 1106 elemental analyser.

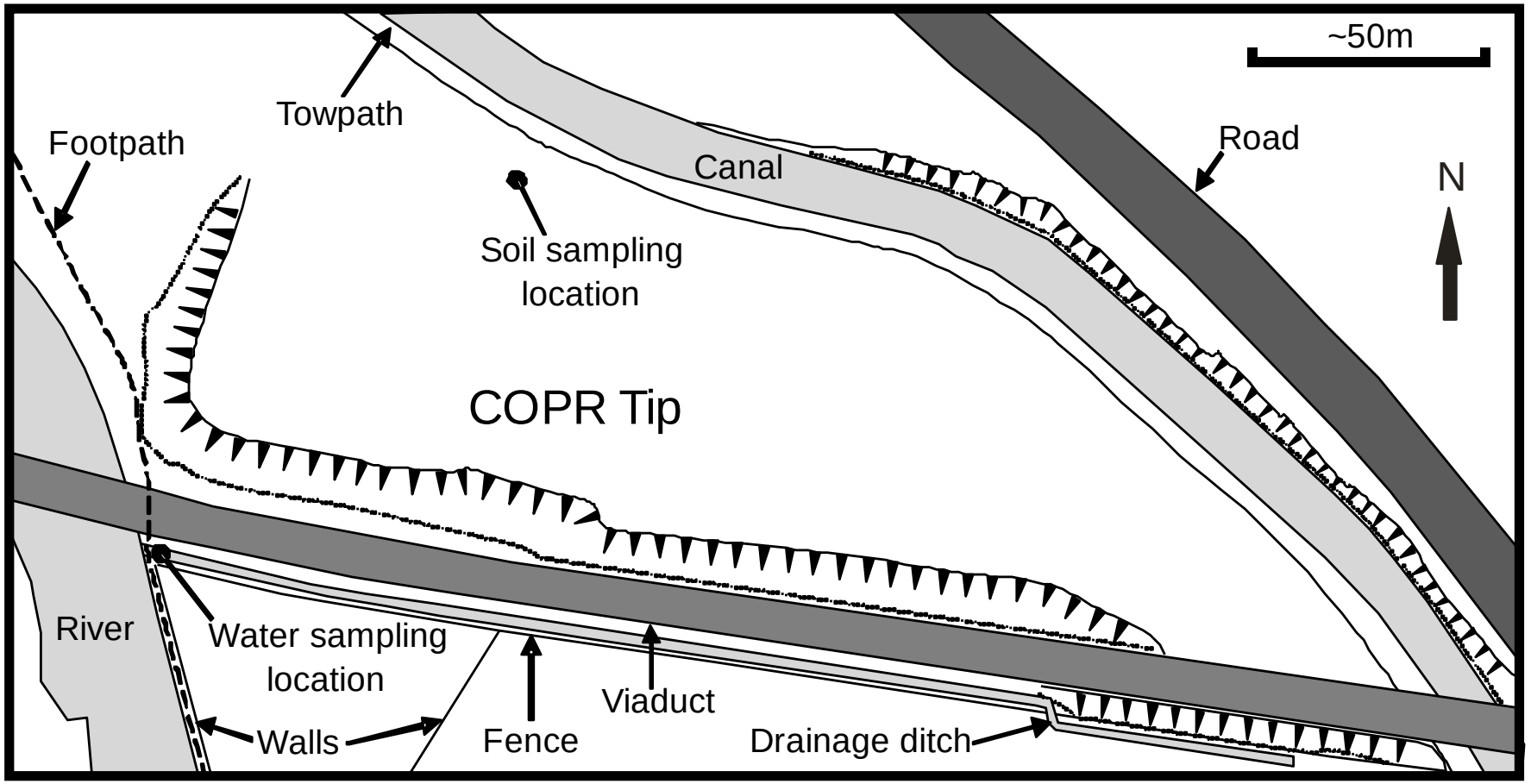

Figure 5.1 Sketch map of the site showing the sampling locations.

5.2.4 Reduction microcosm experiments

Microcosms were prepared using 10g of homogenised soil and 100 ml of ditch water in 120 ml glass serum bottles and sealed with butyl rubber stoppers and aluminium crimps. After sealing, the headspace was purged with nitrogen to displace oxygen present. Two different experimental conditions were established in triplicate microcosms. *Unamended* microcosms contained only the soil and ditch water. *Acetate amended* microcosms also contained sodium acetate to a final concentration of 20 mM. A control was prepared for each experiment in which the soil, sealed in the bottle with a nitrogen purged headspace, was heat sterilised at 120ºC for 20 minutes in an autoclave before filter sterilized ditch water and, in one case, sodium acetate were added. The microcosms and controls were periodically sub-sampled for geochemical and microbiological analysis to produce a progressive time series. At each sample point, microcosms were shaken and 3 ml soil slurry extracted using aseptic technique with sterile syringes and needles (Burke et al., 2006). Samples were centrifuged (5 min, 16,000g) and soil and water were analysed for a range of redox indicators, Cr(VI) and microbiology.

5.2.5 Geochemical methods

The pH was measured using an Orion bench top meter and calibrated electrodes (the pH electrode was calibrated between 4 and 10 using standard buffer solutions). The soil pH was measured using a 1:1 suspension in deionised water (ASTM, 2006). Sulfate, nitrate and chloride concentrations were determined by ion chromatography on a Dionex DX-600 with AS50 autosampler using a 2mm AS16 analytical column, with suppressed conductivity detection and gradient elution to 15 mM potassium hydroxide over 10 minutes. Samples were loaded in a random order to avoid

systematic errors. Standards covering the anticipated range of analyte concentrations were prepared with the addition of 25 µM Cr(VI) as potassium chromate. Between loading samples, the column was flushed with deionised water for 1.5 minutes.

Standard UV/VIS spectroscopy methods based on reactions with diphenycarbazide and ferrozine were used to determine aqueous Cr(VI) and Fe concentrations, respectively, using a Cecil CE3021 UV/VIS Spectrophotometer (USEPA, 1992; Viollier et al., 2000). Fe(II) in solids was determined after extraction by 0.5 N HCl and reaction with ferrozine (Lovley and Phillips, 1986). Standards for each analyte were used regularly. Calibration graphs exhibited good linearity (typically r^2>0.99).

5.2.6 DNA extraction

Soil samples from the triplicate microcosms at a single time point (day 68) were combined (typically ~0.25 g of soil) and microbial DNA was extracted using a FastDNA spin kit (Qbiogene, Inc.) and FastPREP instrument (unless explicitly stated, the manufacturer's protocols supplied with all kits employed were followed precisely). DNA fragments in the size range 3 kb ~20 kb were isolated on a 1% "1x" Tris-borate-EDTA (TBE) gel stained with ethidium bromide to enable viewing under UV light (10x TBE solution from Invitrogen Ltd., UK). The DNA was extracted from the gel using a QIAquick gel extraction kit (QIAGEN Ltd., UK.). This purified DNA was used for subsequent analysis.

5.2.7 16S rRNA gene sequencing

A fragment of the 16S rRNA gene of approximately ~500 bp was PCR amplified using broad-specificity bacterial primers 8f (5´-AGAGTTTGATCCTGGCTCAG-3´) (Eden et al., 1991) and 519r (5´-GWATTACCGCGGCKGCTG-3´) where K = G or

T, W = A or T (Lane et al., 1985). Each PCR reaction mixture contained 20 µl of purified DNA solution, GoTaq DNA polymerase (5 units), 1× PCR reaction buffer, $MgCl_2$ (1.5mM), PCR nucleotide mix (0.2 mM), T4 Gene 32 Protein (100 ng/µl) and 8f and 519r primers (0.6 µM each) in a final volume of 50 µl. The reaction mixtures were incubated at 95ºC for 2 min, and then cycled 30 times through three steps: denaturing (95ºC, 30 s), annealing (50ºC, 30s), primer extension (72ºC, 45 s). This was followed by a final extension step at 72ºC for 7min. The PCR products were purified using a QIAquick PCR Purification Kit. Amplification product sizes were verified by electrophoresis of 10 µl samples in a 1.0% agarose TBE gel with ethidium bromide straining.

The PCR product was ligated into the standard cloning vector pGEM-T Easy (Promega Corp., USA), and transformed into E. coli XL1-Blue supercompetent (Stratagene). Transformed cells were grown on LB-agar plates containing ampicillin (100 $\mu g.ml^{-1}$) at 37ºC for 17 hours. The plates were surfaced dressed with IPTG and X-gal (as per Stratagene protocol) for blue-white colour screening. For each sample, 48 colonies containing an insert were restreaked on LB-ampicillin agar plates and incubated at 37ºC. Single colonies from these plates were incubated overnight in liquid LB-ampicillin. Plasmid DNA was extracted using a QIAprep Spin miniprep kit (QIAGEN Ltd., UK) or PureYield Plasmid Miniprep System (Promega, UK) and sent for automated DNA sequencing on an ABI 3100*xl* Capillary Sequencer using the T7P primer. Sequences were analysed against the EMBL release nucleotide database in April 2009 using the NCBI-BLAST2 program (version 2.2.19 November 2009) and matched to known 16S rRNA gene sequences. Default BLAST parameters were used (match/mismatch scores 2, -3, open gap penalty 5, gap extension penalty

2). The nucleotide sequences described in this study were deposited in the GenBank database (accession numbers FN706451 - FN706510).

5.2.8 Phylogenetic tree building

The EMBOSS needle pairwise alignment program was used to assign similar gene sequences into clades based on sequence homology, using default parameters (open gap penalty 10, gap extension penalty 0.5). Selected sequences were then aligned with known bacterial 16S rRNA gene sequences from the EMBL database using the ClustalX software package (version 2.0.11), and a phylogenetic trees were constructed from the distance matrix by neighbour joining. Bootstrap analysis was performed with 1000 replicates, and resulting phylograms drawn using the TreeView (version 1.6.6) software package.

5.3 Results

5.3.1 Soil characterisation

XRD and XRF analysis of the alluvial soil showed that the major mineral was quartz with small amounts of kaolinite and muscovite. The XRF analysis indicated a concentration of chromium of 3020 $mg.kg^{-1}$ in the solid phase (see Table 5.1). The soil had a pH of 10.5. The total organic carbon (TOC) and total inorganic carbon (TIC) of the soil were found to be 3.6 and 0.2%, respectively. Water from the ditch along the southern edge of the waste had a pH of 11.4, and a Cr(VI), nitrate and sulphate concentrations of 293 µM (15.2 $mg.l^{-1}$), 163 µM (10.1 $mg.l^{-1}$), and 3.29 mM (316 $mg.l^{-1}$), respectively.

Table 5.1 Major elements in fused samples (%) measured by XRF (corrected for loss on ignition at 1000°C).

	SiO_2	Al_2O_3	CaO	MgO	Fe_2O_3	Cr_2O_3	TiO_2	Mn_3O_4	Na_2O	K_2O	SO_3	LOI
Grey silty clay	71.4	9.73	2.29	0.35	3.47	0.45	0.56	0.12	0.56	1.56	0.03	9.30
COPR waste	3.61	4.27	40.29	5.85	7.04	4.93	0.05	0.07	n.d.	0.03	5.10	28.40

5.3.2 Reduction microcosm experiments

The initial pH values of the *unamended* and *acetate-amended* microcosms were both 10.9, whereas the pH values of sterile controls were both 10.8. The active microcosm experiments had an initial aqueous Cr(VI), nitrate and sulphate concentration of 279 ± 2 µM, 96.5 ± 4.87 µM, and 3.01 ± 0.10 mM, respectively (Figure 5.2). The sterile controls had slightly higher initial aqueous Cr(VI) and sulphate concentrations of 287 ± 4 µM and 3.26 ± 0.06 mM, respectively. The *acetate-amended* sterile control had an initial nitrate concentration of 89.7 ± 9 µM. The nitrate concentration of the *unamended* sterile control was not measured due to technical difficulties (there was insufficient sample to repeat measurement). Initially the percentage of the total 0.5 N HCl extractable iron present as Fe(II) was 13.7 ± 1.1% in the active experiments whereas it was 10.0 ± 0.6% the heat treated controls.

In the microbially active *unamended* microcosms the pH of the active microcosms decreased from 10.9 to 9.9 over 175 days of incubation, whereas the pH of the sterile control decreased from 10.8 to 10.4 in the same time period (Figure 5.2). Nitrate removal from aqueous solution commenced shortly after the start of the test, with the concentration dropping by two-thirds by day 5, and was not detected on day 15. Over the test period, we noted very little change in aqueous Cr(VI) concentration in either

the active *unamended* or the control microcosms. Similarly we noted little change in the amount of total Fe(II) extractable by 0.5 N HCl and no discernable change in aqueous sulphate concentration in either the active or the control microcosms (see Figure 5.2). In the active *acetate-amended* microcosms the pH decreased from an initial value of 10.9 to a value of 10.1 on day 175, whereas the pH value of the sterile control decreased from 10.8 to 10.5. The trend in nitrate data was similar to that in the *unamended* microcosms, with nitrate removal commencing shortly after the start of the test and becoming undetectable by day 5. No nitrate removal was observed in the corresponding sterile control. The aqueous Cr(VI) concentration decreased in all three replicates once nitrate was below detection limits, but at different rates. In replicate II in which the aqueous chromate concentration decreased most rapidly, Cr(VI) was not detected on day 118. In replicate III where aqueous chromate concentration decreased least rapidly the concentration on day 175 was two-thirds of the initial value. No change in Cr(VI) concentration occurred in the corresponding controls. The trends in the proportion of the acid extractable iron present as Fe(II) also differed between the three replicates. In the early stages of all three *acetate-amended* microcosms about 20% of the 0.5 N HCl extractable iron was in the Fe(II) oxidation state, and this did not change significantly with time in replicates I and III. However in replicate II there was a significant increase in the proportion of the acid extractable iron present as Fe(II) shortly after Cr(VI) was completely removed from solution. In the *acetate-amended* sterile control (like the *unamended* sterile control), roughly 10% of the 0.5 N HCl extractable iron was present as Fe(II), which did not change with time. There was no discernable change in the aqueous sulphate concentration in either the active *acetate-amended* microcosms or corresponding control.

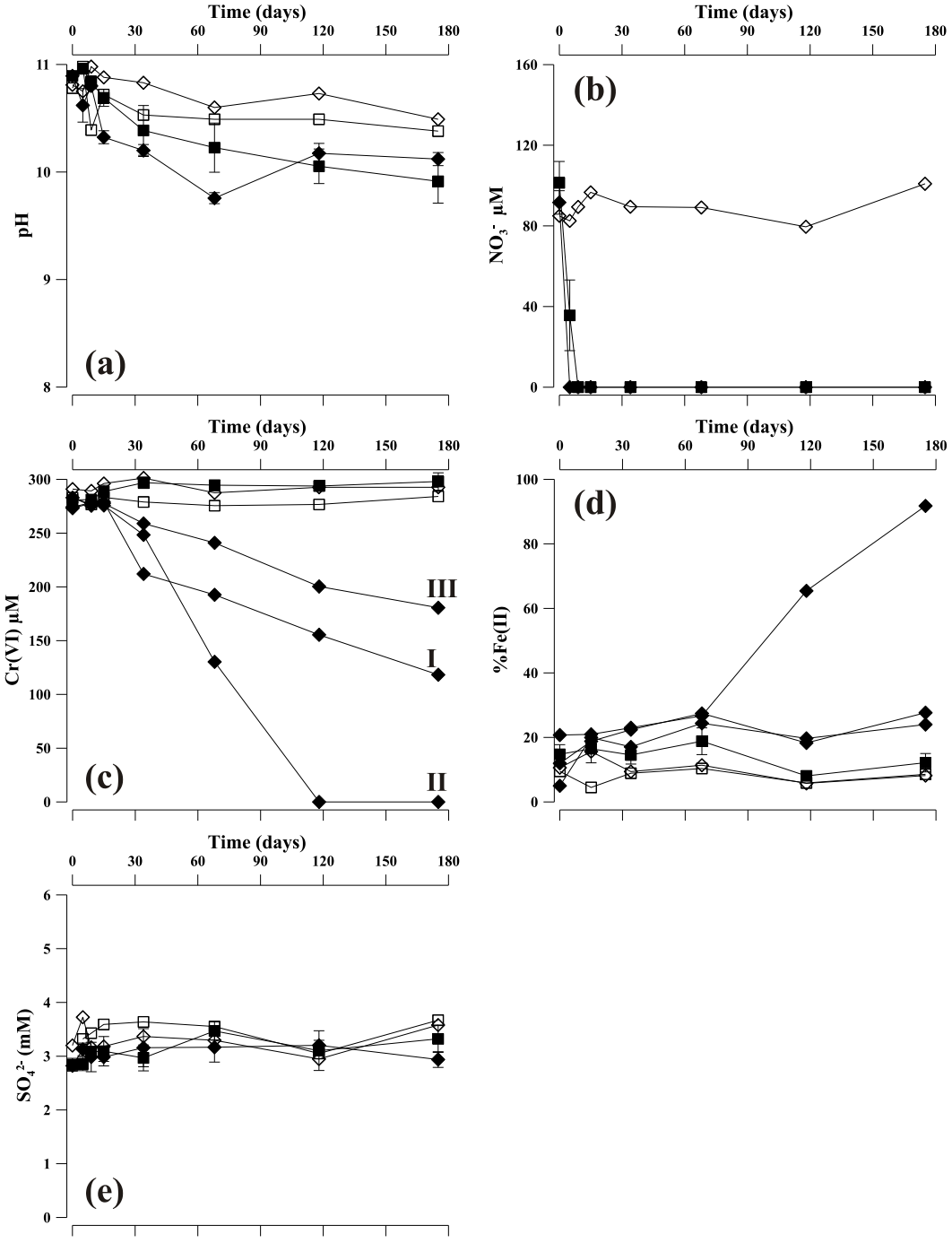

Figure 5.2 Geochemical response of the *unamended* (■) and *acetate-amended* (◆) microcosms: (a) pH, (b) porewater NO_3^- concentration, (c) porewater Cr(VI) concentration (d) % of 0.5 N HCl extractable Fe as Fe(II) in soils, (e) porewater SO_4^{2-} concentration. Response in individual *acetate-amended* microcosms from triplicate series (I-III) are shown in (c) and (d). Error bars shown are one standard deviation from the mean of triplicate experiments. NO_3^- and SO_4^{2-} data were corrected using Cl^- variability to account for instrument variability. Data from sterile controls are shown using open symbols.

5.3.3 Microbiological community analysis

Geochemical analysis indicated aqueous chromate removal was underway by day 68 in the *acetate amended* microcosms, but the behaviour of the three replicate microcosms had not diverged significantly. Therefore, on day 68, we pooled soil from each of the three *unamended* microcosms into one combined sample and from each of the three *acetate-amended* microcosms into a second combined sample. These two combined samples were then used to compare the microbial communities in each with respect to chromate removal from the liquid phase. Thirty 16S rRNA gene sequences recovered from each of the two samples were analyzed.

Initially sequences were assigned to a phylum (or class in the case of proteobacteria) using the NCBI-BLAST2 program, based on >95% identity over a sequence length of >400 bp to a known sequence in the EMBL release database. However, less than a third of sequences could be assigned in this way, although many sequences were more than >95% homologous to sequences from unidentified bacteria recovered from alkaline environments. Sequences that were >95% homologous to the same sequence in the database were further analysed using EMBOSS and grouped based on >98% mutual homology. ClustalX analysis and neighbour joining tree construction of these groups indicated there were four distinct clades amongst the initially unidentified sequences, subsequently called clades A, B, C and E. Further ClustalX analysis and NJ tree construction using characteristic members of each clade was used to assign clade members to a phylum. Members of clade A have been thus assigned to the Comamonadaceae family of β-proteobacteria that appear to be most closely related to the genera Rhodoferax, Hydrogenophaga and Malikia (Figure 5.3). Clade B were members of the Flexibacteraceae family of Bacteroidetes that

appeared to be most closely related to the genera Aquiflexum (Figure 5.4). Clade C were members of the Xanthomonadaceae family of γ-proteobacteria that appeared to be most closely related to the genera Lysobacter (Figure 5.5). Clade E were members of the Sphingomonadaceae family of α-proteobacteria that appeared to be most closely related to the genera Sphingomonas (Figure 5.6).

Of the thirty clones isolated from the *unamended* microcosms on day 68, 14 sequences (46%) were β-proteobacteria including 11 (36%) from clade A, 5 (17%) were α-proteobacteria including 4 (13%) from clade E, 5 (17%) were bacteroidetes including 3 (10%) from clade B, 4 (13%) were γ-proteobacteria all from clade C (see Figure 5.7a). Thus β-proteobacteria are an important component of the bacterial population of the *unamended* microcosms on day 68 and, overall, two-thirds of sequences isolated were from one of four bacterial clades. Of the thirty clones isolated from the *acetate-amended* microcosms on day 68, 28 (93%) were β-proteobacteria including 23 sequences (77%) from clade A, the remaining 2 sequences (7%) being unidentified (see Figure 5.7b). Thus β-proteobacteria, particularly those from clade A, dominated the bacterial population of the *acetate-amended* microcosms on day 68.

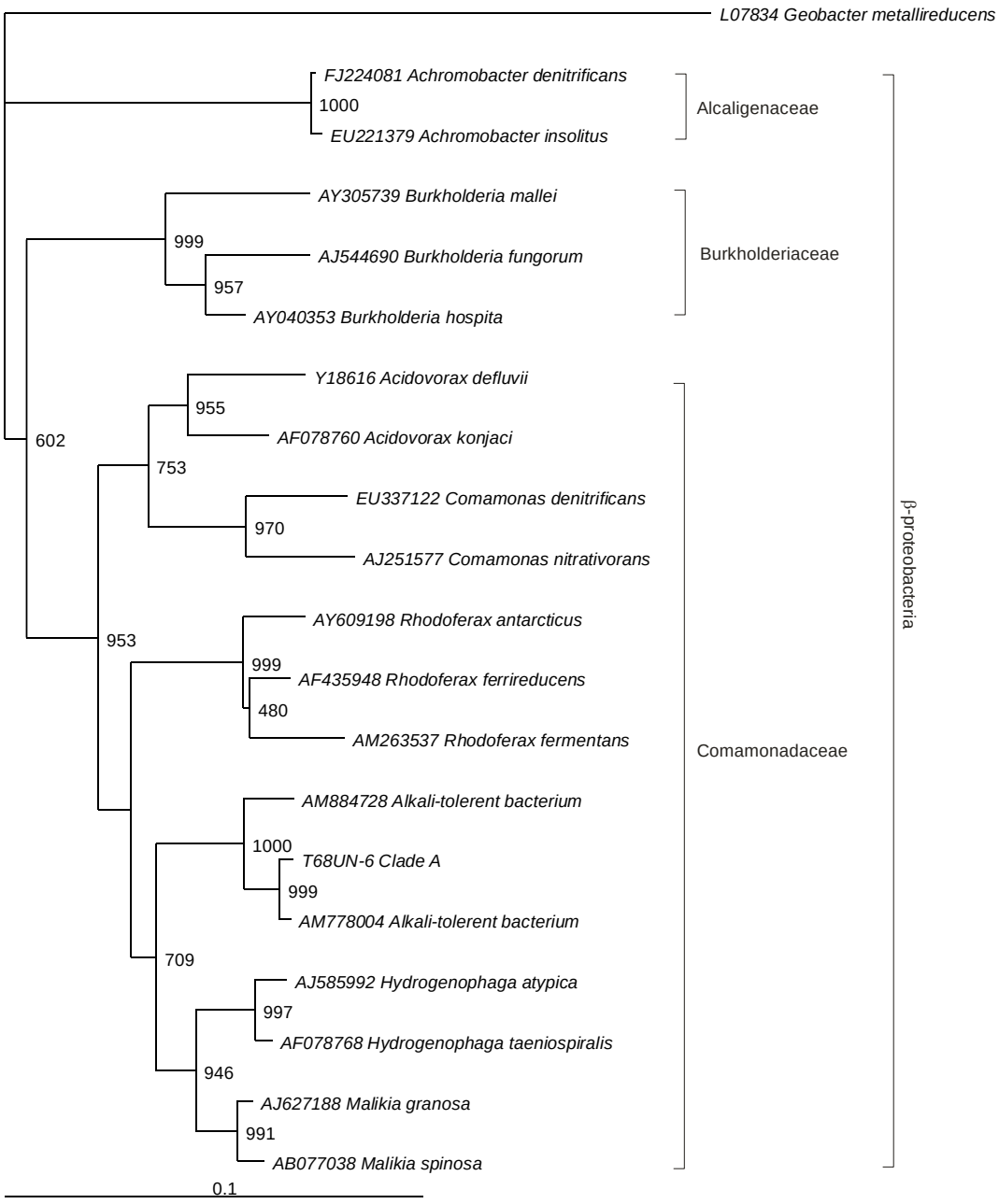

Figure 5.3 Phylogenetic tree showing the relationship between a representative sequence from clade A and 16S rRNA gene sequences of previously described bacteria. *Geobacter metallireducens* was included as an out-group. The scale bar corresponds to 0.1 nucleotide substitutions per site. Bootstrap values (from 1000 replications) are shown at branch points.

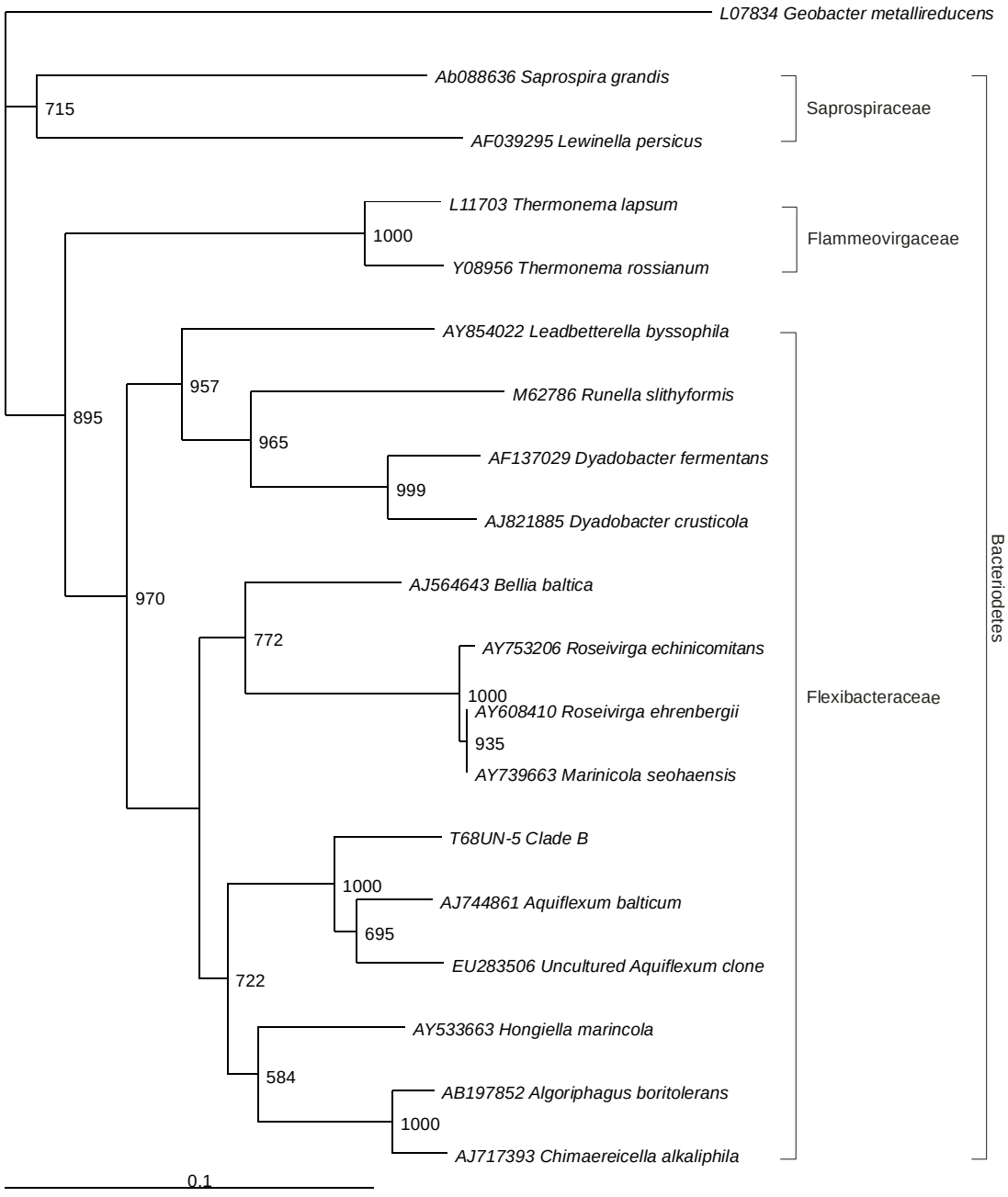

Figure 5.4 Phylogenetic tree showing the relationship between a representative sequence from clade B and 16S rRNA gene sequences of previously described bacteria. *Geobacter metallireducens* was included as an out-group. The scale bar corresponds to 0.1 nucleotide substitutions per site. Bootstrap values (from 1000 replications) are shown at branch points.

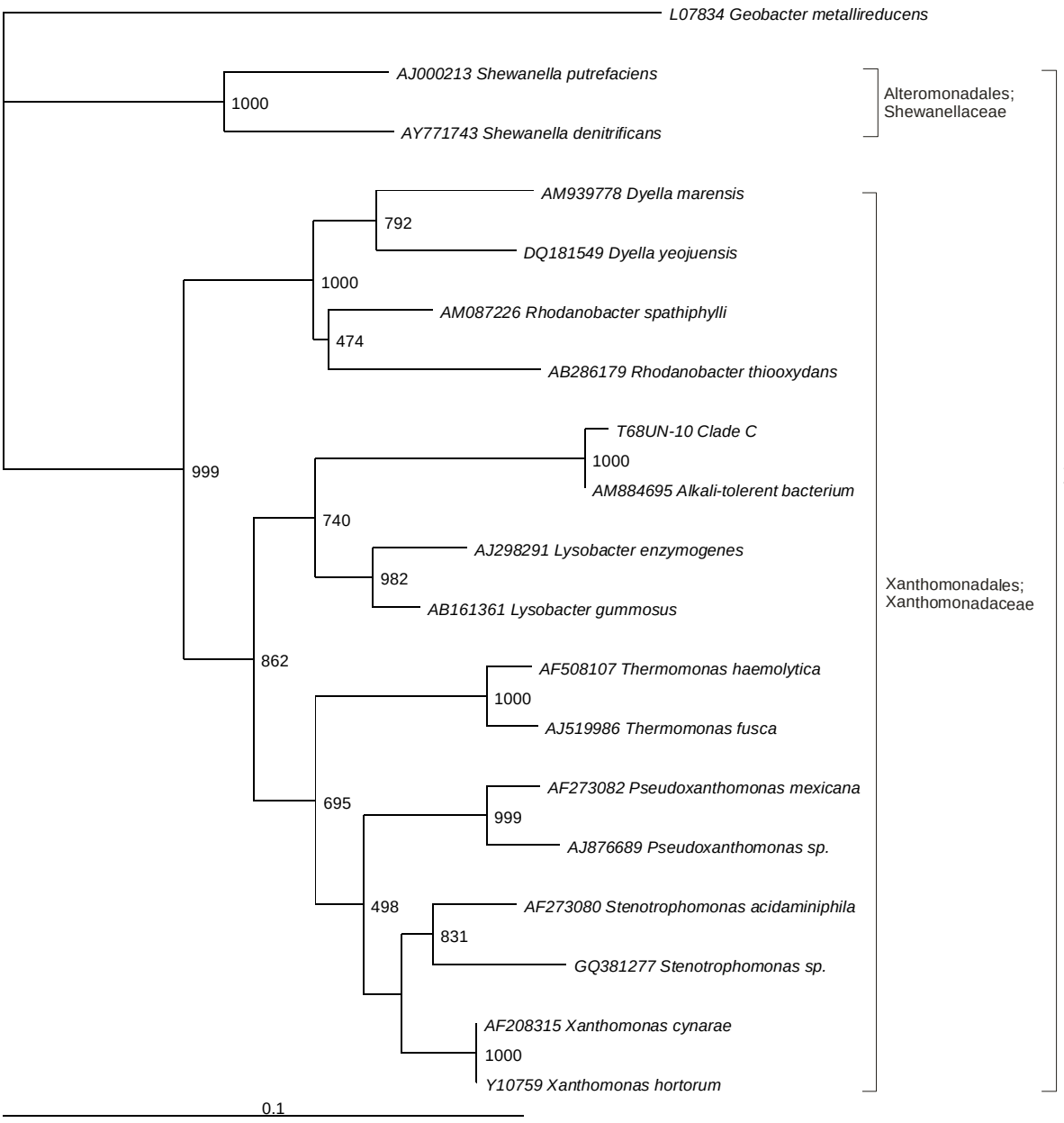

Figure 5.5 Phylogenetic tree showing the relationship between a representative sequence from clade C and 16S rRNA gene sequences of previously described bacteria. *Geobacter metallireducens* was included as an out-group. The scale bar corresponds to 0.1 nucleotide substitutions per site. Bootstrap values (from 1000 replications) are shown at branch points.

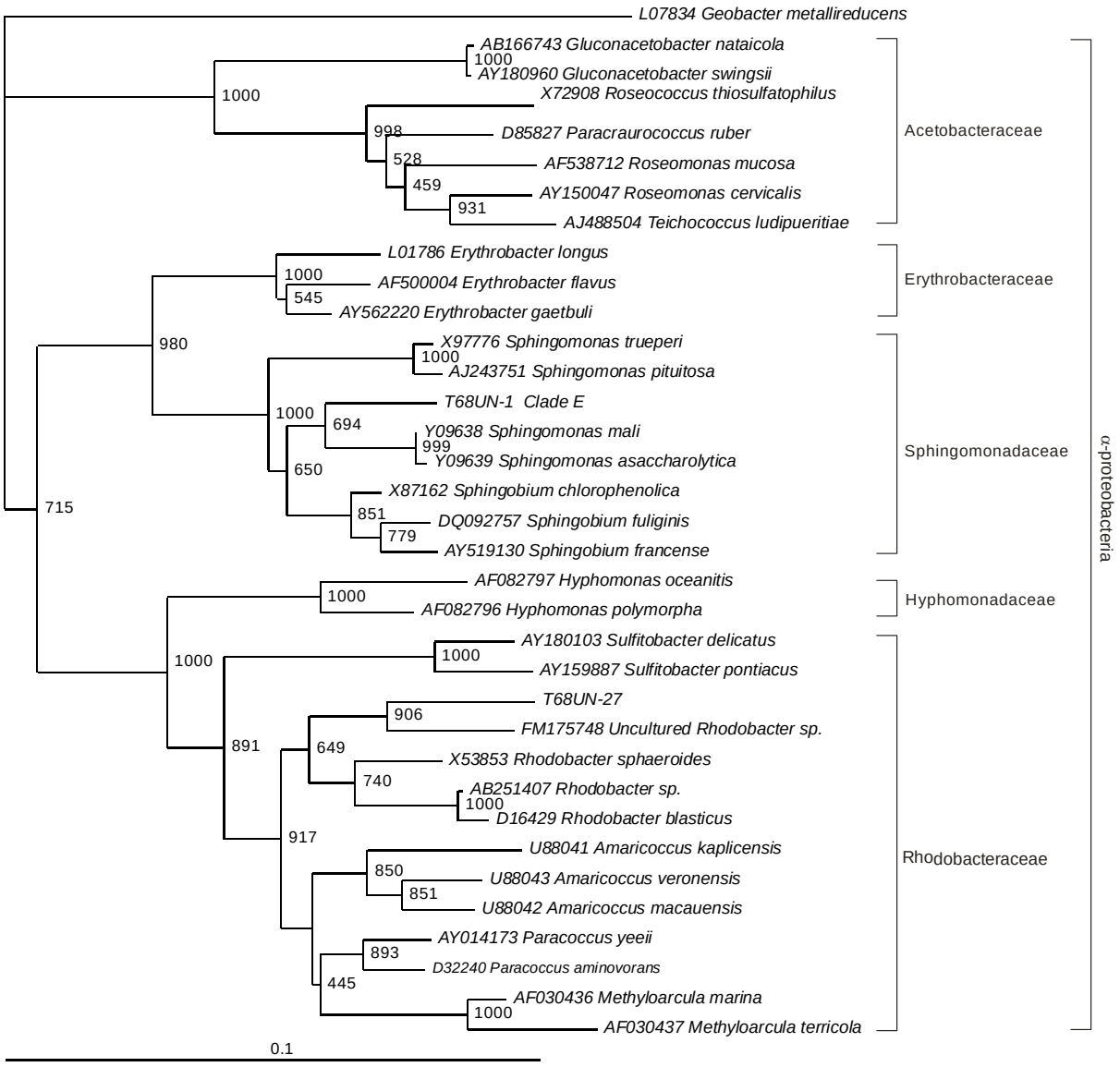

Figure 5.6 Phylogenetic tree showing the relationship between a representative sequence from clade E and 16S rRNA gene sequences of previously described bacteria. *Geobacter metallireducens* was included as an out-group. The scale bar corresponds to 0.1 nucleotide substitutions per site. Bootstrap values (from 1000 replications) are shown at branch points.

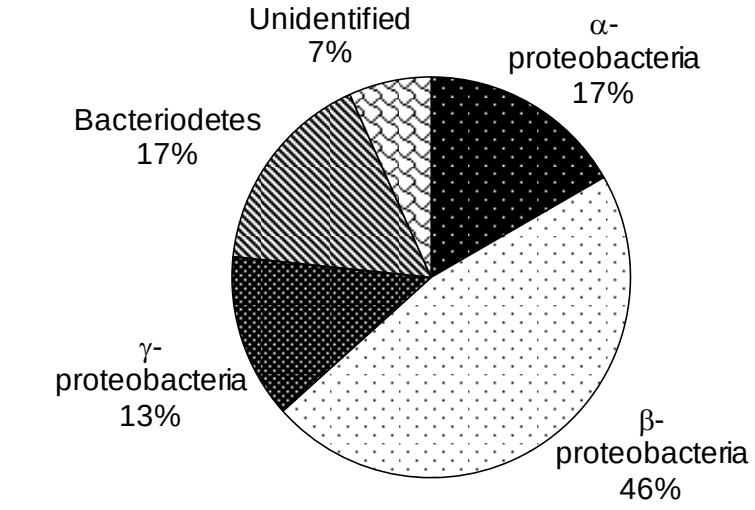

(a)

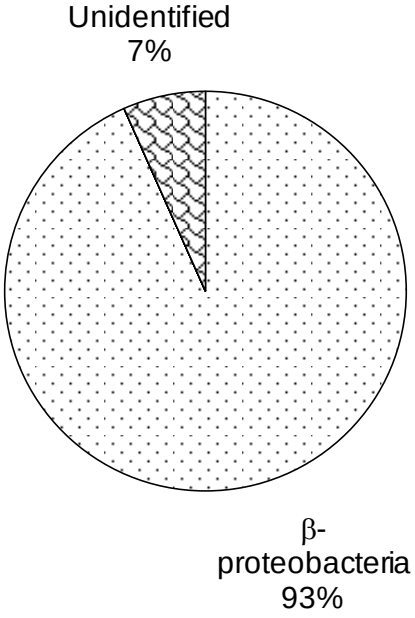

(b)

Figure 5.7 Microbial communities of (a) the unamended microcosms (30 clones) and (b) the acetate-amended microcosms (30 clones) after incubation under anaerobic conditions for 68 days. Charts show phylogenetic affiliation of the 16S rRNA gene sequences

5.4 Discussion

Currently there is a perched water table in the waste pile and downward seepage through the clayey former surface layer into the underlying alluvium where the water table is controlled by the river. Observation of the site over a period of four years suggests these conditions are typical of the site (Studds, pers. comm.). Thus, alkaline, highly oxidising and oxygenated Cr(VI) containing leachate from the tip has been percolating through, and interacting with the former surface soil for over 100 years. Therefore any microorganisms in this soil have had a long time to adapt to the local geochemical environment.

As the leachate from the waste pile seeps downwards it will undergo geochemical changes as it interacts with both the soil and its microbial population. Flow through natural soils can vary greatly spatially and tends to follow preferential paths. These temporal and spatial variations in the flow, and the development of increasingly more reducing conditions down the flow-path, have resulted in the highly variable redox conditions in the clayey former surface soil beneath the waste. For example the percentage of 0.5 N HCl extractable Fe(II) in soils found beneath the waste ranges from less than 5% Fe(II) to more than 90% Fe(II) on a centimetre scale (Tilt, 2009). This distribution probably reflects the balance between the rate of ingress of initially highly oxidising oxygenated Cr(VI)-containing groundwater, and the rate of in situ bioreduction at particular locations.

The initial solution composition in the microcosm experiments reflects the composition of the ditch water, which is a reasonable proxy for the waste leachate (leachate emerging from the waste pile is the main flux into the ditch). The

percentage of 0.5 N HCl extractable solid phase iron as Fe(II) determined when microcosms were established was between 10-20 % Fe(II). Thus the initial conditions in the microcosms are representative of the more oxidised end of the range of conditions observed *in-situ*. Such starting material is likely to have low numbers of obligate anaerobes, whose presence would be anticipated in the more reducing soils on site.

The initial behaviour of the two microcosm systems (*unamended* and *acetate-amended*) was similar. Nitrate was removed rapidly from solution (this occurred slightly more quickly in the *acetate-amended* system but the difference was small). There was no noticeable change in the nitrate concentration in *acetate-amended* sterile control. Thus it is inferred that nitrate removal from the active microcosms is likely to have been microbially mediated, and probably due to the action of nitrate reducing bacteria. It used to be a widely held belief that microbial nitrate reduction is optimal at pH 7 – 8 (Knowles, 1982; Wang et al., 1995). However there is now ample evidence that microbial nitrate reduction can occur at high pH when the microbial community has adapted to the ambient pH (Dhamole et al., 2008; Glass and Silverstein, 1998). Indeed the rate of nitrate reduction to nitrite can increase with increasing pH, although the time taken for complete denitrification at high pH tends to be unaffected as nitrite reduction to N_2 tends to lag behind nitrate reduction to nitrite in alkaline systems (Glass and Silverstein, 1998). Also, as Fe(II) is present in these soils it is possible that nitrate dependant Fe(II) oxidation (Straub et al., 1996) processes may have contributed to nitrate reduction in these experiments, however, we did not observe a reduction in % Fe(II) concurrent with nitrate reduction. Therefore, is not possible to report whether such reduction processes occurred in

these experiments. Once the nitrate was removed from solution the *unamended* system exhibited little further geochemical change. It is unclear from these experiments whether these microcosms had reached a long-term steady-state, or whether further microbially mediated reactions were merely slow in the absence of a readily metabolizable electron donor.

It is likely that bacterial reduction of nitrate in the *unamended* system was coupled to oxidation of soil organic matter (the soil contained 3.6% organic carbon and no exogenic carbon source was added). The complete oxidation of organic matter requires the cooperative activity of a community of microorganisms collectively exhibiting several different metabolic pathways (e.g. hydrolysis of complex organic matter, fermentation of sugars, and oxidation of fatty acids, lactate, acetate and H_2; (Lovley, 1993b). The soil used in the microcosm experiments was covered with COPR waste for over 100 years, and thus it is likely that the labile organic components present prior to burial was already consumed by microorganisms, leaving behind the less labile components such as lignin and cellulose. Anaerobic respiration cannot be supported directly by these polymeric substrates (Stumm and Morgan, 1996), so nitrate reduction in the microcosm experiments suggests that the microbial diversity reported in Figure 5.7a represents a community capable of the complete oxidation of complex organic matter. Thus it is likely that further microbially mediated geochemical reactions would have eventually followed in time, as they did in the *acetate-amended* microcosms.

In *acetate-amended* system Cr(VI) removal followed nitrate removal, however the three replicates responded at different rates and Cr(VI) removal only reached

completion in one microcosm (replicate II). In this replicate there was a significant increase in the proportion of the acid extractable iron present as Fe(II) once Cr(VI) had been removed from solution. In the other two replicates the proportion of the acid extractable iron present as Fe(II) was generally higher than in the *unamended* microcosms or the sterile control, but there was no noticeable increasing trend with time. Comparison with the sterile control, which showed no major change in Cr(VI) concentration with time, suggests that Cr(VI) removal from solution is microbially mediated. Because iron reduction began after Cr(VI) removal ceased, the overall response of the *acetate-amended* system was indicative of a cascade of terminal respiratory processes, which occurred in the normal sequence expected during the progression of microbially induced anoxia (NABIR, 2003).

Because Cr(VI) removal in the *acetate-amended* microcosms occurred as part of a redox cascade, it is likely that it occurred by reduction and precipitation since Cr(III) has very low solubility at high pH (Fendorf, 1995; Fendorf and Zasoski, 1992). However, it is not possible to determine whether Cr(VI) reduction was a direct enzymatic process, or indirect microbially mediated process involving other redox active species (e.g. Fe(III)/Fe(II) cycling). The slightly higher proportion of acid extractable iron in the form of Fe(II) during Cr(VI) reduction may be indicative of iron cycling and thus indicative of the latter mechanism. It is therefore speculated that Cr(VI) reduction in *acetate-amended* microcosms was mediated by reaction with Fe(II) from microbial Fe(III)-reduction. Accumulation of Fe(II) in solids, however, would not be expected in these microcosms until all Cr(VI) was removed from solution. The different response rates of the three replicates may indicate this was a rather marginal environment for bacteria and, as a result, the rate of response was

sensitive to subtle differences in microbiology and geochemistry (e.g. micro-environments).

Addition of acetate to this soil-water system will have preferentially supported the growth of alkaliphilic Cr(VI) tolerant bacteria within the soil that can respire anaerobically on acetate (acetate cannot support fermentative growth). On day 68 these appear to have been predominantly β-proteobacteria, with a single group of closely related bacteria within the family Comamonadaceae dominating (clade A). At this time point Cr(VI) was being removed from all three replicates, probably by reductive precipitation associated with Fe(III)/Fe(II) cycling. Thus it appears likely that members of clade A were able to couple acetate oxidation to iron reduction. At a pH value of 10.5 the coupling of acetate oxidation to the reduction of Fe(III) to Fe(II) is thermodynamically favourable (see Table 2.2), and thus can support energy metabolism by microorganisms. It has been observed that closely related members of the Comamonadaceae family can couple acetate oxidation to Fe(III) reduction (e.g. Rhodoferax ferrireducens; Finneran et al., 2003). However genera in the Comamonadaceae family are phenotypically highly diverse, even when they are phylogenetically closely related (Spring et al., 2005) so the apparent similarity to clade A is not evidence that clade A will have similar metabolism.

Over the period of observation the pH value of both sterile controls decreased slightly with time, reaching a value around 10.5, the measured pH of the soil sample, suggesting the ditch water pH value was chemically buffered by contact with the soil. The pH values of both active microcosms decreased to a value 0.5 pH units

below the measured pH of the soil. This difference is small but was probably due to microbial activity (e.g. the release of metabolic products such as CO_2 by bacteria).

Whilst similarity of the 16S rRNA gene is not evidence that organisms share other genes (e.g. those associated with adaptation to a particular environment) it may nevertheless be significant that each of the four bacterial clades identified in this study appeared to be closely related to genera that are adapted to similar harsh environments. For example the sequences in clade A have ≥97% identity with sequence AM778004 found in a non-saline alkaline environment, and ≥96% identity to sequence AM884728 found in an alkaline, chromium contaminated soil from a COPR disposal site (Stewart et al., 2007). Both these alkali tolerant species are shown for comparative purposes on the phylogenetic tree constructed for β-proteobacteria (Figure 5.3). Sequences within clade B appeared to be closely related to members of the *Aquiflexum* genus (Figure 5.4) and had ≥94% identity to *Aquiflexum* clone EU283506 isolated from sediment from a brackish alkaline lake. Sequences within clade C (Figure 5.5) had ≥98% identity to sequence AM884695 isolated from an alkaline, chromium contaminated soil from a COPR disposal site (Stewart et al., 2007). Members of clade E appeared to be members of the *Sphingomonas* genus (Figure 5.6), which contains hardy species capable of uranium reduction in alkaline solutions (Nilgiriwala et al., 2008). More detailed investigation of these species may provide interesting insights into life in harsh environments.

The findings of this study will have a major impact on the long-term management of the COPR waste site from which the samples were obtained, and offer a potential solution to the downward leaching of chromate at many other COPR legacy sites.

Environmentally sound management of such sites is very unlikely to involve removal of the waste, as industrial scale excavation will almost certainly generate chromate bearing dusts that will act as a pathway to human exposure. Thus remediation of COPR disposal sites will almost always involve three elements:

- Better separation of the waste from the surface environment
- Measures to reduce water infiltration into the waste
- Measures to treat leachate emerging from the waste

The first two elements will usually involve placement of a capillary barrier and a low permeability cover layer over the waste. However such a capping layer is unlikely to reduce the rainwater influx to zero, and thus there will always be the risk that contaminated water from the waste will leach downwards and contaminate underlying water resources.

This study has shown that the microbial community in soil, given time, can adapt to life at high pH. If that community is provided with a suitable electron donor, then progressive anoxia develops and chromium accumulates in the soil by reduction and precipitation at the point in the redox cascade just before iron reduction becomes fully established. Creating such a reductive zone in the soil will act as a barrier to the migration of chromium, which should reduce the impact of the waste on the wider environment. It is not clear from the current study whether the residual organic matter still remaining in the former surface layer can support iron reduction, or if it now needs augmenting with an organic substrate such as acetate, however the widespread presence of Fe(II) and the amount of chromium that has accumulated in that soil layer is evidence that it has done so the past.

5.5 Conclusions

A former surface soil that has been buried beneath a COPR tip for over 100 years has an active microbial population despite it having a pH value of 10.5. Without the addition of an exogenic electron donor this microbial population is able to reduce nitrate using an electron donor(s) that is probably derived from the soil organic matter. With the addition of acetate as a more readily available electron donor, Cr(VI) removal occurred after nitrate reduction, to be followed by iron reduction. It is proposed that Cr(VI) removal from solution was by microbially mediated reductive precipitation. This was either a direct enzymatic process with Cr(VI) being used as an electron acceptor, or more likely an indirect process involving an abiotic reaction with Fe(II) produced by microbial Fe(III) reduction.

5.6 Acknowledgements

RAW would like to acknowledge his funding from a John Henry Garner Scholarship at the University of Leeds. The authors would also like to thank Dr Phil Studds and Mark Bell, Ramboll UK, for help enabling the field work.

5.7 References

ASTM, 2006. D4972-01: standard test method for pH of soils. Annual book of ASTM standards. American Society for Testing and Materials 4, 963-965.

Bopp, L.H., Ehrlich, H.L., 1988. Chromate resistance and reduction in *pseudomonas-fluorescens* strain LB300. Arch. Microbiol. 150, 426-431.

Burke, I.T., Boothman, C., Lloyd, J.R., Livens, F.R., Charnock, J.M., McBeth, J.M., Mortimer, R.J.G., Morris, K., 2006. Reoxidation behavior of technetium, iron, and sulfur in estuarine sediments. Environ. Sci. Technol. 40, 3529-3535.

Cervantes, C., Campos-Garcia, J., Devars, S., Gutierrez-Corona, F., Loza-Tavera, H., Torres-Guzman, J.C., Moreno-Sanchez, R., 2001. Interactions of chromium with microorganisms and plants. FEMS. Microbiol. Rev. 25, 335-347.

Chai, L.Y., Huang, S.H., Yang, Z.H., Peng, B., Huang, Y., Chen, Y.H., 2009. Hexavalent chromium reduction by Pannonibacter phragmitetus BB isolated from soil under chromium-containing slag heap. J. Environ. Sci. Heal. A 44, 615-622.

Chen, J.M., Hao, O.J., 1998. Microbial chromium (VI) reduction. Crit. Rev. Env. Sci. Tec. 28, 219-251.

Cudennec, Y., Lecerf, A., 2006. The transformation of ferrihydrite into goethite or hematite, revisited. J. Solid State Chem. 179, 716-722.

Darrie, G., 2001. Commercial extraction technology and process waste disposal in the manufacture of chromium chemicals from ore. Environ. Geochem. Health 23, 187-193.

Daulton, T.L., Little, B.J., Jones-Meehan, J., Blom, D.A., Allard, L.F., 2007. Microbial reduction of chromium from the hexavalent to divalent state. Geochim. Cosmochim. Acta 71, 556-565.

Detkova, E., Pusheva, M., 2006. Energy metabolism in halophilic and alkaliphilic acetogenic bacteria. Microbiol. 75, 1.

Dhamole, P.B., Nair, R.R., D'Souza, S.F., Lele, S.S., 2008. Denitrification of Highly Alkaline Nitrate Waste Using Adapted Sludge. Appl. Biochem. Biotechnol. 151, 433-440.

Eden, P.A., Schmidt, T.M., Blakemore, R.P., Pace, N.R., 1991. Phylogenetic Analysis of Aquaspirillum-Magnetotacticum Using Polymerase Chain Reaction-Amplified 16s Ribosomal-Rna-Specific DNA. Int. J. Syst. Bacteriol. 41, 324-325.

Farmer, J.G., Graham, M.C., Thomas, R.P., Licona-Manzur, C., Licona-Manzur, C., Paterson, E., Campbell, C.D., Geelhoed, J.S., Lumsdon, D.G., Meeussen, J.C.L., Roe, M.J., Conner, A., Fallick, A.E., Bewley, R.J.F., 1999. Assessment and modelling of the environmental chemistry and potential for remediative treatment of chromium-contaminated land. Environ. Geochem. Health 21, 331-337.

Farmer, J.G., Paterson, E., Bewley, R.J.F., Geelhoed, J.S., Hillier, S., Meeussen, J.C.L., Lumsdon, D.G., Thomas, R.P., Graham, M.C., 2006. The implications of integrated assessment and modelling studies for the future remediation of chromite ore processing residue disposal sites. Sci. Total Environ. 360, 90-97.

Farmer, J.G., Thomas, R.P., Graham, M.C., Geelhoed, J.S., Lumsdon, D.G., Paterson, E., 2002. Chromium speciation and fractionation in ground and surface waters in the vicinity of chromite ore processing residue disposal sites. J. Environ. Monitor. 4, 235-243.

Fendorf, S.E., 1995. Surface-Reactions of Chromium in Soils and Waters. Geoderma 67, 55-71.

Fendorf, S.E., Zasoski, R.J., 1992. Chromium(III) oxidation by δ-MnO_2: 1. Characterization. Environ. Sci. Technol. 26, 79-85.

Finneran, K.T., Johnsen, C.V., Lovley, D.R., 2003. Rhodoferax ferrireducens sp nov., a psychrotolerant, facultatively anaerobic bacterium that oxidizes acetate with the reduction of Fe(III). Int J Syst Evol Microbiol 53, 669-673.

Fonseca, B.M., H. Quintelas, C. Teixeira, A. Tavares, T., 2009. Retention of Cr(VI) and Pb(II) on a loamy sand soil: Kinetics, equilibria and breakthrough. Chem. Eng. J 152, 212-219.

Francis, C.A., Obraztsova, A.Y., Tebo, B.M., 2000. Dissimilatory metal reduction by the facultative anaerobe Pantoea agglomerans SP1. Appl. Environ. Microbiol. 66, 543-548.

Froelich, P.N., Klinkhammer, G.P., Bender, M.L., Luedtke, N.A., Heath, G.R., Cullen, D., Dauphin, P., Hammond, D., Hartman, B., Maynard, V., 1979. Early Oxidation Of Organic-Matter In Pelagic Sediments Of The Eastern Equatorial Atlantic - Suboxic Diagenesis. Geochim. Cosmochim. Acta 43, 1075-1090.

Geelhoed, J.S., Meeussen, J.C.L., Roe, M.J., Hillier, S., Thomas, R.P., Farmer, J.G., Paterson, E., 2003. Chromium remediation or release? Effect of iron(II) sulfate addition on chromium(VI) leaching from columns of chromite ore processing residue. Environ. Sci. Technol. 37, 3206-3213.

Glass, C., Silverstein, J., 1998. Denitrification kinetics of high nitrate concentration water: pH effect on inhibition and nitrite accumulation. Water Res. 32, 831-839.

Han, X., Wong, Y.S., Tam, N.F.Y., 2006. Surface complexation mechanism and modeling in Cr(III) biosorption by a microalgal isolate, Chlorella miniata. J. Colloid Interface Sci. 303, 365-371.

Hansel, C.M., Benner, S.G., Fendorf, S., 2005. Competing Fe(II)-induced mineralization pathways of ferrihydrite. Environ. Sci. Technol. 39, 7147-7153.

Ishibashi, Y., Cervantes, C., Silver, S., 1990. Chromium reduction in *pseudomonas-putida*. Appl. Environ. Microbiol. 56, 2268-2270.

James, B.R., 1994. Hexavalent Chromium Solubility and Reduction in Alkaline Soils Enriched with Chromite Ore Processing Residue. J. Environ. Qual. 23, 227-233.

Knowles, R., 1982. Denitrification. Microbiol. Rev. 46, 43-70.

Krulwich, T.A., Ito, M., Guffanti, A.A., 2001. The Na+-dependence of alkaliphily in Bacillus. BBA-Bioenergetics 1505, 158-168.

Lane, D.J., Pace, B., Olsen, G.J., Stahl, D.A., Sogin, M.L., Pace, N.R., 1985. Rapid determination of 16S ribosomal RNA sequences for phylogenetic analysis. P. Natl. Acad. Sci. USA 82, 6955-6959.

Langmuir, D., 1997. Aqueous Environmental Geochemistry. Englewood Cliffs, NJ: Prentice Hall.

Lee, T., Lim, H., Lee, Y., Park, J.W., 2003. Use of waste iron metal for removal of Cr(VI) from water. Chemosphere 53, 479-485.

Lloyd, J.R., Nolting, H.F., Sole, V.A., Bosecker, K., 1998. Technetium reduction and precipitation by sulfate-reducing bacteria. Geomicrobiol. J. 15, 45-58.

Lovley, D.R., 1993a. Anaerobes into Heavy-Metal - Dissimilatory Metal Reduction in Anoxic Environments. Trends Ecol. Evol. 8, 213-217.

Lovley, D.R., 1993b. Dissimilatory Metal Reduction. Annu. Rev. Microbol 47, 263-290.

Lovley, D.R., Phillips, E.J.P., 1986. Availability of Ferric Iron for Microbial Reduction in Bottom Sediments of the Fresh-Water Tidal Potomac River. Appl. Environ. Microbiol. 52, 751-757.

Morales-Barrera, L., Cristiani-Urbina, E., 2008. Hexavalent chromium removal by a Trichoderma inhamatum fungal strain isolated from tannery effluent. Water Air Soil Poll. 187, 327-336.

NABIR, 2003. Bioremediation of metals and radionuclides: what it is and how it works, A NABIR primer, 2nd ed. NABIR primer prepared for US Department of Energy, p. p.78.

Neal, A.L., Lowe, K., Daulton, T.L., Jones-Meehan, J., Little, B.J., 2002. Oxidation state of chromium associated with cell surfaces of Shewanella oneidensis during chromate reduction. Appl. Surf. Sci. 202, 150-159.

Nilgiriwala, K.S., Alahari, A., Rao, A.S., Apte, S.K., 2008. Cloning and overexpression of alkaline phosphatase PhoK from Sphingomonas sp strain BSAR-1 for bioprecipitation of uranium from alkaline solutions. Appl. Environ. Microbiol. 74, 5516-5523.

Pechova, A., Pavlata, L., 2007. Chromium as an essential nutrient: a review. Vet. Med-Czech 52, 1-18.

Rai, D., Sass, B.M., Moore, D.A., 1987. Chromium(Iii) Hydrolysis Constants and Solubility of Chromium(Iii) Hydroxide. Inorg. Chem. 26, 345-349.

Rehman, A., Zahoor, A., Muneer, B., Hasnain, S., 2008. Chromium tolerance and reduction potential of a Bacillus sp.ev3 isolated from metal contaminated wastewater. B. Environ. Contam. Tox. 81, 25-29.

Richard, F.C., Bourg, A.C., 1991. Aqueous geochemistry of Cr: A review. Water Res. 25, 807-816.

Roadcap, G.S., Sanford, R.A., Jin, Q.S., Pardinas, J.R., Bethke, C.M., 2006. Extremely alkaline (pH > 12) ground water hosts diverse microbial community. Ground Water 44, 511-517.

Romanenko, V.I., Koren'kov, V.N., 1977. Pure culture of bacteria using chromates and bichromates as hydrogen acceptors during development under anaerobic conditions. Mikrobiologiia 46, 414-417.

Sani, R.K., Peyton, B.M., Smith, W.A., Apel, W.A., Petersen, J.N., 2002. Dissimilatory reduction of Cr(VI), Fe(III), and U(VI) by Cellulomonas isolates. Appl. Microbol. Biot. 60, 192-199.

Sau, G.B., Chatterjee, S., Sinha, S., Mukherjee, S.K., 2008. Isolation and Characterization of a Cr(VI) Reducing Bacillus firmus Strain from Industrial Effluents. Polish Journal of Microbiology 57, 327-332.

Schumacher, B.A., 2002. Methods for the Determination of Total Organic Carbon (TOC) in Soils and Sediments. United States Environmental Protection Agency, Las Vegas.

Schwertmann, U., Friedl, J., Stanjek, H., 1999. From Fe(III) ions to ferrihydrite and then to hematite. J. Colloid Interface Sci. 209, 215-223.

Spring, S., Wagner, M., Schumann, P., Kampfer, P., 2005. Malikia granosa gen. nov., sp nov., a novel polyhydroxyalkanoate- and polyphosphate-accumulating bacterium isolated from activated sludge, and reclassification of Pseudomonas spinosa as Malikia spinosa comb. nov. Int J Syst Evol Microbiol 55, 621-629.

Sreeram, K.J., Ramasami, T., 2001. Speciation and recovery of chromium from chromite ore processing residues. J. Environ. Monitor. 3, 526-530.

Stewart, D.I., Burke, I.T., Hughes-Berry, D.V., Whittleston, R.A., 2010. Microbially mediated chromate reduction in soil contaminated by highly alkaline leachate from chromium containing waste. Ecol. Eng. 36, 211-221.

Stewart, D.I., Burke, I.T., Mortimer, R.J.G., 2007. Stimulation of microbially mediated chromate reduction in alkaline soil-water systems. Geomicrobiol. J. 24, 655-669.

Straub, K.L., Benz, M., Schink, B., Widdel, F., 1996. Anaerobic, nitrate-dependent microbial oxidation of ferrous iron. Appl. Environ. Microbiol. 62, 1458-1460.

Stucki, J.W., Lee, K., Goodman, B.A., Kostka, J.E., 2007. Effects of in situ biostimulation on iron mineral speciation in a sub-surface soil. Geochim. Cosmochim. Acta 71, 835-843.

Studds, P.G., pers. comm. Director, Environment and Nature, Ramboll UK

Stumm, W., Morgan, J.J., 1996. Aquatic Geochemistry 3rd ed. John Wiley and Sons, New York.

Suzuki, T., Miyata, N., Horitsu, H., Kawai, K., Takamizawa, K., Tai, Y., Okazaki, M., 1992. NAD(P)H-dependent chromium (VI) reductase of Pseudomonas ambigua G-1: a Cr(V) intermediate is formed during the reduction of Cr(VI) to Cr(III). J. Bacteriol. 174, 5340-5345.

Tilt, Z., 2009. The subsurface migration of Cr(VI) at a chromium waste tip in the North of England., School of Earth and Environment. University of Leeds.

Tinjum, J.M., Benson, C.H., Edil, T.B., 2008. Mobilization of Cr(VI) from chromite ore processing residue through acid treatment. Sci. Total Environ. 391, 13-25.

USEPA, 1992. SW-846 Manual: Method 7196a. Chromium hexavalent (colorimetric). Retrieved 6th Jan 2006.

USEPA, 1998. Toxicological review of hexavalent chromium. Available online at http://www.epa.gov/ncea/iris.

VanEngelen, M.R., Peyton, B.M., Mormile, M.R., Pinkart, H.C., 2008. Fe(III), Cr(VI), and Fe(III) mediated Cr(VI) reduction in alkaline media using a Halomonas isolate from Soap Lake, Washington. Biodegradation 19, 841-850.

Viollier, E., Inglett, P.W., Hunter, K., Roychoudhury, A.N., Van Cappellen, P., 2000. The ferrozine method revisited: Fe(II)/Fe(III) determination in natural waters. Appl. Geochem. 15, 785-790.

Walawska, B., Kowalski, Z., 2000. Model of technological alternatives of production of sodium chromate (VI) with the use of chromic wastes. Waste Manage. 20, 711-723.

Wang, J.H., Baltzis, B.C., Lewandowski, G.A., 1995. Fundamental Denitrification Kinetic-Studies With Pseudomonas-Denitrificans. Biotechnol. Bioeng. 47, 26-41.

Wang, Y.T., 2000. In Lovley D.R. "Environmental Microbe-Metal Interactions" ASM Press. Chapter 10: Microbial Reduction of Chromate, 225-235.

Whittleston, R.A., Hughes-Berry, D.V., Stewart, D.I., Burke, I.T., 2007. A Natural In-situ Reactive Zone beneath a COPR Tip, 3rd International Symposium on Permeable Reactive Barriers and Reactive Zones, Rimini, Italy.

Zhu, W.J., Yang, Z.H., Ma, Z.M., Chai, L.Y., 2008. Reduction of high concentrations of chromate by Leucobacter sp CRB1 isolated from Changsha, China. World J. Microb. Biot. 24, 991-996.

Chapter 6 Enhancing microbial reduction in hyperalkaline, chromium contaminated sediments by pH amendment

Abstract

Soil found beneath a chromite ore processing residue (COPR) disposal site contains a diverse population of anaerobic alkaliphiles, despite the continuous influx of a Cr(VI) contaminated, hyperalkaline leachate (pH12.2). Chromium is accumulating in this soil as a result of an abiotic reaction of Cr(VI) with microbially produced Fe(II). Sodium bicarbonate was added to this soil to investigate whether bioreduction of iron in hyperalkaline, chromium contaminated soils can be enhanced by pH amendment. In anaerobic microcosm experiments without pH amendment soil microorganisms were able to reduce nitrate at pH 11.2 coupled to the oxidation of electron donors derived from the original soil organic matter, but progressive anoxia did not develop to the point of iron reduction over a period of 9 months. The addition of sodium bicarbonate produced a well buffered system with a pH of ~9.3, and promoted the development of iron reducing conditions within 1 month once complete denitrification had occurred. This was also coupled to the oxidation of electron donors derived from the original soil organic matter, and appears to be controlled by members of the phylum *Firmicutes.* Therefore, pH amendment using bicarbonate may provide a suitable strategy for stimulating the bioremediation of COPR contaminated groundwater, where the microbial community have adapted to the alkaline conditions.

6.1 Introduction

Disposal of chromium ore processing residue (COPR) is a globally widespread concern due to the risks associated with potentially harmful Cr(VI) contaminated hyperalkaline liquors leaching into the wider environment (Deakin et al., 2001; Stewart et al., 2010; Weng et al., 2000). Chromium is extracted from its ore, chromite, by roasting it in the presence of air and an alkali carbonate to oxidise Cr(III) to Cr(VI) which can then be extracted with water due to its increased solubility. Originally lime (CaO), and then limestone, was added to the kiln to increase air penetration and thus provide sufficient O_2 for chromite oxidation in a practice known as the "high-lime" process (Farmer et al., 1999). Although technologically superseded by lime-free processing in the 1960s, the high-lime process, until recently, still accounted for 40% of chromium production worldwide (Darrie 2001). The high-lime process is notoriously inefficient and produces large volumes of hyperalkaline wastes with pH> 12 (Higgins et al., 1998). Residual Cr concentrations within COPR typically range from 2000-40,000 $mg.kg^{-1}$, with up to 35% present in the oxidised Cr(VI) (Geelhoed et al., 2002; Tinjum et al., 2008). This can easily become mobile in water as the toxic and carcinogenic chromate anion (CrO_4^{2-}) (Farmer et al., 2006; James, 1994; Tinjum et al., 2008). Remediation of legacy sites contaminated with COPR is challenging, particularly because these sites are often in urban areas and date from times when COPR disposal was quite poorly managed (Breeze, 1973; Geelhoed et al., 2002; Higgins et al., 1998; Jeyasingh and Philip, 2005; Stewart et al., 2007). Traditional "dig and dump" remediation strategies are not only costly due to the large volumes involved, but also inadvisable due to the risk of forming carcinogenic Cr(VI) bearing dusts (USEPA, 1998). In contrast to the harmful properties of Cr(VI), the reduced form Cr(III) is an essential trace nutrient in

plants and animals (Richard and Bourg, 1991), readily sorbs to soil minerals, and (co)-precipitates as insoluble Cr(III) hydroxides in neutral and alkaline environments (Rai et al., 1987; Richard and Bourg, 1991). Thus the reduction of Cr(VI) to Cr(III) *in-situ* significantly reduces the hazard posed by Cr contaminated groundwater.

Soil microorganisms can couple the oxidation of soil organic matter to the reduction of transition metals, such as iron and manganese, in a process known as dissimilatory metabolism (Lovley, 1993b). Iron is the most abundant redox-active metal in soils, and as a result microbial Fe(III) reducing conditions have been described as the most important to develop during the development of anaerobic soils due to its influence on trace metal behaviour (Lovley, 1991, 1997; Pollock et al., 2007; Zavarzina et al., 2006). Numerous iron reducing microorganisms from a range of microbial taxa have been isolated from a broad range of environments, including some alkaliphilic bacteria such as *Bacillus sp* and *Geoalkalibacter ferrihydriticus* (Pollock et al., 2007; Zavarzina et al., 2006). During dissimilative reduction bacteria transfer electrons from organic carbon to Fe(III) and use the energy released from these coupled reactions to translocate protons from the cytoplasm to the periplasm. This produces an electrochemical gradient (or proton motive force) across the cytoplasmic membrane that drives adenosine triphosphate (ATP) synthesis via oxidative phosphorylation of adenosine diphosphate (ATP is the unit used for intracellular energy transfer). In contrast, fermentative bacteria synthesise ATP from the action of internal cytoplasmic enzymes which catalyse the transfer of a phosphate group from the substrate to adenosine diphosphate in a process known as substrate-level phosphorylation (Nelson and Cox, 2005). High pH is a challenging environment for bacteria as it is difficult to maintain a proton motive force when the external pH

exceeds that of the cytoplasm, thus highly alkaline conditions may favour fermentative metabolism over respiration. Some fermentative alkaliphiles in the order Clostridiales been demonstrated to indirectly reduce iron in soils and sediments through the external dumping of electrons to Fe(III) as a method of maintaining internal redox balance within cells (e.g. *Tindallia magadii* (1998); *Clostridium beirjerinckii* (1999); *Anoxynatronum sibiricum* (2003); *Anaerobranca californiensis* (2004)). Soil microorganisms can also reduce contaminant metals, such as chromium, during dissimilatory metabolism. Microbial reduction of Cr(VI) has been reported in a number of Gram negative genera including *Desulfovibro* and *Shewanella*, and members of the Gram positive *Bacillus* and *Cellulomonas* genera (Francis et al., 2000; Lovley, 1993a; Romanenko and Koren'kov, 1977; Sani et al., 2002; Sau et al., 2008), however only a few studies have demonstrated direct microbial Cr(VI) reduction at high pH (Chai et al., 2009; VanEngelen et al., 2008; Zhu et al., 2008). Thus it has been suggested that microbially mediated Cr(VI) reduction in alkaline, chromium contaminated environments usually occurs by an indirect pathway involving extracellular reaction with reduced species (Higgins et al., 1998), for example Fe(II) produced during dissimilative iron reduction coupled to oxidation of soil organic matter(Lovley and Phillips, 1986b).

Bioreduction to achieve a remediation goal is usually induced by addition of an electron donor to environments where the growth of Fe(III)-reducing bacteria is limited by lack of organic matter. However, at high pH and in the presence of Cr(VI), it may be these harsh conditions that limit growth. This chapter investigates a soil recovered from beneath a COPR tip which contains organic matter and acid extractable Fe(II). A previous study suggests that reduction of Fe(III) is probably

occurring *in-situ* but, at pH 11.5, at a rate too slow to prevent the spread of Cr(VI) (Whittleston et al., 2011b). Here the feasibility of enhancing microbial reduction by buffering the soil pH down to about 9.5 (close to the optimum pH value for many alkaliphilic micro-organisms) is investigated. Differences in the microbial community and the rate of development of Fe(III) reducing conditions that occur with and without pH buffering are reported.

6.2 Materials and methods

6.2.1 Field sampling and sample handling

Samples were obtained from a 19th century COPR tip in the north of England (see Whittleston et al. (2011a)). A soil sample (B2-310) was collected from a grey-clay horizon immediately beneath the COPR waste using a hand auger and 1m core sampler in March 2009. Water from within the COPR waste was collected at the same time from a near-by monitoring well using disposable PVC bailers (there is a perched water table within the waste, and this water is percolating downwards into the underlying soil horizons (Atkins, 2009)). Samples were stored in sealed polythene containers with as little headspace as possible, and kept in the dark at 4°C.

6.2.2 Sample characterisation

Soil pH was measured following the ASTM standard method (ASTM, 2006). The total organic carbon content of oven dried and HCl treated subsamples were measured using Carlo-Erba 1106 elemental analyser (Schumacher, 2002). The acid neutralisation capacity was determined with both 1 M HCl and 1 M $NaHCO_3$. Freeze dried soil (10g) was suspended in deionised water (100 ml) in a sealed flask stirred by magnetic flea (to limit CO_2 in-gassing). The titrating solution was added in increments (1 ml) and allowed to equilibrate (4 hrs).

6.2.3 Reduction microcosm experiments

A *pH amended* microcosm series was established in triplicate with corresponding sterile controls. Each microcosm consisted of 10g of homogenised B2-310 soil and 100ml of COPR water in a 120ml glass serum bottles (Whittleston et al., 2011a). After sealing these were buffered to pH 9 using 1 M sodium bicarbonate solution, and the headspace purged with nitrogen. Sterile controls were prepared by autoclaving soil with a nitrogen purged headspace (120°C, 20min) and adding filter sterilised COPR leachate upon cooling. An active *unamended* control microcosm series was prepared using only the soil and COPR water. Bottles (incubated in the dark at 21°C) were periodically sampled aseptically for geochemical analysis. During sampling microcosms were shaken and 3ml soil slurry extracted. Samples were centrifuged (3min, 16,000g) and the water analysed for pH, Eh and Cr(VI), and soil for acid extractable Fe(II). Soil pellets were retained for microbiological community analysis.

6.2.4 Geochemical methods

Eh and pH were measured using an Orion meter (pH calibrated at 7 and 10). Nitrate concentrations were determined by ion chromatography on a Dionex DX-600 with AS50 autosampler using a 2mm AS16 analytical column, with suppressed conductivity detection and gradient elution to 15 mM potassium hydroxide over 10 minutes. Samples were loaded in a random order to avoid systematic errors, and the column was flushed between samples with deionised water for 1.5 minutes. UV/VIS spectroscopy methods were used to determine aqueous Cr(VI) concentrations based on reaction with diphenycarbazide (USEPA, 1992) and aqueous nitrite concentrations following reaction with sulphanilaminde (SAN) and naphthylethylenediamine dihydrochloride (Harris and Mortimer, 2002). Iron was

extracted from solids using 0.5N HCl (a proxy for microbial available iron (Burke et al., 2006; Weber et al., 2001)), and the percentage Fe(II) was determined by reaction with ferrozine (Lovley and Phillips, 1986a). UV/VIS spectroscopy methods were performed on a Cecil CE3021 UV/VIS Spectrophotometer; calibration standards were used regularly.

6.2.5 X-ray absorption spectroscopy (XAS)

XANES spectra were collected from soil recovered from the *pH 9 amended* microcosms on day 153 on station I18 at the Diamond Light Source, UK. Spectra were also collected from potassium chromate and amorphous Cr-hydroxide (precipitated by drop-wise neutralisation of $CrCl_3$ solution using 10M NaOH (Saraswat and Vajpei, 1984)). XANES spectra were summed and normalised using Athena v0.8.056 (see Appendix A.2.7).

6.2.6 Microbial community analysis

Microbial DNA was extracted from a sample of B2-310 soil, and the *pH amended* microcosms on day 153 and *unamended* control microcosms on day 270. A 16S rRNA gene fragment (~500 bp) was amplified from each sample by polymerase chain reaction (PCR) using broad specificity primers. The PCR product was ligated into a standing cloning vector, and transformed into *E. coli* competent cells to isolate plasmids containing the insert, which were sent for sequencing. The quality of each gene sequence was evaluated, and non-chimeric sequences were classified using the Ribosomal Database Project (RDP) naïve Bayesian Classifier (Wang et al., 2007) in August 2010 (see Appendix A.5). Sequences were grouped into operational taxonomic units (OTUs) using the MOTHUR software (Schloss et al., 2009) (>98% nearest neighbour sequence similarity cut-off). Rarefaction curves were constructed

to characterize the diversity of each clone library using the Shannon Index (H') (Krebs, 1999). Phylogenetic trees were constructed using representative sequences from selected OTUs, aligned with type species from the EMBL database using ClustalX (version 2.0.11), and drawn with TreeView (version 1.6.6). Trees were constructed from the distance matrix by neighbour joining, with bootstrap analysis performed with 1000 replicates Sequences were submitted to the EMBL Nucleotide Sequence Database (accession numbers: FR695903-FR696047 and HE573872-HE573888).

6.2.7 Multidimensional scaling analysis

Multidimensional Scaling Analysis (MDS), which is also known as principle coordinate analysis, configures the position of objects in Euclidean space based on their pair-wise dissimilarity, and is used in a number scientific fields to visualize datasets (Son et al., 2011). Here it is used to investigate changes in initial B2-310 microbial community after incubation in the microcosm experiments (*unamended* and *pH amended*). Sequences were aligned using Clustalw2 (http://www.ebi.ac.uk/Tools/msa/clustalw2/) and the distance matrix (a matrix of pair-wise dissimilarity scores) was downloaded into NewMDSX (Coxon, 2004; Roskam et al., 2005). Basic non-metric MDS was undertaken using the Minissa-N algorithm within NewMDSX.

6.3 Results

6.3.1 Sample recovery

Borehole B2 was located near the south-western edge of the COPR tip. It encountered a topsoil layer then entered COPR waste at 190cm, grey sandy clay at 310cm, and terminated in a gravel layer at 365cm. Soil sample B2-310 was collected

from the grey clay just below the soil-waste interface (sample depth 310 – 320 cm). This layer was probably the original surface deposit before the waste was tipped approximately 100 years ago (Stewart et al., 2010).

6.3.2 Sample geochemistry

Soil sample B2-310 has been described in detail by Whittleston et al (2011b). Briefly, it had a pH value of 12.2, contained 1.0% TOC and 53% of 0.5 N HCl extractable iron was present as Fe(II). XRD and XRF measurements showed the major minerals were quartz, kaolinite and albite. The chromium concentration was approximately 3400 $mg.kg^{-1}$, which the chromium K-edge XANES spectra showed was predominately present in Cr(III) oxidation state and EXAFS analysis showed was within a mixed Cr(III)–Fe(III) oxy-hydroxide phase. Tilt (2009) studied the heterogeneity of this soil layer at a cm-scale and found that the proportion of 0.5N HCl acid extractable iron in the Fe(II) oxidation state can vary at this scale from 5% to 90%.

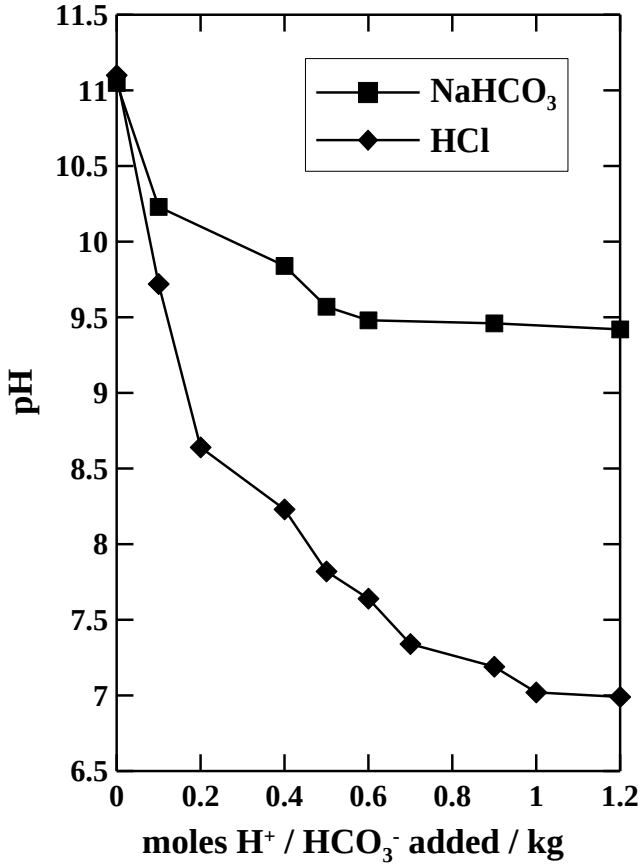

Figure 6.1 ANC titration curves obtained from the acid neutralisation test on freeze dried soil B2-310. Diamond symbol – addition of HCl, Square symbol – HCO_3 addition.

The water from within the COPR has a pH of 12.2, Eh of +90 mV, and a Cr(VI) concentration of 990 µM (51.5 $mg.L^{-1}$). The acid neutralisation capacity of B2-310 soil determined using HCl was approximately 1 mole H^+ per kg of soil (Figure 6.1). The addition of $NaHCO_3^-$ produced a slower decline in pH, with 0.6 moles HCO_3^- per kg of soil required to reach pH 9.5. However, this then remained stable about this value for the remainder of the experiment, up to 1.2 moles HCO_3^- per kg of soil.

6.3.3 Reduction microcosms

The initial pH of the *pH amended* microcosm series was 8.9, while the corresponding sterile control had a slightly lower initial value of 8.6 (see Figure 6.2). In contrast the initial pH of the *unamended* control microcosm series was 12.2. The pH value of *pH*

amended microcosms increased slightly over the first 5 days before levelling off at 9.3, and remained steady about this value until the tests were sampled for microbial community analysis on day 153. The pH value of the sterile control increased from 8.6 $\rightarrow$ 9.2 over the first 15 days, and remained steady about this value for the duration of the experiment. The pH value of the *unamended* control decreased from 12.2 $\rightarrow$ 11.7 over the first 20 days before remaining steady about this value until the tests were terminated for microbial community analysis on day 270.

At the first sample point (~1 hr) the aqueous Cr(VI) concentration in the *pH amended* microcosms had dropped from the initial leachate value of 990 $\rightarrow$ 656 ± 4 µmol L^{-1}, with complete removal observed by 20 days. Similar removal rates were observed in the corresponding sterile and *unamended* controls. Aqueous nitrate concentrations decreased rapidly in the *pH amended* active experiments from an initial value of 144 ± 13 µmol L^{-1} $\rightarrow$ 0 by day 5, with concentrations decreasing at a similar rate in the *unamended* control. Nitrate was also removed from the sterile control, but this occurred very slowly over 137 days (nitrate was not detected in either backup control when they were sampled on day 137). Aqueous nitrite concentration in *pH amended* microcosms increased slightly over the first 5 days, before decreasing over the next 15 days. In contrast, nitrite concentration in the corresponding sterile control increased slightly over the duration of testing (confirmed by both backup sterile experiments). Nitrite concentrations also behaved differently in the *unamended* control, increasing from 66 ± 2 $\rightarrow$ 296 ± 26 µmol L^{-1} by day 41 before decreasing steadily over the remainder of the test.

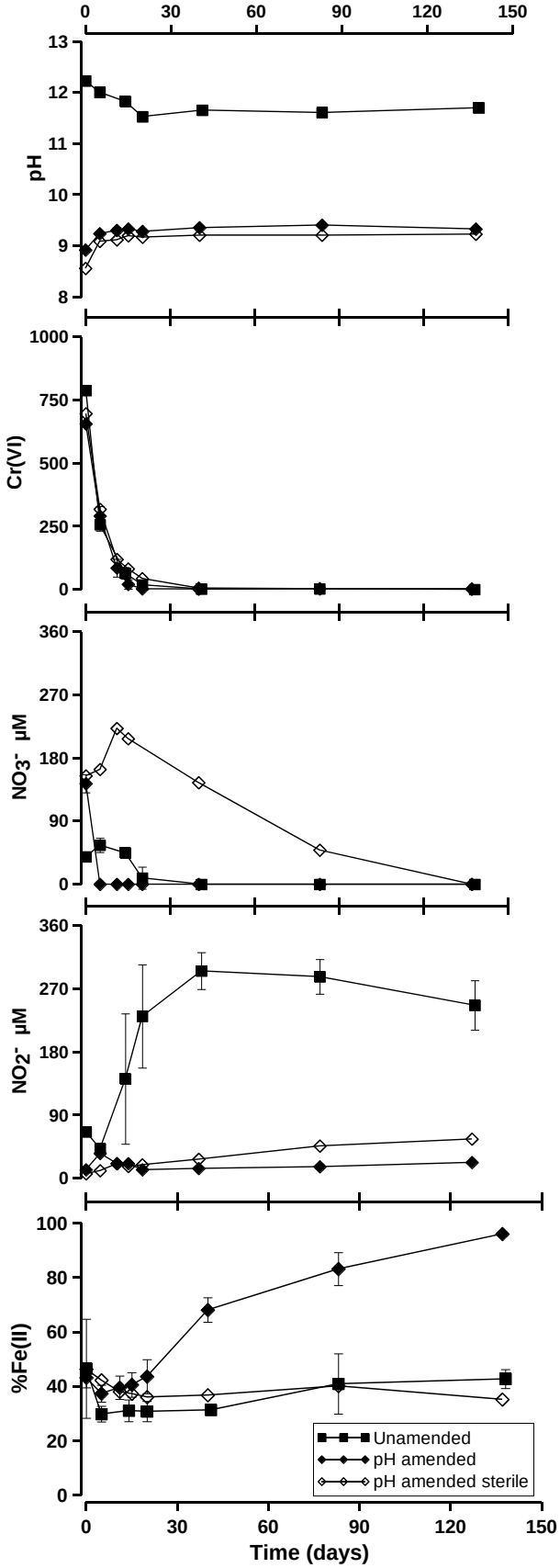

Figure 6.2 Geochemical response of the *pH amended* (◆), *unamended* control (■) and sterile control (◇) microcosms. Top to bottom; pH; pore water Cr(VI) concentration; pore water NO_3^- concentration; pore water NO_2^- concentration; % of 0.5 N HCl extractable Fe as Fe(II) in soils. Error bars shown are one standard deviation from the mean of triplicate experiments.

The percentage of 0.5 N HCl extractable iron present as Fe(II) in the *pH amended* microcosms decreased slightly before recovering to its initial value by day 20, although this change is less than the measurement error. Beyond day 20, the percentage acid extractable iron present as Fe(II) increased steadily from 43 $\rightarrow$ 96% on day 137. No significant increase in Fe(II) percentage was observed in the corresponding sterile and *unamended* controls over the duration of the experiment.

6.3.4 X-ray absorption spectroscopy

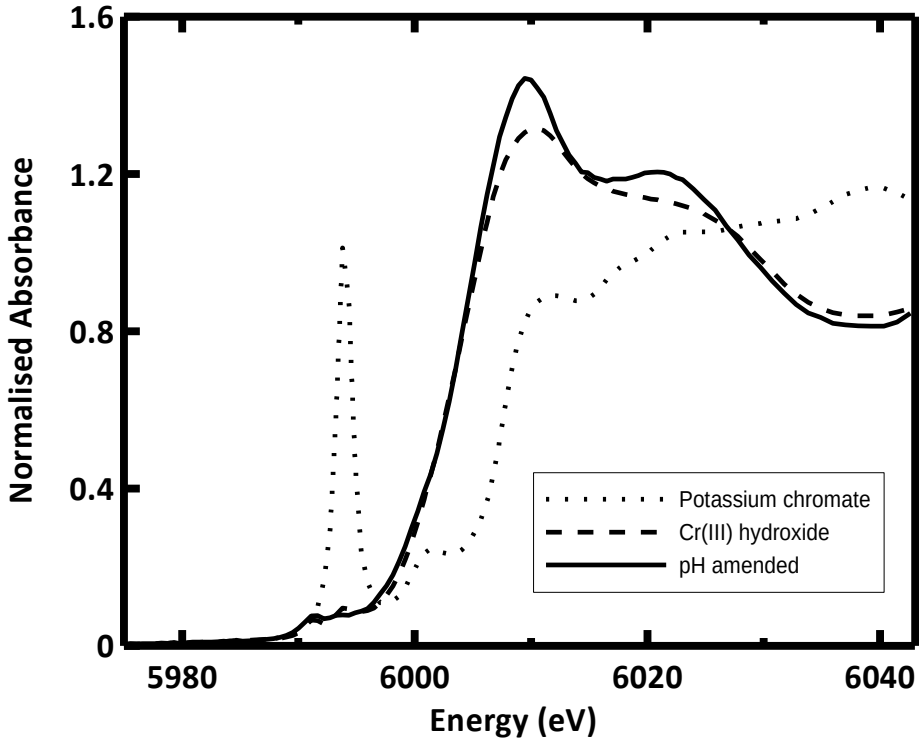

Figure 6.3 Normalised chromium K-edge XANES spectra for soil from the pH 9 amended microcosms on day 153 and for the standards.

The chromium XANES spectra from soil recovered from the pH 9 amended microcosms on day 153 (Figure 6.3) indicated that all the Cr associated with the solid phase was in the Cr(III) oxidation state (i.e. all the Cr(VI) initially present in the COPR water had been reduced to Cr(III)).

6.3.5 Microbial community analysis

Table 6.1 Summary of phylogenetic and OTU assignment from RDP and MOTHUR analysis using 95 and 98% confidence threshold and similarity cut off respectively

	B2-310		pH9 amended		Unamended control	
	Sequences	**OTUs**	**Sequences**	**OTUs**	**Sequences**	**OTUs**
Deinococcus-Thermus	-		-		34	1
Acidobacteria	1	1	-		-	
Verrucomicrobia	2	2	-		-	
Planctomycetes	2	2	-		-	
Nitrospirae	3	2	-		-	
Actinobacteria	6	6	-		-	
Bacteriodetes	9	7	-		-	
Proteobacteria						
α class	2	2	1	1	-	
β class	12	5	2	2	-	
γ class	1	1	-		-	
δ class	1	1	-		-	
Not assigned to class	3	2	2	2		
Firmicutes	13	9	39	15	5	4
Bacteria incertae sedis	1	1	-		-	
Unassigned	6	5	13	9	4	2
Total	62	46	57	29	43	6

A total of 62 rRNA gene sequences were obtained from B2-310. These were assigned to 9 different bacterial phyla (confidence threshold >98%), with approximately 10% of sequences remaining unassigned (see Table 6.1). Three phyla were dominant, with 31%, 19%, and 16% of sequences assigned to *Proteobacteria*, *Firmicutes* and *Bacteriodetes*, respectively. The 57 sequences from the *pH amended* microcosms on day 153 were assigned to just two bacterial phyla, *Firmicutes* and *Proteobacteria* (68% and 9% of sequences, respectively), with the remaining 23% of sequences unassigned. In contrast the 43 sequences obtained from the *unamended* control microcosms on day 270 were also assigned to just two bacterial phyla, *Deinococcus-Thermus* and *Firmicutes* (79% and 12% of sequences, respectively), with 9% of sequences unassigned (see Appendix B.5 for full assignment details).

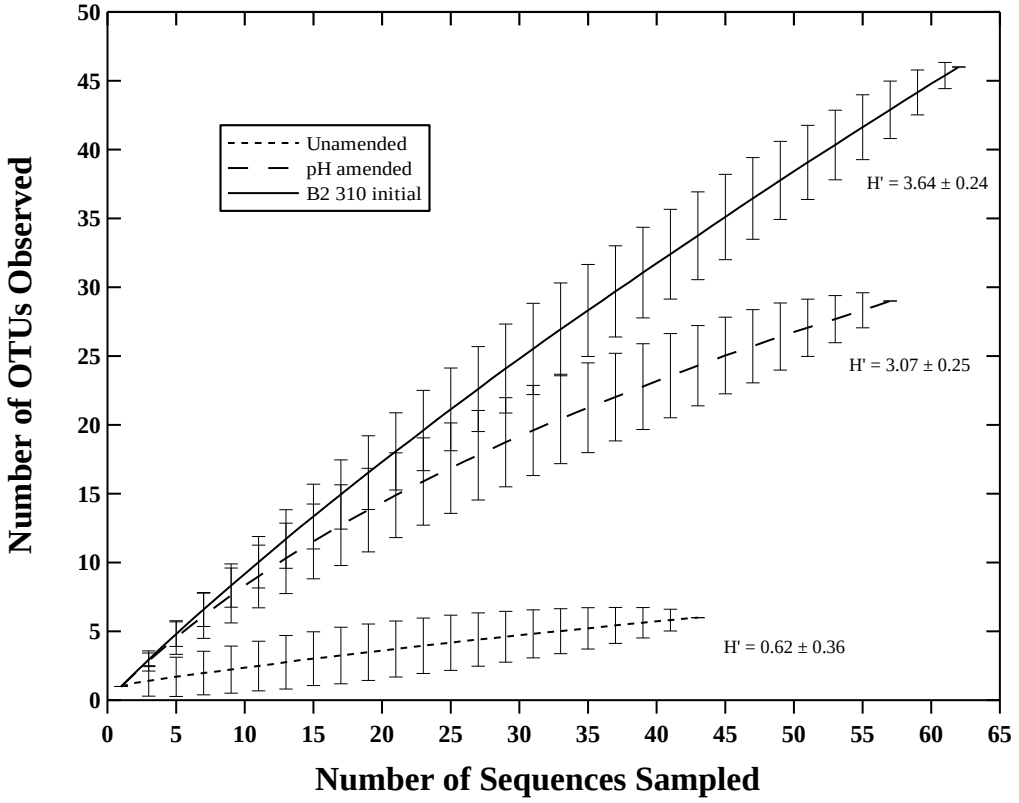

Figure 6.4 Rarefaction curves from MOTHUR analysis using nearest neighbour assignment with 98% similarity cut-off

Rarefaction analysis of the three populations (Figure 6.4) indicates that species richness is highest in the B2-310 sample prior to incubation in microcosm systems (Shannon Index, H' =3.64 ± 0.24). Species richness was slightly lower after 153 days incubation in the *pH amended* microcosm (H' = 3.07 ± 0.25), and lowest in the *unamended* control microcosm on day 270 (H' = 0.62 ± 0.36). The two dimensional MDS representation of the sequence dissimilarity scores (Figure 6.5) largely reflects this species diversity. The sequences recovered from the B2-310 population are scattered widely across the whole area of the MDS plot, demonstrating relatively wide diversity. In contrast the sequences recovered from the *pH amended* microcosm population are grouped more closely together on the plot, with only a small degree of scattering, reflecting that the species present were from significantly fewer phyla (Table 6.1). The sequences from the *unamended* control population show the least

degree of spread across the plot, with most confined to a single area, demonstrating the very limited diversity recovered from this population.

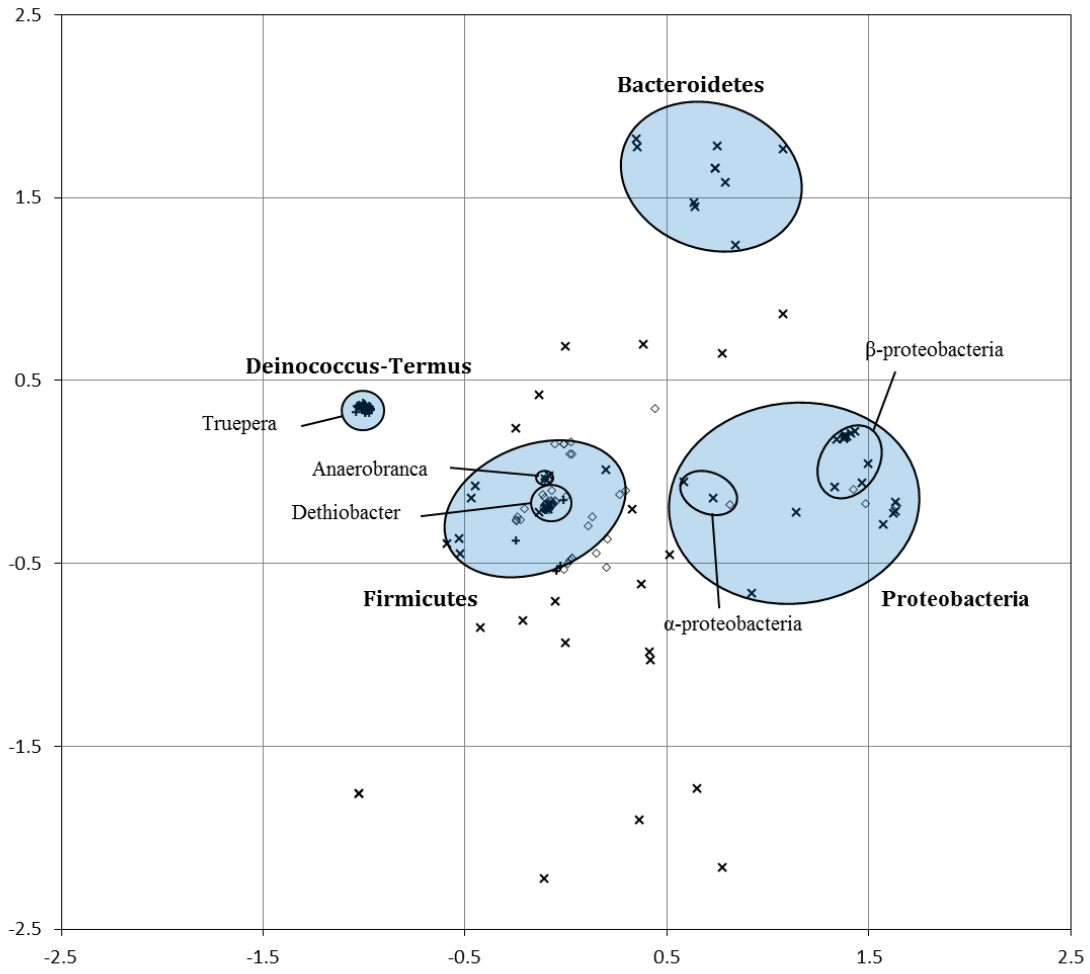

Figure 6.5 Two-dimensional configuration from the MDS analysis of the pair-wise sequence dissimilarity scores: (×) B2-310 population, (◇) *pH amended* microcosm, (+) and *unamended* microcosm (distance scale within this Euclidean space is an arbitrary function of dissimilarity). The "stress" (a measure of lack of fit) associated with this two dimensional representation decreased marginally from 0.20 to 0.17 when the number of dimensions was increased to three, which suggest that two dimensions adequately represent the dissimilaries in the data.

Firmicutes species represented 21% of the initial (B2-310) population, 68% of the *pH-amended* microcosm population on day 153, and just 12% of the *unamended* control microcosm population on day 270. Two genera were common to all three populations. About 6% of the B2-310 population were *Dethiobacter*-like species (4 sequences), as were 5% of the *unamended* control population (2 sequences) and 42%

of the *pH amended* population (24 sequences). Similarly, about 3% of the B2-310 population were *Anaerobranca*-like species (2 sequences), as were 2% of the *unamended* control microcosm population on day 270 (1 sequence) and 4% of the *pH9-amended* microcosm population on day 153 (2 sequences). A phylogenetic tree showing characteristic members of the *Dethiobacter*-like and *Anaerobranca*-like OTUs is shown in Figure 6.6 (the characteristic sequence is the sequence that is the minimum distance from the other members of the OTU (Schloss et al., 2009)). In contrast to the other two populations, the bacterial population of the *unamended* control microcosms on day 270 was dominated by a single OTU (37 of the 43 sequences). This was a *Truepera*-like specie within the phylum Deinococcus-Thermus. A phylogenetic tree showing a characteristic member of the *Truepera*-like OTU is shown in Figure 6.7.

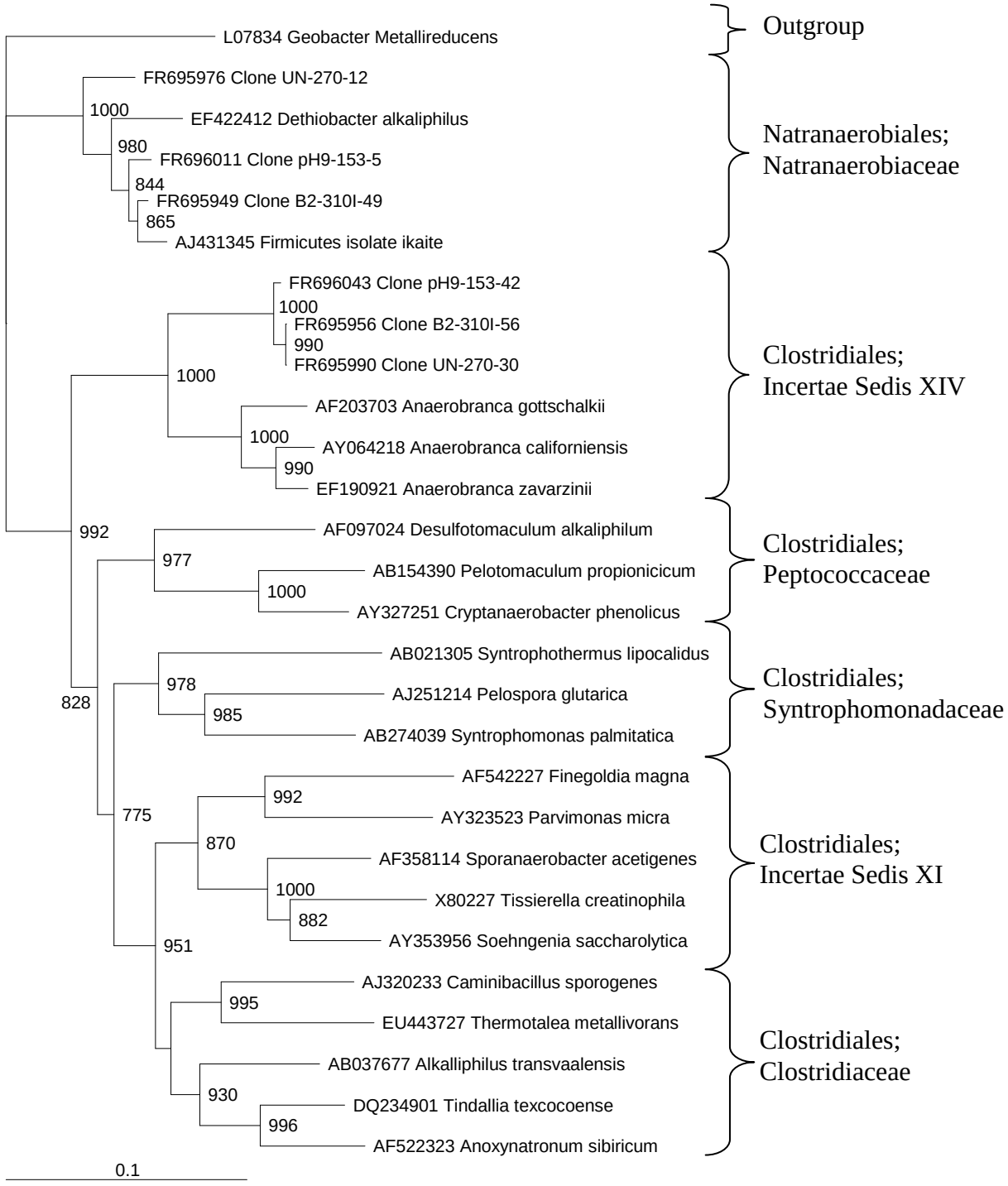

Figure 6.6 Phylogenetic tree showing the relationship between representative sequences from major OTU's recovered from each population and other members of the orders Clostridiales and Natranaerobiales of Firmicutes. *Geobacter metallireducens* (δ-proteobacteria) is included as an out-group. The scale bar corresponds to 0.1 nucleotide substitutions per site. Bootstrap values (from 1000 replications) are shown at branch points.

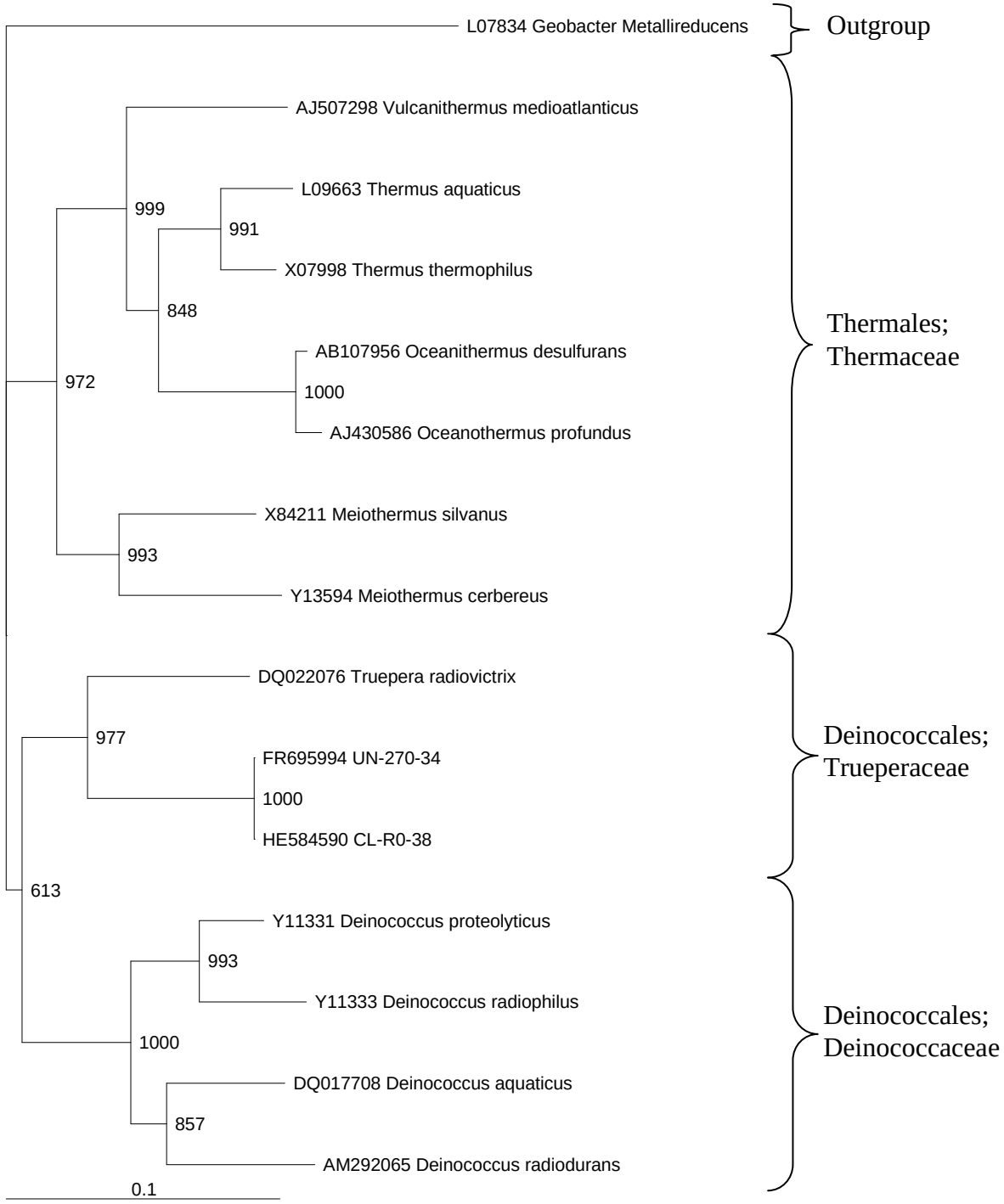

Figure 6.7 Phylogenetic tree showing the relationship between a representative sequence from the major OTU recovered from the *unamended* microcosm series day 270 and other members of the orders Deinococcales and Thermales of the phylum Deinococcus-Thermus. *Geobacter metallireducens* (δ-proteobacteria) is included as an out-group. The scale bar corresponds to 0.1 nucleotide substitutions per site. Bootstrap values (from 1000 replications) are shown at branch points.

6.4 Discussion

The soil immediately beneath the COPR tip is thought to have been the surface layer prior to waste tipping at the end of the 19th century. Cr(VI) bearing leachate from the COPR waste has probably been entering this soil for over 100 years (Stewart et al., 2010). Despite this flux the soil contains a population of bacteria which is relatively diverse (46 different OTUs from 9 different phyla were identified within a clone library of 62 gene sequences). The soil has accumulated ~3400 mg.kg^{-1} Cr, predominately present as Cr(III). As the Cr(III) is within a stable Fe(III) oxide host phase, it has been suggested that it has been reduced by microbially produced Fe(II) (Whittleston et al., 2011b).

When this soil is incubated in microcosm experiments with water from within the waste pile under pH amended conditions, the microbial diversity decreases slightly. In contrast, microbial diversity decreases significantly when there is no pH buffering in the *unamended* control. Initially it might seem surprising that there is loss of diversity in the *unamended* control microcosm experiments, which appear to replicate the conditions *in-situ.* However geochemical conditions vary rapidly in the former topsoil layer as the relatively oxic (Eh +90 mV) COPR water seeps into a reducing environment. Undisturbed the soil would have had fabric that affects seepage at a local scale, and it contains a variety of minerals that would buffer the pH of the COPR water. Together these will have produced a range of geochemical micro-environments within individual soil pores. Different micro-environments within the soil pores would have favoured different bacteria, which would produce a diverse clone library when the sample size is very much larger than the particle size. In contrast the microcosm experiments were prepared from a homogenised soil

sample, and were shaken to produce a soil suspension as part of microcosm sampling. This would have produced more uniform geochemical conditions, which would have put a selective pressure on the microbial population, favouring a sub-set of the initial population to produce a less diverse population under essentially the same bulk average geochemical conditions as those observed *in-situ.*

Aqueous Cr(VI) was completely removed from solution at similar rates in all microcosm experiments, including the sterile *pH amended* control. XANES spectra indicated that soil-associated chromium in the *pH-amended* microcosms was predominately present in Cr(III) oxidation state. Thus, Cr(VI) removal must have been an abiotic process and was probably the result of a reduction reaction with amorphous Fe(II) in the soil. Cr(VI) readily reacts abiotically with Fe(II) to produce Cr(III) and Fe(III) (Lin, 2002). Indeed the capacity of these soils to remove aqueous Cr(VI) from COPR leachate via reductive precipitation as Cr(III)-Fe(III) oxyhydroxides has previously been reported (Whittleston et al., 2011b). A small decrease in the percentage acid extractable iron in the Fe(II) oxidation state concurrent with Cr(VI) removal was also observed in all experiments, but this was less than the measurement error and therefore not significant. However this minor reduction in Fe(II) during Cr(VI) removal is consistent with the calculated Fe(II) : Cr(VI) ratio of 20-30 : 1 present in these experiments.

In the *pH amended* microcosms, aqueous nitrate was removed from the active experiments at least an order of magnitude more quickly than in the corresponding sterile control. In the microbially active experiments, aqueous nitrite concentration increased slightly during nitrate removal but decreased again once the nitrate was

gone. The removal of nitrite was then rapidly followed by an increase in the proportion of acid extractable iron present as Fe(II). The rate of nitrate removal in the active microcosms (in comparison with the control) and subsequent depletion of nitrite and Fe(III) suggests that the reactions are microbially mediated and part of a cascade of terminal electron-accepting processes. The gradual removal of nitrate in the *pH-amended* sterile control was most likely an abiotic process as nitrate was also removed from both backup controls (i.e. if nitrate removal was due to loss of sterility in the sampled control then it is unlikely to have occurred in both back-up controls as these were not sampled until day 137). The reduction of nitrate by Fe^{2+}(aq) is thermodynamically very favourable (even at high pH), but a direct reaction between these ions in solution is kinetically inhibited (Choe et al., 2004; Hansen et al., 1996; Ottley et al., 1997). However, the reaction can be surface catalysed by transition metals and freshly formed Fe(III) precipitates (Fanning, 2000; Ottley et al., 1997; Postma, 1990). Fe(II) oxyhydroxides are still sparingly soluble around pH 9, where Fe^{2+} is the main aqueous species (Langmuir, 1997). It therefore seems reasonable that nitrate reduction by Fe^{2+}(aq) in a surface catalysed reaction was the mechanism by which nitrate was removed from the *pH amended* sterile microcosms.

The biogeochemical behaviour of the *unamended* control microcosms differed from the pH amended microcosms. Nitrate removal was observed over the first 2-3 weeks concurrent with a significant increase in nitrite concentration. Subsequently the nitrite concentration decreased steadily over the remainder of the experiment, suggesting that nitrite reduction was following-on from nitrate reduction. Nitrate reduction has been widely reported in high pH systems where the microbial community has adapted to the ambient pH (Dhamole et al., 2008; Glass and

Silverstein, 1998; Whittleston et al., 2011a), and in such systems it has been observed that nitrite reduction to N_2 tends to lag behind nitrate reduction to nitrite (Glass and Silverstein, 1998). Furthermore, the abiotic reduction of nitrate by $Fe^{2+}(aq)$ is limited by its solubility minima around pH 11 (Smith, 2007), above which $Fe(OH)_3^-$ is the dominant aqueous species (Langmuir, 1997). Thus it seems that nitrate and nitrite reduction in the *unamended* (pH ~11.7) control microcosms were microbially mediated processes, albeit occurring more slowly than with pH amendment. However, the absence of a significant increase in the proportion of acid extractable iron present as Fe(II) over the duration of the *unamended* control experiments suggests that microbial metabolism linked to Fe(III) reduction was inhibited at the unamended pH value.

The microbial community of the *pH-amended* microcosms was sampled when iron reduction was the predominant biogeochemical process. Amendment of the pH to ~9 and the subsequent development of iron reducing conditions favoured bacteria from the phylum *Firmicutes*. Two species, *Dethiobacter* and *Anaerobranca*, were also found in B2-310 soil and *unamended* microcosms. The *Dethiobacter*-like sequences are closely related to a clone, AJ431345, recovered from an alkaline tufa environment (Stougaard et al., 2002) and also to the type species for this genus, *Dethiobacter alkaliphilus* (EF422412), an obligate anaerobic alkaliphile isolated from an soda lake environment (Sorokin et al., 2008). *D. alkaliphilus* is reported to be involved in the reductive sulphur cycle, and is capable of reducing elemental sulphur (Sorokin et al., 2008), but to date no capacity for iron reduction has been reported. *Dethiobacter*-like species were a minor constituent of the original population but clearly thrived when the pH was buffered to 9.3, however it must be

noted that there is no direct evidence that they were responsible for the Fe(III) reduction observed.

The *Anaerobranca*-like species from B2-310 soil and the two actives microcosm series form a distinct clade within the Clostridiales Incertae Sedis XIV, but are closely related to several species of *Anaerobranca*, a genus containing fermentative anaerobic extremophiles (see Figure 6.6). Whilst similarity of the 16S rRNA gene is not evidence that organisms share other genes (e.g. those associated with adaptation to a particular environment) it is nevertheless interesting that *A. californiensis, A. gottschalkii,* and *A. zavarzinii* are all alkaliphilic thermophilic anaerobes (Gorlenko et al., 2004; Kevbrin et al., 2008; Prowe and Antranikian, 2001). Similarly *A. horikoshii* is an alkali-tolerant thermophilic anaerobe (Engle et al., 1995). *A. californiensis, A. gottschalkii and A. horikoshii* are able to reduce iron and sulphur in the presence of organic matter (Gorlenko et al., 2004). There is also evidence that *A. zavarzinii* can reduce Fe(III) to Fe(II) but this is less conclusive (Kevbrin et al., 2008).

The microbial community of the *unamended* microcosms was sampled when nitrite reduction was the predominant biogeochemical process. This population was dominated by a single OTU (37 of the 43 sequences), which is assigned to the order *Deinococcales* and were most probably a *Truepera* species. The phylogenetic tree constructed (Figure 6.7) confirms this classification. The only *Truepera* specie that has been studied in detail is *Truepera Radiovictrix*, the type genus of the family Trueperaceae, which is a radiation resistant, alkaliphilic, slightly halophilic aerobe (Albuquerque et al., 2005).

No exogenic carbon source was added to the microcosm experiments, so microbial metabolism is supported by electron donors derived from the soil organic matter (the soil contains 1% total organic carbon). In anaerobic systems the complete oxidation of organic matter requires the cooperative activity of a community of microorganisms collectively exhibiting several different metabolic pathways (e.g. hydrolysis of complex organic matter, fermentation of sugars, and oxidation of fatty acids, lactate, acetate and H_2 (1995; 1993a)). As processes such as dissimilative nitrate and iron reduction require labile organic carbon (Gottschalk, 1986; Kim and Gadd, 2008) the soil must contain consortium of bacteria capable of the continued breakdown of less labile organic substrates (without replenishment, labile substrates would have been consumed years ago). The development of a cascade of terminal electron accepting processes in the *pH-amended* system suggests that it retained this capability despite the slight decrease in microbial diversity. However, the failure of the *unamended* control microcosms to progress beyond nitrate reduction after 270 days may be due in part to loss of microbial diversity impacting the community's ability to breakdown soil organic matter.

6.5 Engineering implications

Promoting in-situ bioreduction to Cr(III) is a promising way of stopping Cr(VI) leached from legacy COPR disposal sites contaminating groundwater or damaging aquatic ecosystems. However the very high pH of COPR leachate produces an extremely challenging environment to microorganisms capable of dissimilative metal reduction, and thus metabolic rates are slow even where the microbial community has adapted to high pH. This study shows that reducing the pH to closer to the optimum for many alkaliphiles (~pH9) using sodium bicarbonate promoted microbial nitrate and iron reduction coupled to oxidation of electron donors derived from the

soil organic matter. Amendment of pH by this method could therefore enhance the immobilisation of chromium as Cr(VI) is reduced to Cr(III) by microbially reduced Fe(II). The advantage of pH amendment is that supplementing natural groundwater ions such as Na^+ and HCO_3^- may be more acceptable to regulating authorities responsible for groundwater quality than the addition of either nutrients (bio-stimulation) or non-native microorganisms (bio-augmentation). It required about five times more HCO_3^- than acid to buffer the soil pH to pH 9.5 (Figure 6.1). This is because equilibrium is established between CO_3^{2-} and HCO_3^- as this pH value is approached, reducing the effect of further HCO_3^- addition. However, despite the higher addition rate, HCO_3^- is probably the better pH buffer for promoting bioremediation as the pH stability of the CO_3^{2-}/HCO_3^- buffered system will be better for bacterial growth.

6.6 Conclusions

A diverse population of novel anaerobic alkaliphiles exists in the former topsoil layer beneath a COPR tip, despite long-term exposure to oxidising Cr(VI) contaminated hyperalkaline leachate. This population contains taxa capable of coupling the oxidation of soil organic matter to the biogeochemical cycling of nitrate and iron during the progression of microbial anoxia. Addition of HCO_3^- to this soil produces a system with a high buffering capacity at pH values close to the growth optima of many alkaliphiles (Horikoshi, 2004). This promotes bio-reduction of Fe(III), with phylogenetic community analysis indicating that bacteria in the phylum *Firmicutes* are most likely responsible. Bicarbonate amendment of pH is a promising method of stimulating bioremediation of Cr(VI) contaminated groundwater where the microbial community have adapted to alkaline conditions.

6.7 Acknowledgements

RAW is funded by a University of Leeds, John Henry Garner Scholarship. Thanks to: Dr Phil Studds and Mark Bell, Ramboll UK, for enabling fieldwork; Michael Marsden, University of Leeds, for help with fieldwork; and Kalotina Geraki and Prof. Fred Mosselmans for advice during STFC funded XAS experiments at the Diamond Light Source.

6.8 References

Albuquerque, L., Simoes, C., Nobre, M.F., Pino, N.M., Battista, J.R., Silva, M.T., Rainey, F.A., da Costa, M.S., 2005. Truepera radiovictrix gen. nov., sp nov., a new radiation resistant species and the proposal of Trueperaceae fam. nov. FEMS Microbiol. Lett. 247, 161-169.

ASTM, 2006. D4972-01: standard test method for pH of soils. Annual book of ASTM standards. American Society for Testing and Materials 4, 963-965.

Atkins, J., 2009. Modelling groundwater and chromite migration through an old spoil tip in Copley., MSc Dissertation School of Earth and Environment. University of Leeds, Leeds, UK.

Breeze, V.G., 1973. Land Reclamation and River Pollution Problems in Croal Valley Caused by Waste from Chromate Manufacture. J. Appl. Ecol. 10, 513-525.

Burke, I.T., Boothman, C., Lloyd, J.R., Livens, F.R., Charnock, J.M., McBeth, J.M., Mortimer, R.J.G., Morris, K., 2006. Reoxidation behavior of technetium, iron, and sulfur in estuarine sediments. Environ. Sci. Technol. 40, 3529-3535.

Chai, L.Y., Huang, S.H., Yang, Z.H., Peng, B., Huang, Y., Chen, Y.H., 2009. Hexavalent chromium reduction by Pannonibacter phragmitetus BB isolated from soil under chromium-containing slag heap. J. Environ. Sci. Heal. A 44, 615-622.

Choe, S.H., Ljestrand, H.M., Khim, J., 2004. Nitrate reduction by zero-valent iron under different pH regimes. Appl. Geochem. 19, 335-342.

Coxon, A.P.M., 2004. Multidimensional Scaling in M. S. Lewis-Beck, A. Bryman, T. F. Liao, The Sage Encyclopedia of Social Science Research Methods. Sage, Thousand Oaks.

Deakin, D., West, L.J., Stewart, D.I., Yardley, B.W.D., 2001. Leaching behaviour of a chromium smelter waste heap. Waste Manage. 21, 265-270.

Dhamole, P.B., Nair, R.R., D'Souza, S.F., Lele, S.S., 2008. Denitrification of Highly Alkaline Nitrate Waste Using Adapted Sludge. Appl. Biochem. Biotechnol. 151, 433-440.

Dobbin, P.S., Carter, J.P., Garcia-Salamanca San Juan, C., Hobe, M., Powell, A.K., Richardson, D.J., 1999. Dissimilatory Fe(III) reduction by Clostridium beijerinckii isolated from freshwater sediment using Fe(III) maltol enrichment. FEMS Microbiol. Lett. 176, 131-138.

Engle, M., Li, Y.H., Woese, C., Wiegel, J., 1995. Isolation and characterization of a novel alkalitolerant thermophile, Anaerobranca horikoshii gen. nov., sp. nov. Int. J. Syst. Bacteriol. 45, 454-461.

Fanning, J.C., 2000. The chemical reduction of nitrate in aqueous solution. Coord. Chem. Rev. 199, 159-179.

Farmer, J.G., Graham, M.C., Thomas, R.P., Licona-Manzur, C., Licona-Manzur, C., Paterson, E., Campbell, C.D., Geelhoed, J.S., Lumsdon, D.G., Meeussen, J.C.L., Roe, M.J., Conner, A., Fallick, A.E., Bewley, R.J.F., 1999. Assessment and modelling of the environmental chemistry and potential for remediative treatment of chromium-contaminated land. Environ. Geochem. Health 21, 331-337.

Farmer, J.G., Paterson, E., Bewley, R.J.F., Geelhoed, J.S., Hillier, S., Meeussen, J.C.L., Lumsdon, D.G., Thomas, R.P., Graham, M.C., 2006. The implications of integrated assessment and modelling studies for the future remediation of chromite ore processing residue disposal sites. Sci. Total Environ. 360, 90-97.

Francis, C.A., Obraztsova, A.Y., Tebo, B.M., 2000. Dissimilatory metal reduction by the facultative anaerobe Pantoea agglomerans SP1. Appl. Environ. Microbiol. 66, 543-548.

Garnova, E.S., Zhilina, T.N., Tourova, T.P., Lysenko, A.M., 2003. Anoxynatronum sibiricum gen.nov., sp.nov alkaliphilic saccharolytic anaerobe from cellulolytic community of Nizhnee Beloe (Transbaikal region). Extremophiles 7, 213-220.

Geelhoed, J.S., Meeussen, J.C.L., Hillier, S., Lumsdon, D.G., Thomas, R.P., Farmer, J.G., Paterson, E., 2002. Identification and geochemical modeling of processes controlling leaching of Cr(VI) and other major elements from chromite ore processing residue. Geochim. Cosmochim. Acta 66, 3927-3942.

Glass, C., Silverstein, J., 1998. Denitrification kinetics of high nitrate concentration water: pH effect on inhibition and nitrite accumulation. Water Res. 32, 831-839.

Gorlenko, V., Tsapin, A., Namsaraev, Z., Teal, T., Tourova, T., Engler, D., Mielke, R., Nealson, K., 2004. Anaerobranca californiensis sp nov., an anaerobic, alkalithermophilic, fermentative bacterium isolated from a hot spring on Mono Lake. Int J Syst Evol Microbiol 54, 739-743.

Gottschalk, G., 1986. Bacterial Metabolism. Springer-Velag, New York.

Hansen, H.C.B., Koch, C.B., NanckeKrogh, H., Borggaard, O.K., Sorensen, J., 1996. Abiotic nitrate reduction to ammonium: Key role of green rust. Environ. Sci. Technol. 30, 2053-2056.

Harris, S.J., Mortimer, R.J.G., 2002. Determination of nitrate in small water samples (100 mu L) by the cadmium-copper reduction method: A manual technique with application to the interstitial waters of marine sediments. Int. J. Environ. Anal. Chem. 82, 369-376.

Higgins, T.E., Halloran, A.R., Dobbins, M.E., Pittignano, A.J., 1998. In situ reduction of hexavalent chromium in alkaline soils enriched with chromite ore processing residue. Japca J. Air. Waste Ma. 48, 1100-1106.

Horikoshi, K., 2004. Alkaliphiles. P. Jpn. Acad. A-Phys. 80, 166-178.

James, B.R., 1994. Hexavalent Chromium Solubility and Reduction in Alkaline Soils Enriched with Chromite Ore Processing Residue. J. Environ. Qual. 23, 227-233.

Jeyasingh, J., Philip, L., 2005. Bioremediation of chromium contaminated soil: optimization of operating parameters under laboratory conditions. . J. Hazard. Mater. 118, 113-120.

Kevbrin, V., Boltyanskaya, Y., Garnova, E., Wiegel, J., 2008. Anaerobranca zavarzinii sp nov., an anaerobic, alkalithermophilic bacterium isolated from Kamchatka thermal fields. Int J Syst Evol Microbiol 58, 1486-1491.

Kevbrin, V.V., Zhilina, T.N., Rainey, F.A., Zavarzin, G.A., 1998. Tindallia magadii gen. nov., sp. nov.: An alkaliphilic anaerobic ammonifier from soda lake deposits. Curr. Microbiol. 37, 94-100.

Kim, B.H., Gadd, G., 2008. Bacterial Physiology and Metabolism. Cambridge University Press, Cambridge.

Krebs, C.J., 1999. Ecological Methodology, 2nd ed. Addison-Welsey Educational Publishers Inc, Menlo Park, CA.

Langmuir, D., 1997. Aqueous Environmental Geochemistry. Englewood Cliffs, NJ: Prentice Hall.

Leschine, S.B., 1995. Cellulose degradation in anaerobic environments. Annu. Rev. Microbol 49, 399-426.

Lin, C.J., 2002. The chemical transformations of chromium in natural waters - A model study. Water Air Soil Poll. 139, 137-158.

Lovley, D.R., 1991. Dissimilatory Fe(III) and Mn(IV) Reduction. Microbiol. Rev. 55, 259-287.

Lovley, D.R., 1993a. Anaerobes into Heavy-Metal - Dissimilatory Metal Reduction in Anoxic Environments. Trends Ecol. Evol. 8, 213-217.

Lovley, D.R., 1993b. Dissimilatory Metal Reduction. Annu. Rev. Microbol 47, 263-290.

Lovley, D.R., 1997. Microbial Fe(III) reduction in subsurface environments. FEMS. Microbiol. Rev. 20, 305-313.

Lovley, D.R., Phillips, E.J.P., 1986a. Availability of Ferric Iron for Microbial Reduction in Bottom Sediments of the Fresh-Water Tidal Potomac River. Appl. Environ. Microbiol. 52, 751-757.

Lovley, D.R., Phillips, E.J.P., 1986b. Organic-Matter Mineralization with Reduction of Ferric Iron in Anaerobic Sediments. Appl. Environ. Microbiol. 51, 683-689.

Nelson, N.L., Cox, M.M., 2005. Lehninger Principles of Biochemistry. W. H. Freeman and Co., New York.

Ottley, C.J., Davison, W., Edmunds, W.M., 1997. Chemical catalysis of nitrate reduction by iron(II). Geochim. Cosmochim. Acta 61, 1819-1828.

Pollock, J., Weber, K.A., Lack, J., Achenbach, L.A., Mormile, M.R., Coates, J.D., 2007. Alkaline iron(III) reduction by a novel alkaliphilic, halotolerant, Bacillus sp isolated from salt flat sediments of Soap Lake. Appl. Microbol. Biot. 77, 927-934.

Postma, D., 1990. Kinetics of nitrate reduction by detrital Fe(II)-silicates. Geochim. Cosmochim. Acta 54, 903-908.

Prowe, S.G., Antranikian, G., 2001. Anaerobranca gottschalkii sp nov., a novel thermoalkaliphilic bacterium that grows anaerobically at high pH and temperature. Int J Syst Evol Microbiol 51, 457-465.

Rai, D., Sass, B.M., Moore, D.A., 1987. Chromium(Iii) Hydrolysis Constants and Solubility of Chromium(Iii) Hydroxide. Inorg. Chem. 26, 345-349.

Richard, F.C., Bourg, A.C., 1991. Aqueous geochemistry of Cr: A review. Water Res. 25, 807-816.

Romanenko, V.I., Koren'kov, V.N., 1977. Pure culture of bacteria using chromates and bichromates as hydrogen acceptors during development under anaerobic conditions. Mikrobiologiia 46, 414-417.

Roskam, E.E., Coxon, A.P.M., Brier, A.P., Hawkins, P.K., 2005. The NewMDSX Program Series, Version 5. NewMDSX Project, Edinburgh.

Sani, R.K., Peyton, B.M., Smith, W.A., Apel, W.A., Petersen, J.N., 2002. Dissimilatory reduction of Cr(VI), Fe(III), and U(VI) by Cellulomonas isolates. Appl. Microbol. Biot. 60, 192-199.

Saraswat, I.P., Vajpei, A.C., 1984. Characterization of Chromium-Oxide Hydrate Gel. J. Mater. Sci. Lett. 3, 515-517.

Sau, G.B., Chatterjee, S., Sinha, S., Mukherjee, S.K., 2008. Isolation and Characterization of a Cr(VI) Reducing Bacillus firmus Strain from Industrial Effluents. Polish Journal of Microbiology 57, 327-332.

Schloss, P.D., Westcott, S.L., Ryabin, T., Hall, J.R., Hartmann, M., Hollister, E.B., Lesniewski, R.A., Oakley, B.B., Parks, D.H., Robinson, C.J., Sahl, J.W., Stres, B., Thallinger, G.G., Van Horn,

D.J., Weber, C.F., 2009. Introducing mothur: Open-Source, Platform-Independent, Community-Supported Software for Describing and Comparing Microbial Communities. Appl. Environ. Microbiol. 75, 7537-7541.

Schumacher, B.A., 2002. Methods for the Determination of Total Organic Carbon (TOC) in Soils and Sediments. United States Environmental Protection Agency, Las Vegas.

Smith, K.S., 2007. Strategies to predict metal mobility in surficial mining environments. Reviews in Engineering Geology 17, 25-45.

Son, A.J., Schmidt, C.J., Shin, H.J., Cha, D.K., 2011. Microbial community analysis of perchlorate-reducing cultures growing on zero-valent iron. J. Hazard. Mater. 185, 669-676.

Sorokin, D.Y., Tourova, T.P., Mussmann, M., Muyzer, G., 2008. Dethiobacter alkaliphilus gen. nov sp nov., and Desulfurivibrio alkaliphilus gen. nov sp nov.: two novel representatives of reductive sulfur cycle from soda lakes. Extremophiles 12, 431-439.

Stewart, D.I., Burke, I.T., Hughes-Berry, D.V., Whittleston, R.A., 2010. Microbially mediated chromate reduction in soil contaminated by highly alkaline leachate from chromium containing waste. Ecol. Eng. 36, 211-221.

Stewart, D.I., Burke, I.T., Mortimer, R.J.G., 2007. Stimulation of microbially mediated chromate reduction in alkaline soil-water systems. Geomicrobiol. J. 24, 655-669.

Stougaard, P., Jorgensen, F., Johnsen, M.G., Hansen, O.C., 2002. Microbial diversity in ikaite tufa columns: an alkaline, cold ecological niche in Greenland. Environ. Microbiol. 4, 487-493.

Tilt, Z., 2009. The subsurface migration of Cr(VI) at a chromium waste tip in the North of England., School of Earth and Environment. University of Leeds.

Tinjum, J.M., Benson, C.H., Edil, T.B., 2008. Mobilization of Cr(VI) from chromite ore processing residue through acid treatment. Sci. Total Environ. 391, 13-25.

USEPA, 1992. SW-846 Manual: Method 7196a. Chromium hexavalent (colorimetric). Retrieved 6th Jan 2006.

USEPA, 1998. Toxicological review of hexavalent chromium. Available online at http://www.epa.gov/ncea/iris.

VanEngelen, M.R., Peyton, B.M., Mormile, M.R., Pinkart, H.C., 2008. Fe(III), Cr(VI), and Fe(III) mediated Cr(VI) reduction in alkaline media using a Halomonas isolate from Soap Lake, Washington. Biodegradation 19, 841-850.

Wang, Q., Garrity, G.M., Tiedje, J.M., Cole, J.R., 2007. Naive Bayesian classifier for rapid assignment of rRNA sequences into the new bacterial taxonomy. Appl. Environ. Microbiol. 73, 5261-5267.

Weber, K.A., Picardal, F.W., Roden, E.E., 2001. Microbially catalyzed nitrate-dependent oxidation of biogenic solid-phase Fe(II) compounds. Environ. Sci. Technol. 35, 1644-1650.

Weng, C.H., Huang, C.P., Sanders, P.F., 2000. Effect of pH on Cr(VI) leaching from soil enriched in chromite ore processing residue, 18th European Conference of SEGH, Glasgow, Scotland, pp. 207-211.

Whittleston, R.A., Stewart, D.I., Mortimer, R.J.G., Ashley, D.J., Burke, I.T., 2011a. Effect of Microbially Induced Anoxia on Cr(VI) Mobility at a Site Contaminated with Hyperalkaline Residue from Chromite Ore Processing. Geomicrobiol. J. 28, 68-82.

Whittleston, R.A., Stewart, D.I., Mortimer, R.J.G., Tilt, C.Z., Brown, A.P., Geraki, K., Burke, I.T., 2011b. Chromate reduction in Fe(II)-containing soil affected by hyperalkaline leachate from chromite ore processing residue. J. Hazard. Mater.

Zavarzina, D.G., Kolganova, T.V., Boulygina, E.S., Kostrikina, N.A., Tourova, T.P., Zavarzin, G.A., 2006. Geoalkalibacter ferrihydriticus gen. nov sp nov., the first alkaliphilic representative of the family Geobacteraceae, isolated from a soda lake. Microbiol. 75, 673-682.

Zhu, W.J., Yang, Z.H., Ma, Z.M., Chai, L.Y., 2008. Reduction of high concentrations of chromate by Leucobacter sp CRB1 isolated from Changsha, China. World J. Microb. Biot. 24, 991-996.

Chapter 7 Isolation of microbial iron reducers

This chapter reports results from several attempts made at obtaining viable single specie isolates of the iron reducing alkaliphiles indigenous to the reducing zone beneath the COPR (sample B2-310). It begins with an overview of the bioenergetics of microbial iron reduction.

7.1 Introduction

The process of iron metabolism by microorganisms has been around for billions of years, and is believed to have driven the global carbon cycle in the early earth's anaerobic atmosphere (Canfield et al., 2006). This method of metabolism is carried out by a broad range of bacterial phyla, and is still widespread today in many anaerobic niches. Examples of iron metabolising communities have been found in deep sea environments, deep mines, and a broad range of subsurface soils and sediments (Konig et al., 1997; Templeton, 2011; Zavarzina et al., 2006).

As discussed in Chapter 6, microbial reduction of iron is a result of the transfer of electrons from the oxidation of organic carbon (or H_2) to Fe(III) species to obtain energy for growth, in the absence of oxygen. This occurs either directly by use as an terminal electron acceptor in place of oxygen during dissimilatory iron reduction (respiration), or indirectly via the external dumping of electrons from a cell to maintain a suitable redox balance as a consequence of the enzymatic transformation of organic substrates (fermentation) (Nelson and Cox, 2005). In both processes electrons are eventually transferred from the cell outer membrane to Fe(III) by either the direct transfer of c-type cytochromes, indirect transfer via electron shuttles, or

indirect transfer to solubilised Fe(III) species produced by organic chelators (Newman, 2001). The use of each mechanism is not mutually exclusive, and is dependent on the form of iron available and the physiology of the microorganism present (Bird et al., 2011).

Complex soil organic matter is a primary source of organic carbon for microorganisms in subsurface soils and sediments. Its complete breakdown by microorganisms occurs with the production of a series of organic intermediates. The initial hydrolysis of complex organic matter by bacterial hydrolytic enzymes yields macronutrients such as proteins (amino acids), carbohydrates and long chain fatty acids (Lovley, 1993). These in turn are broken down by microorganisms into simpler organic molecules or H_2 which are then further oxidised by bacteria to eventually form CO_2. For example, fermentative bacteria gain energy through the fermentation of complex sugars and proteins, with the reduction of Fe(III) reported in a wide range of bacteria including *Bacillus sp.* (Pollock et al., 2007), *Clostridium beirjerinckii* (Dobbin et al., 1999), *Anoxynatronum sibiricum* (Garnova et al., 2003) and *Anaerobranca californiensis* (Gorlenko et al., 2004). The products of fermentation include simpler organic compounds such as short chained fatty acids e.g. lactate and acetate and H_2. These in turn can be respired by dissimilatory Fe(III) reducers, for example acetate by *Geobacter metalireducens* (Lovley et al., 1993), lactate by *Cellulomonas flavigena* (Sani et al., 2002) and H_2 by *Geobacter sulfurreducens* (Caccavo et al., 1994). Simplified microbial dissimilatory iron reducing reactions with acetate and H_2 are described below *(Eqn. 14 - 15)* (Lovley, 1993);

$$Acetate^- + 8Fe(III) + 4H_2O \rightarrow 2HCO_3^- + 8Fe(II) + 9H^+ \quad (14)$$

$$H_2 + 2Fe(III) \rightarrow 2Fe(II) + 2H^+ \quad (15)$$

Bacteria respiring on these simpler organic substrates are reliant on the continued breakdown of larger organic components by the action of fermentative bacteria to provide substrates for their metabolism. The complete breakdown of complex soil organic matter *in-situ* therefore requires the collaborative action of a community of microorganisms utilising different metabolic pathways, which in anoxic environments can be coupled to the reduction of iron.

The ability of microorganisms to reduce iron has been known since the 19th century. However, it was not until more recently that the transformation of Fe(III) to Fe(II) has become regarded as the most important chemical change that occurs in the development of anaerobic soils, due to its influence on trace metal behaviour (Bird et al., 2011; Lovley, 1991, 1997; Pollock et al., 2007; Zavarzina et al., 2006). The production of Fe(II) species by iron metabolising microorganisms has therefore been suggested as a useful mechanism for the remediation of metal contaminated subsurface environments, as well as other decontamination processes such as dechlorination (Lovley, 1997). In COPR effected environments where pH values easily can exceed 6.0 ferrous iron, Fe(II), is regarded as the most important reductant of Cr(VI) (Lin, 2002). The microbial transformation of iron can therefore catalyse the reduction of chromium by providing a source of Fe(II) for the abiotic reduction of Cr(VI). If iron reducing conditions are maintained, the Fe(III) produced via this reaction may subsequently be re-reduced, effectively replenishing the supply of

Fe(II) in the soils available for the abiotic reduction of Cr(VI). This has been suggested as a possible mechanism for the remediation of Cr(VI) contaminated environments in both laboratory studies (Wielinga et al., 2001), and during field study's where Cr(VI) enters an organic rich reducing zone (Higgins et al., 1998).

For this COPR site the results presented in chapter's 4-6 strongly suggest that this biotic-abiotic coupling is responsible for the natural attenuation of Cr(VI) as Cr(III) *in-situ*. It appears that this mechanism is controlled by a community of indigenous microorganisms containing anaerobic alkaliphiles, capable of iron reduction in microhabitats where the pH is lower than the bulk soil value. Although the capacity of this community to directly reduce Cr(VI) cannot be ruled out, it is impossible to distinguish from the Cr(VI) removal observed in microcosm experiments due to the presence of significant proportions of Fe(II). This is because the abiotic reduction of Cr(VI) by Fe(II) is reported to occur at a much faster rate than biological Cr(VI) reduction (Wielinga et al., 2001).

The biostimulation method of bioremediation would involve the *in-situ* addition of nutrients to nutrient starved systems or altering of conditions that is known to stimulate the growth of the desired microbial community. The stimulation of these indigenous iron reducing microorganisms *in-situ* could therefore increase the Fe(II) content in sediments and theoretically result in the increased attenuation of chromium. For this study site, it has been demonstrated that soil organic matter present in the horizon beneath the COPR waste is providing a supply of nutrients to the indigenous microorganisms, allowing them to respire successfully. The results from Chapter 6 show that pH amendment favours the development of microbial iron

metabolism by the indigenous alkaliphilic population. This suggests that pH amendment of the soil horizon *in-situ* as may provide a suitable bioremediation strategy through the enhancement of iron bioreduction by indigenous alkaliphiles.

Due to the numerous metabolic pathways employed by microorganisms outlined above, it is important to characterise the bioenergetics of the organisms responsible for iron reduction at this site. This includes the organic substrates used and mechanism of electron transfer to Fe(III). This ensures that when implementing biostimulation the correct amendments can be made that will have the best chance at successfully stimulating the iron metabolising population *in-situ*. To do this, pure single specie cultures capable of iron reduction are required. This chapter reports the results of several methods employed in an attempt to produce such an isolate from the soils beneath the COPR at this site.

7.2 Methods

7.2.1 Iron reducing consortium

It was identified in Chapter 4 that a consortium of iron reducing alkaliphiles could be successfully cultured at pH 9.2 from soil B2-310 when incubated in the presence of Fe(III) citrate and yeast extract as the sole electron acceptor and donor respectively (full details see Appendix A.4.1**)**. This population was dominated by members of the phylum *Firmicutes*, which accounted for 43 of the 44 clones successfully classified to phylum level based on >95% similarity using the RDP classifier (Wang et al., 2007). It is therefore reasonable to assume that members of this phylum are capable of Fe(III) reduction. The remaining clone was classified as a *β-proteobacterium.* A detailed breakdown of the structure of the *Firmicutes* population recovered based on

>95% similarity cut-off using the RDP classifier is shown in (Figure 7.1). Full clone libraries for this population can be found in Table B.4.

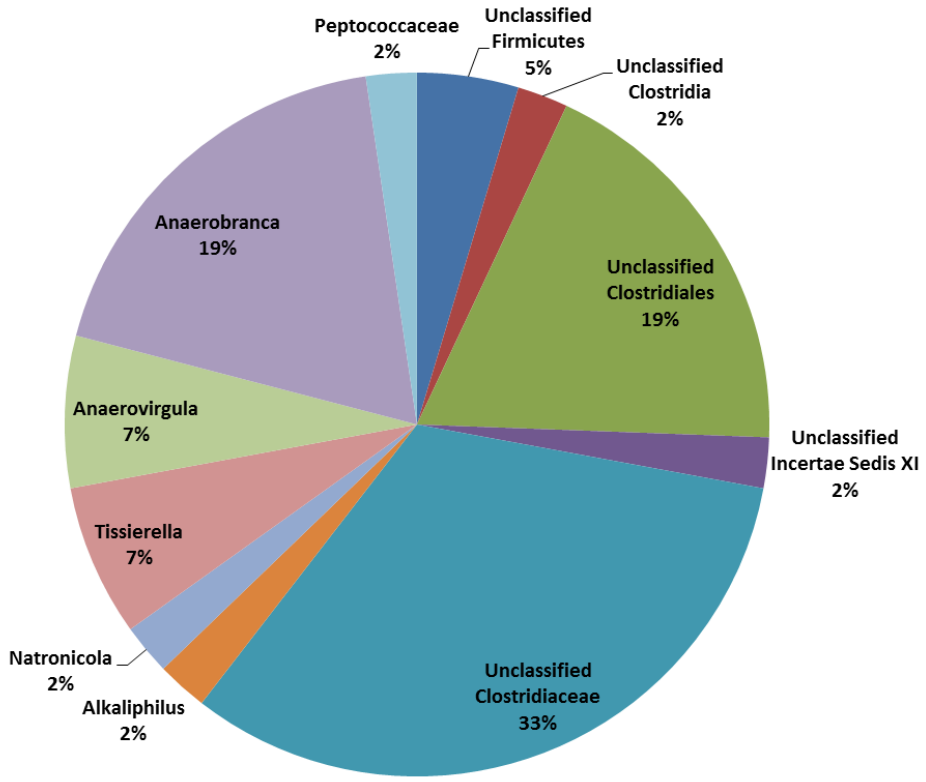

Figure 7.1 Microbial community structure of the *Firmicutes* population (43 clones) recovered from the iron reducing consortium.

It was clear from the structure of the *Firmicutes* population recovered (Figure 7.1) that the population remains relatively diverse, with genera from a range of families including *Peptococcaceae*, *Clostridiaceae, Incertae Sedis XI* and *Incertae Sedis XIV* represented. A number of different experiments were subsequently designed to try and isolate individual species from this initial consortium.

7.2.2 Iron reducing agar plates

In an attempt to produce isolates from the growth of individual microbial colonies, 2% agar plates composed of sterile iron reducing pH 9.2 media were produced and

poured using aseptic technique (for full protocol see Appendix A.4.2). Once solidified they were prepared from the iron consortium following two methods:

1. *Streak plating*

To produce streaked plates; 100 µl aliquots of iron reducing consortium exhibiting successful growth were extracted using needles and aseptic technique. These were transferred into 8 sterile 1.5 ml centrifuge tubes containing 400 µl sterile iron reducing media and mixed. Immediately, a sterile loop was immersed into the centrifuge tubes and used to streak across the surface of a pre-prepared agar plate. This was repeated for the remaining 7 aliquots. All 8 streaked plates were then transferred into a sealed plastic container and incubated in an anaerobic atmosphere produced using Anaerogen^{tm} sachets, at 21°C.

2. *Dilution spreading*

Plates were also prepared from a series of dilutions from the original iron reducing consortium. Briefly, 5, 10, 20, 40 and 50 µl of the iron reducing consortium was pipetted into a pool of sterile iron reducing media on the surface of the pre-prepared agar plates, to a final volume of 100 µl. Each dilution was then spread across the entire surface of the plates using aseptic technique. These were immediately transferred into a sealed plastic container and incubated in an anaerobic atmosphere produced using Anaerogen^{tm} sachets, at 21°C.

During preparation, all steps were progressed as quickly as possible to reduce the impact of exposure to atmospheric O_2 as excessive exposure may harm obligate anaerobic microorganisms. Successful growth was indicated by the clearing of the agar and/or appearance of colonies. Where a colony could be identified it was

transferred into a 1.5ml centrifuge tube containing sterile growth media using a sterile needle. This was then mixed and injected into sterile growth media bottles using aseptic technique and incubated in the dark at 21°C.

7.2.3 Serial dilution

The second method employed in an attempt to produce an isolate culture was the serial dilution of the iron reducing consortium into fresh growth media. This method is based on the theory of most probable number (MPN) analysis that suggests successive dilutions of a population will eventually produce a system where the population is absent or consist of a single individual. In microbiology this therefore gives the potential for a dilution of an initially mixed culture to consist of a single cell which can therefore grow into a culture containing a single species. The iron reducing consortium was repeatedly progressed into fresh sterile iron reducing media bottles, producing a series of 10^1 – 10^{10} dilutions (for full protocol see Appendix A.4.3). These were then incubated in the dark at 21°C.

7.2.4 DNA extraction

Successful growth in media bottles from methods was indicated by precipitate colour change from orange to black, and confirmed using the ferrozine method (for full protocol see appendix A.3.2). Any successful growth was then progressed to fresh media bottles to confirm a viable iron reducing culture had been obtained. DNA was then extracted from the viable cultures and prepared for 16s rRNA sequence analysis (for full protocol see Appendix A.5.2). Sequencing was performed by GATC biotech Ltd.

7.2.5 Phylogenetic assignment

The sequences recovered from each culture were classified using the Ribosomal Database Project (RDP) naïve Bayesian Classifier with a confidence threshold of 95%. A full description of the RDP Classifier can be found in Wang et al. (2007). The sequences were also grouped into operational taxonomic units (OTUs) using the MOTHUR software (Schloss et al., 2009) with a >98% nearest neighbour sequence similarity cut-off value (see Appendix B.5 for full clone libraries detailing phylogenetic assignment from each culture). Representative sequences from selected OTUs from each culture were aligned with known 16S rRNA gene type sequences of the phylum *Firmicutes* retrieved from the EMBL database, using the ClustalX software package (version 2.0.11). Phylogenetic trees were constructed from the distance matrix by neighbour joining, with bootstrap analysis performed with 1000 replicates. Resulting phylograms were drawn using the TreeView (version 1.6.6) software package, and rooted to *Geobacter Metallireducens* (L07834), included as an out-group.

7.3 Results

7.3.1 Streaked plating

The agar plates began to clear where they had been streaked after approximately 1 week of incubation (Figure 7.2). Despite this, individual colonies could not easily be identified. Instead, several media bottles were inoculated from needles touched into the plate at the edge of the cleared area. Two viable iron reducing cultures were obtained from these inoculations, P-2-3 and P-2-9.

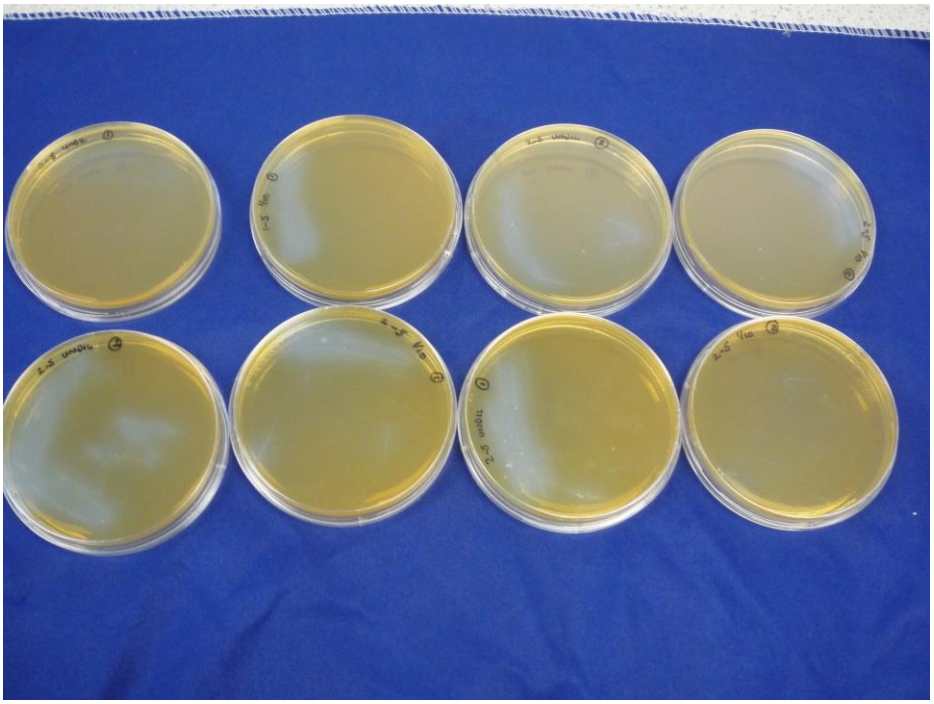

Figure 7.2 Clearing of iron reducing agar plates after 1 week of streaked incubation with iron reducing consortium

A total of 11 rRNA gene sequences were obtained from culture P-2-3, and all were assigned to the order *Clostridiales* within the phylum *Firmicutes* (confidence threshold of >95%). Within this order, 7 of the 11 sequences were assigned to the family *Incertae Sedis XI,* specifically the genera *Tissierella* (6), with the final 4 sequences remaining unassigned. MOTHUR analysis assigned this population to 4 distinct operational taxonomic units (OTUs), with 45% of the sequences recovered (5 of 11) contained within the largest OTU (E1). Sequences within OTU E1 were assigned to the genus *Tissierella*.

A total of 12 rRNA sequences were obtained from culture P-2-9, and all were assigned to the phylum *Firmicutes*. All but one of these sequences were assigned to the order *Clostridiales* (confidence threshold of >95%). The remaining sequence was assigned to the order *Bacillus.* Within the order *Clostridiales*, 9 of the 11 sequences were assigned to the family *Incertae Sedis XIV,* specifically the genera

Anaerovirgula (7) and *Anaerobranca* (2). The remaining 3 *Clostridiales* sequences were assigned to the genus *Tissierella.* MOTHUR analysis assigned this population to 4 OTUs, with 58% of the sequences recovered (7 of 12) contained within the largest OTU (F1). Sequences within OTU F1 were assigned to the genus *Anaerovirgula.*

7.3.2 Dilution spreading

The plates that had been spread with different concentrations of the initial iron reducing consortium began to clear after approximately 3 days incubation, starting with the plates that had received the highest concentration. After 2 weeks incubation all plates had cleared. Unfortunately these plates cleared in a uniform manner without the appearance of distinct individual colonies clearing the area of agar around them. It was therefore again difficult to identify individual colonies under a microscope and transfer to fresh media bottles using a needle. Despite this, one viable culture was obtained, PD-2-9. A total of 18 rRNA sequences were recovered from this culture, with 17 assigned to the order *Clostridiales* within the phylum *Firmicutes* (confidence threshold of >95%). The final sequence remained assigned as an unclassified bacterium. Within the order *Clostridiales*, 13 sequences were assigned to the family *Incertae Sedis XIV,* specifically the genera *Anaerovirgula* (6) and *Anaerobranca* (6), and 3 sequences assigned to the genus *Tissierella* within the family *Incertae Sedis XI.* MOTHUR analysis assigned this population to 5 OTUs, with 39% of the sequences recovered (7 of 18) contained within the largest OTU (G3). Sequences within OTU G3 were assigned to the genus *Anaerobranca.*

7.3.3 Serial dilution

Iron reducing conditions were established in all the dilutions produced, and developed in series with the highest dilution, 10^{10}, taking the longest period of incubation, approximately 1 month, before growth was observed. A total of 17 rRNA sequences were therefore recovered from the culture produced from the highest dilution, SD-10. All 17 sequences were assigned to the order *Clostridiales* within the phylum *Firmicutes* (confidence threshold of >95%), with 15 assigned to the family *Incertae Sedis XI,* specifically the genus *Tissierella* (14). The remaining 2 sequences were assigned to the genera *Anaerobranca* and *Anaerovirgula* within the family *Incertae Sedis XIV.* MOTHUR analysis assigned this population to 3 OTUs, with 88% of the sequences recovered (15 of 17) contained within the largest OTU (H1). Sequences within OTU H1 were assigned to the genus *Tissierella.*

Table 7.1 Summary of phylogenetic assignment from RDP classifier (95% confidence threshold) and MOTHUR analysis (>98% nearest neighbour similarity cut-off). Full sequence assignments can be found in Appendix B.5.

Source:	Streaked plate	Streaked plate	Plate spreading	Serial dilution
Culture:	P-2-3	P-2-9	PD-2-9	SD10
Number of sequences:	11	12	18	17
Firmicutes	100%	100%	94%	100%
Clostridiales	100%	92%	94%	100%
Incertae Sedis XI	64%	17%	17%	88%
Tissierella	55%	17%	17%	82%
Unclassified XI	9%	-	-	6%
Incertae Sedis XIV	-	75%	72%	12%
Anaerovirgula	-	58%	33%	6%
Anaerobranca	-	17%	33%	6%
Unclassified XIV	-		6%	-
Unclassified Clostridiales	36%	-	6%	-
Bacillales	-	8%	-	-
Bacillaceae	-	8%	-	-
Unclassified	-	8%	-	-
Unclassified	-	-	6%	-
Number of OTUs	4	4	5	3
Number in largest OTU	45%	58%	39%	88%

7.4 Discussion

It is clear that despite multiple attempts, a single specie culture was not isolated from the original iron reducing consortium. Each of the 4 populations characterised from

the isolation attempts were found to contain multiple OTUs, and were assigned to a variety of genera. A successful experiment was expected to only contain sequences from a single species, indistinguishable from one other with the distances between them easily within the 98% nearest neighbour threshold applied during MOTHUR analysis. Therefore 100% of these sequences would be expected to be contained within a single large operational taxonomic unit. Several factors may have attributed to the failings of these methods. Distinct colonies were not observed during the plate methods as were expected, and instead cleared in a uniform manner. This made it impossible to be certain that individual colonies were transferred to the media bottles for incubation, and may account for the range in species observed if more than one species was carried on the needle. In addition it was noted that microbial growth progressed downward into the gel, which made it difficult to be precise in transferring individual colonies without disturbing a wider area and increasing the risk of carrying multiple species.

Although no viable isolate was produced, the vast majority of the sequences recovered from each population were assigned using the RDP classifier to just 3 microbial genera within the *Firmicutes* phylum, *Anaerobranca, Anaerovirgula* and *Tissierella.* These populations were found to contain 3-5 OTUs, with the amount of sequences contained within the largest OTU ranging from 39% in the viable culture obtained from dilution spreading, to 88% of the population recovered from 10^{10} serial dilution. As the phylogenetic identity of the largest OTU also varied between samples, this suggests that the methods used had varying degrees of success in reducing the initial consortiums diversity, and/or favoured the growth of a particular OTU. For example, the major OTUs recovered from P-2-3 and SD10 (E1 and H1

respectively) were both assigned to the genera *Tissierella.* However, OTU H1 contained 88% of the sequences recovered compared to E1 which contained only 45%. The largest OTUs in the remaining two populations P-2-9 (F1) and PD-2-9 (G3) accounted for 58% and 39% of the sequences recovered, and were assigned to the genera *Anaerovirgula* and *Anaerobranca* respectively. Each of these three genera were represented in the original iron reducing consortium (Figure 7.1). *Anaerobranca* and *Tissierella* like sequences were also recovered from the initial B2-310 population (clone FR695956 and FR695962 respectively). The lack of *Anaerovirgula* like sequences in the original soil is likely due to it being a very minor constituent of the original population.

A phylogenetic tree was constructed to show the relationship between representative sequences from the largest OTU in each population to known *Firmicutes* type species, and to other sequences recovered from the initial soil and microcosm populations (Figure 7.3). This tree confirms the RDP classification of the dominant OTUs E1 and H1 as most likely members of the genus *Tissierella*, and OTU G3 as most likely members of the genus *Anaerobranca.* OTU G3 forms a clade with other *Anaerobranca*-like species recovered from the initial population and microcosm experiments, and share the closest type species *Anaerobranca gottschalkii* (Prowe and Antranikian, 2001), *Anaerobranca californiesis* (Gorlenko et al., 2004) and *Anaerobranca zavarzinii* (Kevbrin et al., 2008). These anaerobic extremophiles, discussed in detail in Chapter 6, are reported to be metabolise via fermentation on a variety of organic substrates, including yeast extract, and are capable of reducing iron (Gorlenko et al., 2004; Kevbrin et al., 2008; Prowe and Antranikian, 2001). The nearest type species to OTU E1 and H1, *Tissierella creatinophila* and *Tissierella*

praeacuta, are also fermentative anaerobes capable of metabolism with a variety of organic substrates, including yeast extract. However, their growth optima of pH of ~7.5 is lower than that of the reported *Anaerobranca sp.* and to date any ability to reduce Fe(III) has not been reported (Farrow et al., 1995; Harms et al., 1998). These two OTUs appear to form a distinct clade separate from their nearest type specie and original soil clone B2-310I-62, suggesting they may represent a different species within the same genus.

The position and high bootstrap value of OTU F1 to the closest type specie *Anaerovirgula multivorans* confirms its RDP classification as most likely a member of this genus. *Anaerovirgula multivorans* is an obligate anaerobic, alkaliphilic bacterium isolated from a soda lake environment (Pikuta et al., 2006). It is capable of growth at a pH value up to 10 by fermentation on a number of substrates including sugars, amino acids, and cellulose in the presence of yeast extract, but is not reported to reduce Fe(III) (Pikuta et al., 2006). Although the RDP classifier assigns this genus to the family *Incertae Sedis XIV*, its actual family classification appears to be poorly understood. The authors who isolated *A. Multivorans* suggest it belongs to the clostridial cluster XI, however the phylogenetic tree constructed for this study places this sequence distant from both cluster XI and XIV, closest to members of the family *Clostridiaceae*. The presence of relatively low bootstrap values amongst this family highlights the uncertainty of its classification to family level, and is likely due to the lack of other known *Anaerovirgula* type species.

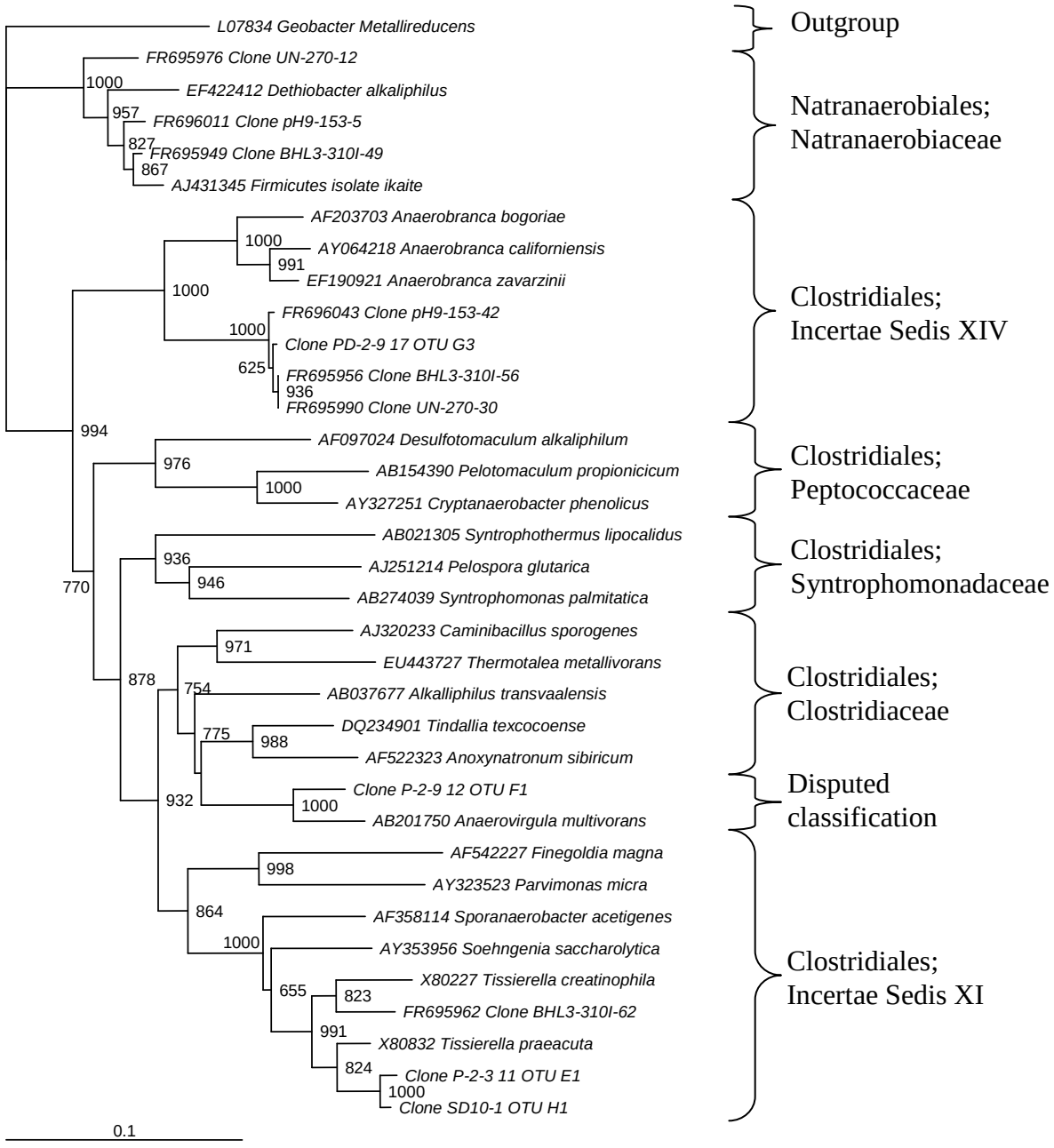

Figure 7.3 Phylogenetic tree showing the relationship between representative sequences from major OTU's recovered from each population, other members of the orders *Clostridiales* and *Natranaerobiales* of *Firmicutes* and representative sequences from major OTU's recovered from previously reported populations. *Geobacter metallireducens* (δ-proteobacteria) is included as an out-group. The scale bar corresponds to 0.1 nucleotide substitutions per site. Bootstrap values (from 1000 replications) are shown at branch points.

In-situ microbial populations will frequently rely on each other to break down complex organic matter to liberate the substrates required for various metabolic pathways, existing in symbiotic relationships. Yeast extract was used in these experiments as it is a broad specificity electron donor, providing many different substrates required for fermentative metabolism in anaerobic environments. The fermentation of yeast extract also yields acetate, H_2 and CO_2 (Lovley, 1993), which may further act as substrates for microbial respiration. The complexity of yeast extract as a carbon source could therefore mean that some organisms in these cultures are reliant on its break it down into simpler substrates required for their metabolism. This could also explain the difficulties encountered in producing an isolated culture as symbiotic relationships may be essential for the survival of an organism. However, whilst similarity of the 16S rRNA gene is not evidence that organisms share genes (such as those controlling metabolic pathway) the closest type species to the dominant OTU's recovered from these populations are all reported to metabolise via fermentation on multiple substrates, including yeast extract (Gorlenko et al., 2004; Harms et al., 1998; Kevbrin et al., 2008; Pikuta et al., 2006; Prowe and Antranikian, 2001).

7.5 Conclusions and future considerations

Although a number of viable cultures were recovered from the experiments, the methods employed were unsuccessful at isolating a single species from the original iron reducing consortium for extensive characterisation. This may be due to the microorganisms, specifically *Anaerobranca, Anaerovirgula* and *Tissierella*-like clones, reliant on symbiotic relationships for successful metabolism. Failure may also be the result of the difficulties encountered with the methods used. It would

therefore be prudent to make the following considerations when attempting to isolate species from the iron reducing consortium in the future:

- Plate incubation techniques appear to be unsuitable due to the growth characteristics of the microorganisms contained within the iron reducing consortium.
- The presence of the fewest OTUs (3) and relative proportion contained within the largest OTU (H1 88%) suggests that the serial dilution method has been most successful at reducing the diversity from the initial consortium. Producing serial dilutions with dilution factors beyond 10^{10} is therefore an obvious adaptation to this method.
- Research into the metabolism of the nearest type species may identify a more specific fermentative substrate that may be unique to the metabolism of a single species. Use of this substrate in the place of yeast extract may therefore aid in the isolation of a single species.

Despite the lack of an isolated culture, the sequences recovered displayed clear similarity to known iron reducing species, to genera recovered from the original iron reducing consortium, and to members of the original soil population. The use of a variety of isolation techniques produced similar populations dominated by one or more of just three clostridia species within the *Anaerobranca*, *Anaerovirgula* and *Tissierella* genera. It can therefore be said with some confidence that these microorganisms will at least in part be responsible for iron reduction within *in-situ* microhabitats, and should be the target of future characterisation studies. This population of iron metabolising microorganisms are therefore responsible for

mediating the subsequent abiotic attenuation of chromium. It is likely that the collaborative action of multiple microorganisms capable of iron reduction is responsible for producing Fe(II) *in-situ.* Thus, it may be more applicable for the purposes of this research to characterise the iron reducing consortium as a whole. For example, the susceptibility of the consortium to pH change and Cr(VI) toxicity would provide more useful information in order to advise future bioremediation strategies for this site, than the response of a single microorganism.

7.6 References

Bird, L.J., Bonnefoy, V., Newman, D.K., 2011. Bioenergetic challenges of microbial iron metabolisms. Trends in Microbiology 19, 330-340.

Caccavo, F., Lonergan, D.J., Lovley, D.R., Davis, M., Stolz, J.F., McInerney, M.J., 1994. Geobacter sulfurreducens sp. nov., a hydrogen- and acetate-oxidizing dissimilatory metal-reducing microorganism. Appl. Environ. Microbiol. 60, 3752-3759.

Canfield, D.E., Rosing, M.T., Bjerrum, C., 2006. Early anaerobic metabolisms. Phil. Trans. R. Soc. B 361, 1819-1834.

Dobbin, P.S., Carter, J.P., Garcia-Salamanca San Juan, C., Hobe, M., Powell, A.K., Richardson, D.J., 1999. Dissimilatory Fe(III) reduction by Clostridium beijerinckii isolated from freshwater sediment using Fe(III) maltol enrichment. FEMS Microbiol. Lett. 176, 131-138.

Farrow, J.A.E., Lawson, P.A., Hippe, H., Gauglitz, U., Collins, M.D., 1995. Phylogenetic evidence that the gram-negative nonsporulating bacterium Tissierella (Bacteroides) praeacuta is a member of the Clostridium subphylum of the gram-positive bacteria and description of Tissierella creatinini sp. nov. Int. J. Syst. Bacteriol. 45, 436-440.

Garnova, E.S., Zhilina, T.N., Tourova, T.P., Lysenko, A.M., 2003. Anoxynatronum sibiricum gen.nov., sp.nov alkaliphilic saccharolytic anaerobe from cellulolytic community of Nizhnee Beloe (Transbaikal region). Extremophiles 7, 213-220.

Gorlenko, V., Tsapin, A., Namsaraev, Z., Teal, T., Tourova, T., Engler, D., Mielke, R., Nealson, K., 2004. Anaerobranca californiensis sp nov., an anaerobic, alkalithermophilic, fermentative bacterium isolated from a hot spring on Mono Lake. Int J Syst Evol Microbiol 54, 739-743.

Harms, C., Schleicher, A., Collins, M.D., Andreesen, J.R., 1998. Tissierella creatinophila sp. nov., a Gram-positive, anaerobic, non-spore-forming, creatinine-fermenting organism. Int. J. Syst. Bacteriol. 48, 983-993.

Higgins, T.E., Halloran, A.R., Dobbins, M.E., Pittignano, A.J., 1998. In situ reduction of hexavalent chromium in alkaline soils enriched with chromite ore processing residue. Japca J. Air. Waste Ma. 48, 1100-1106.

Kevbrin, V., Boltyanskaya, Y., Garnova, E., Wiegel, J., 2008. Anaerobranca zavarzinii sp nov., an anaerobic, alkalithermophilic bacterium isolated from Kamchatka thermal fields. Int J Syst Evol Microbiol 58, 1486-1491.

Konig, I., Drodt, M., Suess, E., Trautwein, A.X., 1997. Iron reduction through the tan-green color transition in deep-sea sediments. Geochim. Cosmochim. Acta 61, 1679-1683.

Lin, C.J., 2002. The chemical transformations of chromium in natural waters - A model study. Water Air Soil Poll. 139, 137-158.

Lovley, D.R., 1991. Dissimilatory Fe(III) and Mn(IV) Reduction. Microbiol. Rev. 55, 259-287.

Lovley, D.R., 1993. Anaerobes into Heavy-Metal - Dissimilatory Metal Reduction in Anoxic Environments. Trends Ecol. Evol. 8, 213-217.

Lovley, D.R., 1997. Microbial Fe(III) reduction in subsurface environments. FEMS. Microbiol. Rev. 20, 305-313.

Lovley, D.R., Giovannoni, S.J., White, D.C., Champine, J.E., Phillips, E.J.P., Gorby, Y.A., Goodwin, S., 1993. Geobacter metallireducens gen. nov. sp. nov., a microorganism capable of coupling

the complete oxidation of organic compounds to the reduction of iron and other metals. Arch. Microbiol. 159, 336-344.

Nelson, N.L., Cox, M.M., 2005. Lehninger Principles of Biochemistry. W. H. Freeman and Co., New York.

Newman, D.K., 2001. Microbiology - How bacteria respire minerals. Science 292, 1312-1313.

Pikuta, E.V., Itoh, T., Krader, P., Tang, J., Whitman, W.B., Hoover, R.B., 2006. Anaerovirgula multivorans gen. nov., sp nov., a novel spore-forming, alkaliphilic anaerobe isolated from Owens Lake, California, USA. Int J Syst Evol Microbiol 56, 2623-2629.

Pollock, J., Weber, K.A., Lack, J., Achenbach, L.A., Mormile, M.R., Coates, J.D., 2007. Alkaline iron(III) reduction by a novel alkaliphilic, halotolerant, Bacillus sp isolated from salt flat sediments of Soap Lake. Appl. Microbol. Biot. 77, 927-934.

Prowe, S.G., Antranikian, G., 2001. Anaerobranca gottschalkii sp nov., a novel thermoalkaliphilic bacterium that grows anaerobically at high pH and temperature. Int J Syst Evol Microbiol 51, 457-465.

Sani, R.K., Peyton, B.M., Smith, W.A., Apel, W.A., Petersen, J.N., 2002. Dissimilatory reduction of Cr(VI), Fe(III), and U(VI) by Cellulomonas isolates. Appl. Microbol. Biot. 60, 192-199.

Schloss, P.D., Westcott, S.L., Ryabin, T., Hall, J.R., Hartmann, M., Hollister, E.B., Lesniewski, R.A., Oakley, B.B., Parks, D.H., Robinson, C.J., Sahl, J.W., Stres, B., Thallinger, G.G., Van Horn, D.J., Weber, C.F., 2009. Introducing mothur: Open-Source, Platform-Independent, Community-Supported Software for Describing and Comparing Microbial Communities. Appl. Environ. Microbiol. 75, 7537-7541.

Templeton, A.S., 2011. Geomicrobiology of iron in Extreme Environments. Elements 7, 95-100.

Wang, Q., Garrity, G.M., Tiedje, J.M., Cole, J.R., 2007. Naive Bayesian classifier for rapid assignment of rRNA sequences into the new bacterial taxonomy. Appl. Environ. Microbiol. 73, 5261-5267.

Wielinga, B., Mizuba, M.M., Hansel, C.M., Fendorf, S., 2001. Iron promoted reduction of chromate by dissimilatory iron-deducing bacteria. Environ. Sci. Technol. 35, 522-527.

Zavarzina, D.G., Kolganova, T.V., Boulygina, E.S., Kostrikina, N.A., Tourova, T.P., Zavarzin, G.A., 2006. Geoalkalibacter ferrihydriticus gen. nov sp nov., the first alkaliphilic representative of the family Geobacteraceae, isolated from a soda lake. Microbiol. 75, 673-682.

Chapter 8 Summary and future considerations

8.1 Summary

The significant financial costs and hazards associated with the relocation of COPR waste mean there is a clear need to develop *in-situ* remediation strategies for these environments. The success of these strategies is reliant on the detailed assessment of chromium mobility at COPR sites due to the high mobility of Cr(VI) contained within contaminated subsurface hyperalkaline leachates. It was therefore the objective of this project to develop a thorough understanding of the complex biogeochemical interactions occurring within the subsurface at a site of COPR disposal. The roles these play on the fate and stability of the toxic contaminant Cr(VI) have subsequently been investigated in detail. These results have presented evidence supporting the existence of a microbially mediated zone of natural attenuation beneath the waste which itself significantly limits the mobility of Cr(VI). This reactive zone is facilitating the reductive precipitation of Cr(VI) as it percolates vertically from the waste above by reaction with microbially produced Fe(II). This is forming a Cr(III)-Fe(III) oxyhydroxide phase which is resistant to remobilisation by oxygenated DIW, therefore providing a stable hosting environment for chromium leached from waste. A novel population of anaerobic alkaliphilic microorganisms capable of replenishing the supply of Fe(II) required for this abiotic reduction has been identified within this horizon. The biostimulation of this indigenous population *in-situ* may therefore provide a suitable remediative strategy to increase Cr(VI) immobilisation. A wide range of geochemical, microbiological and analytical

techniques were employed to investigate the processes occurring within this zone. The findings of this thesis are summarised below.

Chapter 4 identified the effects of a Cr(VI) contaminated hyperalkaline plume migrating away from the COPR tip as it enters adjacent soil horizons. Sub-oxic soils immediately beneath the waste were found to be accumulating chromium as a result of interaction with this contaminant plume. Microcosm studies showed these soils were able to remove Cr(VI) from solution when mixed with contaminated groundwater. Cr K-edge XANES analysis demonstrated that all of the chromium within these sediments was accumulating in the reduced Cr(III) form. A microbial population capable of iron reduction was found to be indigenous to this horizon, and appear to be producing significant amounts of Fe(II) *in-situ.* As Fe(II) is the principle transformer of Cr(VI) at pH >6 (Lin, 2002), this provides a viable mechanism for the reductive precipitation of Cr(VI) as it is leached vertically from the waste, due to the low solubility of the resulting Cr(III) phase. The existence of this mechanism was further supported by the association of chromium with iron in these soils identified from (S)TEM elemental mapping, and Cr K-edge EXAFS modelling indicating the presence of a mixed Cr(III)-Fe(III) oxy-hydroxide phase. This phase was deemed a stable hosting environment for Cr(III) as it was shown to be resistant to remobilisation via air oxidation. These results demonstrate the importance of biogeochemical interactions occurring within the subsurface to influence Cr(VI) mobility, and have identified the presence of a natural zone of chromium attenuation beneath the waste itself. Harnessing this microbially mediated coupled biotic/abiotic mechanism of chromium immobilisation provides a potential strategy for

implementing *in-situ* remediation through the biostimulation of the controlling population.

The effect of the development of microbial anoxia on oxidised sediments recovered from directly beneath the COPR when mixed with Cr(VI) contaminated surface waters was investigated in Chapter 5. The microbial population was found to be able to metabolise using electron donors derived from soil organic matter present within the sediments despite a pH value of 10.5. This population was capable of reducing nitrate without the addition of an exogenic electron donor. However, the addition of acetate as a more readily accessible electron donor was required in order to progress to Cr(VI) and Fe(III) reducing conditions. This follows the cascade of microbial terminal electron accepting processes expected with the development of microbial anoxia (Froelich et al., 1979). The removal of Cr(VI) could theoretically be attributed to direct microbial reduction of Cr(VI). However, it is more likely the result of the onset of Fe(III) reduction producing Fe(II) available for the reductive precipitation of Cr(VI) as described in Chapter 4. The complete removal of aqueous Cr(VI) by this coupled mechanism would then account for the subsequent accumulation of Fe(II) observed within these experiments. These results highlight the ability of the indigenous microbial population to progressively influence biogeochemical cycling under extreme conditions. Their successful metabolism despite the high pH and Cr(VI) toxicity was also observed in Chapter 4. This is indicative of evolutionary adaptations in the indigenous population, and suggested the presence of alkaliphiles. These adaptations to the novel indigenous population and their ability to influence the biogeochemical cycling of iron and chromium are important as they would form the basis for the implementation of future bioremediation strategies.

Chapter 6 investigated the response of the alkaliphilic population indigenous to the reduced COPR affected sediments when incubated with contaminated groundwater under differing conditions. The results have demonstrated the potential of pH amendment as a strategy to enhance the bioreduction of iron. By reducing the pH to 9.2 using sodium bicarbonate, a well buffered system close to the growth optima for many alkaliphiles (Horikoshi, 2004) was established. This was found to favour the development of iron reducing conditions, without the need for the addition of an exogenic electron donor. Phylogenetic assignment of the community recovered from the iron reducing population revealed initial species diversity had been lost, and the population had become dominated by members of the phylum *Firmicutes.* In contrast although slow nitrate reduction did occur, incubation without pH amendment did not result in the onset of iron reduction. Instead this population was dominated by extremophiles from the phylum *Deinococcus-Thermus.* The enhancement of Fe(III) reduction therefore appears to be a result of the reduction in metabolic stresses associated with hyperalkalinity on the indigenous microorganisms. These results and the stability of the bicarbonate buffered system suggest it may be a suitable strategy to employ *in-situ* to stimulate bioreduction. As a result, this could increase the amount of Fe(II) available for the reductive precipitation of Cr(VI) as it enters the reducing horizon within migrating COPR leachates. This method may therefore be applicable for a wide variety of metal contaminated subsurface environments where the influential indigenous microorganisms are specifically adapted to alkaline conditions. Thus, these results have broad implications when discussing future *in-situ* remediation strategies of metal contaminated environments derived from alkaline solid wastes (e.g. coal fly ash, bauxite processing waste (red mud) and a range of steel industry slags (Cornelis et al., 2008; Mayes et al., 2011; Mayes et al., 2008)).

Although a reduction in pH has been shown to stimulate iron metabolism, further information on the physiology of the influential species would increase the likelihood of success when implementing any future remediation via biostimulation. Chapter 7 reported the difficulties associated with attempting to isolate novel iron reducing alkaliphiles from a consortium of iron reducers indigenous to the reducing horizon. Although the isolation attempts resulted in a decrease in diversity from the original consortium, a single species was not successfully cultured. Despite this, the vast majority of the sequences recovered were assigned to just three genera from the phylum *Firmicutes.* The repeated appearance of these *Anaerobranca, Anaerovirgula* and *Tissierella*-like clones recovered from the iron reducing alkaline cultures strongly suggest that these species have the capacity for iron metabolism at high pH. These results showed that; 1) further method refinement is required in order to successfully culture individual species; and 2) it is likely the collaborative action of multiple microorganisms capable of iron reduction is responsible for producing Fe(II) *in-situ.* Indeed, just 0.1-10% of bacteria in soils are believed to be cultivable (Torsvik et al., 2002). It was concluded that it may both be more successful and beneficial to characterise the iron reducing consortium as a whole prior to advising the bioremediation by biostimulation of this site.

8.2 Future considerations

Despite having identified the presence of a natural microbially mediated reactive zone that provides a mechanism acting to reduce chromium mobility within the subsurface, our understanding of the extent of Cr(VI) contamination on site is still incomplete. The continuity and extent of this reducing horizon and thus its fundamental efficiency at intercepting Cr(VI) containing leachates is not clear. Indeed, there may be areas under the site where the horizon is absent or suitably thin

that Cr(VI) enters the underlying alluvial gravels. As the underlying groundwater within these alluvial gravels poses a possible pathway for wider contamination, additional research into the mobility of Cr(VI) within this material is required.

Our understanding of fate of chromium entering the reducing horizon adjacent to the COPR is now more advanced; however the precise implications this may have on future *in-situ* remediation strategies is still not fully understood. The results from laboratory studies have clearly identified the potential of harnessing the natural microbial process of iron reduction occurring within these sediments to reduce Cr(VI) subsurface mobility. The experimental procedures employed throughout this investigation were designed to replicate *in-situ* interactions as closely as possible. Despite this, the use of microcosm experiments to replicate the biogeochemical processes occurring within the sediment-leachate interface does not produce an ideal proxy for subsurface environments. These closed systems allow the development of steady state geochemical conditions during the progression of microbial anoxia, where in reality the subsurface is a dynamic, open system. For example, *in-situ* soils are likely to be receiving a seasonally variable flux of Cr(VI) contained within hyperalkaline leachates. These may act to suppress microbial activity to varying degrees due to the toxicity of Cr(VI), and continued pressure of hyperalkalinity. The effect this would have on the potential for the biostimulation of the indigenous population is not known, and neither is the capability of the bicarbonate buffered system to maintain its stability under such dynamic conditions. Therefore, column tests and small scale *in-situ* field trials are a logical progression to help clarify the feasibility of pH amendment using sodium bicarbonate as a method of stimulating microbial iron reduction within site sediments. Furthermore, the detailed

characterisation of the consortium of iron reducing alkaliphiles would increase our understanding of their fundamental physiology. This would aid the implementation of successful biostimulation at this site. For example by measuring the effects of a different growth conditions on the rate of iron reduction, it may be possible to identify ways of increasing the efficiency of the stimulation of bioreduction *in-situ*. This may include the use of less broad specificity organic substrates, to enable greater control on the stimulation of the beneficial microbial metabolic processes. The tolerance of this community to Cr(VI) toxicity should also be investigated.

The deliberate stimulation of indigenous alkaliphilic microorganisms as a method of enhanced natural attenuation of Cr(VI) contaminated groundwaters within the subsurface is a novel concept. As a treatment, this would rely on the development of a steady alkaline pH to promote the metabolism of indigenous alkaliphilic microorganisms which have the capacity for iron reduction in anoxic sediments. pH amendment strategies traditionally aim to reach circumneutral values. It is therefore likely that this method will be less costly due to the as smaller volumes of chemicals required to achieve the desired pH. These amendments could also be applied *in-situ* via the injection of buffering solutions directly to the subsurface. Thus, this may provide a suitable intervention strategy for COPR contaminated environments where the relocation of waste itself poses significant danger to health.

In addition, the findings of this thesis have wider implications applicable to the remediation of similar contaminated environments. Numerous other industrial processes produce large volumes of alkaline solid wastes, which are often found at poorly managed legacy disposal sites across the globe (Cornelis et al., 2008; Mayes

et al., 2011; Mayes et al., 2008). These wastes have the potential to form heavy metal contaminated hyperalkaline leachates which can travel within the subsurface, similar to those derived from COPR. It is possible that in these environments similar adaptations to the indigenous microbial population exist which allow for successful metabolism despite high pH and metal toxicity. In subsurface anoxic soils, the importance of Fe(II) produced from microbial iron metabolism is well known, due to its influence on the behaviour of many trace metals, not just chromium (Lovley, 1991). Thus, pH amendment could be considered as a potential remediative strategy to enhance the bioreduction of iron *in-situ,* where the presence of microbially produced Fe(II) results in the beneficial transformation of a contaminant.

8.3 References

Cornelis, G., Johnson, C.A., Van Gerven, T., Vandecasteele, C., 2008. Leaching mechanisms of oxyanionic metalloid and metal species in alkaline solid wastes: A review. Appl. Geochem. 23, 955-976.

Froelich, P.N., Klinkhammer, G.P., Bender, M.L., Luedtke, N.A., Heath, G.R., Cullen, D., Dauphin, P., Hammond, D., Hartman, B., Maynard, V., 1979. Early Oxidation Of Organic-Matter In Pelagic Sediments Of The Eastern Equatorial Atlantic - Suboxic Diagenesis. Geochim. Cosmochim. Acta 43, 1075-1090.

Horikoshi, K., 2004. Alkaliphiles. P. Jpn. Acad. A-Phys. 80, 166-178.

Lin, C.J., 2002. The chemical transformations of chromium in natural waters - A model study. Water Air Soil Poll. 139, 137-158.

Lovley, D.R., 1991. Dissimilatory Fe(III) and Mn(IV) Reduction. Microbiol. Rev. 55, 259-287.

Mayes, W.M., Jarvis, A.P., Burke, I.T., Walton, M., Feigl, V., Klebercz, O., Gruiz, K., 2011. Dispersal and Attenuation of Trace Contaminants Downstream of the Ajka Bauxite Residue (Red Mud) Depository Failure, Hungary. Environ. Sci. Technol. 45, 5147-5155.

Mayes, W.M., Younger, P.L., Aumonier, J., 2008. Hydrogeochemistry of alkaline steel slag leachates in the UK. Water Air Soil Poll. 195, 35-50.

Torsvik, V., Ovreas, L., Thingstad, T.F., 2002. Prokaryotic diversity - Magnitude, dynamics, and controlling factors. Science 296, 1064-1066.

Appendix A Materials and methods

A.1 Materials

A.1.1 Soils sampling and storage

Initial soil samples were acquired by D. I. Stewart and I. T. Burke from exploratory boreholes produced using cable percussion drilling during a professional site investigation in March 2007. These samples were taken from approximately 1 metre below the COPR, at a depth approximately 7 metres below ground level. Samples were stored in the dark at 4°C until use in March 2008, with sample manipulation kept to a minimum prior to use as the oxidised COPR affected soils discussed in Chapter 5.

In March 2009, further soil samples were taken at varying depths from 6 boreholes produced in transect leading away from the south-western edge of the waste using a using a hand auger and 1 metre core sampler. Bulk samples for use in microcosm incubations and XRD/XRF measurements were stored in the dark at 4°C in sealed polythene containers with experimental conditions established rapidly after sampling to limit the effects of sample ageing. Samples to be used in initial microbial community analysis were also kept in sealed containers in the dark at 4°C, but further stored in an anaerobic atmosphere produced using Anaerogen^{tm} sachets. These sachets were specifically selected due to their ability to consume oxygen while not producing hydrogen which would facilitate microbial respiration. Soil samples for XAS analysis were stored at −80°C in glass vials prior to preparation. These soils were used in the research presented in Chapters 4 and 6.

A.1.2 Water sampling and storage

All water samples were stored in polythene containers in the dark at 4°C. Site ditch water was collected by hand in February 2008, and stored in sealed polythene containers until use in March 2008 for the research presented in Chapter 5. Groundwater from within the waste itself was collected in March 2009 using disposable PVC bailers from a monitoring standpipe (BH5) screened into the waste by a professional site investigation in 2002. This groundwater was used in the research presented in Chapters 4 and 6.

A.2 Sample characterisation

A.2.1 Soil pH

Soil pH was measured following the ASTM (2006) standard method for pH in soils. 10g of soil was made up to a 1:1 suspension with deionised water and left for 1 hour before measurement was taken using an Orion bench top meter. Electrodes were regularly calibrated between 7 and 10 using standard buffer solutions.

A.2.2 Leachable Cr(VI) in soils

Water soluble Cr(VI) content in soils was measured to provide information on the concentration of Cr(VI) compounds contained within samples and thus their potential to become mobile and leach into the wider environment, following the method of Vitale et al. (1997). Initially, a 10:1 suspension of soil to deionised water was incubated for 24 hours with shaking at 150 rpm in 15ml centrifuge tubes. 1.5 ml was then extracted and centrifuged (3 min, 16,000 g). Aqueous Cr(VI) concentration in the supernatant was then determined using standard UV/VIS spectroscopy methods described below. Due to the suspected presence of freshly precipitated Cr(III) hydroxides in soils, alkaline extraction methods where not performed as method

induced oxidation of Cr(III) is likely in these samples (USEPA, 1996; Vitale et al., 1997)

A.2.3 X-ray powder diffraction (XRD) and X-ray fluorescence (XRF)

XRD is a method of analysis used to identify bulk crystalline phases present within samples (Slaughter and Falco, 1992). X-rays are fired at a sample, and diffract to varying degrees based on varying distances between crystal lattices. Different crystals have different lattice distances and thus diffract X-rays to different extents (Zacharia, 1967). These diffractions can be detected to enable the production of a diffractogram unique to the crystals present. By varying the angles of X-rays fired at the material (theta, θ), polycrystalline structures can be identified and separated dependent on the diffraction produced

Sequential XRF analyses provide information on elemental concentration within the sample. It is able to identify elements at trace levels below 1 ppb, and up to 100%. The sample is first powdered and fused into a glass bead, and then primary X-ray photons fired at it. This energy is absorbed and promotes electrons from within the element to be ejected from its inner orbital. Replacement of these electrons happens by transition of electrons from outer to inner orbitals and results in the emission of a secondary X-ray photon (the florescence measured). This emission corresponds to both the energy required to eject the initial electron, and the distance travelled by the replacing electron (Beckhoff et al., 2006). The length of the transition path between the different electron orbitals and energy required to eject the initial electron is unique to different elements. Thus, the emitted secondary X-ray wavelength corresponds to the element present and enables identification of the elemental makeup of a sample. The intensity of the secondary X-ray emitted corresponds to

concentration, and can be calculated by comparison to known standard materials. By rotating the detector angle to measure each wavelength, a comprehensive step by step analysis of the elements present can be established.

X-ray powder diffraction (XRD) was performed on a Philips PW1050 Goniometer and X-ray fluorescence (XRF) on a Philips PW2404 wavelength dispersive sequential X-ray spectrometer. Borehole soil samples recovered in 2009 were first freeze dried, ground to < 75 μm prior to XRD analysis, and further fused into a bead prior to XRF analysis. Data were corrected for loss on ignition (LOI).

A.2.4 Total organic carbon (TOC)

Approximately 25g of homogenised soil was oven dried at 105°C and disaggregated with a mortar and pestle for carbon content determination. A portion of each sample was pre-treated with 10% HCl to remove any carbonates present following the method of Schumacher (2002). The total organic and inorganic carbon content of oven dried and HCl treated subsamples was then measured using a Carlo-Erba 1106 elemental analyser.

A.2.5 Electron microscopy

Electron microscopy uses focussed beams of electrons passing through a low pressure atmosphere to provide high resolution images of a sample via their interaction with it. The much higher wavelength of an electron beam to that of light enables higher resolution images to that of traditional light microscopes to be constructed. The beam itself is produced by an electron gun usually consisting of a tungsten cathode selected for its high melting point, which emits electrons as it is heated with high voltage (Goldstein et al., 2003). The beam is then focussed to a

point of between 0.4 nm and 5 nm using one or two condenser lenses and aimed at a sample.

During scanning electron microscopy (SEM) this beam is passed over the sample in a raster pattern and in doing so some of the high energy electrons are reflected. The amount of reflection or backscattering by these backscatter electrons (BSE) is dependent on the atomic number of the element, with heavier elements scattering electrons to a greater degree than lighter elements (Reed, 2005). As a result, an image can be produced using a detector designed to collect and interpret BSE. An Electron Probe Micro-Analyser (EPMA) can be used in conjunction with a SEM in order to gain location specific quantative information on the elements present within the sample. As well as the BSE, the EPMA allows the detection of secondary X-ray radiation produced when the electron beam is of high enough intensity to eject an inner electron from an element within the sample. This electron gets replaced by an electron from a higher shell orbital, shedding energy as it does so in the form of an secondary X-ray photon (Reed, 2005). These X-rays are characteristic of the element, and enable element identification and abundance in a similar fashion to XRF analysis.

During transmission electron microscopy (TEM) the beam of high energy electrons is passed through an ultra-thin sample. The degree of interaction of the electrons transmitted through the sample before it reaches a detector on the other side enables the construction of an image. Some electrons pass straight through the specimen and reach the detector, while others are adsorbed by the sample or scattered away from the detector (Pennycook et al., 2003). The amount of scattering and adsorption is

dependent on the density of the material encountered by the beam, with the densest material resulting in the largest degree of interference. This therefore produces an image where denser materials appear lighter as fewer electrons are reaching that area of the detector. These microscopes can be equipped with scanning transmission electron microscopy units ((S)TEM) and moveable detectors to enable mapping of chemical composition in a raster pattern. This is done by measuring the X-rays produced when an element becomes ionized by the beam and inner shell electrons are displaced as described for EPMA. This unit also enables Energy dispersive X-ray (EDX) spectroscopy, which provides high resolution location specific chemical composition by measuring these characteristic secondary X-rays.

In preparation for analysis, a freeze dried sample of soil B2-310 was embedded in a block of epoxy resin under a vacuum and prepared for SEM analysis by polishing in non-aqueous oils and carbon coated (approximately 5-10 nm thickness). The carbon coating is important to reduce drift as a result of charging of the sample under the electron beam. Scanning Electron Microscopy (SEM) was performed on a FEI Quanta 650 FEG-ESEM to produce backscatter electron images. Elemental quantification was carried out on the ESEM using an electron probe micro analyser (EPMA). Thirty-three 15 x 15 µm regions of the fine matrix material of B2-310 resin embedded thin section were analysed for common rock forming oxides. The measured elemental wt% was then corrected by assuming a total oxide weight of 100% to account for the influence of resin infilling into pore spaces. An average composition of these 33 regions is reported, with error given as the range of results.

Soil B2-310 was prepared for (S)TEM imaging by freeze drying and sieving at 150 mesh to collect the less than 104 µm sized fraction. Approximately 0.05 g was then mixed with 1 ml of LR White^{TM} resin and polymerised for 24 hours at 70°C. A thin section of resin embedded soil was then cut using a microtome (80 nm), placed on a Cu support grid (Agar Scientific, UK), and carbon coated (~5 um) prior to (S)TEM analysis. The specimen was examined using a Philips/FEI CM200 field emission gun TEM fitted with a scanning unit and an ultra-thin window energy dispersive X-ray detector (Oxford Instruments ISIS EDX). The total Cr concentration in this soil was ~0.3 % w/w, which if homogeneously dispersed is close to the limit of detection for EDX analysis.

A.2.6 Ion chromatography (IC)

Sulphate, nitrate and chloride concentrations were determined by ion chromatography. This initially involves the loading of aqueous samples onto a stationary phase that has an affinity to anions, which is contained within an analytical column. An ionic eluent is then passed through the column, displacing the retained analyte ions. The degree of displacement varies dependant on the ion present due to their differing affinity to the stationary phase. This therefore enables separation based on the time taken for the analyte to be carried along the column by the eluting solution. On exiting the column a detector measures the presence of anions and thus can identify the analyte present by matching the measured elution peaks with that of known standard materials. The concentration of this eluent can be increased over the course of a single elution, reducing the time taken for specific analytes to become displaced from the stationary phase. This gradient elution has the effect of both increasing peak separation, and reducing overall experimental time.

Experiments were performed on a Dionex DX-600 with AS50 autosampler using a 2 mm AS16 analytical column, with suppressed conductivity detection and gradient elution to 15 mM potassium hydroxide over 10 minutes. Samples were loaded in a random order to avoid systematic errors. Standards covering the anticipated range of analyte concentrations were prepared with the addition of 25 µM Cr(VI) as potassium chromate in an attempt to replicate the matrix of Cr(VI) affected aqueous samples. Between loading samples, the column was flushed with deionised water for 1.5 minutes. Analyte concentrations were determined with reference to standard materials, and final concentrations were adjusted in ratio with the average chloride concentration in order to account for instrumental drift (Thompson and Ellison, 2005).

A.2.7 X-ray absorption spectroscopy (XAS)

X-ray absorption spectroscopy (XAS) is an X-ray analytical technique that allows information on the oxidation state (or speciation) and association of individual atoms of an element to be gathered. This technique has several advantages over other X-ray analytical methods such as XRD and XRF, as it utilises synchrotron radiation (SR) that can be produced at intensities several orders of magnitude greater than traditional X-rays. This allows for a reduction in data acquisition time. SR is produced by firing electrons around a curved trajectory, systematically using a magnetic field to accelerate them to near the speed of light. The energy of these electrons can vary from hundreds of eV to several GeV dependant on the facility (Zubavichus and Slovokhotov, 2001). As these travel round a closed storage ring, they emit extremely intense electromagnetic radiation, SR, which is then fed into spectroscopy stations situated about the ring. In contrast to conventional X-rays where the radiation falls within a relatively narrow spectral range, the high intensity

of SR is uniformly distributed across the entire X-ray spectrum, increasing its application potential (Zubavichus and Slovokhotov, 2001).

XAS is the measurement of absorption of SR by a specific element across its absorption edge. For chromium, this absorption edge falls around 5989 eV (Parsons et al., 2007). As has previously been discussed, elements behave differently from one another when exposed to X-ray radiation. There are two main types of signal detectors in XAS, fluorescence and transmission. Where the synchrotron X-rays are absorbed strongly by the sample, an inner shell electron is excited to the point of ejection, which subsequently gets replaced by an outer electron, expelling energy as it does so as fluorescent secondary X-rays (Kawai, 1999). It is this energy that is detected when performing XAS in fluorescence mode. In transmission mode, absorption spectra are constructed as a function of the intensity incident on the sample of the SR beam to that transmitted through the sample (De Sio et al., 2008). Both these modes enable the construction of spectra which are typically described in two distinct regions, the X-ray absorption near edge structure (XANES) and extended X-ray absorption fine structure (EXAFS). The XANES region comprises of the area just before the absorption edge and the edge itself, and is used to calculate the oxidation state and geometry of an element. Oxidation state determination of chromium is made easier by the presence of a characteristic feature associated with Cr(VI) in the pre-edge region at 5998 eV. This is due to the transition of a 1s electron to a 3d orbital which is possible in tetrahedral compounds (Parsons et al., 2007). This feature is not present for Cr(III) compounds, and thus calibration of the peaks magnitude in a spectra allows for the determination of Cr(VI):Cr(III) ratio within a sample. Beyond the absorption edge of a sample, the EXAFS region allows for the

determination of the atomic association of the element in the sample being studied. The electromagnetic interference from neighbouring elements produces oscillations within the absorption spectra as ejected photoelectrons interact with surrounding atoms. These oscillations can be interpreted using modelling software to provide information on coordination number, inter-atomic distances and amount of thermal disorder (Debye-Waller factor) of a sample (Parsons et al., 2007).

Samples for XAS analysis were chosen from a range of undisturbed environmental borehole samples stored at -80°C and experimental samples. Standard materials were produced from laboratory chemicals. Cr-substituted goethite was synthesised via precipitation of goethite from $Fe(NO)_3$ as described in Cornell and Schwertmann (2003), with 2% by molar ratio of $Fe(NO)_3$ substituted by $CrCl_3$. Cr-hydroxide was prepared following the method of Saraswat and Vajpei (1984). Precipitation of Cr-hydroxide was achieved through dropwise neutralisation of $CrCl_3$ solution by sodium hydroxide. The resulting precipitate was then washed with distilled water to remove all impurities and dried in an oven at 60°C for 24 hours. XRD spectra of standards were compared to published work to ensure the correct compound was synthesised at an appropriate purity.

In order to determine the speciation and atomic association of chromium within the samples, Cr K-edge spectra were collected on beamline I18 at the Diamond Light Source, Harwell Science and Innovation Campus, Didcot, Oxfordshire. This beamline operates at 3 GeV with a typical current of 200 mA, using a nitrogen cooled Si(111) double crystal monochromator and focussing optics. A pair of plane mirrors was used to reduce the harmonic content of the beam and microfocusing was

achieved using Kirkpatrick-Baez mirrors. The beam size at the sample window was approximately 150 µm. For standard materials Cr K-edge spectra were collected in transmission mode at room temperatures (approximately 295 °K). Standards where prepared as 50 mg pressed pellets and diluted with boron nitride (BN) as required. For soil samples data were collected in fluorescence mode using a 9 element solid state Ge detector. Sediment samples were spun down to form moist pellets and were mounted at 1 mm thickness in aluminium holders with Kapton™ widows. Experiments were performed at liquid nitrogen temperatures (approximately 78 °K) and multiple scans averaged to improve the signal / noise ratio using Athena version 0.8.056 (Ravel and Newville, 2005). For XANES spectra absorption was also normalised in Athena over the full data range and plotted from 5980 eV to 6030 eV with no correction required for drift in E_0. For EXAFS analysis data was background subtracted using PySpline v1.1 (Tenderholt et al., 2007).

A.2.8 EXAFS modelling

Background subtracted EXAFS spectra were analysed in DLexcurv v1.0 (Tomic et al., 2005) using full curved wave theory (Gurman et al., 1984). Phase shifts were derived from *ab initio* calculations using Hedin-Lundqvist potentials and von-Barth ground states (Binsted, 1998). Fourier transforms of the EXAFS spectra were used to obtain an approximate radial distribution function around the central Cr atom (the absorber atom). The peaks of these Fourier transforms can be related to "shells" of surrounding backscattering ions characterised by atom type, number of atoms (n), absorber-scatterer distance (R), and the Debye-Waller factor ± 25% ($2\sigma^2$). Atomic distances calculated by DLexcurv have an error of approximately ± 0.02 and ± 0.05 Å in the first and outer shells respectively (Burke et al., 2005). The data were fitted for each sample by defining a theoretical model and comparing the calculated

EXAFS spectrum with experimental data and published spectra for Cr-substituted compounds (Charlet and Manceau, 1992). Shells of backscatterers were added around the Cr and by refining an energy correction E_f (the Fermi Energy; which for final fits typically varied between -19 and -17) the absorber-scatterer distance, and the Debye-Waller factor for each shell, a least squares residual (the *R* factor) was minimised (Binsted et al., 1992). The amplitude factor (or AFAC in DLexcurv V1.0) was retained as the default of 1 throughout. Shells or groups of shells were only included if the overall fit (*R*-factor) was reduced overall by >5%. For shells of scatterers around the central Cr, the number of atoms in the shell was chosen as an integer to give the best fit, but not further refined.

A.2.9 Reoxidation experiments

Air reoxidation experiments were carried out in order to investigate the stability of Cr(III) containing phases within COPR affected soils. This was done as a proxy for the effects of traditional dig and dump remediative strategies which would expose the sediments directly below to oxygen and oxygenated rainwater. Its exposure could potentially cause further Cr(VI) leaching from remobilisation of Cr(VI) phases within the soil, and secondary release from the reoxidation of accumulated Cr(III).

A 10:1 suspension was achieved through mixing of 10g of sediment with 100 ml deionised water in a 500 ml conical flask. These systems were left open and kept on an orbital shaker at 150 rpm, in the dark at 21ºC ± 2ºC. To enable sampling, tubing was placed into the suspension, with one end attached to a 5 ml syringe and held in place by a foam stopper. Experiments were performed in triplicate, and periodically sampled in a logarithmic fashion to produce a time series of progressive oxidation. At each time point, 1.5 ml soil slurry was extracted, centrifuged for 3 minutes at

16,000 g, and the resulting soil pellet and porewaters analysed for solid phase acid extractable Fe as Fe(II) and aqueous Cr(VI) respectively (see above). The system was then weighed and replaced on the orbital shaker. At the next time point, before slurry was extracted the system is again weighed and deionised water added to account for loss caused by evaporation. The system is then mixed, and sampling continued as before.

A.3 Geochemical spectrophotometric methods

Ultraviolet-Visible (UV-VIS) spectroscopy was used to determine a variety of chemical concentrations using colorimetric methods. Colorimetric methods are based on chemical reaction of a reagent with an analyte resulting in the formation of a coloured solution. Light in the visible to near-ultraviolet spectrum is then passed through the sample at given a wavelength and measured by a detector on the other side. The degree of absorbance by a species is a function of the reagent chemicals molar absorptivity at that given wavelength. The actual absorbance, *A*, is dependent on the pathlength and concentration of the species, and can be calculated using the Beer-Lambert law:

$$A = \varepsilon c l \qquad (16)$$

Where l is the path length (usually 1 cm for standard laboratory cuvettes), c is the concentration of the species and ε is its molar absorptivity. Thus, by comparing the absorbance of unknown samples to that of known calibration standards, the concentration of the analyte within the sample can be determined. All spectrophotometric measurements were performed on a CECIL CE 3021

spectrophotometer, and compared to matrix matched calibration standards. These standards were produced in the range of 0-60, 0-300, and 0-2000 µM for iron, Cr(VI) as chromate, and nitrite respectively, and were selected to cover the expected analyte range. These standards were measured regularly (linear r^2 = 0.99 or better). Where the analyte concentrations in the sample exceeded the range of standards used, a suitable dilution factor was applied to the solution using deionised water, and the method repeated to yield a result within standard range.

A.3.1 Aqueous Cr(VI) determination

Aqueous Cr(VI) was determined by reaction with diphenylcarbazide to produce a red-violet colour, following an adapted version of the USEPA (1992) method 7196a. This method can be used to measure samples containing between 0.5 and 50 $mg.l^{-1}$ dissolved hexavalent chromium. As the colour produced is reported to fade most rapidly at high pH values, the maximum colour formation from reaction with diphenylcarbazide is achieved through prior acidification of the sample (Pflaum and Howick, 1956). The adapted procedure follows: Samples were prepared for analysis by centrifugation for 3 min at 16,000g. 100 µl of the resulting supernatant was then added to a 1.4 ml cuvette. The sample was then acidified by the addition of 900 µl 0.01M H_2SO_4 and mixed with 100 µl diphenylcarbazide solution. The reaction was left for 10 minutes to allow colour development, and absorbance then measured at 540 nm (USEPA, 1992).

A.3.2 Iron determination

Both total dissolved iron and percentage of microbially available iron as the reduced Fe(II) oxidation state in solids were measured using reaction with ferrozine reagent. Ferrozine (a disodium salt of 3-(2-pyridyl)5,6-bis(4-phenylsulfonic acid)-1,2,4-

triazine) was first introduced as a reagent for iron determination in 1974, as a cheaper and easier to acquire alternative to existing chemicals (Stookey, 1970). Ferrozine salt is dissolved in ammonium acetate to produce a reagent that reacts with the ferrous ion to form an intense magenta colour that exhibits maximum absorbance at 562 nm (Stookey, 1970). This allows for its use in UV-VIS spectroscopic determination of iron in natural waters. Since its introduction, the ferrozine method has been adapted for numerous applications of iron determination. The use of hydroxylamine hydrochloride and ammonium acetate (pH 9.5) as a reducing agent and buffer respectively, allow for the determination of total dissolved Fe in porewaters by transforming all Fe(III) present to Fe(II) (Viollier et al., 2000).

Total dissolved Fe in porewater samples was measured following the method of Viollier, Inglett et al. (2000). Samples were prepared for analysis by centrifugation for 3 min at 16,000 g with 1000 µl of the resulting supernatant was transferred to a 1.4 ml cuvette. This was then mixed in order with 100 µl ferrozine solution, 200 µl hydroxylamine hydrochloride and ammonium acetate pH 9.5 buffer. The reaction was left for 10 minutes to allow for colour development before the absorbance was measured at 562 nm (Viollier et al., 2000).

During the development of microbial iron reducing conditions, the ratio of solid phase Fe(II):Fe(III) increases as bacteria couple the oxidation of organic matter to the reduction of soil bound ferric iron (Lovley, 1997). Extraction with 0.5 N HCl for 1 hour with shaking is generally accepted to be the concentration of acid and time required to mobilise poorly crystalline, amorphous iron phases (Lovley and Phillips, 1986). These are considered to be the forms of iron readily available in subsurface

environments for microbes to utilise in metabolic processes. The measurement of the change in Fe(II)/Fe(III) ratio of these phases over time can therefore be used to monitor the progression of microbial iron reduction. This ratio can be determined by comparing the reaction with ferrozine solution of extracted solutions in the presence of the reducing agent hydroxylamine hydrochloride, and without.

Percentage of microbial available Fe as Fe(II) in solids was determined following a method adapted from Lovley and Phillips (1986). First, a pellet of sediment was recovered via centrifugation of 1.5 ml sediment slurry for 3 min, at 16,000 g. This was then resuspended by pipetting in 1 ml 0.5 N HCl, transferred to a 13 ml polyethylene tube containing 4 ml 0.5 N HCl, and shaken at 150 rpm for 1 hour. Upon completion, this was filtered using a 0.2 µm syringe filter, and two 100 µl sub-aliquots added to two 4ml cuvettes. 2900 µl deionised H_2O and 300 µl ferrozine solution was added to cuvette 1, with 2000 µl deionised H_2O, 300 µl ferrozine solution, 600 µl hydroxylammonium hydrochloride and 300 µl buffer (pH 9.5) solution added to cuvette 2. Cuvette 1 provided information on solely Fe(II) ions present in the extracted sample due to the lack of a reduction step, and cuvette 2 total dissolved iron. Colour was allowed to develop for 10 minutes before absorbance was measured at 562 nm. The percentage of acid extractable Fe as Fe(II) could then be calculated using the following formula:

$$Percentage\ extractable\ Fe\ as\ Fe(II) = \left(\frac{\text{A562 } cuvette\ 1}{\text{A562 } cuvette\ 2}\right) * 100 \quad (17)$$

A.3.3 Aqueous nitrite

Aqueous nitrite concentration was also determined following reaction with sulphanilaminde (SAN) and naphthylethylenediamine dihydrochloride (NED) reagents as described by Harris and Mortimer (2002). Samples were prepared for analysis by centrifugation for 3 min at 16,000 g. 100 µl of the resulting supernatant was then added to a 1.4 ml cuvette, and mixed in order with 100 µl ammonium chloride buffer (pH 8.5), 25 µl SAN, 25 µl NED and 750 µl deionised H_2O. Colour was allowed to develop for 10 minutes before absorbance was measured at 536.5 nm.

A.4 Culturing techniques

A.4.1 Growth media

An alkaline growth media recipe was developed in order to culture alkaliphilic anaerobes capable of iron reduction which are indigenous to the COPR affected soils beneath the waste. To prepare the media, 500 ml deionised H_2O was first degassed through boiling and purging with oxygen free nitrogen for 1 hour. The ingredients are then added upon cooling in order as listed in Table A.1, with ferric citrate added as the sole electron acceptor (Fe(III)), and yeast extract added as the sole electron donor. The vitamins and mineral mixes were produced as previously described by Bruce, Achenbach et al. (1999), following the recipes shown in Table A.2 and Table A.3. The pH of the media is then buffered to 9.2 with dropwise addition of sodium carbonate solution. 4.5 ml aliquots of the media was transferred to 5 ml glass serum bottles under a nitrogen atmosphere, sealed using butyl rubber stoppers and aluminium crimps, and heat sterilised at 120°C for 20 minutes. The media was adjusted to pH 9.2 as this value is well within the growth optima of a number of different species of alkaliphiles (Horikoshi, 2004).

Table A.1 Iron reducing media recipe

Ingredient	Quantity (g)
$NaH_2PO_4.H_2O$	0.178
KCl	0.05
$FeC_6H_5O_7$ (ferric citrate)	1
Vitamin mix	5 (ml)
Mineral mix	5 (ml)
Yeast extract	1
Deionised water	490 (ml)

Table A.2 Vitamin mix (Bruce et al., 1999)

Ingredient	Quantity (mg/l)
Biotin	2
Folic acid	2
Pyridoxine HCl	10
Riboflavin	5
Thiamine	5
Nicotinic acid	5
Pantothenic acid	5
Vitamin B-12	0.1
p-aminobenzoic acid	5
Thioctic acid	5

Table A.3 Mineral mix (Bruce et al., 1999)

Ingredient	Quantity (g/l)
NTA	1.5
$MgSO_4$	3
$MnSO_4.H_2O$	0.5
NaCl	1
$FeSO_4.7H_2O$	0.1
$CaCl_2.2H_2O$	0.1
$CoCl_2.6H_2O$	0.1
$ZnCl_2$	0.13
$CuSO_4.5H_2O$	0.01
$AlK(SO_4)_2.12H_2O$	0.01
H_3BO_3	0.01
Na_2MoO_4	0.025
$NiCl_2.6H_2O$	0.024
$Na_2WO_4.2H_2O$	0.025

For inoculation, 100 mg of sample B2-310 was suspended in 0.5 ml of alkaline growth media under a nitrogen atmosphere. This was then injected into the sealed bottles containing 4.5 ml of alkaline growth media and incubated at 21°C. The presence of iron reduction was indicated by precipitate colour change from orange to black (Figure A.1) and confirmed using the ferrozine method described above. Successful cultures were progressed repeatedly into fresh media to ensure a viable culture had been obtained.

Figure A.1 Colour indication of successful iron reduction in media bottles (left to right)

A.4.2 Plate techniques

In order to isolate individual colonies from iron reducing consortiums, agar plates based on the iron reducing pH 9.2 media were produced. 10 g of agar was added to 500 ml of the media, produced following the protocol described above. However, it was found that addition of sodium carbonate buffer prior to heat sterilisation produced dark coloured plates that made it difficult to identify any microbial growth. Instead, the media was first heat sterilised at 120°C for 20 minutes, and then allowed to cool to 55°C in a water bath. The pH was then adjusted to 9.2 using drop-wise addition of filter sterilised sodium carbonate solution, with 5 ml removed from the sterilised media after each addition and separately measured using a Orion bench top

meter and calibrated electrodes. This was done in order to remove the risk of contamination from the apparatus. Plates were prepared in two methods; Streak plates were prepared using loops initially immersed in a mixture of 100 µl of successful iron reducing consortium extracted using aseptic techniques and 400 µl sterile growth media in a 1.5 ml centrifuge tube. Plates were also prepared by spreading from series of dilutions; 5, 10, 20, 40 and 50 µl of the iron reducing consortium were pipetted into a pool of sterile iron reducing media to a final volume of 100 µl and spread evenly across the plate surface. When producing all growth plates it was important that all steps were progressed as quickly as possible to limit the effect exposure to atmospheric O_2. All plates were incubated in an anaerobic atmosphere produced using Anaerogen^{tm} sachets, at 21°C.

Successful growth on plates was indicated by the clearing of the agar and/or appearance of colonies. Where possible, colonies were then picked using a sterile needle, and suspended in sterile growth media. This was then injected into sterile growth media bottles using aseptic technique and incubated in the dark at 21°C. Successful growth was indicated by the presence of iron reduction.

A.4.3 Serial dilution

A series of dilutions were produced from the initial iron reducing consortium in an effort to produce a pure culture. This method is based on the theory of most probable number (MPN) analysis that suggests successive dilutions of a population will eventually produce a system where the population is absent or consist of a single individual. In microbiology this therefore gives the potential for a dilution of an initially mixed culture to consist of a single cell which can therefore grow into a culture containing a single species. To produce the dilutions, 500 µl of the iron

reducing consortium produced from soil B2-310 was transferred into a sealed media bottle containing 4.5 ml sterile iron reducing alkaline growth media using a needle and aseptic technique. This produced a tenfold (10^1) dilution of the original consortium. This was then mixed, and a further 500 µl transferred to the next sterile media bottle, producing a further tenfold dilution (10^2). This process was repeated up to a final dilution factor of 10^{10}, which represents a 10,000,000,000 times dilution of the original consortium. Once inoculated, all media bottles were incubated in the dark at 21°C.

A.5 Microbial community analysis

Microbial DNA was extracted from soils and microcosm sediment pellets using a FastDNA spin kit (Qbiogene, Inc.) and FastPREP instrument (unless explicitly stated, the manufacturer's protocols supplied with all kits employed were followed precisely). In order to extract microbial DNA from the successful iron reducing cultures, culture bottles were opened, transferred into a 15 ml centrifuge tube and centrifuged at 3500 rpm for 10 minutes. Supernatant was then discarded and pellet resuspended in 978 µl of sodium phosphate buffer supplied in the FastDNA spin kit. The suspension was then transferred to a Lysing Matrix E tube also supplied in the FastDNA spin kit, and manufacturers' protocols subsequently followed precisely. DNA fragments in the size range 3 kb ~20 kb were isolated on a 1% "1x" Tris-borate-EDTA (TBE) gel stained with ethidium bromide to enable viewing under UV light (10x TBE solution from Invitrogen Ltd., UK). The DNA was extracted from the gel using a QIAquick gel extraction kit (QIAGEN Ltd., UK.) and stored at -20°C in preparation for amplification by polymerase chain reaction (PCR).

A.5.1 Ribosomal integenic spacer analysis (RISA)

A fragment of DNA of unknown length from the spacer region between the 16S and 23S rRNA genes was amplified by PCR using the universal primers S-D-Bact-1522-b-S-20 (5´-TGCGGCTGGATCCCCTCCTT-3´) and L-D-Bact-132-a-A-18 (5´-CCGGGTTTCCCCATTCGG-3´) that target the end of the 16S rRNA gene and beginning of 23S rRNA gene (Cardinale et al., 2004). Although amplification by this method does not identify individual specie type, the spacer region is highly variable in both its length and sequence, and so produces a fingerprint of the microbial populations diversity (Garcia-Martinez et al., 1999). In turn this enables the comparison of populations as they develop over time. Each 50 µl PCR reaction mix contained 25 µl of purified 3-20 kb DNA fragments, 0.5 µl of 5 $\mu g.\mu l^{-1}$ GoTaq DNA polymerase containing 1.5 mM $MgCl_2$ (Promega Corp., USA), 10 µl 5 x PCR reaction buffer, 1 µl of 10 mM PCR nucleotide mix (Promega Corp., USA), 10.8 µl ultraPURE H_2O (Invitrogen, USA), and 1.25 µl of both SD and LD primers (20 mM). Using a Mastercycler gradient thermal cycler (Eppendorf, Germany), the reaction mixtures were incubated at 94ºC for 3 min, and then cycled 25 times through three steps: denaturing (94ºC, 1 min), annealing (55ºC, 30 s), and primer extension (72ºC, 60 s). This is followed by a final extension step at 72ºC for 5 min. The PCR products were then purified using a QIAquick PCR purification Kit (QIAGEN Ltd, UK) and eluted to a final volume of 50 µl. DNA concentration was then measured by UV/VIS spectroscopy on a Biomate 3 spectrophotometer with 1 mm path length nanocell (Thermo Fisher Scientific, Inc). Purified PCR product was then amended using ultraPURE H_2O (Invitrogen, USA) and mixed with 6 x loading dye (New England BioLabs, Inc) to give a total of 480 µg DNA loaded onto a 1.0%

agarose TBE gel with ethidium bromide straining and separated by electrophoresis. After suitable separation gel was photographed under UV light. Results not shown.

A.5.2 16s rRNA gene sequencing

A fragment of the 16s rRNA gene of approximately 500bp was amplified using broad-specificity bacterial primers 8f (5´-AGAGTTTGATCCTGGCTCAG-3´) (Eden et al., 1991) and 519r (5´-GWATTACCGCGGCKGCTG-3´) where K = G or T, W = A or T (Lane et al., 1985). Each PCR reaction mixture contained 20 µl of purified DNA solution, GoTaq DNA polymerase (5 units), 1× PCR reaction buffer, $MgCl_2$ (1.5mM), PCR nucleotide mix (0.2 mM), T4 Gene 32 Protein (100 ng/µl) and 8f and 519r primers (0.6 µM each) in a final volume of 50 µl. The reaction mixtures were incubated at 95ºC for 2 min, and then cycled 30 times through three steps: denaturing (95ºC, 30 s), annealing (50ºC, 30s), primer extension (72ºC, 45 s). This was followed by a final extension step at 72ºC for 7min. The PCR products were purified using a QIAquick PCR Purification Kit. Amplification product sizes were verified by electrophoresis of 10 µl samples in a 1.0% agarose TBE gel with ethidium bromide straining.

The PCR product was ligated into the standard cloning vector (pGEM-T Easy; Promega Corp., USA), and transformed into E. coli competent cells (XL1-Blue; Agilent Technologies UK Ltd). Transformed cells were grown on LB-agar plates containing ampicillin (100 $\mu g.ml^{-1}$) at 37ºC for 17 hours. The plates were surfaced dressed with IPTG and X-gal (as per the XL1-Blue protocol) for blue-white colour screening. After 17 hours, colonies which had successfully incorporated the inserted plasmid with ligated 16s rRNA gene fragment were restreaked onto LB-ampicillin agar plates and incubated at 37ºC for a further 15 hours. Successful transformations

were identifiable as white colonies as the successful insertion into the pGEM-T Easy vector disrupts a gene responsible for blue colour production. Therefore, the E. coli competent cells that contain the desired insert containing plasmid were easily selected for restreaking using a sterile toothpick. After incubation, single colonies for each condition from restreaked plates were stab inoculated into an LB-agar ampicillin 96 well plate and sent for sequencing using the T7 primer (GATC Biotech Ltd).

In order to increase confidence that a suitable representation of the diverse B2-310 initial soil population had been collected, a further 16 plasmids were sent for sequencing. Single colonies from restreaked plates were incubated overnight at 37°C in LB media. Bacterial plasmids were then extracted from the resulting broth using the Promega Pureyield™ Plasmid Miniprep Purification system (Promega Corp., USA). The concentration of plasmid DNA was then determined using UV spectroscopy, and adjusted to 50 $ng.\mu l^{-1}$ with deionised water. 12µl of each plasmid mixture was then sent for sequencing at the Faculty of Biological Sciences, University of Leeds, Leeds, UK.

A.5.3 Phylogenetic assignment

16s rRNA bacterial sequence fragments recovered by GATC Biotech Ltd were checked with both Bellerophon (Huber et al., 2004) and Mallard v 1.02 (Ashelford et al., 2006) online chimera checkers in order to exclude putative chimeras from subsequent analyses. Sequences were then assigned to bacterial phyla using the online Ribosomal Database Project (RDP) naïve Bayesian Classifier version 2.2 (available online: http://rdp.cme.msu.edu/classifier/classifier.jsp) in August 2010. The sequences were assigned to the taxonomical hierarchy: RDP training set 6, based

on nomenclatural taxonomy and Bergey's Manual, with a confidence threshold of 95% (assignments to a phylum reported in Figure 4 are based on >98% confidence). Full details of this algorithm, its development and its performance can be found in Wang et al. (2007). Good quality sequences were uploaded to the EMBL GenBank database.

A.5.4 Phylogenetic tree building

The EMBOSS needle pairwise alignment program (available from http://www.ebi.ac.uk/Tools/emboss/align/) was used to assign similar gene sequences into clades based on sequence homology, using default parameters (open gap penalty 10, gap extension penalty 0.5). The sequences were also grouped into operational taxonomic units (OTUs) using a >98% sequence similarity cut-off value in the MOTHUR software (Schloss et al., 2009). The diversity within the clone library for each sample was characterized using the Shannon index (H′)(Krebs, 1999) and rarefaction curves constructed. Rarefaction analysis is designed to compare species richness within a sample, but is not a true representation of species diversity. It can be used to compare species diversity between samples as long as the methods employed are consistent, with accuracy improving with increased sample number (Leadbetter, 2005). Selected sequences were then aligned with known bacterial 16S rRNA gene sequences from the EMBL database using the ClustalX software package (version 2.0.11), and a phylogenetic trees were constructed from the distance matrix by neighbour joining. Bootstrap analysis was performed with 1000 replicates, and resulting phylograms drawn using the TreeView (version 1.6.6) software package.

A.5.5 Multidimensional scaling analysis (MDS)

Multidimensional Scaling analysis, which is also known as principle coordinate analysis, configures the position of objects in Euclidean space based on their pair-wise dissimilarity, and is used in a number scientific fields to visualize datasets (Son et al., 2011). For the purpose of this research it was used to represent graphically the changes in the initial B2-310 microbial community after incubation in the microcosm experiments reported in Chapter 6 (*unamended* and *pH amended*), based on the dissimilarity between the sequences recovered. In order to produce a suitable input file, sequences were first aligned using the online Clustalw2 tool (http://www.ebi.ac.uk/Tools/msa/clustalw2/), and used to produce a distance matrix constructed of pair-wise dissimilarity scores between sequences. This was loaded into the NewMDSX program, and basic non-metric MDS undertaken using the Minissa-N algorithm (Coxon, 2004; Roskam et al., 2005).

A.6 References

Ashelford, K.E., Chuzhanova, N.A., Fry, J.C., Jones, A.J., Weightman, A.J., 2006. New screening software shows that most recent large 16S rRNA gene clone libraries contain chimeras. Appl. Environ. Microbiol. 72, 5734-5741.

ASTM, 2006. D4972-01: standard test method for pH of soils. Annual book of ASTM standards. American Society for Testing and Materials 4, 963-965.

Beckhoff, B., Kanngießer, R., Langhoff, N., Wedell, R., Wolff, H., 2006. Handbook of practical X-ray fluorescence analysis. Springer, Germany.

Binsted, N., 1998. CLRC Daresbury Laboratory EXCURV98 program, CLRC Daresbury Laboratory, Warrington, UK.

Binsted, N., Strange, R.W., Hasnain, S.S., 1992. Constrained and Restrained Refinement in Exafs Data-Analysis with Curved Wave Theory. Biochemistry-US 31, 12117-12125.

Bruce, R.A., Achenbach, L.A., Coates, J.D., 1999. Reduction of (per)chlorate by a novel organism isolated from paper mill waste. Environ. Microbiol. 1, 319-329.

Burke, I.T., Boothman, C., Lloyd, J.R., Mortimer, R.J.G., Livens, F.R., Morris, K., 2005. Effects of progressive anoxia on the solubility of technetium in sediments. Environ. Sci. Technol. 39, 4109-4116.

Cardinale, M., Brusetti, L., Quatrini, P., Borin, S., Puglia, A.M., Rizzi, A., Zanardini, E., Sorlini, C., Corselli, C., Daffonchio, D., 2004. Comparison of different primer sets for use in automated ribosomal intergenic spacer analysis of complex bacterial communities. Appl. Environ. Microbiol. 70, 6147-6156.

Charlet, L., Manceau, A., 1992. X-Ray Absorption Spectroscopic Study of the Sorption of Cr(Iii) at the Oxide Water Interface .2. Adsorption, Coprecipitation, and Surface Precipitation on Hydrous Ferric-Oxide. J. Colloid Interface Sci. 148, 443-458.

Cornell, R.M., Schwertmann, U., 2003. The Iron Oxides: Structure, Properties, Reactions, Occurances and Uses, 2nd ed. WILEY-VCH, Weinheim.

Coxon, A.P.M., 2004. Multidimensional Scaling in M. S. Lewis-Beck, A. Bryman, T. F. Liao, The Sage Encyclopedia of Social Science Research Methods. Sage, Thousand Oaks.

De Sio, A., Bocci, A., Pace, E., Castellano, C., Cinque, G., Tartoni, N., D'Acapito, F., 2008. Diamond solid state ionization chambers for x-ray absorption spectroscopy applications. Appl. Phys. Lett. 93.

Eden, P.A., Schmidt, T.M., Blakemore, R.P., Pace, N.R., 1991. Phylogenetic Analysis of Aquaspirillum-Magnetotacticum Using Polymerase Chain Reaction-Amplified 16s Ribosomal-Rna-Specific DNA. Int. J. Syst. Bacteriol. 41, 324-325.

Garcia-Martinez, J., Acinas, S.G., Anton, A.I., Rodriguez-Valera, F., 1999. Use of the 16S-23S ribosomal genes spacer region in studies of prokaryotic diversity. J. Microbiol. Methods 36, 55-64.

Goldstein, J.I., Newbury, D.E., Echlin, P., Joy, D.C., Lyman, C.E., Lifshin, E., Sawyer, L.C., Michael, J.R., 2003. Scanning Electron Microscopy and X-Ray Microanalysis: A text for biologists, materials scientists, and geologists. Plenum Press.

Gurman, S.J., Binsted, N., Ross, I., 1984. A Rapid, Exact Curved-Wave Theory for Exafs Calculations. J. Phys. C. Solid State 17, 143-151.

Harris, S.J., Mortimer, R.J.G., 2002. Determination of nitrate in small water samples (100 mu L) by the cadmium-copper reduction method: A manual technique with application to the interstitial waters of marine sediments. Int. J. Environ. Anal. Chem. 82, 369-376.

Horikoshi, K., 2004. Alkaliphiles. P. Jpn. Acad. A-Phys. 80, 166-178.

Huber, T., Faulkner, G., Hugenholtz, P., 2004. Bellerophon: a program to detect chimeric sequences in multiple sequence alignments. Bioinformatics 20, 2317-2319.

Kawai, J., 1999. A survey of novel X-ray analysis methods. Journal of Analytical Atomic Spectrometry 14, 455-459.

Krebs, C.J., 1999. Ecological Methodology, 2nd ed. Addison-Welsey Educational Publishers Inc, Menlo Park, CA.

Lane, D.J., Pace, B., Olsen, G.J., Stahl, D.A., Sogin, M.L., Pace, N.R., 1985. Rapid determination of 16S ribosomal RNA sequences for phylogenetic analysis. P. Natl. Acad. Sci. USA 82, 6955-6959.

Leadbetter, J.R., 2005. Environmental microbiology. Gulf Professional Publishing.

Lovley, D.R., 1997. Microbial Fe(III) reduction in subsurface environments. FEMS. Microbiol. Rev. 20, 305-313.

Lovley, D.R., Phillips, E.J.P., 1986. Organic-Matter Mineralization with Reduction of Ferric Iron in Anaerobic Sediments. Appl. Environ. Microbiol. 51, 683-689.

Parsons, J.G., Dokken, K., Peralta-Videa, I.R., Romero-Gonzalez, J., Gardea-Torresdey, J.L., 2007. X-ray absorption near edge structure and extended X-ray absorption fine structure analysis of standards and biological samples containing mixed oxidation states, of chromium(III) and Chromium(VI). Appl. Spectrosc. 61, 338-345.

Pennycook, S.J., Lupini, A.R., Borisevich, A., Varela, M., Peng, Y., Nellist, P.D., Duscher, G., Buczko, R., Pantelides, S.T., 2003. Transmission electron microscopy: Overview and challenges, in: Seiler, D.G., Diebold, A.C., Shaffner, T.J., McDonald, R., Zollner, S., Khosla, R.P., Secula, E.M. (Eds.), Characterization and Metrology for Ulsi Technology, pp. 627-633.

Pflaum, R.T., Howick, L.C., 1956. The chromium-diphenylcarbazinde reaction. J. Am. Chem. Soc. 78, 4862-4866.

Ravel, B., Newville, M., 2005. ATHENA, ARTEMIS, HEPHAESTUS: data analysis for X-ray absorption spectroscopy using IFEFFIT. J. Synchrot. Radiat. 12, 537-541.

Reed, S.J.B., 2005. Electron Microprobe Analysis and Scanning Electron Microscopy in Geology, 2 ed. Cambridge University Press, Cambridge, UK.

Roskam, E.E., Coxon, A.P.M., Brier, A.P., Hawkins, P.K., 2005. The NewMDSX Program Series, Version 5. NewMDSX Project, Edinburgh.

Saraswat, I.P., Vajpei, A.C., 1984. Characterization of Chromium-Oxide Hydrate Gel. J. Mater. Sci. Lett. 3, 515-517.

Schloss, P.D., Westcott, S.L., Ryabin, T., Hall, J.R., Hartmann, M., Hollister, E.B., Lesniewski, R.A., Oakley, B.B., Parks, D.H., Robinson, C.J., Sahl, J.W., Stres, B., Thallinger, G.G., Van Horn, D.J., Weber, C.F., 2009. Introducing mothur: Open-Source, Platform-Independent, Community-Supported Software for Describing and Comparing Microbial Communities. Appl. Environ. Microbiol. 75, 7537-7541.

Schumacher, B.A., 2002. Methods for the Determination of Total Organic Carbon (TOC) in Soils and Sediments. United States Environmental Protection Agency, Las Vegas.

Slaughter, J.M., Falco, C.M., 1992. Advances in multilayer X-ray optics. Nucl. Instrum. Methods Phys. Res. Sect. A-Accel. Spectrom. Dect. Assoc. Equip. 319, 163-169.

Son, A.J., Schmidt, C.J., Shin, H.J., Cha, D.K., 2011. Microbial community analysis of perchlorate-reducing cultures growing on zero-valent iron. J. Hazard. Mater. 185, 669-676.

Stookey, L.L., 1970. Ferrozine - A new spectrophotometric reagent for iron. Anal. Chem. 42, 779-&.

Tenderholt, A., Hedman, B., Hodgson, K.O., 2007. PySpline: A modern, cross-platform program for the processing of raw averaged XAS edge and EXAFS data, in: Hedman, B., Painetta, P. (Eds.), X-Ray Absorption Fine Structure-XAFS13, pp. 105-107.

Thompson, M., Ellison, S.L.R., 2005. A review of interference effects and their correction in chemical analysis with special reference to uncertainty. Accredit. Qual. Assur. 10, 82-97.

Tomic, S., Searle, B.G., Wander, A., Harrison, N.M., Dent, A.J., Mosselmans, J.F.W., Inglesfield, J.E., 2005. CCLRC Technical Report DL-TR-2005-001, ISSN 1362-0207(2005).

USEPA, 1992. SW-846 Manual: Method 7196a. Chromium hexavalent (colorimetric). Retrieved 6th Jan 2006.

USEPA, 1996. Alkaline Digestion for Hexavalent Chromium, USEPA Method 3060A (SW-846, 1996) Washington D.C.: Office of Solid Waste and Emerging Response; 1996b.

Viollier, E., Inglett, P.W., Hunter, K., Roychoudhury, A.N., Van Cappellen, P., 2000. The ferrozine method revisited: Fe(II)/Fe(III) determination in natural waters. Appl. Geochem. 15, 785-790.

Vitale, R.J., Mussoline, G.R., Petura, J.C., James, B.R., 1997. Cr(VI) soil analytical method: A reliable analytical method for extracting and quantifying Cr(VI) in soils. J. Soil Contam. 6, 581-593.

Wang, Q., Garrity, G.M., Tiedje, J.M., Cole, J.R., 2007. Naive Bayesian classifier for rapid assignment of rRNA sequences into the new bacterial taxonomy. Appl. Environ. Microbiol. 73, 5261-5267.

Zacharia, W.H., 1967. A general theory of X-ray diffraction in crystals. Acta Crystallographica 23, 558-&.

Zubavichus, Y.V., Slovokhotov, Y.L., 2001. X-Ray synchrotron radiation in physicochemical studies. Russian Chemical Reviews 70, 373-403.

Appendix B Additional results

B.1 Historical OS maps

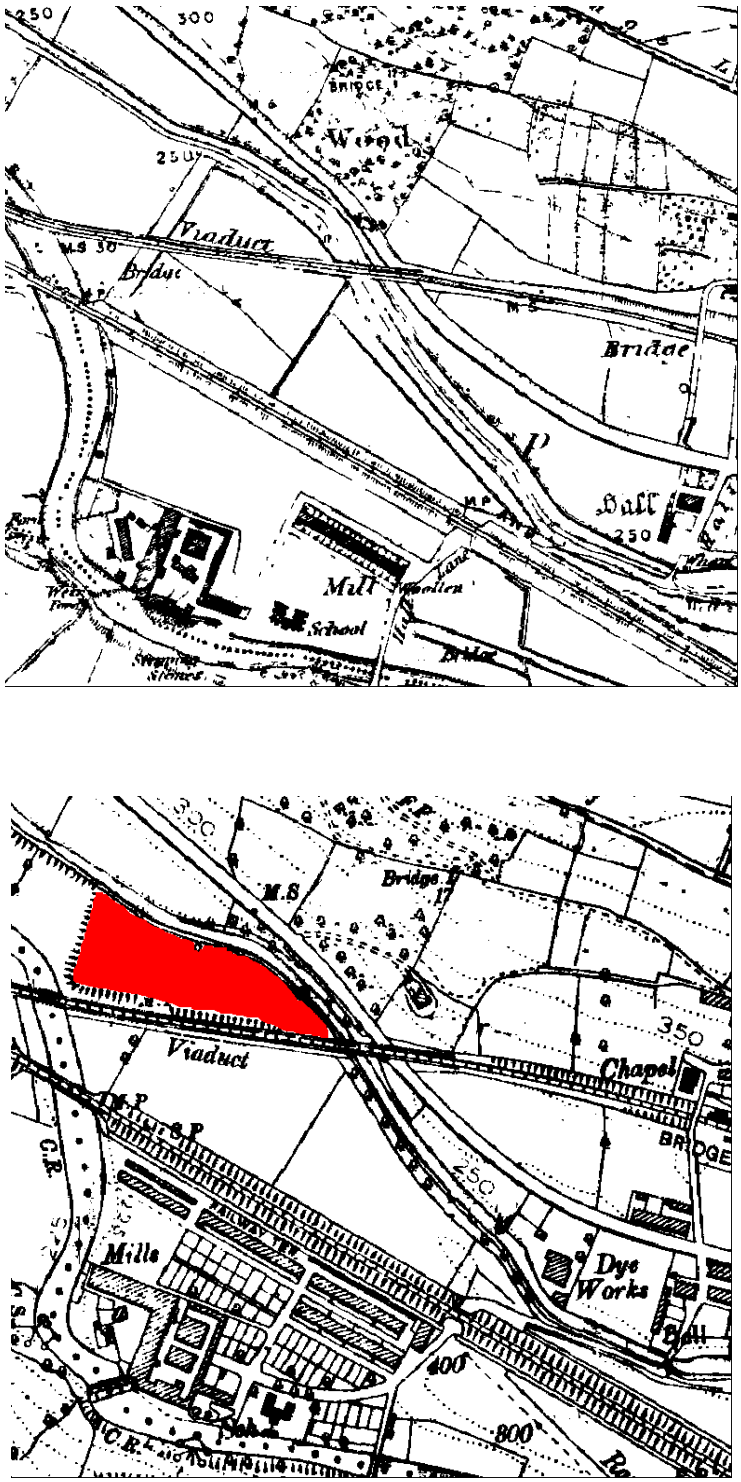

Figure B.1 Historical Ordinance Survey maps from 1899 (top) and 1914 (bottom) depicting the appearance of the COPR landform (shaded red), as well as the location of the Dye Works. *1:10560 County series first edition, 1849, 1888. © Crown Copyright and Landmark Information Group Limited 2009. All rights reserved 1848-1914.*

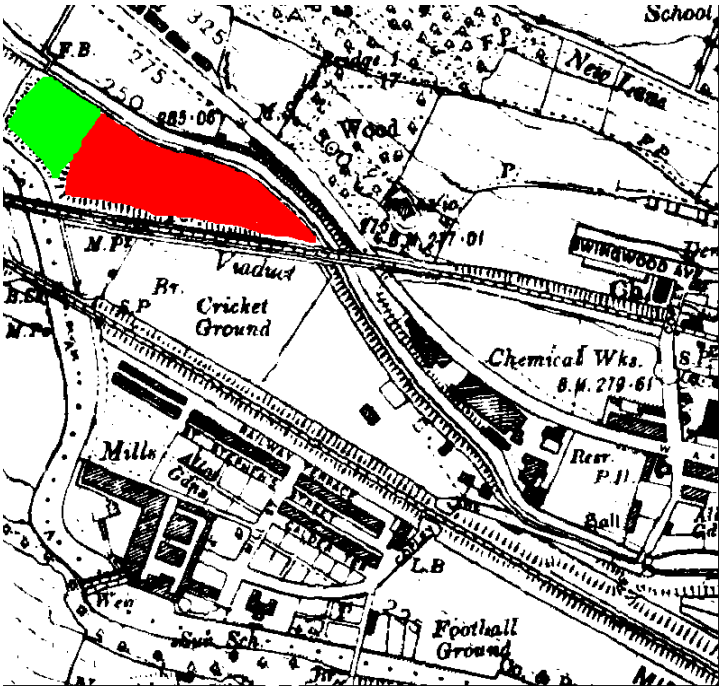

Figure B.2 Historical Ordinance Survey map from 1922 showing the appearance of the second landform (shaded green) to the west of the COPR (shaded red). *1:10560 County series third revision, 1922. © Crown Copyright and Landmark Information Group Limited 2009. All rights reserved. 1922-1969.*

B.2 Hydrogeological investigation

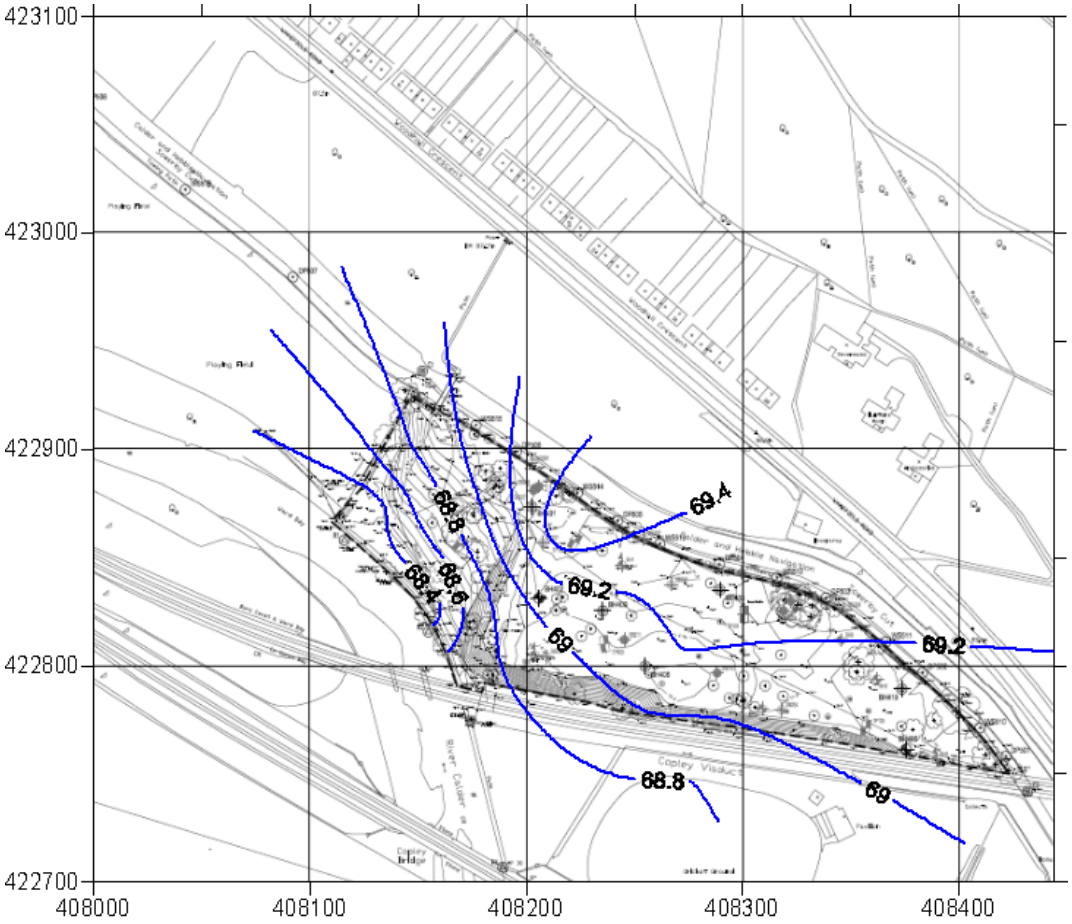

Figure B.3 Hydrogeological map of ground water flow direction at COPR site (Atkins, 2009)

B.3 Borehole geochemical profiles

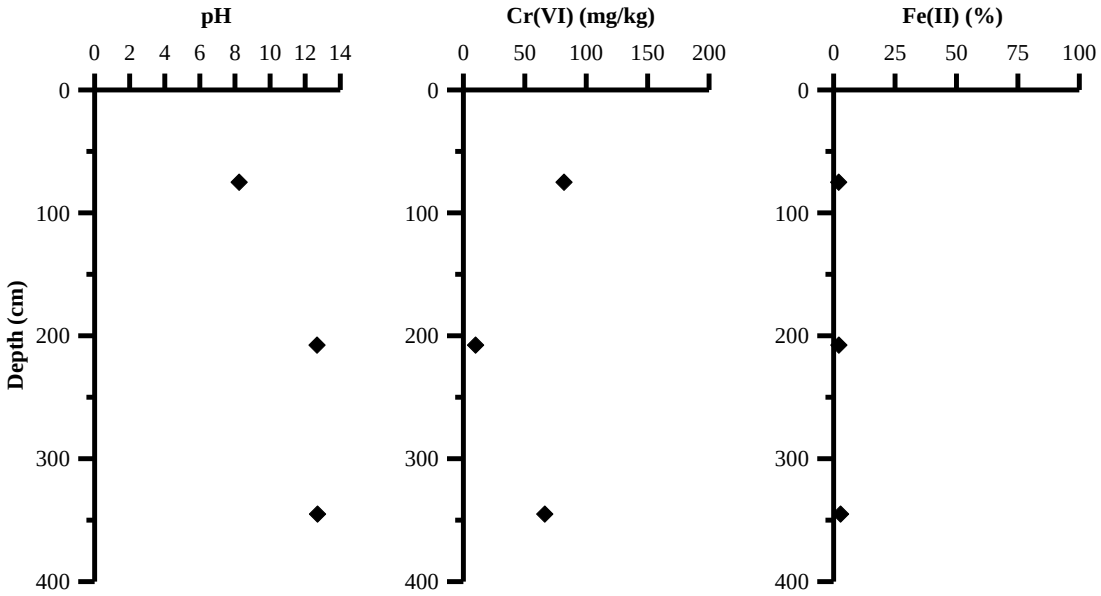

Figure B.4 Geochemical profile BHL2 (renumbered B1 prior to publication)

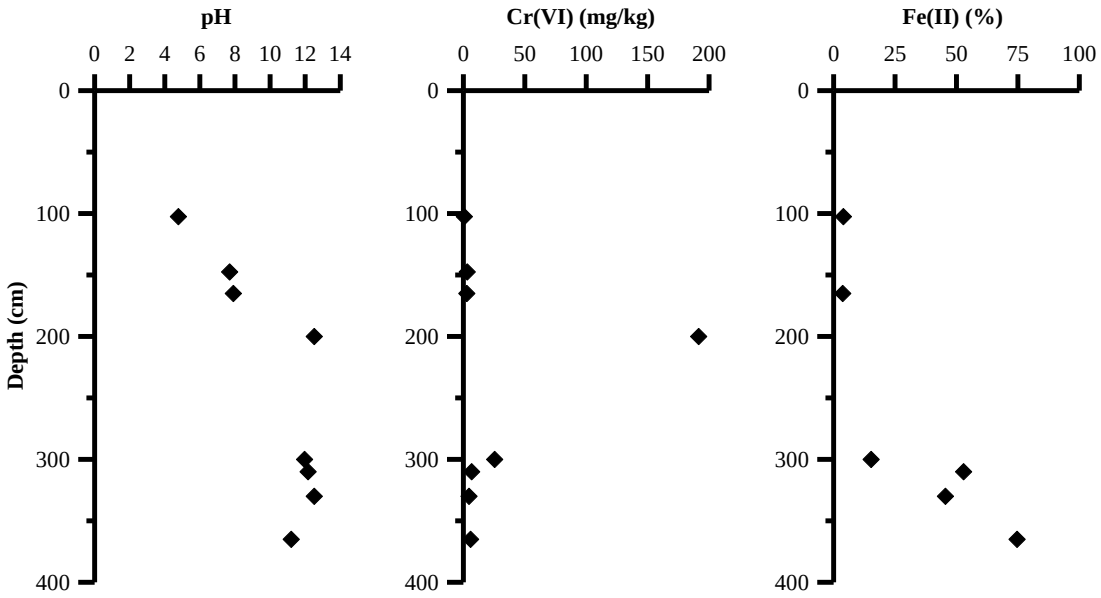

Figure B.5 Geochemical profile BHL3 (renumbered B2 prior to publication)

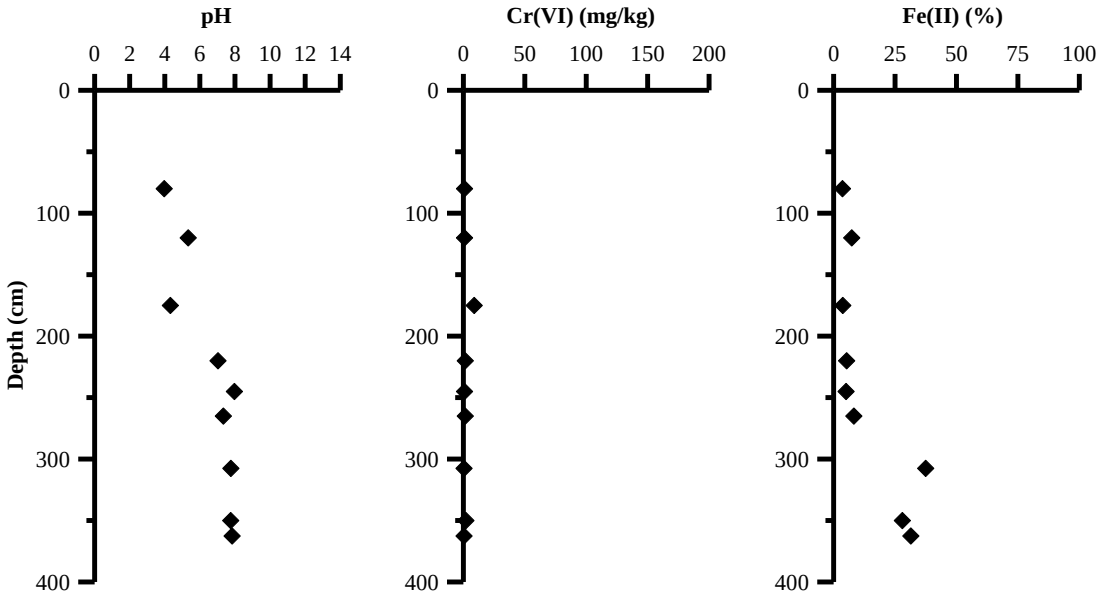

Figure B.6 Geochemical profile BHL1 (renumbered B3 prior to publication)

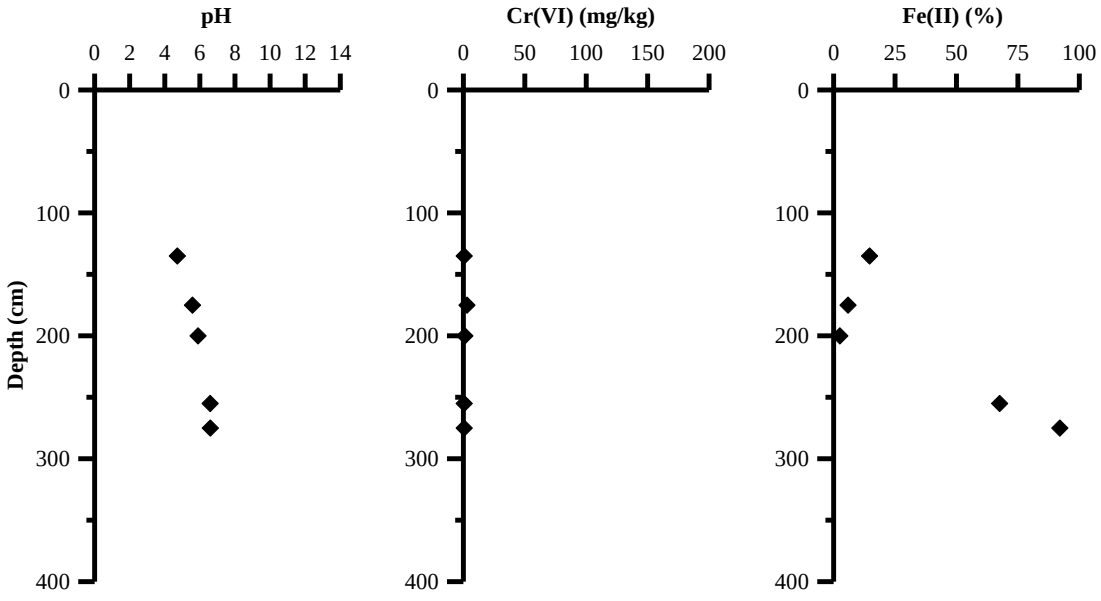

Figure B.7 Geochemical profile BHL5 (renumbered B4 prior to publication)

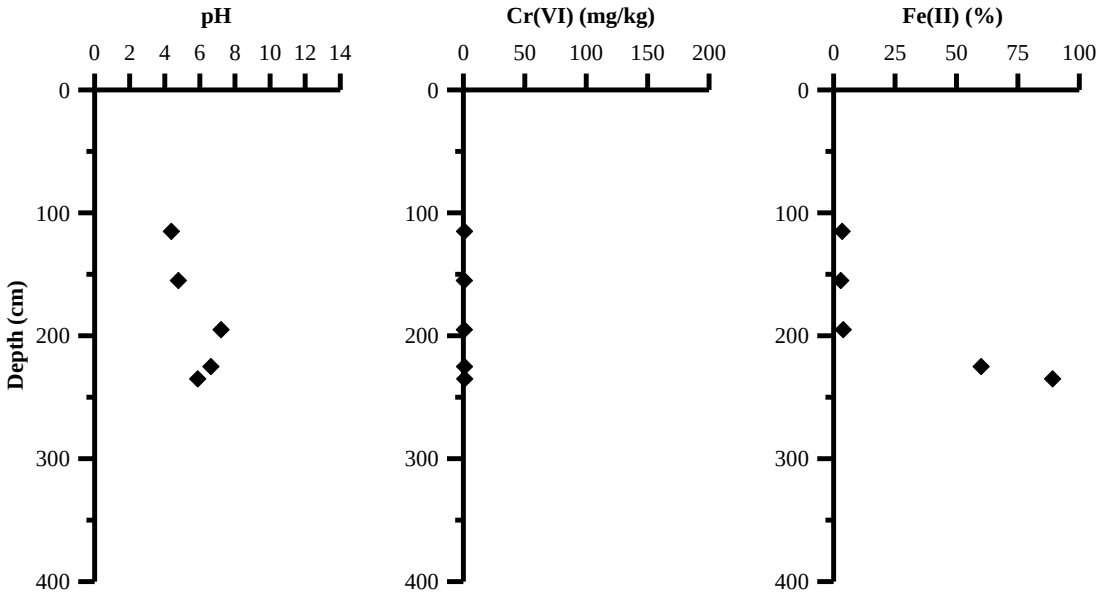

Figure B.8 Geochemical profile BHL6 (renumbered B5 prior to publication)

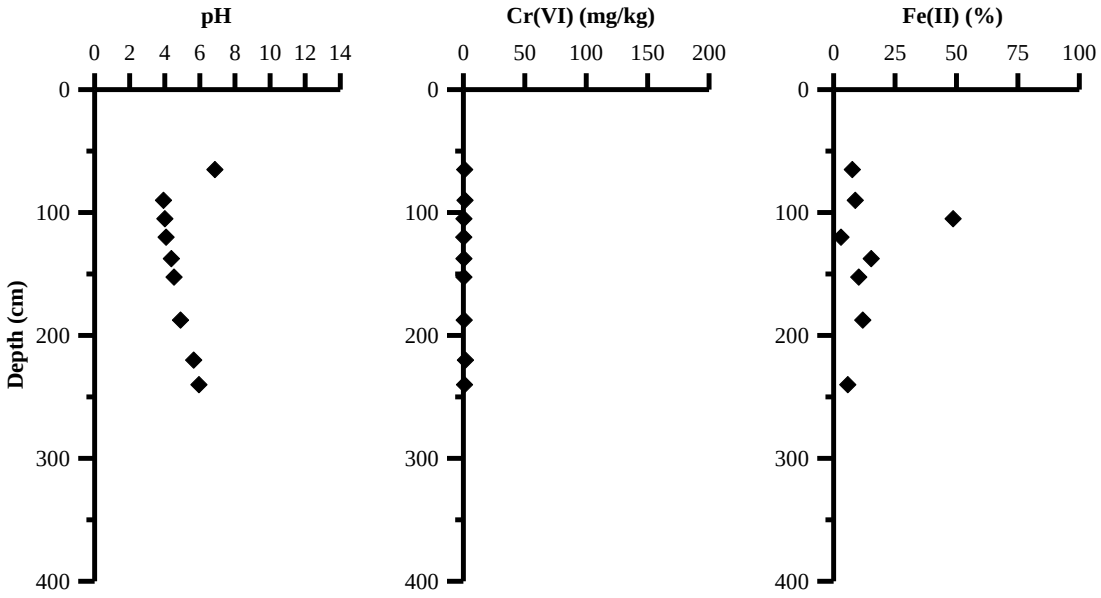

Figure B.9 Geochemical profile BHL4 (renumbered B6 prior to publication)

B.4 X-ray diffraction

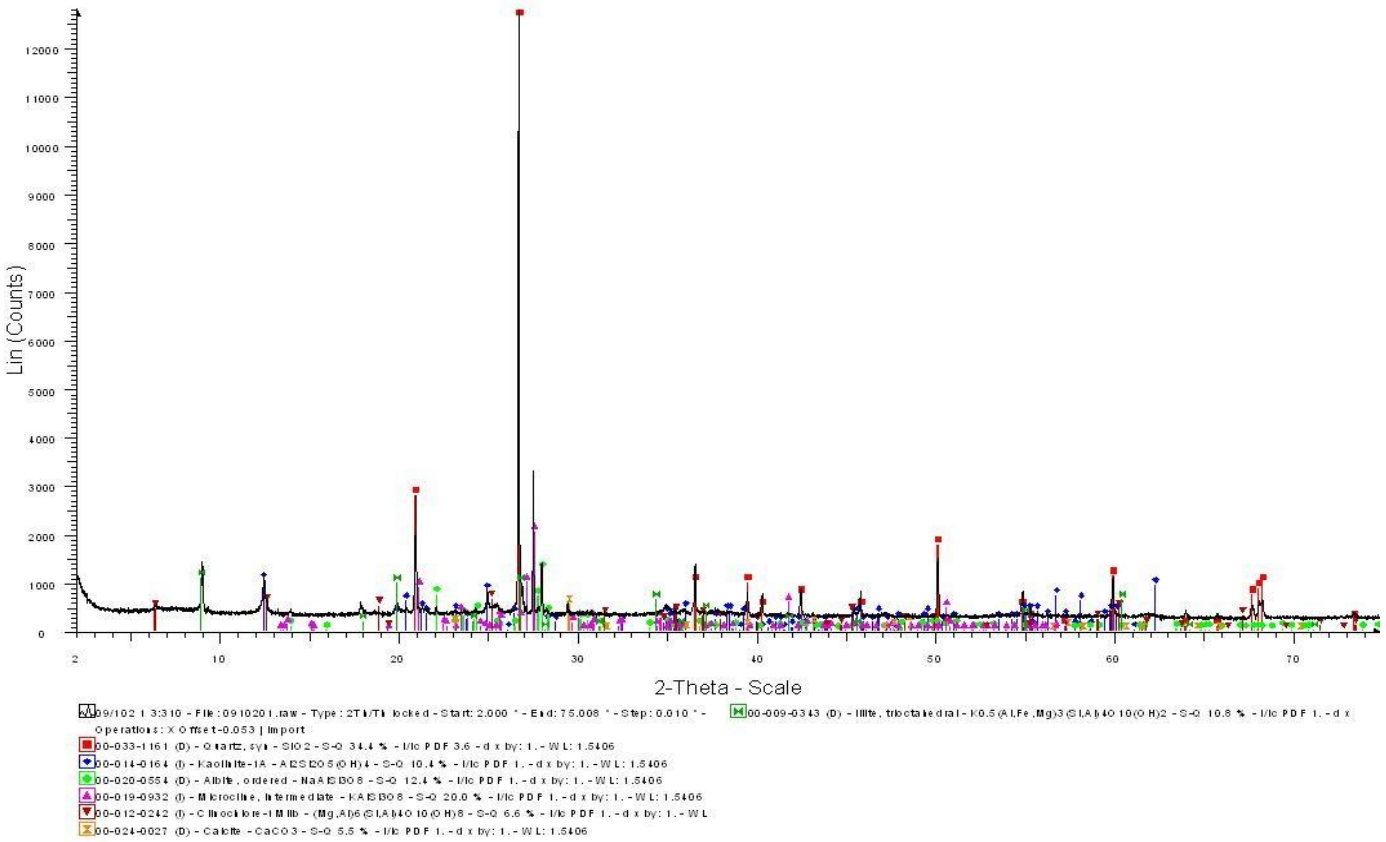

Figure B.10 B2-310 soil X-ray diffractogram

B.5 Clone libraries

Table B.1 RDP classification with 95% confidence threshold and OTU assignment for sequences obtained from B2 310 initial sample.

ID*	Accession number	Sequence length	OTU	Classification using the RDP classifier (Wang et al., 2007) (95% Confidence threshold)
BHL3-310I-1	FR695903	536	A1	Firmicutes, Bacilli, Bacillales, Bacillaceae
BHL3-310I-2	FR695904	527	A2	Proteobacteria, Betaproteobacteria
BHL3-310I-3	FR695905	547	A3	Verrucomicrobia, Subdivision3, Subdivision3_genera_incertae_sedis
BHL3-310I-4	FR695906	470	A4	Proteobacteria, Alphaproteobacteria
BHL3-310I-5	FR695907	517	A5	Actinobacteria, Actinobacteria, Rubrobacteridae, Solirubrobacterales
BHL3-310I-6	FR695908	527	A2	Proteobacteria, Betaproteobacteria
BHL3-310I-7	FR695909	535	A6	Firmicutes, Bacilli, Bacillales, Bacillaceae, Bacillus
BHL3-310I-8	FR695910	527	A2	Proteobacteria, Betaproteobacteria
BHL3-310I-9	FR695911	527	A2	Proteobacteria, Betaproteobacteria
BHL3-310I-10	FR695912	499	A7	Firmicutes, Clostridia, Clostridiales
BHL3-310I-11	FR695913	545	A8	Verrucomicrobia, Subdivision3, Subdivision3_genera_incertae_sedis
BHL3-310I-12	FR695914	510	A9	Firmicutes, Clostridia, Natranaerobiales, Natranaerobiaceae, Dethiobacter
BHL3-310I-14	FR695915	526	A10	Nitrospira, Nitrospira, Nitrospirales, Nitrospiraceae, Nitrospira
BHL3-310I-15	FR695916	527	A11	Bacteroidetes, Sphingobacteria, Sphingobacteriales, Chitinophagaceae
BHL3-310I-16	FR695917	510	A9	Firmicutes, Clostridia, Natranaerobiales, Natranaerobiaceae, Dethiobacter
BHL3-310I-17	FR695918	531	A12	Proteobacteria
BHL3-310I-18	FR695919	510	A13	Firmicutes, Clostridia, Clostridiales, IncertaeSedisXIV, Anaerobranca
BHL3-310I-19	FR695920	517	A14	Bacteroidetes, Flavobacteria, Flavobacteriales, Flavobacteriaceae, Flavobacterium
BHL3-310I-20	FR695921	525	A15	Proteobacteria, Betaproteobacteria
BHL3-310I-21	FR695922	509	A16	Actinobacteria, Actinobacteria, Actinobacteridae, Actinomycetales, Micrococcineae, Microbacteriaceae
BHL3-310I-22	FR695923	523	A17	Bacteroidetes, Sphingobacteria, Sphingobacteriales, Chitinophagaceae
BHL3-310I-23	FR695924	549	A18	Firmicutes, Clostridia, Clostridiales, Peptococcaceae, Peptococcaceae1, Desulfosporosinus
BHL3-310I-24	FR695925	525	A19	Proteobacteria, Gammaproteobacteria

ID*	Accession number	Sequence length	OTU	Classification using the RDP classifier (Wang et al., 2007) (95% Confidence threshold)
BHL3-310I-25	FR695926	522	A20	
BHL3-310I-26	FR695927	527	A2	Proteobacteria, Betaproteobacteria, Burkholderiales
BHL3-310I-27	FR695928	532	A21	Proteobacteria
BHL3-310I-28	FR695929	525	A22	Proteobacteria, Betaproteobacteria
BHL3-310I-29	FR695930	517	A23	Bacteroidetes, Flavobacteria, Flavobacteriales, Flavobacteriaceae, Flavobacterium
BHL3-310I-30	FR695931	500	A24	Planctomycetes, Planctomycetacia, Planctomycetales, Planctomycetaceae, Gemmata
BHL3-310I-31	FR695932	536	A25	Acidobacteria, Acidobacteria_Gp6, Gp6
BHL3-310I-32	FR695933	515	A23	Bacteroidetes, Flavobacteria, Flavobacteriales, Flavobacteriaceae, Flavobacterium
BHL3-310I-34	FR695934	542	A26	Nitrospira, Nitrospira, Nitrospirales, Nitrospiraceae, Leptospirillum
BHL3-310I-35	FR695935	509	A27	Actinobacteria, Actinobacteria
BHL3-310I-36	FR695936	525	A28	Proteobacteria, Betaproteobacteria
BHL3-310I-37	FR695937	507	A29	Actinobacteria, Actinobacteria, Actinobacteridae, Actinomycetales, Micrococcineae
BHL3-310I-38	FR695938	528	A30	Bacteroidetes, Sphingobacteria, Sphingobacteriales, Chitinophagaceae, Ferruginibacter
BHL3-310I-39	FR695939	543	A31	
BHL3-310I-40	FR695940	536	A32	Proteobacteria, Deltaproteobacteria, Myxococcales, Nannocystineae
BHL3-310I-41	FR695941	526	A10	Nitrospira, Nitrospira, Nitrospirales, Nitrospiraceae, Nitrospira
BHL3-310I-42	FR695942	526	A2	Proteobacteria, Betaproteobacteria
BHL3-310I-43	FR695943	508	A33	Planctomycetes, Planctomycetacia, Planctomycetales, Planctomycetaceae
BHL3-310I-44	FR695944	531	A34	Actinobacteria, Actinobacteria, Rubrobacteridae, Solirubrobacterales
BHL3-310I-45	FR695945	549	A18	Firmicutes, Clostridia, Clostridiales, Peptococcaceae, Peptococcaceae1, Desulfosporosinus
BHL3-310I-46	FR695946	541	A35	
BHL3-310I-47	FR695947	541	A35	
BHL3-310I-48	FR695948	510	A36	
BHL3-310I-49	FR695949	510	A9	Firmicutes, Clostridia, Natranaerobiales, Natranaerobiaceae, Dethiobacter
BHL3-310I-50	FR695950	527	A2	Proteobacteria, Betaproteobacteria
BHL3-310I-51	FR695951	522	A37	Bacteroidetes, Sphingobacteria, Sphingobacteriales, Cyclobacteriaceae
BHL3-310I-52	FR695952	531	A38	

ID*	Accession number	Sequence length	OTU	Classification using the RDP classifier (Wang et al., 2007) (95% Confidence threshold)
BHL3-310I-53	FR695953	522	A37	Bacteroidetes, Sphingobacteria, Sphingobacteriales, Cyclobacteriaceae
BHL3-310I-54	FR695954	531	A12	Proteobacteria
BHL3-310I-55	FR695955	527	A2	Proteobacteria, Betaproteobacteria
BHL3-310I-56	FR695956	512	A39	Firmicutes, Clostridia, Clostridiales, IncertaeSedisXIV, Anaerobranca
BHL3-310I-57	FR695957	523	A40	Bacteroidetes
BHL3-310I-58	FR695958	532	A41	Actinobacteria, Actinobacteria, Rubrobacteridae, Solirubrobacterales, Solirubrobacteraceae, Solirubrobacter
BHL3-310I-59	FR695959	513	A42	Bacteria_incertae_sedis, Ktedonobacteria, Ktedonobacterales, Ktedonobacteraceae, Ktedonobacter
BHL3-310I-60	FR695960	510	A9	Firmicutes, Clostridia, Natranaerobiales, Natranaerobiaceae, Dethiobacter
BHL3-310I-61	FR695961	516	A43	Proteobacteria, Betaproteobacteria, Burkholderiales, Comamonadaceae, Pelomonas
BHL3-310I-62	FR695962	521	A44	Firmicutes, Clostridia, Clostridiales, IncertaeSedisXI, Tissierella
BHL3-310I-63	FR695963	537	A45	Firmicutes, Bacilli, Bacillales, Bacillaceae, Bacillus
BHL3-310I-64	FR695964	474	A46	Proteobacteria, Alphaproteobacteria, Rhizobiales

* BHL3 was renumbered B2 after sequences had been submitted to GenBank

Table B.2 RDP classification with 95% confidence threshold and OTU assignment for sequences obtained from *unamended* microcosm day 270

ID	Accession number	Sequence length	OTU	Classification using the RDP classifier (Wang et al., 2007) (95% Confidence threshold)
UN-270-1	FR695965	522	B1	Firmicutes,
UN-270-2	FR695966	503	B2	Deinococcus-Thermus, Deinococci, Deinococcales, Trueperaceae, Truepera
UN-270-3	FR695967	503	B2	Deinococcus-Thermus, Deinococci, Deinococcales, Trueperaceae, Truepera
UN-270-4	FR695968	503	B2	Deinococcus-Thermus, Deinococci, Deinococcales, Trueperaceae, Truepera
UN-270-5	FR695969	503	B2	Deinococcus-Thermus, Deinococci, Deinococcales, Trueperaceae, Truepera
UN-270-6	FR695970	503	B2	Deinococcus-Thermus, Deinococci
UN-270-7	FR695971	503	B2	Deinococcus-Thermus, Deinococci
UN-270-8	FR695972	503	B2	Deinococcus-Thermus, Deinococci, Deinococcales, Trueperaceae, Truepera
UN-270-9	FR695973	503	B2	Deinococcus-Thermus, Deinococci
UN-270-10	FR695974	509	B3	Firmicutes, Clostridia, Natranaerobiales, Natranaerobiaceae, Dethiobacter
UN-270-11	FR695975	503	B2	Deinococcus-Thermus, Deinococci, Deinococcales, Trueperaceae, Truepera
UN-270-12	FR695976	507	B4	Firmicutes, Clostridia, Natranaerobiales, Natranaerobiaceae, Dethiobacter
UN-270-13	FR695977	503	B2	Deinococcus-Thermus, Deinococci, Deinococcales, Trueperaceae, Truepera
UN-270-15	FR695978	503	B2[+]	
UN-270-16	FR695979	503	B2	Deinococcus-Thermus, Deinococci, Deinococcales, Trueperaceae, Truepera
UN-270-17	FR695980	504	B5	
UN-270-18	FR695981	503	B2	Deinococcus-Thermus, Deinococci, Deinococcales, Trueperaceae, Truepera
UN-270-19	FR695982	503	B2	Deinococcus-Thermus, Deinococci, Deinococcales, Trueperaceae, Truepera
UN-270-20	FR695983	503	B2	Deinococcus-Thermus, Deinococci, Deinococcales, Trueperaceae, Truepera
UN-270-21	FR695984	503	B2	Deinococcus-Thermus, Deinococci, Deinococcales, Trueperaceae, Truepera
UN-270-22	FR695985	503	B2	Deinococcus-Thermus, Deinococci, Deinococcales, Trueperaceae, Truepera
UN-270-23	FR695986	502	B2	Deinococcus-Thermus, Deinococci, Deinococcales, Trueperaceae, Truepera
UN-270-24	FR695987	503	B2	Deinococcus-Thermus, Deinococci, Deinococcales, Trueperaceae, Truepera
UN-270-25	FR695988	503	B2	Deinococcus-Thermus, Deinococci, Deinococcales, Trueperaceae, Truepera
UN-270-28	FR695989	503	B2	Deinococcus-Thermus, Deinococci, Deinococcales, Trueperaceae, Truepera
UN-270-30	FR695990	512	B6	Firmicutes, Clostridia, Clostridiales, Incertae Sedis XIV, Anaerobranca
UN-270-31	FR695991	503	B2	Deinococcus-Thermus, Deinococci, Deinococcales, Trueperaceae, Truepera
UN-270-32	FR695992	503	B2	Deinococcus-Thermus, Deinococci, Deinococcales, Trueperaceae, Truepera

ID	Accession number	Sequence length	OTU	Classification using the RDP classifier (Wang et al., 2007) (95% Confidence threshold)
UN-270-33	FR695993	503	B2	Deinococcus-Thermus, Deinococci
UN-270-34	FR695994	503	B2	Deinococcus-Thermus, Deinococci, Deinococcales, Trueperaceae, Truepera
UN-270-35	FR695995	503	B2	Deinococcus-Thermus, Deinococci, Deinococcales, Trueperaceae, Truepera
UN-270-36	FR695996	503	B2	Deinococcus-Thermus, Deinococci, Deinococcales, Trueperaceae, Truepera
UN-270-38	FR695997	503	B2	Deinococcus-Thermus, Deinococci, Deinococcales, Trueperaceae, Truepera
UN-270-39	FR695998	503	B2[+]	
UN-270-40	FR695999	503	B2[+]	
UN-270-41	FR696000	503	B2	Deinococcus-Thermus, Deinococci
UN-270-42	FR696001	503	B2	Deinococcus-Thermus, Deinococci, Deinococcales, Trueperaceae, Truepera
UN-270-43	FR696002	498	B2	Deinococcus-Thermus, Deinococci, Deinococcales, Trueperaceae, Truepera
UN-270-44	FR696003	503	B2	Deinococcus-Thermus, Deinococci, Deinococcales, Trueperaceae, Truepera
UN-270-45	FR696004	503	B2	Deinococcus-Thermus, Deinococci, Deinococcales, Trueperaceae, Truepera
UN-270-46	FR696005	503	B2	Deinococcus-Thermus, Deinococci, Deinococcales, Trueperaceae, Truepera
UN-270-47	FR696006	503	B2	Deinococcus-Thermus, Deinococci, Deinococcales, Trueperaceae, Truepera
UN-270-48	FR696007	522	B1	Firmicutes

[+] 26 members of OTU C2 were assigned to Deiococcus-Thermus while 3 members were unassigned

Table B.3 RDP classification with 95% confidence threshold and OTU assignment for sequences obtained from *pH9 amended* microcosm day 153

ID	Accession number	Sequence length	OTU	Classification using the RDP classifier (Wang et al., 2007) (95% Confidence threshold)
pH9-153-1	FR696008	508	C1	Firmicutes, Clostridia, Natranaerobiales, Natranaerobiaceae, Dethiobacter
pH9-153-2	FR696009	517	C2	
pH9-153-4	FR696010	510	C3	Firmicutes, Clostridia, Natranaerobiales, Natranaerobiaceae, Dethiobacter
pH9-153-5	FR696011	510	C4	Firmicutes, Clostridia, Natranaerobiales, Natranaerobiaceae, Dethiobacter
pH9-153-6	FR696012	531	C5	Proteobacteria
pH9-153-7	FR696013	522	C6	Firmicutes
pH9-153-8	FR696014	522	C6	Firmicutes
pH9-153-9	FR696015	514	C7	Firmicutes
pH9-153-10	FR696016	510	C3	Firmicutes, Clostridia, Natranaerobiales, Natranaerobiaceae, Dethiobacter
pH9-153-12	FR696017	522	C6*	
pH9-153-13	FR696018	510	C3	Firmicutes, Clostridia, Natranaerobiales, Natranaerobiaceae, Dethiobacter
pH9-153-14	FR696019	510	C8	
pH9-153-15	FR696020	510	C3	Firmicutes, Clostridia, Natranaerobiales, Natranaerobiaceae, Dethiobacter
pH9-153-16	FR696021	510	C3	Firmicutes, Clostridia, Natranaerobiales, Natranaerobiaceae, Dethiobacter
pH9-153-17	FR696022	533	C9	Proteobacteria
pH9-153-18	FR696023	517	C10	Firmicutes
pH9-153-20	FR696024	522	C6*	
pH9-153-22	FR696025	511	C11	Firmicutes, Clostridia, Clostridiales, Incertae Sedis XIV, Anaerobranca
pH9-153-23	FR696026	510	C8	
pH9-153-24	FR696027	507	C1	Firmicutes, Clostridia, Natranaerobiales, Natranaerobiaceae, Dethiobacter
pH9-153-25	FR696028	511	C12	
pH9-153-26	FR696029	510	C4	Firmicutes, Clostridia, Natranaerobiales, Natranaerobiaceae, Dethiobacter
pH9-153-28	FR696030	515	C13	Firmicutes, Clostridia, Clostridiales, Ruminococcaceae, Acetivibrio
pH9-153-30	FR696031	511	C3	Firmicutes, Clostridia, Natranaerobiales, Natranaerobiaceae, Dethiobacter
pH9-153-31	FR696032	506	C14	Firmicutes, Clostridia
pH9-153-32	FR696033	494	C15	Proteobacteria, Alphaproteobacteria
pH9-153-33	FR696034	510	C3	Firmicutes, Clostridia, Natranaerobiales, Natranaerobiaceae, Dethiobacter
pH9-153-34	FR696035	516	C16	Firmicutes, Clostridia

ID	Accession number	Sequence length	OTU	Classification using the RDP classifier (Wang et al., 2007) (95% Confidence threshold)
pH9-153-35	FR696036	511	C17	Firmicutes, Clostridia, Natranaerobiales, Natranaerobiaceae, Dethiobacter
pH9-153-36	FR696037	496	C18	Firmicutes
pH9-153-37	FR696038	508	C19	Firmicutes, Clostridia, Natranaerobiales, Natranaerobiaceae, Dethiobacter
pH9-153-38	FR696039	508	C20	
pH9-153-39	FR696040	510	C3	Firmicutes, Clostridia, Natranaerobiales, Natranaerobiaceae, Dethiobacter
pH9-153-40	FR696041	509	C21	Firmicutes, Clostridia
pH9-153-41	FR696042	510	C22	Firmicutes, Clostridia
pH9-153-42	FR696043	512	C11	Firmicutes, Clostridia, Clostridiales, Incertae Sedis XIV, Anaerobranca
pH9-153-43	FR696044	511	C17	Firmicutes, Clostridia, Natranaerobiales, Natranaerobiaceae, Dethiobacter
pH9-153-44	FR696045	510	C17	Firmicutes, Clostridia, Natranaerobiales, Natranaerobiaceae, Dethiobacter
pH9-153-45	FR696046	510	C3	Firmicutes, Clostridia, Natranaerobiales, Natranaerobiaceae, Dethiobacter
pH9-153-48	FR696047	510	C8	
pH9-153-50	HE573872	525	C23	Proteobacteria, Betaproteobacteria, Burkholderiales, Oxalobacteraceae, Herbaspirillum
pH9-153-51	HE573873	516	C16	Firmicutes, Clostridia
pH9-153-53	HE573874	496	C18	
pH9-153-56	HE573875	527	C24	Proteobacteria, Betaproteobacteria
pH9-153-57	HE573876	511	C25	Firmicutes, Clostridia, Natranaerobiales, Natranaerobiaceae, Dethiobacter
pH9-153-59	HE573877	509	C26	Firmicutes, Clostridia, Natranaerobiales, Natranaerobiaceae, Dethiobacter
pH9-153-60	HE573878	510	C3	Firmicutes, Clostridia, Natranaerobiales, Natranaerobiaceae, Dethiobacter
pH9-153-61	HE573879	506	C14	Firmicutes, Clostridia
pH9-153-62	HE573880	516	C16	
pH9-153-63	HE573881	509	C26	Firmicutes, Clostridia, Natranaerobiales, Natranaerobiaceae, Dethiobacter
pH9-153-64	HE573882	509	C8	
pH9-153-66	HE573883	522	C6	Firmicutes
pH9-153-68	HE573884	509	C26	Firmicutes, Clostridia, Natranaerobiales, Natranaerobiaceae, Dethiobacter
pH9-153-69	HE573885	509	C27	Firmicutes, Clostridia, Natranaerobiales, Natranaerobiaceae, Dethiobacter
pH9-153-70	HE573886	512	C28	
pH9-153-71	HE573887	519	C29	
pH9-153-72	HE573888	510	C4	Firmicutes, Clostridia, Natranaerobiales, Natranaerobiaceae, Dethiobacter

* Two member of OTU B6 are classified as Firmicutes while two were unclassified

Table B.4 RDP classification with 95% confidence threshold and OTU assignment for sequences obtained from iron reducing consortium isolated from B2 310 sample.

ID*	Accession number	Sequence length	OTU	Classification using the RDP classifier(Wang et al., 2007) (95% Confidence threshold)
BHL3_Fe_Consort_1	FR820910	521	D1	Firmicutes, Clostridia, Clostridiales, Incertae Sedis XI, Tissierella
BHL3_Fe_Consort_2	FR820911	511	D2	
BHL3_Fe_Consort_3	FR820912	516	D3	Firmicutes, Clostridia, Clostridiales, Clostridiaceae
BHL3_Fe_Consort_4	FR820913	506	D4	Firmicutes, Clostridia, Clostridiales, Clostridiaceae, Clostridiaceae 2, Natronincola
BHL3_Fe_Consort_5	FR820914	516	D3	Firmicutes, Clostridia, Clostridiales, Clostridiaceae
BHL3_Fe_Consort_6	FR820915	512	D5	Firmicutes, Clostridia, Clostridiales, Incertae Sedis XIV, Anaerobranca
BHL3_Fe_Consort_7	FR820916	517	D6	Firmicutes, Clostridia, Clostridiales, Clostridiaceae
BHL3_Fe_Consort_8	FR820917	516	D3	Firmicutes, Clostridia, Clostridiales, Clostridiaceae
BHL3_Fe_Consort_9	FR820918	514	D7	Firmicutes, Clostridia
BHL3_Fe_Consort_10	FR820919	515	D3	Firmicutes, Clostridia, Clostridiales, Clostridiaceae
BHL3_Fe_Consort_11	FR820920	521	D8	Firmicutes, Clostridia, Clostridiales, Incertae Sedis XI, Tissierella
BHL3_Fe_Consort_12	FR820921	516	D3	Firmicutes, Clostridia, Clostridiales, Clostridiaceae
BHL3_Fe_Consort_13	FR820922	496	D9	Firmicutes
BHL3_Fe_Consort_14	FR820923	516	D3	Firmicutes, Clostridia, Clostridiales, Clostridiaceae
BHL3_Fe_Consort_15	FR820924	516	D3	Firmicutes, Clostridia, Clostridiales, Clostridiaceae
BHL3_Fe_Consort_16	FR820925	586	D10	Firmicutes, Clostridia, Clostridiales
BHL3_Fe_Consort_17	FR820926	516	D3	Firmicutes, Clostridia, Clostridiales, Clostridiaceae
BHL3_Fe_Consort_18	FR820927	557	D11	Firmicutes, Clostridia, Clostridiales, Peptococcaceae, Peptococcaceae 1, Desulfitibacter
BHL3_Fe_Consort_19	FR820928	521	D12	Firmicutes, Clostridia, Clostridiales
BHL3_Fe_Consort_20	FR820929	521	D8	Firmicutes, Clostridia, Clostridiales, Incertae Sedis XI
BHL3_Fe_Consort_21	FR820930	518	D13	Firmicutes, Clostridia, Clostridiales, Incertae Sedis XIV, Anaerovirgula
BHL3_Fe_Consort_22	FR820931	589	D14	Firmicutes, Clostridia, Clostridiales
BHL3_Fe_Consort_23	FR820932	512	D5	Firmicutes, Clostridia, Clostridiales, Incertae Sedis XIV, Anaerobranca
BHL3_Fe_Consort_24	FR820933	521	D12	Firmicutes, Clostridia, Clostridiales
BHL3_Fe_Consort_25	FR820934	518	D15	Firmicutes, Clostridia, Clostridiales, Incertae Sedis XIV, Anaerovirgula
BHL3_Fe_Consort_26	FR820935	511	D2	
BHL3_Fe_Consort_27	FR820936	584	D10	Firmicutes, Clostridia, Clostridiales
BHL3_Fe_Consort_28	FR820937	512	D5	Firmicutes, Clostridia, Clostridiales, Incertae Sedis XIV, Anaerobranca

ID*	Accession number	Sequence length	OTU	Classification using the RDP classifier(Wang et al., 2007) (95% Confidence threshold)
BHL3_Fe_Consort_30	FR820938	521	D16	Proteobacteria, Betaproteobacteria, Burkholderiales, Comamonadaceae, Comamonas
BHL3_Fe_Consort_31	FR820939	512	D5	Firmicutes, Clostridia, Clostridiales, Incertae Sedis XIV, Anaerobranca
BHL3_Fe_Consort_32	FR820940	583	D17	Firmicutes, Clostridia, Clostridiales
BHL3_Fe_Consort_33	FR820941	630	D18	Firmicutes, Clostridia, Clostridiales, Incertae Sedis XIV, Anaerovirgula
BHL3_Fe_Consort_34	FR820942	582	D19	Firmicutes, Clostridia, Clostridiales, Incertae Sedis XIV, Anaerobranca
BHL3_Fe_Consort_35	FR820943	511	D20	Firmicutes, Clostridia, Clostridiales, Incertae Sedis XIV, Anaerobranca
BHL3_Fe_Consort_36	FR820944	516	D3	Firmicutes, Clostridia, Clostridiales, Clostridiaceae
BHL3_Fe_Consort_37	FR820945	516	D3	Firmicutes, Clostridia, Clostridiales, Clostridiaceae
BHL3_Fe_Consort_38	FR820946	512	D5	Firmicutes, Clostridia, Clostridiales, Incertae Sedis XIV, Anaerobranca
BHL3_Fe_Consort_39	FR820947	521	D12	Firmicutes, Clostridia, Clostridiales, Peptococcaceae
BHL3_Fe_Consort_40	FR820948	512	D5	Firmicutes, Clostridia, Clostridiales, Incertae Sedis XIV, Anaerobranca
BHL3_Fe_Consort_41	FR820949	584	D10	Firmicutes, Clostridia, Clostridiales
BHL3_Fe_Consort_42	FR820950	521	D21	Firmicutes, Clostridia, Clostridiales, Incertae Sedis XI, Tissierella
BHL3_Fe_Consort_43	FR820951	516	D3	Firmicutes, Clostridia, Clostridiales, Clostridiaceae, Clostridiaceae 2, Alkaliphilus
BHL3_Fe_Consort_44	FR820952	516	D3	Firmicutes, Clostridia, Clostridiales, Clostridiaceae
BHL3_Fe_Consort_45	FR820953	516	D3	Firmicutes, Clostridia, Clostridiales, Clostridiaceae
BHL3_Fe_Consort_46	FR820954	511	D2	Firmicutes
BHL3_Fe_Consort_47	FR820955	504	D22	
BHL3_Fe_Consort_48	FR820956	516	D3	Firmicutes, Clostridia, Clostridiales, Clostridiaceae

* BHL3 was renumbered B2 after sequences had been submitted to GenBank

Table B.5 RDP classification with 95% confidence threshold and OTU assignment for sequences obtained from viable cultures produced from plate streaking isolation attempts from the iron reducing consortium.

ID*	Sequence length	OTU	Classification using the RDP classifier (Wang et al., 2007) (95% Confidence threshold)
P-2-9-1	517	F1	Firmicutes, Clostridia, Clostridiales, Incertae Sedis XIV, Anaerovirgula
P-2-9-2	512	F2	Firmicutes, Clostridia, Clostridiales, Incertae Sedis XIV, Anaerobranca
P-2-9-3	517	F1	Firmicutes, Clostridia, Clostridiales, Incertae Sedis XIV, Anaerovirgula
P-2-9-4	540	F3	Firmicutes, Bacilli, Bacillales, Bacillaceae ,
P-2-9-5	521	F4	Firmicutes, Clostridia, Clostridiales, Incertae Sedis XI, Tissierella
P-2-9-6	517	F1	Firmicutes, Clostridia, Clostridiales, Incertae Sedis XIV, Anaerovirgula
P-2-9-7	521	F4	Firmicutes, Clostridia, Clostridiales, Incertae Sedis XI, Tissierella
P-2-9-8	517	F1	Firmicutes, Clostridia, Clostridiales, Incertae Sedis XIV, Anaerovirgula
P-2-9-9	517	F1	Firmicutes, Clostridia, Clostridiales, Incertae Sedis XIV, Anaerovirgula
P-2-9-10	512	F2	Firmicutes, Clostridia, Clostridiales, Incertae Sedis XIV, Anaerobranca
P-2-9-11	517	F1	Firmicutes, Clostridia, Clostridiales, Incertae Sedis XIV, Anaerovirgula
P-2-9-12	517	F1	Firmicutes, Clostridia, Clostridiales, Incertae Sedis XIV, Anaerovirgula

Table B.6 RDP classification with 95% confidence threshold and OTU assignment for sequences obtained from viable cultures produced from plate streaking isolation attempts from the iron reducing consortium.

ID*	Sequence length	OTU	Classification using the RDP classifier (Wang et al., 2007) (95% Confidence threshold)
P-2-3-2	521	E1	Firmicutes, Clostridia, Clostridiales, Incertae Sedis XI, Tissierella
P-2-3-3	516	E2	Firmicutes, Clostridia, Clostridiales,
P-2-3-4	516	E2	Firmicutes, Clostridia, Clostridiales,
P-2-3-5	521	E3	Firmicutes, Clostridia, Clostridiales, Incertae Sedis XI, Tissierella
P-2-3-6	521	E1	Firmicutes, Clostridia, Clostridiales, Incertae Sedis XI, Tissierella
P-2-3-7	521	E3	Firmicutes, Clostridia, Clostridiales, Incertae Sedis XI
P-2-3-8	521	E1	Firmicutes, Clostridia, Clostridiales, Incertae Sedis XI, Tissierella
P-2-3-9	521	E1	Firmicutes, Clostridia, Clostridiales, Incertae Sedis XI, Tissierella
P-2-3-10	216	E4	Firmicutes, Clostridia, Clostridiales,
P-2-3-11	520	E1	Firmicutes, Clostridia, Clostridiales, Incertae Sedis XI, Tissierella
P-2-3-12	516	E2	Firmicutes, Clostridia, Clostridiales

Table B.7 RDP classification with 95% confidence threshold and OTU assignment for sequences obtained from viable cultures produced from plate spreading isolation attempts from the iron reducing consortium.

ID*	Sequence length	OTU	Classification using the RDP classifier (Wang et al., 2007) (95% Confidence threshold)
PD-2-9-1	517	G1	Firmicutes, Clostridia, Clostridiales, Incertae Sedis XIV, Anaerovirgula
PD-2-9-2	517	G1	Firmicutes, Clostridia, Clostridiales, Incertae Sedis XIV, Anaerovirgula
PD-2-9-3	520	G2	
PD-2-9-4	512	G3	Firmicutes, Clostridia, Clostridiales, Incertae Sedis XIV, Anaerobranca
PD-2-9-5	521	G4	Firmicutes, Clostridia, Clostridiales, Incertae Sedis XI, Tissierella
PD-2-9-6	582	G3	Firmicutes, Clostridia, Clostridiales, Incertae Sedis XIV, Anaerobranca
PD-2-9-7	517	G1	Firmicutes, Clostridia, Clostridiales, Incertae Sedis XIV, Anaerovirgula
PD-2-9-8	512	G3	Firmicutes, Clostridia, Clostridiales, Incertae Sedis XIV, Anaerobranca
PD-2-9-9	512	G3	Firmicutes, Clostridia, Clostridiales, Incertae Sedis XIV, Anaerobranca
PD-2-9-10	512	G3	Firmicutes, Clostridia, Clostridiales, Incertae Sedis XIV, Anaerobranca
PD-2-9-11	521	G4	Firmicutes, Clostridia, Clostridiales, Incertae Sedis XI, Tissierella
PD-2-9-12	521	G4	Firmicutes, Clostridia, Clostridiales, Incertae Sedis XI, Tissierella
PD-2-9-13	517	G1	Firmicutes, Clostridia, Clostridiales, Incertae Sedis XIV, Anaerovirgula
PD-2-9-14	582	G3	Firmicutes, Clostridia, Clostridiales, Incertae Sedis XIV,
PD-2-9-15	517	G1	Firmicutes, Clostridia, Clostridiales, Incertae Sedis XIV, Anaerovirgula
PD-2-9-16	519	G5	Firmicutes, Clostridia, Clostridiales, Incertae Sedis XIV, Anaerovirgula
PD-2-9-17	512	G3	Firmicutes, Clostridia, Clostridiales, Incertae Sedis XIV, Anaerobranca
PD-2-9-18	520	G2	Firmicutes, Clostridia, Clostridiales,

Table B.8 RDP classification with 95% confidence threshold and OTU assignment for sequences obtained from the 10^{10} serial dilution culture produced from the iron reducing consortium.

ID*	Sequence length	OTU	Classification using the RDP classifier (Wang et al., 2007) (95% Confidence threshold)
SD-10-1	521	H1	Firmicutes, Clostridia, Clostridiales, Incertae Sedis XI, Tissierella
SD-10-2	521	H1	Firmicutes, Clostridia, Clostridiales, Incertae Sedis XI, Tissierella
SD-10-3	521	H1	Firmicutes, Clostridia, Clostridiales, Incertae Sedis XI, Tissierella
SD-10-4	521	H1	Firmicutes, Clostridia, Clostridiales, Incertae Sedis XI, Tissierella
SD-10-6	521	H1	Firmicutes, Clostridia, Clostridiales, Incertae Sedis XI, Tissierella
SD-10-7	521	H1	Firmicutes, Clostridia, Clostridiales, Incertae Sedis XI, Tissierella
SD-10-8	521	H1	Firmicutes, Clostridia, Clostridiales, Incertae Sedis XI, Tissierella
SD-10-9	513	H2	Firmicutes, Clostridia, Clostridiales, Incertae Sedis XIV, Anaerobranca
SD-10-10	521	H1	Firmicutes, Clostridia, Clostridiales, Incertae Sedis XI, Tissierella
SD-10-11	521	H1	Firmicutes, Clostridia, Clostridiales, Incertae Sedis XI, Tissierella
SD-10-12	521	H1	Firmicutes, Clostridia, Clostridiales, Incertae Sedis XI, Tissierella
SD-10-13	521	H1	Firmicutes, Clostridia, Clostridiales, Incertae Sedis XI,
SD-10-14	516	H3	Firmicutes, Clostridia, Clostridiales, Incertae Sedis XIV, Anaerovirgula
SD-10-15	521	H1	Firmicutes, Clostridia, Clostridiales, Incertae Sedis XI, Tissierella
SD-10-16	521	H1	Firmicutes, Clostridia, Clostridiales, Incertae Sedis XI, Tissierella
SD-10-17	521	H1	Firmicutes, Clostridia, Clostridiales, Incertae Sedis XI, Tissierella
SD-10-18	521	H1	Firmicutes, Clostridia, Clostridiales, Incertae Sedis XI, Tissierella

B.6 References

Atkins, J., 2009. Modelling groundwater and chromite migration through an old spoil tip in Copley., MSc Dissertation School of Earth and Environment. University of Leeds, Leeds, UK.

Wang, Q., Garrity, G.M., Tiedje, J.M., Cole, J.R., 2007. Naive Bayesian classifier for rapid assignment of rRNA sequences into the new bacterial taxonomy. Appl. Environ. Microbiol. 73, 5261-5267.

Appendix C Associated publications

Included within this section are publications associated with the work presented in this thesis. In addition, publications and conference proceedings that have included contributions from the author, Mr R. A. Whittleston, are also attached.

C.1 Relevant publications

Whittleston, R.A., Stewart, D.I., Mortimer, R.J.G., Tilt, C.Z., Brown, A.P., Geraki, K., Burke, I.T., 2011b. Chromate reduction in Fe(II)-containing soil affected by hyperalkaline leachate from chromite ore processing residue. Journal of Hazardous. Materials *(in press).*

Whittleston, R.A., Stewart, D.I., Mortimer, R.J.G., Ashley, D.J., Burke, I.T., 2011a. Effect of Microbially Induced Anoxia on Cr(VI) Mobility at a Site Contaminated with Hyperalkaline Residue from Chromite Ore Processing. Geomicrobiology Journal. 28, 68-82.

C.2 Other publications

Stewart, D.I., Burke, I.T., Hughes-Berry, D.V., Whittleston, R.A., 2010. Microbially mediated chromate reduction in soil contaminated by highly alkaline leachate from chromium containing waste. Ecological Engineering. 36, 211-221.

Burke, I.T., Mortimer, R.J.G., Palani, S., Whittleston, R.A., Lockwood, C.L., Ashley, D.J., Stewart, D.I. Biogeochemical reduction processes in a hyper-alkaline affected leachate soil profile. Geomicrobiology Journal *(in press).*

C.3 Conference proceedings

Whittleston RA, Burke IT, Stewart DI, Mortimer RJG. Geomicrobiology of hyperalkaline Cr(VI) contaminated land. Goldschmidt, Prague, CZ, 14 Aug 2011 - 19 Aug 2011. Mineralogical Magazine. 75 (3): pp.A2155.

Whittleston, RA; Stewart, DI; Mortimer, RJG; Burke, IT Biostimulation of nitrate, iron and chromate reduction at hyperalkaline conditions in. Goldschmidt, Davos, CH, 21 Jun 2009. Geochmica et Cosmochimica Acta, vol. 73, pp.A1436.

Whittleston, RA; Stewart, DI; Mortimer, RJG; Burke, IT Microbially mediated chromate reduction in hyperalkaline conditions. Geological Society William Smith Meeting, London, England, 2009 *(DIS oral).*

Libert, M; Pointeau, I; Sellier, R; Lillo, M; Burke, IT; Stewart, DI; Whittleston, RA; Albrecht, A. Nitrate-reducing bacterial activity under alkaline conditions such as bituminous nuclear waste repositories. 1st International Symposium on Cement-based Materials for Nuclear Wastes, Avignon, France, 2011